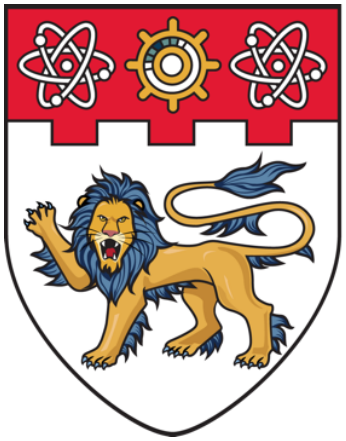

NANYANG TECHNOLOGICAL UNIVERSITY
SINGAPORE

HTRA AND CRORS TWO-COMPONENT SIGNAL TRANSDUCTION SYSTEM MONITOR SORTASE-ASSEMBLED PILUS BIOGENESIS IN *ENTEROCOCCUS FAECALIS*

ADELINE YONG MEI HUI

SCHOOL OF BIOLOGICAL SCIENCES

2019

HtrA and CroRS two-component signal transduction system monitor sortase-assembled pilus biogenesis in *Enterococcus faecalis*

Adeline Yong Mei Hui

School of Biological Sciences

A thesis submitted to the Nanyang Technological University in partial fulfillment of the requirement for the degree of Doctor of Philosophy

2019

STATEMENT OF ORIGINALITY

I hereby certify that the work embodied in this thesis is the result of original research done by me except where otherwise stated in this thesis. The thesis work has not been submitted for a degree or professional qualification to any other university or institution. I declare that this thesis is written by myself and is free of plagiarism and of sufficient grammatical clarity to be examined. I confirm that the investigations were conducted in accord with the ethics policies and integrity standards of Nanyang Technological University and that the research data are presented honestly and without prejudice.

18th February 2019

. . . . . .

18th February 2019

. . . . . .

Adeline Yong Mei Hui

SUPERVISOR DECLARATION STATEMENT

I have reviewed the content and presentation style of this thesis and declare it of sufficient grammatical clarity to be examined. To the best of my knowledge, the thesis is free of plagiarism and the research and writing are those of the candidate's except as acknowledged in the Author Attribution Statement. I confirm that the investigations were conducted in accord with the ethics policies and integrity standards of Nanyang Technological University and that the research data are presented honestly and without prejudice.

18th February 2019

. . . . . .

18th February 2019

. . . . . .

Associate Prof. Kimberly Kline

AUTHORSHIP ATTRIBUTION STATEMENT DECLARATION

Thesis Title:

HtrA and CroRS two-component signal transduction system monitor sortase-assembled pilus biogenesis in *Enterococcus faecalis*

I have excluded the Authorship Attribution Statement declaration because the thesis does not contain any published material.

. . . . . .
Adeline Yong Mei Hui

Date: 18th February 2019

. . . . . .
Associate Prof. Kimberly Kline

Date: 18th February 2019

ACKNOWLEDGMENT

This Ph.D. has been an aspiring and exciting journey for me. It would not have been possible without the love and supports from my family, friends, supervisors, mentors, members of the Thesis advisory committee, and colleagues. I would like to give special thanks to all the people who have, in some way contributed to the work in this thesis.

First and foremost, I would like to give my deepest gratitude to my supervisor, **Assoc Prof Kimberly Kline**, for taking me into her lab, to become her first FYP student, then a research assistant before converting to a Ph.D. student. I am grateful and fortunate to work side-by-side with her for the past 6 years. Without her invaluable guidance, wisdom, and support throughout my Ph.D. candidature, I would not have achieved what I have today.

I would also like to take this opportunity to thank the following lab members- **Dr. Kelvin Chong** and **Dr. Mohammad Hafiz** for their wisdom and advice; **Dr. Mark Veleba, Dr. Sumitra Mitra**, **Dr. Irina Afonina, Ms. Pei Yi Choo** for their friendship and all the help in the lab; **Dr. Joey Yam** and **Dr. Artur Matysik** for the help with microscopic-related technical problems; members of the localization group for the critical feedbacks during localization meetings as well as everyone in the Kline lab.

I would like to extend my thanks to **Assoc Prof. Wandy Beatty** at Washington University in St. Louis for all transmission electron microscopic images used in this work. They are fantastically done. I would also like to extend my thanks to the **NTU Protein Production Platform** for the cloning, expression tests and purification of all protein constructs used in this thesis.

I am also grateful for the support from friends and colleagues from the Graduate Student Offices from the School of Biological Sciences (SBS, NTU) and Singapore Centre on Environmental Life Sciences Engineering (SCELSE, NTU); SCELSE Laboratory Management, Administration, Finance, Sequencing and IT department for making my study life in SCELSE a very enjoyable place. Special thanks to **Dr. Song Lin Chua**, **Dr. Grant Tan**, **Ms. Ying Ting Loh**, **Ms. Priscilla Lefort**, **Dr. Krager Koh**, **Ms. Ley Byan Chew**, **Mr. Zhei Hwee Yap**, **Dr. Wey Yeeng Chee**, **Ms. Thanalachmy Karunanithy** and **Ms. Siti Fatimah**.

I would also like to extend my heartfelt gratitude to my family, my fiancé, **Dr. Joey Yam**, whose love, support and understanding throughout these years have been of great comfort.

Lastly, I acknowledge **NTU research scholarship** and **SCELSE for** providing the scholarship funding and financial support throughout my Ph.D. candidature.

This work is also supported by the **National Research Foundation** and **Ministry of Education Singapore** under its Research Centre of Excellence Programme and by the National Research Foundation under its Singapore NRF Fellowship Programme (NRF-NRFF201111).

TABLE OF CONTENT

STATEMENT OF ORIGINALITY i

SUPERVISOR DECLARATION STATEMENT ii

AUTHORSHIP ATTRIBUTION STATEMENT DECLARATION iii

ACKNOWLEDGMENT iv

TABLE OF CONTENT vi

LIST OF FIGURES xiv

LIST OF TABLES xvii

LIST OF ABBREVIATIONS xix

LIST OF PUBLICATIONS xxiii

ABSTRACT xxv

CHAPTER I: INTRODUCTION 1

1.1 Background 1

1.2 Objectives and scope 3

CHAPTER II: LITERATURE REVIEW 5

2.1 *Enterococcus faecalis* Endocarditis and biofilm-associated pili (Ebp) 8

2.1.2 Sortase-catalysed transpeptidation 16

2.1.3 Regulation of Ebp expression 17

2.1.3.1 Endocarditis and biofilm-associated pilus regulator (EbpR) 17

2.1.3.2 Environmental factors 17

2.1.3.3 The *fsr* quorum-sensing system 18

2.2 Two-component signal transduction pathways 22

2.2.1 TCS in *E. faecalis* OG1RF 23

2.2.2 TCS involved in antibiotic resistance and cell wall stress 27

2.3 High-temperature requirement A (HtrA) serine protease 30

2.3.1 Role of HtrA in other Gram-positive bacteria 33

2.3.2 Role of Deg proteases in *E. coli* 35

2.3.2.1 DegP and the Cpx system 37

2.3.2.2 DegP, DegS, and the Sigma E pathway 37

2.3.3 HtrA in virulence and in anti-bacterial therapy 40

CHAPTER 3: CONSTRUCTION AND CHARACTERIZATION OF HIGH-TEMPERATURE REQUIREMENT A (HTRA) MUTANT IN *ENTEROCOCCUS FAECALIS* 46

3.1 INTRODUCTION 46

3.2 MATERIALS AND METHODS 48

3.2.1 Bacterial strains and growth conditions 48

3.2.2 Competent cell preparation and electro-transformation of *E. coli* and *E. faecalis* 49

3.2.3 Molecular techniques 50

3.2.4 Construction of *htrA* deletion mutant 51

3.2.5 pGPC123-*htrA* plasmid construction 52

3.2.6 Whole genome sequencing (WGS) of WT and *htrA* deletion mutant 53

3.2.7 Generation of antibodies 53
3.2.8. Bacterial cell preparation for immunofluorescence staining 55
3.2.9 Identification of protein localization using SR-SIM microscopy 55
3.2.10 Growth Kinetic Assay 56
3.2.11 Biofilm Assay 56
3.2.12 Environmental stress tolerance assays 57
3.2.13 Bacterial cell fractionation 57
3.2.14 Immunoblotting 58
3.2.15 Murine wound infection model 58
3.2.16 Alkaline Phosphatase (AP) Secretion assay 60
3.2.17 Statistical analyses 60
3.2.18 Ethics Statement 61
3.3 RESULTS 62
3.3.1 Genetic organization and bioinformatics prediction of OG1RF_12305 coding for *htrA* 62
3.3.2 Construction of in-frame deletion of *htrA* in *E. faecalis* 67
3.3.3 HtrA is enriched at the septum in *E. faecalis* 69
3.3.4 Characterization of HtrA functions in *E. faecalis* 71
3.3.4.1 Growth of *E. faecalis* is not affected by *htrA* gene disruption under high temperature 71

3.3.4.2 $HtrA_{EF}$ is not essential in biofilm formation 73

3.3.4.3 Growth of *E. faecalis* is not affected by *htrA* gene disruption under various environmental stresses 74

3.3.5 Deletion of *htrA* does not affect pilus protein expression in *E. faecalis* 75

3.3.6 $HtrA_{EF}$ contributes to colonization fitness during chronic wound infection 76

3.3.7 Attenuated fitness of the Δ*htrA* mutant *in vivo* is not due to a growth defect in mixed culture 81

3.3.8 The Δ*htrA* mutant exhibits a severe defect in protein maturation 82

3.4 DISCUSSION 84

CHAPTER 4: HTRA MONITORS SORTASE-ASSEMBLED PILUS BIOGENESIS IN *ENTEROCOCCUS FAECALIS* 87

4.1 INTRODUCTION 87

4.2 MATERIALS AND METHODS 88

4.2.1 Bacterial strains and growth conditions 88

4.2.2 OG1RF Δ*srtA*Δ*htrA* mutant construction 89

4.2.3 OG1RFΔ*ebpABC*Δ*srtA*Δ*htrA* mutant construction 89

4.2.4 *pGPC123-srtA* construction 90

4.2.5 Growth Kinetic Assay 90

4.2.6 Biofilm assay 92

4.2.7 Construction of HtrA and EbpC point mutations using site-directed mutagenesis (SDM) 92

4.2.8 Bacterial cell fractionation and Immunoblotting 93

4.2.9 Generation of antibodies 93

4.2.10 Bacterial cell preparation for immunofluorescence staining 93

4.2.11 Visualization of bacterial chain length with phase contrast microscopy 94

4.2.12 Transmission Electron Microscopy (TEM) 95

4.2.13 Quantitative analysis of fluorescent foci and cell length 95

4.2.14 RNA extraction and purification 96

4.2.15 mRNA library preparation and Illumina sequencing 97

4.2.16 pP_{ftsW}-*ftsW/rodA* construction 97

4.2.17 qRT-PCR 98

4.2.18 Statistical analyses 98

4.3 RESULTS 100

4.3.1 Construction of Δ*srtA*Δ*htrA* and Δ*srtC*Δ*htrA* mutations in *E. faecalis* OG1RF 100

4.3.2 Growth kinetics and biofilm formation by Δ*srtA*Δ*htrA* mutant 101

4.3.3 HtrA is needed for the removal of mistargeted Ebp pili in *E. faecalis* 104

4.3.4 HtrA chaperone function is sufficient to restore Ebp pilus expression 108

4.3.5 HtrA interacts with EbpC, DnaK, and SrtA 108

4.3.6 Localization of Ebp pili is not affected in a Δ*srtA*Δ*htrA* mutant 111

4.3.7 Absence of *srtA* and *htrA* results in chaining of cells 114

4.3.8 Deletion of *E. faecalis srtA* and *htrA* results in aberrant cell morphology..... 116

4.3.9 Aberrant cell morphology in Δ*srtA*Δ*htrA* mutant is pilus-dependent..... 119

4.3.10 Accumulated monomeric or polymerized pili in the membrane can lead to aberrant cell morphology 120

4.3.11 Transcriptomic analysis reveals differential expression of *ebp* genes in Δ*srtA*Δ*htrA* mutant 121

4.3.12 Identification of genes induced in the presence of membrane stress 123

4.3.12.1 Differential expression of several cell division/separation genes 125

4.3.12.2 Differential expression of genes involved in signal transduction pathways 128

4.4 DISCUSSION..... 131

CHAPTER 5: POTENTIAL ROLE OF CRORS IN GOVERNING CELL CYCLE CHECKPOINT DURING MEMBRANE STRESS IN *ENTEROCOCCUS FAECALIS*... 138

5.1 INTRODUCTION..... 138

5.2 MATERIALS AND METHODS 139

5.2.1 Bacterial strains and growth conditions 139

5.2.2 Validation of *croR::Tn* and *croS::Tn*..... 140

5.2.3 Construction of *E. faecalis croR::Tn*Δ*srtA*Δ*htrA* and *croS::Tn*Δ*srtA*Δ*htrA* mutants in OG1RF..... 140

5.2.4 pCroR$_{promoter}$-*croRS* plasmid construction 140

5.2.5 Generation of antibodies..... 143

5.2.6 Growth Kinetic Assay 143

5.2.7 Bacterial cell fractionation 144

5.2.8 Bacterial cell preparation for TEM, immunofluorescence staining and visualization 144

5.2.9 Quantitative analysis of cell length 144

5.2.10 Antibiotic susceptibility determinations 145

5.2.11 RNA extraction, purification, and sequencing 145

5.2.12 mRNA library preparation and Illumina sequencing 146

5.2.13 Statistical analysis 147

5.3 RESULTS 148

5.3.1 CroR confers resistance to cell wall antibiotics 148

5.3.2 Construction of *E. faecalis croR::TnΔsrtAΔhtrA* and *croS::TnΔsrtAΔhtrA* mutants in OG1RF 149

5.3.3 Absence of *croR* restores piliation levels during membrane stress 151

5.3.4 CroR induction correlates with cell morphology 153

5.3.5 Identification of potential CroR targets by RNA sequencing 158

5.3.6 Genes of the *fsr* system and cell wall synthesis and elongation are potential CroR targets 162

5.4 Discussion 164

CHAPTER 6: CONCLUSION AND FUTURE RECOMMENDATIONS 171

6.1 CONCLUSIONS 171

6.2 FUTURE RECOMMENDATIONS 175
6.2.1 Investigation of the phosphorylation state of CroRS 175
6.2.2 Investigation of the interaction between CroRS and non-cognate CisRS 176
6.2.3 Identification of the CroR regulon 176
6.2.4 Involvement of FsrA-FsrC two-component systems in membrane stress response in *Enterococcus faecalis* 177
6.2.5 Investigating the role of HtrA in processing pilin monomers 178
6.2.6 *E. faecalis* HtrA roles in virulence 179
PERMISSIONS 181
CHAPTER 7: APPENDICES 182
APPENDIX A 182
APPENDIX B 187
APPENDIX C 193
REFERENCES 246

LIST OF FIGURES

Figure 2.1 | *In vivo* systems for modeling and studying *E. faecalis* and *E. faecium* virulence. 7
Figure 2.2 | A scanning electron micrograph (SEM) of Ebp pili on the cell surface of *E. faecalis*. 8
Figure 2.3 | Mechanism of sortase-mediated polymerized pili anchoring to the cell wall. 12
Figure 2.4 | Co-localization of Sortase enzymes and the Sec secretion machinery focally at the *E. faecalis* division septum. 15
Figure 2.5 | The *fsr* quorum-sensing system and its regulation in *E. faecalis*..... 20
Figure 2.6 | Genomic organization and domain architecture of *croRS* locus in *E. faecalis* OG1RF. 28
Figure 2.7 | Localization of HtrA in *S. pyogenes* and *S. pneumoniae*..... 33
Figure 2.8 | RpoE and Cpx pathways regulate transcription of *degP* (*htrA*) expression in *E. coli*. 39
Figure 3.1 | Genomic organization of the *htrA* locus in the sequenced genome of *E. faecalis* OG1RF. 62
Figure 3.2 | Architecture of HtrA proteases. 64
Figure 3.3 | HtrA is conserved across all domains of life. 65
Figure 3.4 | Locus and the genetic disruption of *htrA* in *E. faecalis* OG1RF..... 68
Figure 3.5 | $HtrA_{EF}$ is localized to multiple foci around the membrane but enriched at the septum. 70
Figure 3.6 | $HtrA_{EF}$ does not play a role in high-temperature growth. 72
Figure 3.7 | $HtrA_{EF}$ does not play a role in biofilm formation in *E. faecalis*..... 74
Figure 3.8 | Pili was expressed at equivalent levels in OG1RF WT and Δ*htrA*. 76
Figure 3.9 | HtrA is required for persistent wound infection. 79
Figure 3.10 | Co-culture with OG1X does not cause slower growth of 81
Figure 3.11 | The *E. faecalis* Δ*htrA* mutant exhibits a severe defect in protein maturation. 83
Figure 4.1 | Construction and validation of Δ*srtA*Δ*htrA* mutant. 101
Figure 4.2 | Growth kinetics and biofilm formation by Δ*srtA*Δ*htrA*..... 103

Figure 4.3 | Increased EbpC protein levels in Δ*srtA*Δ*htrA*. 106
Figure 4.4 | Increased pilin expressing cells in Δ*srtA*Δ*htrA*..... 107
Figure 4.5 | HtrA interacts with EbpC, DnaK, and SrtA. 109
Figure 4.6 | Localization pattern of Ebp pili on Δ*srtA*Δ*htrA*. 113
Figure 4.7 | Localization pattern of Ebp pili on Δ*srtA*Δ*htrA* using PSICIC. 114
Figure 4.8 | Chaining morphology observed in Δ*srtA*Δ*htrA*..... 115
Figure 4.9 | Absence of SrtA and HtrA resulted in aberrant fluorescent-vancomycin staining. 117
Figure 4.10 | Δ*srtA*Δ*htrA* exhibits cells with wider cell width. 118
Figure 4.11 | TEM revealed cells morphology defects in Δ*srtA*Δ*htrA*..... 119
Figure 4.12 | Ebp effects on cell morphology in the absence of *srtA* and *htrA*. 121
Figure 4.13 | *ebpABC* transcription is higher in Δ*srtA*Δ*htrA*. 122
Figure 4.14 | Transcriptional gene expression profile of Δ*srtA*Δ*htrA*..... 124
Figure 4.15 | Complementation of Δ*srtA*Δ*htrA* with p*ftsW/rodA* partially alleviates the morphology defect. 127
Figure 4.16 | *croRS* transcription is higher in Δ*srtA*Δ*htrA*. 129
Figure 5.1 | Locus and genetic disruption of *srtA* and *htrA* in *croR::Tn* and *croS::Tn* transposon mutants 150
Figure 5.2 | *croR* is responsible for Ebp pili expression. 152
Figure 5.3 | CroR induction correlates with cell morphology. 154
Figure 5.4 | *croS::Tn*Δ*srtA*Δ*htrA* cells are wider in cell width and shorter in length. 155
Figure 5.5 | Growth kinetic profiles of *croS* mutant variants. 156
Figure 5.6 | Transcriptional gene expression profile of predicted CroR-regulated genes. 160
Figure 5.7 | A simplified cartoon of the *fsr* quorum-sensing system and its regulation in *E. faecalis*. 169
Figure 6.1 | A model for CroR-regulated hyper-piliation induced stress response. 174
Supplementary Figure B1 | Increased Ebp pilus expression in Δ*srtA*Δ*htrA*. 187
Supplementary Figure B2 | Genetic organization of pp2 phage in V583. 188
Supplementary Figure B3 | Different subset of genes regulated in the presence of different stress stimulus. 188

Supplementary Figure B4 | Complementation of *croR:Tn*Δ*srtA*Δ*htrA* p*croR(D52A)* does not phenocopy Δ*srtA*Δ*htrA*. 189
Supplementary Figure B5 | Optimization of nisin concentration for CroR expression. 189
Supplementary Figure B6 | Hyper-piliation observed in strains that lack both SrtA and HtrA. 190
Supplementary Figure B7 | Decreased Ebp pili protein expression in Δ*srtC*Δ*htrA*. 190
Supplementary Figure B8 | Decrease in pili monomers expressed in Δ*srtC*Δ*htrA*..... 191
Supplementary Figure B9 | Ebp pilus expression in Δ*srtC*Δ*htrA* was transcriptionally affected. 192
Supplementary Figure B10 | $HtrA_{EF}$ is released from cells in the absence of lysis. 192

LIST OF TABLES

Table 2.1 | Sortase substrates found in V583 and OG1RF. 10
Table 2.2 | Histidine kinases identified in the *E. faecalis* OG1RF genome aligned against V583. 25
Table 2.3 | Response regulators identified in the *E. faecalis* OG1RF genome aligned against V583. 26
Table 2.4 | HtrA contributions to virulence in various disease models. 43
Table 3.1 | Bacterial Strains and Plasmids used in this study 49
Table 3.2 | Primers used in this study. 52
Table 3.3 | Antibodies used in this chapter. 54
Table 3.4 | Function predictions of HtrA against known functions of HtrA in the database using I-TASSER. 66
Table 4.1 | Bacterial Strains and Plasmids used in this study 88
Table 4.2 | Primers used in this study. 91
Table 4.3 | Cycling Parameters for QuikChange Site-Directed Mutagenesis. 92
Table 4.4 | Antibodies used in this chapter. 94
Table 4.5 | Expression of several cell envelope proteins are differentially regulated. . 126
Table 4.6 | List of genes classified under signaling and regulation. 130
Table 5.1 | Bacterial Strains and Plasmids used in this study 139
Table 5.2 | Primers used in this study. 142
Table 5.3 | Antibodies used in this chapter. 143
Table 5.4 | MICs of various antibiotics for *E. faecalis* mutants. 149
Table 5.5 | Known CroR-targets differently regulated during membrane stress. 161
Table 5.6 | Potential CroR-regulated genes of interest. 162
Supplementary Table A1 | Protein sequences used to raise antibodies in animals. 182
Supplementary Table A2 | HtrA DNA sequences used for sequence alignment. 184
Supplementary Table A3 | mRNA transcriptomics profile between WT and Δ*htrA*. 185
Supplementary Table A4 | List of genes classified under phages. 186
Supplementary Table C1 | RNA-Seq results comparing WT and *ΔsrtAΔhtrA*. 193

Supplementary Table C2 | RNA-Seq results comparing *ΔhtrA* and *ΔsrtAΔhtrA*..... **Error! Bookmark not defined.**
Supplementary Table C3 | RNA-Seq results comparing *ΔsrtA* and *ΔsrtAΔhtrA.* 210
Supplementary Table C4 | RNA-Seq results comparing *croR::TnΔsrtAΔhtrA* and *ΔsrtAΔhtrA.* 216
Supplementary Table C5 | RNA-Seq results showing 164 consensus genes identified when compared across 3 sets of RNA data. 222
Supplementary Table C6 | 81 genes which show opposite in fold-change expression in *croR::TnΔsrtAΔhtrA* vs *ΔsrtAΔhtrA*; *ΔsrtA* vs *ΔsrtAΔhtrA* postulated as CroR-regulated genes. 227
Supplementary Table C7 | RNA-Seq results comparing *ΔsrtA* and WT. 229
Supplementary Table C8 | RNA-Seq results comparing *croS::TnΔsrtAΔhtrA* and *ΔsrtAΔhtrA.* 230

LIST OF ABBREVIATIONS

°C	Degree Celsius
AP	Alkaline Phosphatase
BacTH	Bacteria Two-Hybrids
BGYT	BHI, Glucose, Yeast extract, Tryptone
BHI	Brain Heart Infusion
bp	Base pair
CA	C-terminal catalytic and ATP-binding
CAUTI	Catheter-associated Urinary Tract Infection
CFU	Colony Forming Unit
ChIP	Chromatin Immuno-Precipitation
CI	Competitive Index
CisR	CroRS-interacting system Regulator
CisS	CroRS-interacting system Sensor kinase
Cm	Chloramphenicol
cm	Centimeter
CroR	Ceftriaxone Resistance Regulator
CroS	Ceftriaxone Resistance Sensor kinase
CV	Crystal Violet
CWSS	Cell Wall Sorting Signal
DAPI	4',6-Diamidino-2-Phenylindole, Dihydrochloride
DBD	DNA Binding Domain
DHp	dimerization and histidine phosphor-transfer
dpi	Days Post Infection
DTT	dithiothreitol
Ebp	Endocarditis and Biofilm-associated Pili
EDTA	Ethylene Diamine Tetra Acetic acid
Em	Erythromycin
EMSA	Electromobility Shift Assay
EPS	Extracellular Polymeric Substances
FDR	False Discovery Rate

FM™ 4-64	(N-(3-Triethylammoniumpropyl)-4-(6-(4-(Diethylamino)Phenyl) Hexatrienyl) Pyridinium Dibromide)
Fus	Fusidic acid
GBAP	Gelatinase Biosynthesis-Activating Pheromone
GI	Gastrointestinal
H	Hours
HA	Human influenza hemagglutinin
HAI	Hospital Acquired Infection
HCl	Hydrochloric acid
hpi	Hours Post infection
HIS-tag	Histidine tag
HK	Histidine kinase
HMWL	High Molecular Weight Ladder
HRP	Horse Radish Peroxidase
HtrA	High Temperature Requirement A
IACUC	Institutional Animal Care and Use Committee
IFA	Immuno-Fluorescence Assay
IMAC	Immobilized Metal Affinity Chromatography
IPTG	Isopropyl β-D-1thiogalactopyranoside
I-TASSER	Iterative Threading ASSEmbly Refinement
Km	Kanamycin
kb	Kilo Bases
KDa	Kilo Daltons
LOD	Limit of Detection
M	Molar
MH	Muller Hinton
MIC	Minimum Inhibitory Concentration
MIDAS	Metal Ion-Dependent Adhesion Site
Mins	Minutes
mL	Milliliters
mM	Millimolar

MS	Mass Spectrometry
NaCl	Sodium Chloride
ng	Nanogram
nm	Nanometer
OD	Optical Density
OMP	Outer Membrane Protein
P2CS	Prokaryotic 2-Component Systems
PBP	Penicillin-Binding Protein
PBS	Phosphate Buffered Saline
P-BSA	Phosphate Buffered Saline-Bovine Serum Albumin
PCR	Polymerase Chain Reaction
PDZ	Post-synaptic density protein, Disc large and Zo-1 proteins
PG	Peptidoglycan
pNPP	*Para*-Nitrophenyl Phosphate
pp2	Prophage 2
PPIase	Peptidyl-Prolyl cis-trans Isomerase
PSICIC	Projected System of Internal Coordinates from Interpolated Contours
PTS	Phosphotransferase System
REC	Receiver
Rif	Rifampicin
RpoE	RNA Polymerase σ^E
RR	Response Regulator
sCMOS	Scientific Complementary Metal Oxide Silicon
SDM	Site-Directed Mutagenesis
SDS-PAGE	Sodium Dodecyl Sulfate–Polyacrylamide Gel Electrophoresis
Secs	Seconds
SEM	Scanning Electron Microscope
SMART	Simple Modular Architecture Research Tool
SpeB	Streptococcal pyrogenic exotoxin B
SrtA	Sortase A
SrtC	Sortase C

SR-SIM	Super-Resolution-Structured illumination microscopy
SS	Signal Sequence
Str	Streptomycin
TM	Transmembrane
TMH	Transmembrane Helix
Tn	Transposon mutant
TSBG	Tryptic Soy Broth supplemented with Glucose
µL	Microliters
µg	Micrograms
UTI	Urinary Tract Infection
Van-FL	Vancomycin BODIPY® Fluorescein
VWA	Von Willebrand factor A
WT	Wildtype

LIST OF PUBLICATIONS

Publications

1. Chong K.K.L., Tay W.H., Janela B., **Yong A.M.H.,** Liew T.H., Madden L., Keogh D., Barkham T.M.S., Ginhoux F., Becker D.L., Kline K.A., 2017, ***Enterococcus faecalis* Modulates Immune Activation and Slows Healing During Wound Infection.** The Journal of infectious diseases, Volume 216, Issue 12, Pages 1644–1654.
2. Goh H. M. S., **Yong A.M.H.,** Chong K.K.L., Kline K. A., 2016, **Model Systems for the Study of Enterococcal Colonization and Infection.** Virulence, Volume 8, Issue 8, Pages 1525-1562.

Conferences

1. **Yong A.M.H.,** Kline K. A., 2016. The function of the Serine Protease, HtrA in *Enterococcus faecalis.* Conference presentation at Gordon Research Seminar on Microbial Stress Response (GRS) 2016, Mount Holyoke College in South Hadley MA United States. (Poster presentation).
2. **Yong A.M.H.,** Kline K. A., 2016. The function of the Serine Protease, HtrA in *Enterococcus faecalis.* Conference presentation at Gordon Research Conference on Microbial Stress Response (GRC) 2016, Mount Holyoke College in South Hadley MA United States. (Poster presentation).

3. **Yong A.M.H.,** Kline K. A., 2016. HtrA Monitors Sortase-Assembled Pilus Biogenesis in *Enterococcus faecalis.* Conference presentation at ISME16 2016, Montreal Canada. (Poster presentation).
4. **Yong A.M.H.,** Kline K. A., 2017. HtrA Monitors Sortase-Assembled Pilus Biogenesis in *Enterococcus faecalis.* Conference presentation at IUMS2017, Singapore (Poster presentation) – Awarded with SSMB travel grant award.
5. **Yong A.M.H.,** Chong K. K. L., Chen S. L. and Kline K. A., 2018. HtrA and CroRS two-component signal transduction system monitor sortase-assembled pilus biogenesis in *Enterococcus faecalis.* Conference presentation at 5th International Conference for Enterococci, 2018, Le Majestic Congress Centre, Chamonix, France (Poster presentation).

ABSTRACT

Enterococcus faecalis is one of the leading causes of hospital-acquired infections (HAIs). One of the most commonly associated virulence factors in these HAIs is the endocarditis and biofilm-associated pilus (Ebp) which is often implicated in biofilm formation. *E. faecalis* is associated with urinary tract infections (UTI), bacteremia, endocarditis, surgical wounds, and many other infections. These infections likely give rise to unfolded or misfolded proteins, leading to the accumulation of potentially harmful protein aggregates. *E. faecalis* must evolve strategies to combat these stresses encountered during colonization and infection. It is not known how these misfolded proteins, including Ebp, are processed. In this study, we determined the contribution of a highly conserved serine protease, HtrA, to membrane stress tolerance in *E. faecalis*. We found that $HtrA_{EF}$ is not involved in growth or survival under a wide range of stress conditions, nor is it involved in biofilm formation. However, the Δ*htrA* mutant was attenuated in a competitive murine wound infection, suggesting its contribution to colonization and infection in host tissues. In many bacteria, HtrA deals with accumulated protein stresses and/or is part of a proteolytic pathway. The absence of HtrA alone does not result in accumulation of proteins. We postulated that the induction of protein accumulation in the absence of HtrA in *E. faecalis* may reveal a true role for $HtrA_{EF}$. We created a Δ*srtA*Δ*htrA* to mimic membrane stress where sortase substrates, such as Ebp pili, accumulate on the cell membrane. In this mutant background, we observed hyperpiliation as compared to single mutants. Furthermore, Δ*srtA*Δ*htrA* formed chains and displayed aberrant placement of septa in addition to increased pilus expression.

Δ*srtA*Δ*htrA* cells appeared coccoid and wider at the cell width than WT. In addition, this phenotype was pilus-dependent, as we no longer observed these aberrant cell morphologies in a Δ*srtA*Δ*ebpABC*Δ*htrA* strain. Transcriptomic analysis revealed upregulation of the CroR-CroS two-component system (TCS) in altering cell shape in a Δ*srtA*Δ*htrA* mutant strain. Deletion of *croR* in Δ*srtA*Δ*htrA* resulted in a reversal of cell morphology and piliation level to WT, suggesting that CroR mediates reparative transcriptional responses during membrane stress. Global expression analysis using RNA-seq identified possible CroR target genes, suggesting a possible novel role of this TCS in *E. faecalis* pilus biogenesis. This thesis is the first comprehensive study of HtrA in *E. faecalis*. We have discovered novel roles for HtrA and the CroR-CroS TCS in monitoring pilus biogenesis, providing potential inhibitory targets to limit the biogenesis of this important virulence factor.

CHAPTER I: INTRODUCTION

1.1 Background

Enterococci are facultative anaerobic bacteria commonly found as commensals in the gastrointestinal tracts (GI) of mammals, insects and even fish (Lebreton, Willems et al. 2014). However, Enterococci can cause opportunistic, polymicrobial infections in immunocompromised hosts or in hosts with underlying health conditions, such as the presence of catheter implants (Gold 2001, Agudelo Higuita and Huycke 2014, Lebreton, Willems et al. 2014). Opportunistic infections associated with enterococci include urinary tract infection (UTI), catheter-associated UTI (CAUTI), endocarditis, bacteremia, and a range of wound infections including surgical site infections (Agudelo Higuita and Huycke 2014).

E. faecalis produces an array of virulence factors and one of the most well-characterized is the sortase-assembled pilus. The **E**ndocarditis and **B**iofilm-associated **P**ilus (Ebp) is encoded by an operon consisting of three pilin genes, *ebpA, ebpB* and *ebpC,* and an adjacent downstream gene, *srtC,* whose expression is controlled by a second promoter (Nallapareddy, Singh et al. 2006). These pili are typical of most Gram-positive bacteria and pilin monomers are translocated across the membrane via the Sec secretion machinery, assembled into fibers by sortase enzyme C (SrtC) on the membrane, and are subsequently attached to the cell wall by sortase enzyme A (SrtA), encoded elsewhere on the chromosome (Schneewind and Missiakas 2014). These pili are often implicated in biofilm formation during infection (Nallapareddy, Singh et al. 2006, Sillanpaa, Chang et al. 2013).

Ebp regulation occurs at the transcription level, where it is positively regulated by EbpR and RNase J2 (*rnjB*), while the FsrA response regulator of the *fsr* quorum-sensing system acts as a weak repressor of *ebpR* expression (Nakayama, Chen et al. 2006, Bourgogne, Singh et al. 2007, Gao, Pinkston et al. 2010, Frank, Guiton et al. 2013). e*bp* expression can also be induced by environmental stimuli, including serum, bicarbonate, and fibrinogen secreted by the host during infection (Bourgogne, Thomson et al. 2010, Gao, Pinkston et al. 2010, Nallapareddy, Sillanpaa et al. 2011, Flores-Mireles, Pinkner et al. 2014).

Even though a substantial number of studies have characterized pili and their contribution to infection, most of the studies to date focus on pilus regulation and biogenesis under optimal laboratory growth conditions, which may not fully recapitulate physiological conditions of *E. faecalis* growth. For example, during infection, endogenous cellular stresses or harsh exogenous conditions can give rise to protein folding defects (Clausen, Kaiser et al. 2011). In the case of pili, this type of stress could result in the accumulation of misfolded pilins and potentially harmful protein aggregates and *E. faecalis* would need to have strategies to combat these stresses for optimal survival.

This situation has been described in *E. coli,* where misfolded pilins give rise to protein aggregates that are driven 'off-pathway', rather than being assembled into pili, via non-productive interactions which subsequently activate the Cpx two-component system (TCS) and RNA polymerase σ^E (RpoE) pathway (Mecsas, Rouviere et al. 1993, Danese and Silhavy 1997, Walsh, Alba et al. 2003). Both the Cpx and RpoE pathways activate a conserved serine protease, DegP (HtrA homolog), leading to proteolysis of misfolded pilins (Hung, Raivio et al. 2001). How *E. faecalis* handles and responds to 'off-pathway'

pilus biogenesis to modulate clearance of misfolded proteins and how this stress response interferes with the coupled processes of secretion, sorting and proteolysis at the cell membrane are currently unknown.

In this thesis, we focus on the membrane-anchored HtrA due to its role in both protein quality control and cellular responses to stress in a variety of bacterial species (Gottesman, Wickner et al. 1997, Poquet, Saint et al. 2000, Biswas and Biswas 2005, Kang, Lee et al. 2010, Boehm, Lind et al. 2015, Zhang, Li et al. 2016). HtrA has been extensively studied in *E. coli*, and it has been described in Gram-positive bacteria but its functions in *E. faecalis* are not known. It is our interest to understand the functions of HtrA in *E. faecalis* in order to understand how normal pilus biogenesis proceeds.

1.2 Objectives and scope

Our overall hypothesis for this thesis is that HtrA plays a role in processing misfolded pilins in *E. faecalis* and this process may involve a Cpx-like TCS to mediate stress responses in *E. faecalis*.

The specific objectives and scope for this thesis are:

Chapter 3: To characterize the functions of HtrA in *E. faecalis* strain OG1RF under *in vitro* and *in vivo* conditions, we create a markerless, in-frame deletion of *htrA* in *E. faecalis* OG1RF. This chapter examines the role of HtrA in various environmental stress conditions, such as acid, oxidative stress, temperature, as well as protein secretion in *E. faecalis*. The contribution of *htrA* in pathogenesis during an *in vivo* wound murine model is also presented.

Chapter 4: To elucidate the role of HtrA in monitoring 'off-pathway' pilus biogenesis in *E. faecalis*, this chapter examines HtrA roles in monitoring sortase-assembled pilus assembly under conditions where pilus biogenesis goes 'off-pathway'.

Chapter 5: To determine how the CroRS two-component system (TCS) responds to membrane stress associated with HtrA-dependent 'off-pathway' pilus biogenesis, this chapter describes work that couples genetic analyses with RNA sequencing to identify potential CroR targets involved in cell envelope homeostasis, pilus biogenesis, stress responses, and substrate transport.

Chapter 6: This concluding chapter provides a general discussion of implications and applications of the current findings reported in this thesis, and includes preliminary studies performed that serve as possible directions and starting points for future work. Based on the knowledge and insights obtained from this thesis project, a working model of the pilus biogenesis in *E. faecalis* is presented.

CHAPTER II: LITERATURE REVIEW

Enterococci are Gram-positive, facultative anaerobic diplococci that reside in a variety of hosts — humans and other mammals, birds, reptiles, fish and insects (Lebreton, Willems et al. 2014). Enterococci can survive and grow in harsh environments, such as 6.5% NaCl, a broad range of temperatures (10°C-45°C), and high pH (pH 9.6) (Lebreton, Willems et al. 2014). Enterococci belong to the low GC branch of Gram-positive bacteria, containing about 37.5% GC in the *E. faecalis* chromosome (Agudelo Higuita and Huycke 2014). Enterococci can cause opportunistic infection in susceptible hosts and they are the second most common cause of nosocomial infections, associated with as many as 14% of all the hospital-acquired infections (HAIs) in the United States between 2011-2014 (Weiner, Webb et al. 2016). Among all the Enterococcus species, *Enterococcus faecalis* and *Enterococcus faecium* are the two most commonly identified in human HAIs. These enterococcus species are robust and are often associated with several opportunistic infections such as urinary tract infections (UTI), catheter-associated UTI (CAUTI), endocarditis, bacteremia, peritonitis, endodontic infections, GI infections and colitis, and a range of wound infections including surgical site infections and diabetic foot ulcers (Maki and Agger 1988, Patterson, Sweeney et al. 1995, Gjodsbol, Christensen et al. 2006, Citron, Goldstein et al. 2007, Agudelo Higuita and Huycke 2014, Pinholt, Ostergaard et al. 2014, Garcia-Granja, Lopez et al. 2015). *E. faecalis*- and *E. faecium*-associated opportunistic infections have been studied in various animal models (**Fig 2.1**) (Goh, Yong et al. 2017). In CAUTI, enterococcal species are the second most common bacterial species detected (Hidron, Edwards et al. 2008). Efficient colonization of the host during

infection usually involves the formation of biofilms, which enables the bacteria to better withstand antimicrobial insults and environmental stresses. Bacterial biofilms are formed by a cluster of bacterial species that produce extracellular polymeric substances (EPS) (Flemming, Wingender et al. 2016). Biofilms are often polymicrobial and bacteria in these biofilm biomasses produce a plethora of virulence factors consisting of proteases, transcription factors, two-component systems, and secreted and cell wall-associated factors to form better biofilms to resist environmental stresses, such as antimicrobial agents (McNeill and Hamilton 2003, Kristich, Nguyen et al. 2008, Guiton, Hung et al. 2009, Frank, Guiton et al. 2013, Sillanpaa, Chang et al. 2013, Goh, Yong et al. 2017).

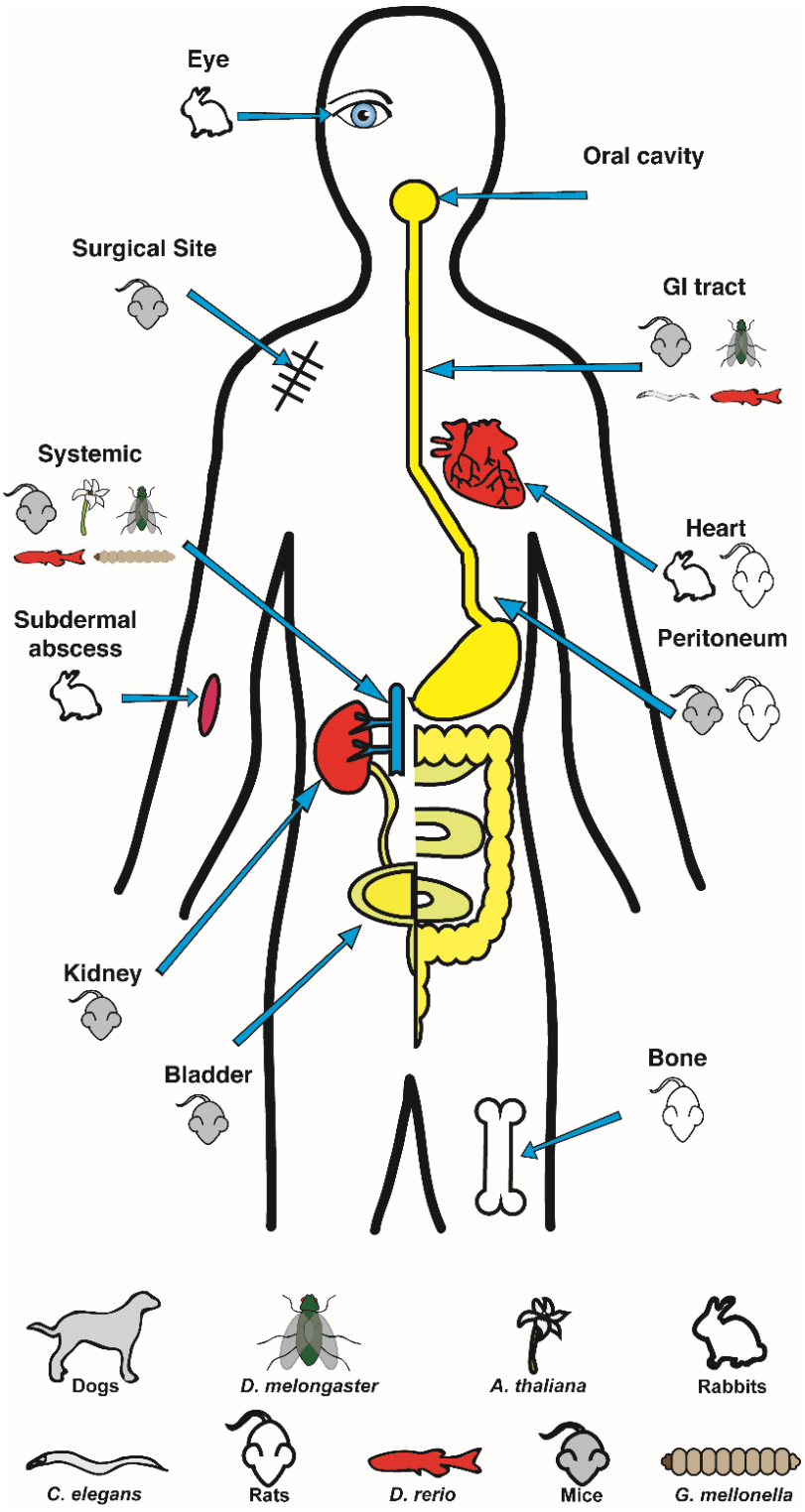

Figure 2.1 | *In vivo* systems for modeling and studying *E. faecalis* and *E. faecium* virulence. A cartoon depiction of the different host model systems that have been used to study niche-specific Enterococcal diseases (Figure was adapted with permission from Goh, Yong *et al*, 2017).

2.1 *Enterococcus faecalis* Endocarditis and biofilm-associated pili (Ebp)

One of the best studied biofilm-associated virulence factors present in *E. faecalis* is the **E**ndocarditis and **B**iofilm-associated **P**ilus (Ebp) as shown in the scanning electron micrograph (Schlievert, Gahr et al. 1998, Shankar, Lockatell et al. 2001, Nallapareddy, Singh et al. 2006, Kemp, Singh et al. 2007) (**Fig 2.2**). The Ebp pilus represents one of the most important virulence determinants for bacterial infection of a mammalian host (Kemp, Singh et al. 2007, Guiton, Hung et al. 2010, Nallapareddy, Sillanpaa et al. 2011, Sillanpaa, Chang et al. 2013).

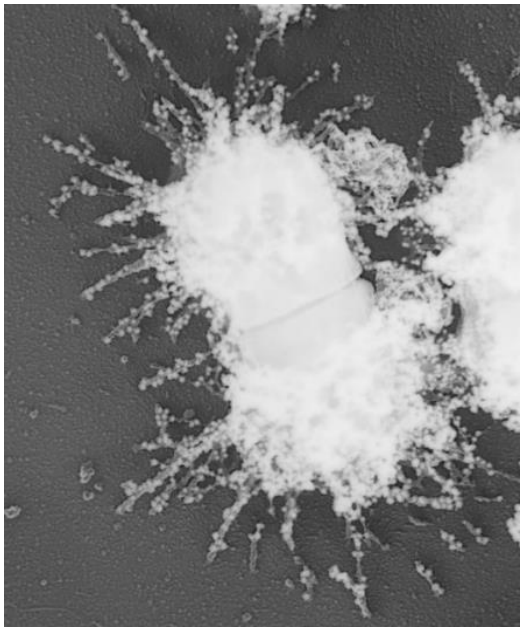

Figure 2.2 | A scanning electron micrograph (SEM) of Ebp pili on the cell surface of *E. faecalis*. Pili were immunolabeled with α-EbpC immune serum (Photo was taken by Hailyn Nielsen, Robyn Roth, and John Heuser, Washington University in St. Louis).

The Ebp pili of *E. faecalis* are typical of most Gram-positive pili in that they are assembled by dedicated machinery involving conserved enzymes known as sortases (Kemp, Singh et al. 2007). There are two main sortases in *E. faecalis*, sortase A (SrtA) and sortase C (SrtC) (Kemp, Singh et al. 2007, Nielsen, Flores-Mireles et al. 2013, Sillanpaa, Chang et al. 2013). SrtA is a housekeeping enzyme that recognizes the sortase recognition motif (Leu-Pro-Xaa-Thr-Gly or LPXTG-like motif) at the carboxyl terminus (C-terminus) of most cell wall surface anchor proteins conserved in *E. faecalis* (Schneewind and Missiakas 2014). With reference from the *E. faecalis* genome papers and literature available in the NCBI database, we compiled a list of sortase substrates identified in strain OG1RF (Bourgogne, Garsin et al. 2008). To identify homologous substrates in V583, we used BLASTp to search the V583 genome (NCBI accession: NC_004668.1) with OG1RF sortase substrates (**Table 2.1**). OG1RF is derived from an oral isolate (OG1), while V583 is derived from a vancomycin-resistant clinical isolate. The genomic sequences of both strains were available, and they are commonly used for molecular manipulation and virulence studies. It is worth noting that the list of substrates in **Table 2.1** does not include predicted sortase substrates found in V583 but not OG1RF. SrtC, on the other hand, is a pilin-specific sortase that polymerizes the Ebp pili by a transpeptidation reaction, prior to their attachment to the cell wall by SrtA (Ton-That and Schneewind 2003, Kemp, Singh et al. 2007, Nielsen, Flores-Mireles et al. 2013).

Table 2.1 | Sortase substrates found in V583 and OG1RF.

V583	OG1RF	Coverage/ identity (%) [#]	Annotation (LPXTG-motif)
EF0062	OG1RF_10056	100/ 98	5-nucleotidase family protein (LPKTG)
EF0089	OG1RF_10084	100/ 99	Conserved collagen binding domain (LPKTN)
EF0093	OG1RF_10088	10/ 98	Cell wall surface anchor family protein (FPKTG)
EF0750	OG1RF_10485	98/ 99	Cell wall surface anchor family protein (LPKTG)
EF0775	OG1RF_10508	94/ 95	Putative von Willebrand factor type A domain (LPMTN)
EF1033	OG1RF_10766	100/ 91	6-aminohexanoate-cyclic-dimer hydrolase (LPKAG)
EF1091	OG1RF_10869	100/ 99	Von Willebrand factor type A domain protein, EbpA (LPETG)
EF1092	OG1RF_10870	100/ 99	Cell wall surface anchor family protein, EbpB (LPKTN)
EF1093	OG1RF_10871	100/ 99	Cell wall surface anchor family protein, EbpC (LPSTG)
EF1099	OG1RF_10878	100/ 98	Collagen adhesin protein, ACE (LPKTG)
EF1269	OG1RF_11037	100/ 98	Cell wall surface anchor family protein (LPKTG)
EF1824	OG1RF_11531	100/ 99	Glycosyl hydrolase, family 31/fibronectin type III domain protein (LPKAN)
EF1896	OG1RF_10785	57/ 63	Cell wall surface anchor family protein (LDQTK)
	OG1RF_10786	42/ 59	Cell wall surface anchor family protein (FPNTG)
EF2224	OG1RF_11764	100/ 97	Cell wall surface anchor family protein (LPKTG)
EF2347	OG1RF_10785	57/ 63	Cell wall surface anchor family protein (LDQTK)
	OG1RF_10786	42/ 60	Cell wall surface anchor family protein (FPNTG)
EF2465	OG1RF_11897	100/ 100	Hypothetical protein (VISTG)

V583	OG1RF	Coverage/ identity (%) [#]	Annotation (LPXTG-motif)
EF2505	OG1RF_11924	100/ 93	Cell wall surface anchor family protein (YPKTG)
EF2968	OG1RF_12251	100/ 98	Cell wall surface anchor family protein (LPSTG)
EF2986	OG1RF_12268	100/ 100	ABC transporter, ATP-binding protein (LPDKG)
EF3023	OG1RF_12303	100/ 99	Polysaccharide lyase, family 8 (LPSTG)
EF3076	OG1RF_12346	100/ 95	Cell wall surface anchor family protein (LPRTG)
EF3187	OG1RF_12054	100/ 99	Cell wall surface anchor family protein (LPRTG)
EF3253	OG1RF_12506	100/ 97	Cell wall surface anchor family protein (LPRTG)
EF3314	OG1RF_12558	100/ 99	Cell wall surface anchor family protein (LPSTG)

[#]Coverage/ identity between *E. faecalis* V583 and OG1RF. Both V583 and OG1RF are the commonly used *E. faecalis* reference strains.

2.1.1 Characteristics of Ebp pili

Ebp pili are encoded by an operon that is made up of three structural pilin genes, *ebpA*, *ebpB* and *ebpC*, and an adjacent downstream gene, *srtC* (**Fig 2.3**). Studies have demonstrated that the three *ebp* genes, together with the gene encoding the sortase enzyme, *srtC,* produce a single polycistronic transcript and that transcription of *srtC* is regulated by a second promoter (Sillanpaa, Chang et al. 2013). Each pilus subunit contains a cell wall sorting signal (CWSS) at the C-terminus comprised of a LPXTG-like motif, a hydrophobic transmembrane domain, and a positively charged C-terminal tail (Nallapareddy, Singh et al. 2006, Nielsen, Flores-Mireles et al. 2013, Sillanpaa, Chang et al. 2013).

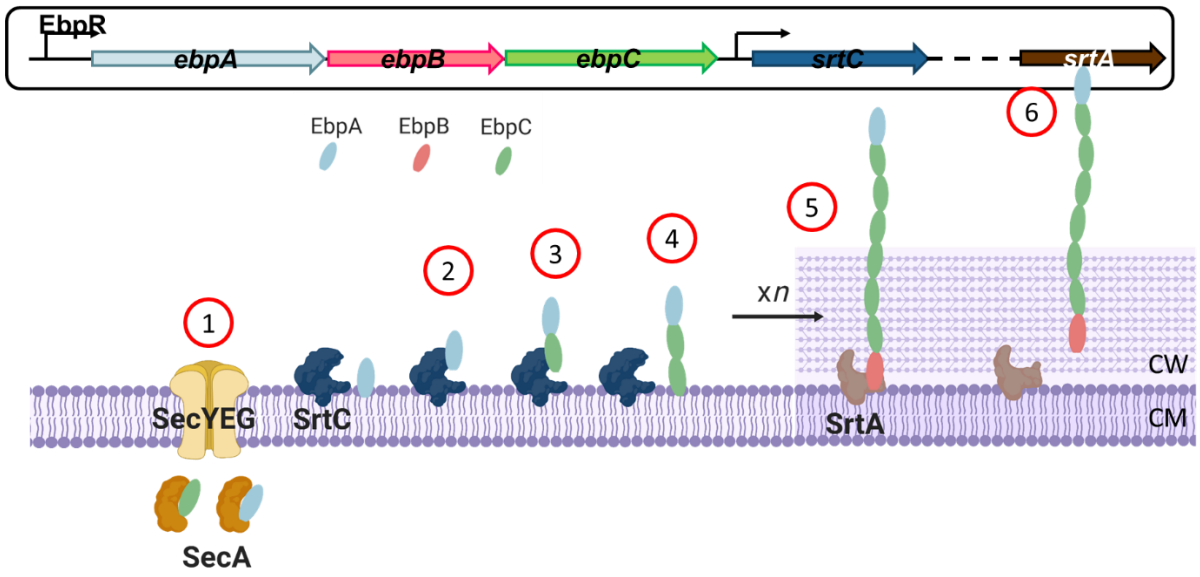

Figure 2.3 | Mechanism of sortase-mediated polymerized pili anchoring to the cell wall. The *ebp* operon consists of the three *ebp* genes, *ebpA* (blue), *ebpB* (pink) and *ebpC* (green), and *srtC* (blue) produced a single polycistronic transcript and *srtC* transcription is additionally regulated by a second promoter. *srtA* (brown) is encoded elsewhere in the chromosome. Pilus biogenesis proceeds from Step 1 through 6. Polymerized pili are anchored onto the cell wall by SrtA. Refer to **2.1.2** for a detailed description of sortase-mediated transpeptidation.

The first pilin gene of the *ebpABC* operon is *ebpA* (blue) (**Fig 2.3**). It encodes the EbpA pilin subunit which forms the tip of the pilus (Nallapareddy, Singh et al. 2006). The EbpA tip pilin subunit functions as an adhesin that mediates bacterial attachment to host fibrinogen (Flores-Mireles, Pinkner et al. 2014). Efficient attachment of pili to fibrinogen occurs via the metal ion-dependent adhesion site (MIDAS) motif present in EbpA's von Willebrand factor A (VWA) domain (Nielsen, Guiton et al. 2012) found near the N-terminus of the subunit. EbpA also binds to collagen as well as human platelets (Nallapareddy, Sillanpaa et al. 2011).

The EbpB pilin subunit is encoded by the second gene of the *ebpABC* operon, *ebpB* (pink), and forms the base of the fully polymerized pilus prior to covalent attachment of the pilus onto the cell wall by SrtA, which is encoded by *srtA* (brown). Out of the 3 Ebp pilin subunits, EbpB has a minor effect on pilus polymerization but affects cell-wall anchoring as an *ebpB* mutant showed an increased amount of pilus polymer released into the culture medium relative to the WT strain (Sillanpaa, Chang et al. 2013). EbpB is thought to be the only SrtA substrate among the three pilin subunits because only EbpB monomers migrate to a higher molecular weight (50 kDa) in the Δ*srtC*Δ*srtA* mutant background due to loss of SrtA to perform posttranslational cleavage of EbpB CWSS (Nielsen, Flores-Mireles et al. 2013). Thus, once pilus polymerization is complete, SrtA cleaves EbpB subunits to achieve cell wall anchoring (Nallapareddy, Singh et al. 2006, Nielsen, Flores-Mireles et al. 2013).

The last gene of the *ebpABC* operon, *ebpC* (green), encodes the EbpC pilin subunit, which is the major subunit that forms the shaft of the pilus. EbpC can polymerize into longer pilus polymers in the absence of EbpA and EbpB subunits. However, this long

polymer is unable to be anchored onto the cell wall in the absence of the 2 minor subunits, especially EbpB due to the reason mentioned above, and is therefore secreted into the culture supernatant (Sillanpaa, Chang et al. 2013).

The pilin monomers are translocated across the membrane through the general Sec secretion machinery prior to polymerization by SrtC (blue) and subsequent attachment by SrtA to the growing cell wall at the septum of the cell (Ton-That and Schneewind 2003, Schneewind and Missiakas 2014). In *E. faecalis*, both SrtC and SrtA are focally localized at the division septum together with the Sec secretion machinery (Kline, Kau et al. 2009, Kandaswamy, Liew et al. 2013) (**Fig 2.4**) to ensure efficient processing, attachment, and subsequent distribution of mature pili around the cell.

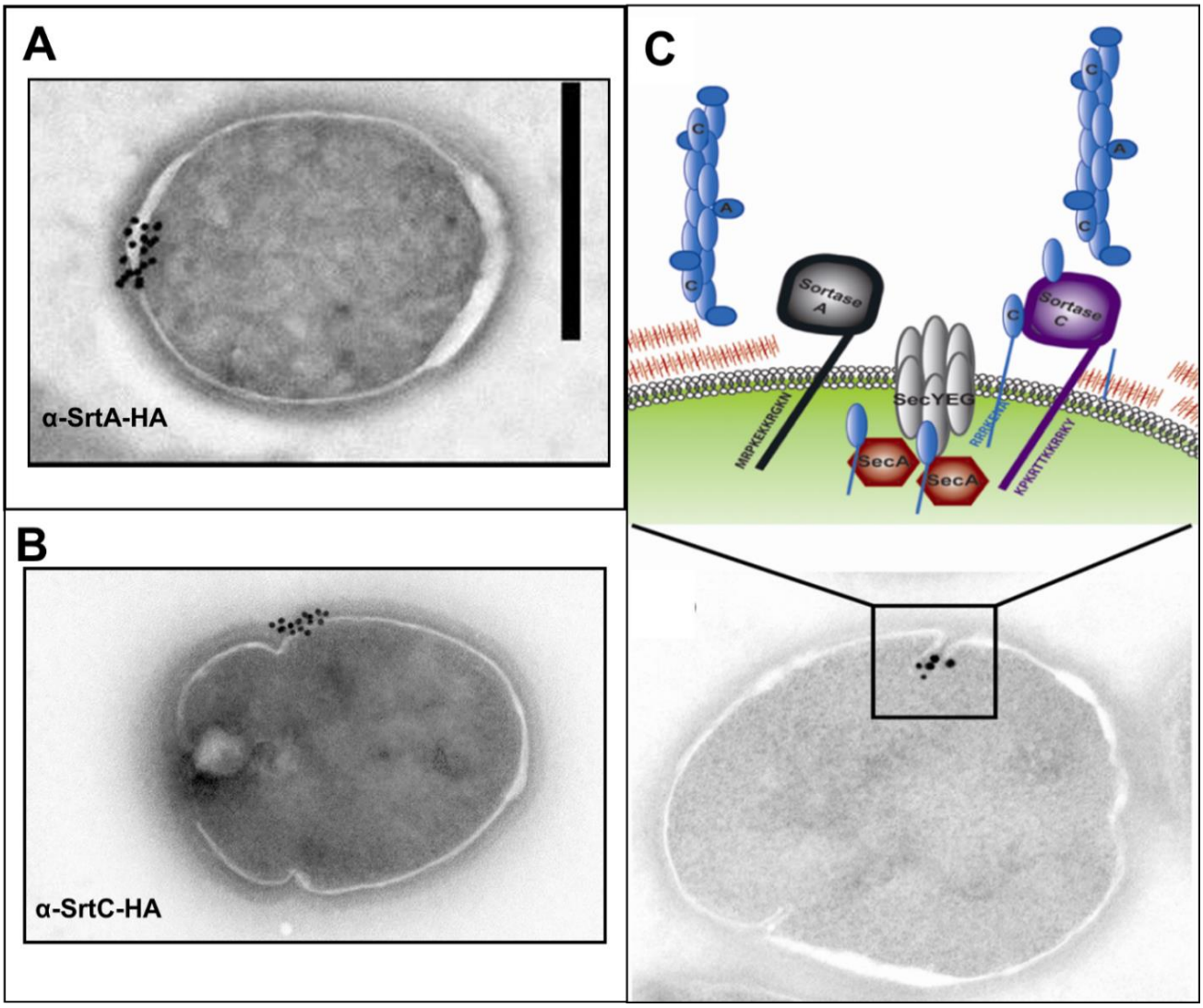

Figure 2.4 | Co-localization of Sortase enzymes and the Sec secretion machinery focally at the *E. faecalis* division septum. (**A**) Immunoelectron microscopy of Δ*srtA* complemented with *srtA-HA* expressed under its native promoter using the anti-HA immune serum. SrtA-HA is focally localized to a single domain on the cell membrane (**B**) Immunoelectron microscopy of Δ*srtC* complemented with p*srtC-HA* using the anti-HA immune serum. SrtC-HA is focally localized to a single domain on the cell membrane. (**C**) SecA (large beads) and SrtA (small beads) are co-localized at the septum of the cell (Figure was obtained and modified with permission from Kline *et al*, 2009 and Kandaswamy *et al,* 2013).

2.1.2 Sortase-catalysed transpeptidation

After translocation of pilin proteins across the membrane via the Sec secretion machinery, the tip pilin EbpA (blue) initiates polymerization and is the first subunit processed by SrtC (green), (**Fig 2.3 step 1**) that cleaves the subunit between the threonine and glycine residues in the LPXTG-motif prior to sequential incorporation of pilin subunits into a growing fiber (**Fig 2.3 step 2**). It has been proposed in *Streptococcus suis* and *Actinomyces oris* that tip pilins are required for efficient initiation of the sortase-mediated polymerization process (Okura, Osaki et al. 2011, Wu, Mishra et al. 2011). The EbpA pilin subunit is processed by SrtC, creating an enzyme-pilin intermediate consisting of a sortase-substrate thioacyl intermediate. This thioacyl intermediate is resolved upon nucleophilic attack by an acceptor molecule, in the EbpC (orange) pilin subunit (**Fig 2.3 step 3**) at the pilin-like motif. The Lys 186 residue of the pilin-like motif (ELAVVHIYPK [conserved residues are underlined]) in the EbpC monomer participates in the formation of inter-pilin isopeptide bonds (Nallapareddy, Singh et al. 2006, Nielsen, Flores-Mireles et al. 2013). This process goes on for *n* number of times, with the growing pilus embedded in the membrane throughout this process (**Fig 2.3 step 4**). Pilus polymerization will end once the base pilin subunit, EbpB (pink), gets attached to the pilus. Once the pili are fully assembled, SrtA (brown) accepts the cross-bridge peptide of the lipid II cell wall precursor as a nucleophile, leading to covalent attachment of polymerized pili onto the cell wall (**Fig 2.4 step 5 and 6**). In WT cells, pili become attached to the cell wall and are distributed around the perimeter of the cell as the cell wall grows. However, in the absence of the SrtA enzyme, pili are not attached to the cell wall but are instead retained focally on the cell membrane (Kline, Kau et al. 2009). It is not known what happens to these surface

proteins that are stuck on the membrane and how *E. faecalis* deals with these forms of membrane stress.

2.1.3 Regulation of Ebp expression

2.1.3.1 Endocarditis and biofilm-associated pilus regulator (EbpR)

ebpABC expression is positively regulated by a transcriptional regulator located upstream of the *ebpABC* operon, encoded by *ebpR*. In an *ebpR* null mutant, a 100-fold reduction in pilin gene expression was observed as compared to the isogenic WT strain (Bourgogne, Singh et al. 2007). Even though *ebpABC* is primarily regulated by EbpR, there is still a basal expression of *ebpABC* in the *ebpR* mutant. Typically, in the WT strain, even in the presence of functional EbpR, pilus fibers are present on 5-20% of the total cell population during exponential phase (Bourgogne, Singh et al. 2007). However, when the WT strain is further complemented with *ebpR* overexpression on the plasmid, the number of cells expressing pili increased to 70%, as compared to the introduction of the same plasmid into Δ*ebpR*, where only 17% of the total cell population expressed pili (Bourgogne, Singh et al. 2007). Another gene, *rnjB*, encoding a putative RNase J2, was discovered through a whole-cell ELISA-based screening of a Tn insertion mutant library to identify gene products that regulate the expression of the *ebpABC* operon and that also affect biofilm formation (Gao, Pinkston et al. 2010, Dale, Nilson et al. 2017). In the most recent study, the *ahrC* gene that codes for a predicted ArgR transcription factor, together with another ArgR transcription factor, *argR2* activates *ebpR* expression, indirectly affecting *ebp* transcription (Manias and Dunny 2018).

2.1.3.2 Environmental factors

Apart from transcriptional regulators, many environmental factors have been identified that can also increase pilus production. The presence of 5% sodium bicarbonate

(CO_2/$NaHCO_3$) in the media increases the percentage of the cell population expressing pili from 53% when grown in aerobic conditions to 87% in CO_2HCO_3 (anaerobic) in the early stationary growth phase (Bourgogne, Thomson et al. 2010). EbpR shares homology to the AtxA/Mga transcriptional regulator family where regulators respond to CO_2/ HCO_3 (Caparon, Geist et al. 1992, Dai and Koehler 1997) and since bicarbonate is a major compound found in the mammalian body, it was plausible that *ebpR* expression could be induced in the presence of bicarbonate (Bourgogne, Thomson et al. 2010). However, other transcriptional changes in the same experiment suggested the involvement of other components, such as the *fsr* quorum-sensing mechanism, a putative glycine betaine/L-proline ABC transporter, and permease protein that shares homology with a bicarbonate transporter described in *Bacillus anthracis*, and the Ers regulon (Bourgogne, Thomson et al. 2010). Expression of *ebp* was also induced by serum and culture medium (tryptic soy broth supplemented with 0.25% glucose (TSBG) vs brain heart infusion (BHI) broth) (Nallapareddy, Sillanpaa et al. 2011).

2.1.3.3 The *fsr* quorum-sensing system

The *fsr* locus of *E. faecalis* encodes a two-component system (TCS) that is a weak repressor of the *ebpABC* operon, by negatively regulating *ebpR* transcription (Bourgogne, Hilsenbeck et al. 2006). The locus is comprised of four genes – *fsrA, fsrB*, *fsrC*, *fsrD* – which are also essential for direct induction of g*elE* and *sprE* and EF1097 (**Fig 2.5**) (Teixeira, Varahan et al. 2013). The *fsrA* gene encodes the FsrA protein, whose transcription is under the control of a weak constitutive promoter and is phosphorylated by FsrC sensor histidine kinase (Qin, Singh et al. 2001, Pinkston, Gao et al. 2011). FsrA is the response regulator of the *fsr* quorum-sensing system where phosphorylated FsrA

binds to LytTR-binding sites in the upstream region of EF1097, *fsrB* and *gelE* (Del Papa and Perego 2011). *fsrB* encodes the FsrB protein, which is a transmembrane protein responsible for processing pro-peptide FsrD (encoded by *fsrD*) to generate gelatinase biosynthesis-activating pheromone (GBAP) (**Fig 2.5**). *fsrC* codes for FsrC protein, a sensor kinase that senses accumulated GBAP in the extracellular milieu and activates FsrA and subsequent downstream expression of 75 other virulence factor genes, some of which are involved in cell-cell communication (Nakayama, Cao et al. 2001). Both *fsrB* and *fsrC* are regulated by a common promoter located upstream of *fsrB* (Bourgogne, Hilsenbeck et al. 2006). The involvement of the *fsr* system as a weak repressor of *ebp* expression is independent of bicarbonate-mediated regulation (Bourgogne, Thomson et al. 2010).

The *gelE* and *sprE*, encoding the metalloproteinase gelatinase (GelE) and serine protease (SprE), respectively, are regulated by a common promoter located at the upstream region of *gelE* (**Fig. 2.5**) (Mylonakis, Engelbert et al. 2002, Hancock and Perego 2004, Bourgogne, Hilsenbeck et al. 2006, Nakayama, Chen et al. 2006, Pinkston, Gao et al. 2011). The absence of these two major proteases resulted in CAUTI attenuation and defective biofilm formation (Xu et al., 2017). The absence of *fsrA, fsrB,* or *fsrC* can affect also subsequent gene expression of *gelE* and *sprE* (Qin, Singh et al. 2000). EF1097, also known as *entV,* encodes enterocin O16, an antimicrobial peptide that is effective against three lactobacilli species but ineffective against enterococci, lactococci, *listeria,* and staphylococci species (Dundar, Brede et al. 2015). The *fsr* quorum-sensing system also mediates autolysin-dependent DNA release during enterococcal biofilm formation (Thomas, Thurlow et al. 2008) and regulates expression of a well-described virulence

factor, EfaA, an antigen involved in infective endocarditis (Lowe, Lambert et al. 1995). The *fsr* quorum-sensing system has been widely studied for its role in virulence in different disease models, and mutants are attenuated in rat endocarditis, mouse peritonitis, *Caenorhabditis elegans*, and *Arabidopsis thaliana* infection models (Goh, Yong et al. 2017).

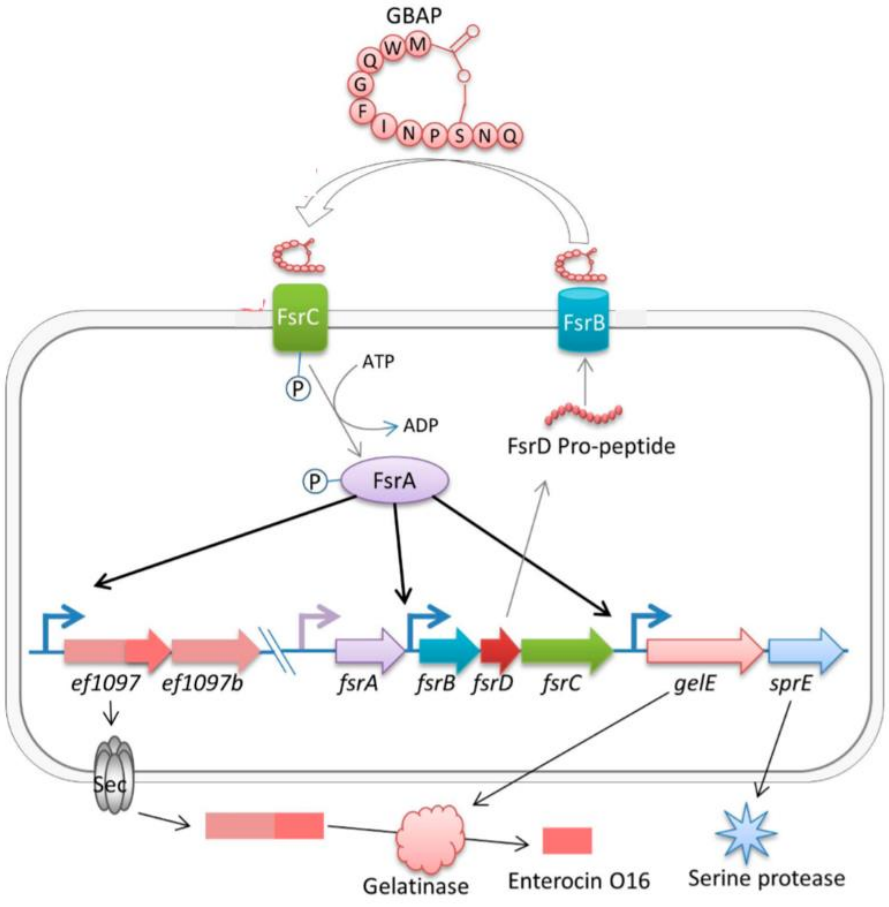

Figure 2.5 | The *fsr* quorum-sensing system and its regulation in *E. faecalis*.

FsrA auto-regulates its own gene, *fsrA*, as well as *fsrB* (co-transcribed with *fsrD* and *fsrC*) and *gelE* (co-transcribed with *sprE*). *fsrB* encodes a transmembrane protein responsible for processing FsrD pro-peptide to generate gelatinase biosynthesis-activating pheromone (GBAP). Accumulated quorum-sensing molecule GBAP in the extracellular environment is sensed by FsrC sensor kinase, leading to activation of the FsrA-FsrC TCS. (Figure adapted with permission from Ali.*et al*, 2017)

2.2 Two-component signal transduction pathways

Apart from alternative sigma factors, bacteria commonly use two-component signaling pathways to sense and respond to environmental stimuli (Capra and Laub 2012). For example, *E. faecalis* activates the *fsrABCD* system to control gene expression of pili and proteases in response to environmental changes at different stages of infection. The two-component systems (TCSs) can be found in all domains of life (Capra & Laub, 2012; Schaller, Shiu, & Armitage, 2011) and apart from their roles in virulence, they are also involved in numerous cellular processes including housekeeping functions, chemotaxis, sporulation, and response to environmental stresses (Chakraborty & Kenney, 2018; Djoric & Kristich, 2017; Kellogg, Little, Hoff, & Kristich, 2017; Kenney, 2018). A typical TCS consists of a membrane-anchored sensor histidine kinase (HK) that detects certain environmental signals and a cognate response regulator (RR) that mediates adaptive responses. Genes encoding cognate HK and RR are often co-transcribed as a single transcript. The TCS becomes activated in response to specific signals that bind to the HK via an N-terminal membrane-bound extracellular sensing domain or act via cytoplasmic stimulation (Ghosh et al., 2017; Wang, Morgan, Godakumbura, Kenney, & Anand, 2012).

Upon signal detection, the HK dimerizes and autophosphorylates at a conserved histidine residue located in the cytoplasmic portion of the HK protein. The HK transduces the signal by catalyzing the transfer of this phosphoryl group to a conserved aspartate residue within the receiver (REC) domain on its cognate cytoplasmic RR. This phosphorylation induces conformational changes of the regulatory protein leading to RR dimerization and activation, usually resulting in action as a transcription factor, resulting

in a change in downstream gene expression (Wang et al., 2012). However, there is also recent accumulating evidence that many RR can function non-canonically, either without a kinase or without the requirement for phosphorylation (Chakraborty, Winardhi, Morgan, Yan, & Kenney, 2017) (Liu & Hulett, 1997) (Boucher, Murakami, Ishihama, & Stibitz, 1997) (Desai et al., 2016), although phosphorylation can increase the binding affinity of the RR to DNA (Kenney, 2002).

In a prototypical HK, the cytoplasmic domain is made up of a less-conserved dimerization and histidine phosphotransfer (DHp) domain and a well-conserved C-terminal catalytic and ATP-binding (CA) domain. In addition to their kinase activity, most HKs are bifunctional and act as a phosphatase towards their cognate phosphorylated RR when they are not stimulated to autophosphorylate (Capra & Laub, 2012). For example, see *E. faecalis* CroS below in section **2.2.2**.

2.2.1 TCS in *E. faecalis* OG1RF

The search for TCSs in *E. faecalis* was first performed in V583, with a total of 17 TCSs and one orphan regulator identified (Hancock and Perego 2002). Using BLASTp to search the OG1RF genome with V583 TCSs, and a cut-off of > 95% identity with V583 genes, we identified candidates for TCSs in OG1RF. Moreover, using Prokaryotic 2-Component Systems (P2CS) (Barakat, Ortet et al. 2009), we identified an additional two TCS in OG1RF that do not exhibit more than 95% similarity with any TCS found in V583. As shown in **Table 2.2 and 2.3**, a total of 15 TCS and two orphan response regulators were identified in OG1RF. The HKs found in OG1RF were expected to be homo-dimeric proteins, consisting of one histidine kinase (HisKA) domain that is involved in dimerization and phosphorelay, and a HATPase domain at the C-terminus. The HKs varied in the

number of transmembrane domains (TM), with some having only one TM (i.e. OG1RF_12536, OG1RF_10966) and others having as many as five TMs (i.e. OG1RF_12463). Some HKs have one or more intracellular sensing domain, such as a cytoplasmic linker region (HAMP), predicted to be involved in regulating trans-autophosphorylation by transmitting a conformational change from the external ligand-binding domain to the cytoplasmic signaling kinase domain (Gushchin et al., 2017) Another intracellular sensing domain, the PAS domain, is predicted to serve as an input sensor component of light, oxygen, redox potential, and small ligands (Taylor and Zhulin 1999). The most widespread family of homo-dimeric RR among bacteria are RRs belonging to the OmpR family (Martinez-Hackert and Stock 1997). Each RR in the OmpR family is made up of a highly conserved N-terminal receiver (REC) domain and a less conserved C-terminal domain. The REC domain comprises three highly conserved motifs- DD-box, D-box, and K-box. The C-terminal domain contains a winged helix-turn-helix predicted structure that binds to DNA of the downstream effector genes (Le Breton, Boel et al. 2003).

Table 2.2 | Histidine kinases identified in the *E. faecalis* OG1RF genome aligned against V583.
(With hits that are >95% similarity to the entire length of the indicated HK protein)

Group[a]	V583 Locus[b]	OG1RF locus[c]	Alignment in OG1RF[d]	TM/ HK input domain features[e]	Size (bp)	Length (amino acids)	Coordinates in OG1RF[f]	Annotation (V583)	Annotation (OG1RF)	Similarity to V583[g]
I	EF2219	OG1RF_11759	QSQINP**H**FLYNTLEYI	3 / HAMP	1713	576	1842174	YesM	Hypothetical protein	99%
	EF3197	OG1RF_12463	QAQVNP**H**FFFNAINTI	5 /	1770	589	2600192	LytS	LytS	100%
II	EF2912	OG1RF_12212	RLAREL**H**DSVSQQLFA	2 /	1434	367	2332788	YvqE, VraS		100%
IIIA	EF1704	OG1RF_11415	DFVSNVS**H**ELKTPVTS	2 / PAS	1776	591	1473805	PhoR	PhoR	99%
	EF3290	OG1RF_12536	ELITNVS**H**DIRTPLTSI	1 / HAMP	1182	393	2694245		CroS*	99%
	EF3290	OG1RF_12162[a]	DLIVYLA**H**DLKTPLT	2 /	1113	370	2282219		CisS*	31%
	EF1261	OG1RF_11030	QFMADAS**H**EMRTPLT	3 / HAMP	1470	489	1074471	YclK	YclK	99%
	EF1194	OG1RF_10966	EFVSNVS**H**ELRTPLTS	1 / HAMP, PAS	1830	609	1007895	VicK	VicK/WalK	99%
	EF0927	OG1RF_10654	YIDSWV**H**EIKVPLAAI	2 /	1026	341	689550		YxdK	99%
	EF1051	OG1RF_10784	QFVEDVS**H**ELRTPVAI	1 / HAMP	1509	502	818271	LisK	CsrS	100%
	EF0373	OG1RF_10260	LIANIS**H**DLKTPITSII	3 /	1482	493	270494			99%
IV	EF1209	OG1RF_10981	SALQSQS**H**EFMNKMH	2 / PAS	1551	516	1021352			100%
	EF1820	OG1RF_11527	EELAMFR**H**DYKNLLYS	4 /	1344	447	1590621	FsrC	FsrC	99%
	EF1820	OG1RF_12377[a]	EIRKFR**H**DYKNILNSL	6 /	1329	442	2515119	FsrC		19%
	EF1632	OG1RF_11346	AIREIH**H**RVKNNLQSV	0 /	1434	477	1409730			99%

*Indicates manual curation.
[a] Grouping is based on the homology of the kinase region surrounding the phosphorylatable histidine (Fabret, Feher, & Hoch, 1999; Mizuno, 1997).
[b] Listed are the locus numbers for V583 according to The Institute for Genomic Research [TIGR] as of 01 Jan 2016.
[c] Listed are the locus numbers for OG1RF according to The Institute for Genomic Research [TIGR] as of 01 Jan 2016.
[d] Shown is the region surrounding the histidine involved in phosphor-transfer (**boldface**).
[e] Some HK contains additional features - PAS (input sensor component PAS domain) and HAMP (cytoplasmic HAMP linker domain).
[f] Listed as coordinates as of 30 Jun 2018.
[g] Percentages refer to the similarity of HK proteins in OG1RF that span across the entire length of the HK protein in V583.

Table 2.3 | Response regulators identified in the *E. faecalis* OG1RF genome aligned against V583.
(With hits that are >95% similarity to the entire length of the indicated RR proteins)

Group[a]	V583 Locus[b]	OG1RF Locus[c]	Family	Gene order[d]	Size (bp)	Length (amino acids)	Coordinates in OG1RF[e]	Annotation (V583)	Annotation (OG1RF) *	Similarity to V583[f]
I	EF2218	OG1RF_11758	YesN	HK-RR	1482	493	1838969	YesN	YesN	99%
	EF3196	OG1RF_12462	LytTR	HK-RR	729	242	2598442	LytR	LytR	100%
II	EF2911	OG1RF_12211	NarL	HK-RR	633	210	2331078	YvqC; VraR		100%
IIIA	EF1703	OG1RF_11414	OmpR	RR-HK	711	236	1471323	PhoP	PhoP	100%
	EF3289	OG1RF_12535	OmpR	RR-HK	690	229	2692385	BacR	CroR*	100%
	EF3289	OG1RF_12163[a]	OmpR	HK-RR	705	234	2283324	BacR	CisR*	48%
	EF1260	OG1RF_11029	OmpR	RR-HK	720	239	1072283	YclJ	YclJ	100%
	EF1193	OG1RF_10965	OmpR	RR-HK	705	234	1005355	YycF		100%
	EF0926	OG1RF_10653	OmpR	RR-HK	675	224	687837			99%
	EF1050	OG1RF_10783	OmpR	RR-HK	687	228	816066	LisR		100%
	EF0372	OG1RF_10259	OmpR	RR-HK	693	230	268324	SrrA		100%
	EF3329	**OG1RF_12574**	**OmpR**	**Orphan**	**723**	**240**	**2735717**			**100%**
IV	EF1210	OG1RF_10982	Unclassified	HK-RR	693	230	1021333	YufM; DcuR	DcuR	98%
	EF1822	OG1RF_11529	LytTR	HK-P-RR	744	247	1591435	FsrA	FsrA	99%
	EF1822	OG1RF_12376[a]	LytTR	RR-HK	747	248	2514398	FsrA		30%
	EF1633	OG1RF_11347	Amir_NasR	HK-RR	582	193	1411164	CitB	CitB	99%
	EF1714	OG1RF_11425[a]	Unclassified	**Orphan**	939	312	1484612	pyrD-2	pyrDB	99%

*Indicates manual curation. Orphan regulators are in **boldface**.
[a] Grouping is based on the homology of the corresponding kinase region surrounding the phosphorylatable histidine (Fabret et al., 1999; Mizuno, 1997).
[b] Listed are the locus numbers for V583 according to The Institute for Genomic Research [TIGR] as of 01 Jan 2016.
[c] Listed are the locus numbers for OG1RF according to The Institute for Genomic Research [TIGR] as of 01 Jan 2016.
[d] HK, histidine kinase; RR, response regulator; HK-P-RR, histidine kinase-peptide-response regulator.
[e] Listed as coordinates as of 30 Jun 2018.
[f] Percentages refer to the similarity of RR proteins in OG1RF that span across the entire length of the RR protein in V583.

2.2.2 TCS involved in antibiotic resistance and cell wall stress

E. faecalis produces a low-affinity penicillin-binding protein (PBP5) which is essential for intrinsic resistance to the broad-spectrum cephalosporin class of β-lactam antibiotics, such as ceftriaxone, which is often used to treat *E. faecalis* infections (Hollenbeck and Rice 2012). Previous investigations identified the key determinant to intrinsic cephalosporin antibiotic resistance in *E. faecalis* as the CroR-CroS TCS, encoded by *croRS*. *croRS* is a bicistronic operon that is co-transcribed from the *croR* promoter. The operon is flanked by a gene encoding a 16S ribosomal RNA protein upstream and a gene encoding a serine-tRNA ligase protein downstream (**Fig 2.6A**), both of whose gene expression are not targets of CroRS regulation (Comenge, Quintiliani et al. 2003).

The CroR REC domain contains a conserved aspartic acid residue important for phosphorelay between CroS and a DNA-binding domain (DBD) (**Fig 2.6B**). CroS is a classical HK consisting of two transmembrane domains (TM), a DHp domain, and a CA domain. CroS is bifunctional and can facilitate de-phosphorylation of CroR through the action of a conserved threonine (T176) in the DHp domain, located near the histidine residue involved in kinase activity (Kellogg and Kristich 2016).

Deletion of *croRS* leads to a 4000-fold reduction in MIC against ceftriaxone (Comenge, Quintiliani et al. 2003, Kellogg, Little et al. 2017). However, a *croRS* null mutant still expresses PBP5 and complementation with PBP5 on a plasmid does not restore resistance to ceftriaxone, suggesting that CroRS controls other factors related to cell wall-mediated stress responses that have yet-to-be identified (Depardieu, Podglajen et al. 2007). Phosphorylated CroR is necessary to drive resistance against a range of

antibiotics targeting the cell wall, suggesting its involvement in the regulation of cell wall synthesis.

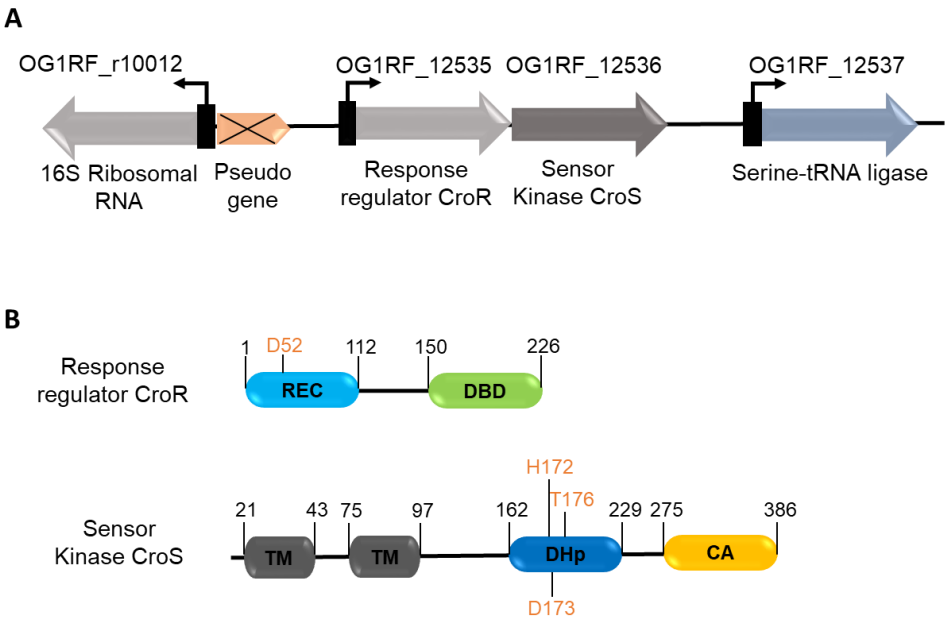

Figure 2.6 | Genomic organization and domain architecture of *croRS* locus in *E. faecalis* OG1RF. (A) Schematic presentation of the *croRS* locus in *E. faecalis* OG1RF. **(B)** Schematic presentation of the domain architecture of CroRS. The residues involved in phosphor-transfer (orange) in CroR and CroS are identified based on (Kellogg and Kristich 2016). Abbreviations: REC, response domain; DBD, DNA-binding domain; TM, transmembrane; DHp, dimerization and histidine phosphotransfer domain; CA, catalytic and ATP-binding domain.

Using alanine site-directed mutagenesis of residues important for phosphorelay in both CroR and CroS, Kellogg and Kristich demonstrated that phosphorylated CroR drives resistance to cephalosporin antibiotics and CroS performs dual functions as a phosphatase and a kinase to regulate CroR phosphorylation (Kellogg and Kristich 2016). In the same study, they also discovered that CroR activity can also be phosphorylated by a non-cognate HK, OG1RF_12162, which was annotated as CisS for **C**roRS-**i**nteracting **s**ystem **s**ensor kinase, in the absence of CroS phosphatase activity. The absence of both TCSs can decrease *E. faecalis* resistance to ceftriaxone, vancomycin, and bacitracin

(Kellogg and Kristich 2016). In another study, cell envelope damage caused by H_2O_2 activates the CroR-CroS TCS, triggering adaptive responses to promote cell envelope repair, which can also elevate resistance to cephalosporins (Djoric and Kristich 2015). Using a protein fragment complementation assay, CroR and the HPr protein of the phosphotransferase system (PTS) are responsible for carbohydrate uptake and catabolite control of gene expression, that can also drive antibiotic resistance in *E. faecalis* (Snyder, Kellogg et al. 2014). In *E*. *faecalis* strain JH2-2, a mutant harboring *croRS* deletions exhibits growth and cell morphology defects (Le Breton, Boel et al. 2003), emphasizing its importance in maintaining cell wall integrity.

Some genes that are directly regulated by CroR have been identified: *salB*, a gene encoding a secreted protein; *glnQ*, a predicted glutamine transport system of the *glnQHMP* operon; and *croR* itself (Muller, Le Breton et al. 2006, Le Breton, Muller et al. 2007). Using a 'domain-swapping' method, Muller, Massier *et al*. created a hybrid RR comprised of the REC domain of a RR from a well-characterized TCS, NisRK, with CroR DBD (Muller, Massier et al. 2018). The method avoids unnecessary cross-talk that may influence the end results because it will only be stimulated to respond to nisin levels. This enabled the identification of potential CroR-regulated genes (Muller, Massier et al. 2018). Using this domain-swapped hybrid RR, the group conducted global gene expression analysis using RNA sequencing and identified 50 genes that are potential CroR targets involved in cell envelope regulation, transport, signaling, stress response, and antibiotic resistance. However, only 11 genes among the 50 CroR targets were selected for **E**lectro**M**obility **S**hift **A**ssay (EMSA) to validate interaction between CroR with promoters of identified CroR targets (Muller, Massier et al. 2018). Seven genes were demonstrated

to have direct interaction with CroR via EMSA. The remaining four genes, namely, the bicistronic operon *metC-cysK*, *pbp5,* and *ace* do not result in DNA retardation on EMSA, reflecting an indirect effect of CroR on the transcription of these genes.

2.3 High-temperature requirement A (HtrA) serine protease

There is increasing evidence that bacterial proteases play an important role in virulence (Boehm, Lind et al. 2015). These proteases can respond to infection in two ways. First, they can be part of the protein quality control machinery that is required for repairing misfolded proteins. Second, there is growing evidence that supports a conserved role of proteases in specific and controlled proteolysis of regulatory proteins in response to environmental stimuli (Day and Hinds 2002, Ingmer and Brondsted 2009, Clausen, Kaiser et al. 2011). Proteolysis plays an important role in post-translational regulation of gene expression (Biswas and Biswas, 2005). Proteolysis includes processing and maturation of various surface associated proteins (Gottesman et al., 1997). How *E. faecalis* monitors protein quality control, including protein processing and maturation during colonization and infection has not been explored.

High-**T**emperature **R**equirement **A** (HtrA) represents an important class of heat-shock-induced serine proteases. HtrA is an ATP-independent serine protease, highly conserved across all kingdoms of life (Page and Di Cera 2008). With the exception of *Mycoplasma genitalium* and *Methanococcus janaschii*, based on BLAST searches, gene encoding HtrA are present in all sequenced prokaryotic and eukaryotic species, including plants and humans (Clausen, Kaiser, Huber, & Ehrmann, 2011; Kim & Kim, 2005; Lu, Yamaoka, & Graham, 2005; Wessler, Schneider, & Backert, 2017). HtrA primarily

functions as a protease involved in quality control, degrading un- or misfolded proteins during stress conditions. In addition, HtrA can function as a chaperone in protein assembly and targeting to the cell surface or extracellular sites in a variety of bacteria including *Escherichia coli*, *Campylobacter jejuni*, *Staphylococcus aureus, Lactococcus lactis*, *Lactobacillus helveticus*, *Streptococcus mutans*, *Streptococcus pyogenes,* and *Streptococcus pneumoniae* (Smeds, Varmanen et al. 1998, Poquet, Saint et al. 2000, Kang, Lee et al. 2010, Baek, Vegge et al. 2011, Kochan and Dawid 2013, Ge, Wang et al. 2014, Heimesaat, Alutis et al. 2014). A typical HtrA protein is made up of a trypsin protease domain with conserved predicted catalytic residues and at least one PDZ domain. The PDZ domain is named after three eukaryotic proteins (**P**ost-synaptic density protein, **D**isc large, and **Z**o-1 proteins), which is a common structure found in signaling proteins in most eukaryotes and prokaryotes (Fanning and Anderson 1996, Ponting 1997) and permits intermolecular protein-protein interactions. Unlike the classic eukaryotic PDZ, PDZ domains in HtrA are thought to harbor several additional structural features that are important for protein oligomerization and cellular localization of HtrA (Clausen, Kaiser et al. 2011). The PDZ domain in HtrA serves as a regulatory element that recognizes and binds to specific hydrophobic amino acid sequences within the C-termini of substrates or regulatory peptides. This binding induces a conformation change in HtrA, from a disordered structure into an ordered conformation of active HtrA protease (Zurawa-Janicka et al., 2017).

HtrA and many proteases, in general, do not attack their substrate randomly. Instead, they display a high degree of specificity for processing substrates, which depends on a variety of factors. One of the factors includes the co-localization of

proteases and substrates in the same cellular compartment (Ehrmann and Clausen 2004). Proper localization of HtrA is necessary for normal processing in *E. coli*, where they are predominately localized within the periplasmic space. By contrast, since Gram-positive bacteria do not have a canonical periplasmic space in the Gram-negative sense, most HtrA in Gram-positive bacteria have a transmembrane domain at the N-terminus and are anchored in the cytoplasmic membrane with the bulk of the C-terminus on the extracellular side of the cell. In *S. pyogenes*, septal focal co-localization of membrane-associated HtrA and the Sec secretion machinery, along with Trigger factor that functions as a ribosome-associated chaperone, and the peptidyl-prolyl cis-trans isomerase (PPIase) are required for proper maturation of nascent streptococcal pyrogenic exotoxin B (SpeB) at the septum (Lyon and Caparon 2003, Rosch and Caparon 2004, Rosch and Caparon 2005). The absence of Trigger factor results in the failure to direct SpeB to the Sec machinery for secretion and maturation (Lyon and Caparon 2003, Lyon and Caparon 2004, Rosch and Caparon 2004, Cole, Aquilina et al. 2007) (**Fig 2.7A**). By contrast, a study by Tsui *et al* showed that instead of a single site of SecA and HtrA focal localization at the septum in *S. pneumoniae*, localization of the Sec machinery and HtrA is cell-cycle dependent and forms many distinct foci on the surface of this organism (**Fig 2.7B**) (Tsui, Keen et al. 2011).

Therefore, two different patterns of localization of HtrA have been described in Gram-positive bacteria. In **Chapter 3** of this thesis, we asked what is the localization pattern of HtrA in *E. faecalis*?

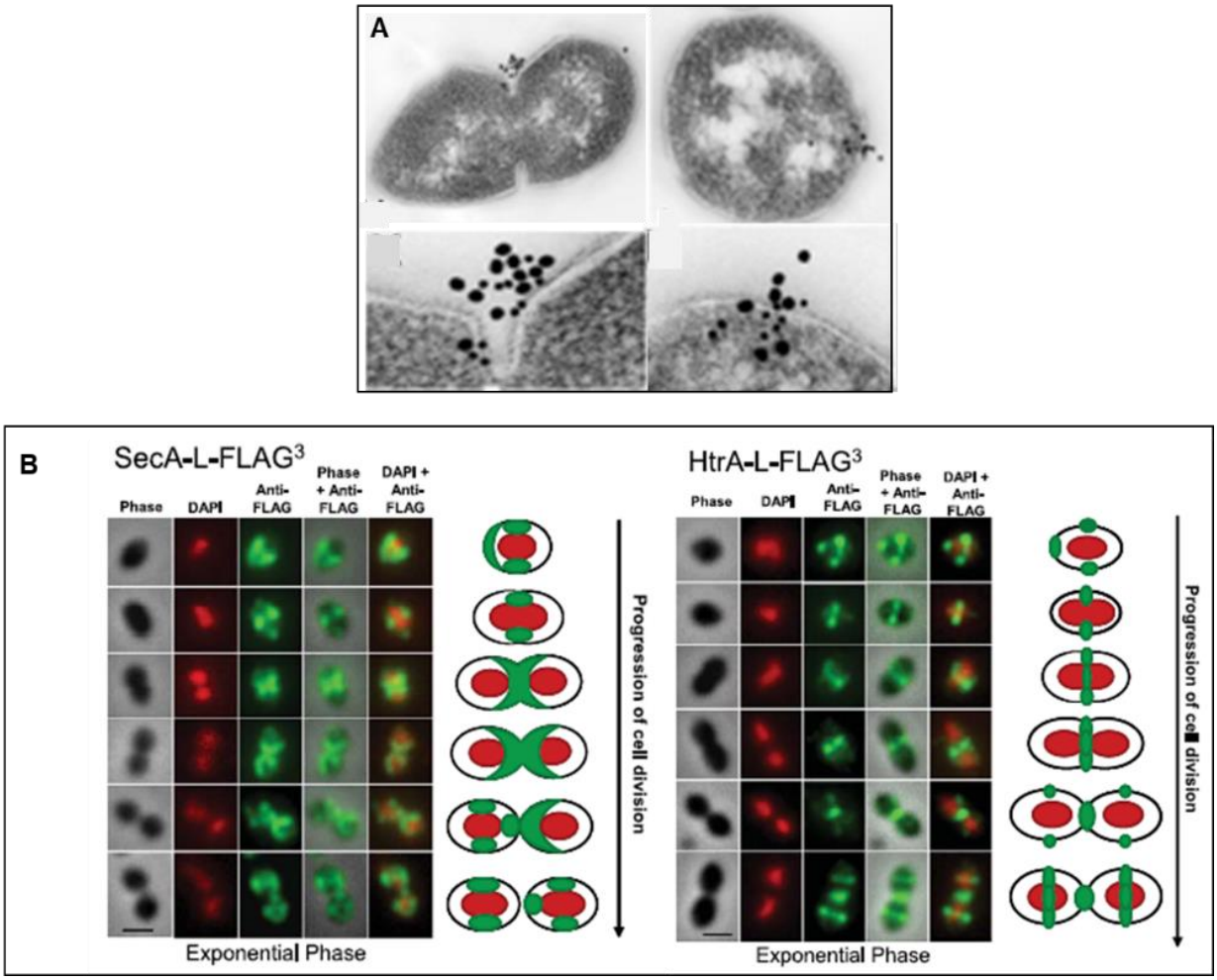

Figure 2.7 | Localization of HtrA in *S. pyogenes* and *S. pneumoniae*. (**A**) Focal localization of SpeB and HtrA on the cytoplasmic membrane of *S. pyogenes*. Double labeling with antisera against HtrA (12 nm bead) and SpeB (18 nm bead), viewed via immunogold electron microscopy (Figure adapted with permission from Rosch and Caparon, 2005). (**B**) Dynamic distribution of SecA and HtrA in *S. pneumoniae* during the exponential phase of the cell cycle. (Figure adapted with permission from Tsui *et al*., 2011).

2.3.1 Role of HtrA in other Gram-positive bacteria

Three homologs of HtrA have been identified in *B. subtilis.* Of these, two of the HtrA homologs, HtrA and HtrB, are the main components responsible for post-translocational protein folding (Sarvas, Harwood et al. 2004). HtrA and HtrB are encoded by *htrA* and *htrB*, respectively, and their transcription is dependent on the CssR-CssS

TCS, which is activated in response to heat and secretion stress (Hyyrylainen, Bolhuis et al. 2001, Darmon, Noone et al. 2002). Among all the 34 potential histidine kinases present in *B. subtilis*, CssS is the only histidine kinase in *B. subtilis* that shows sequence similarity to CpxA of the *E. coli* Cpx TCS system (46% identical residues in a stretch of 228 residues) (Hyyrylainen, Bolhuis et al. 2001), while response regulator, CssR, shows sequence similarity to CpxR of the *E*. *coli* Cpx TCS (35% identical residues in a stretch of 230 residues). Transcription of genes encoding both the CssR-CssS and CpxA-CpxR TCS is autoregulated and these two TCSs control transcription of the gene encoding HtrA (Darmon, Noone et al. 2002).

In *S*. *aureus*, two homologs of HtrA, *htrA*$_{1,}$ and *htrA*$_{2}$, are involved in proper folding and maturation of virulence factors that are positively regulated by the quorum-sensing AgrC/A TCS (Rigoulay, Entenza et al. 2005). *S. aureus* requires both HtrA$_1$ and HtrA$_2$ for thermal stress survival (Rigoulay, Entenza et al. 2005). The functions of HtrA vary across two genetically different virulent *S*. *aureus* strains. In virulent strain RN6390, the absence of *htrA*$_{1}$ resulted in increased sensitivity to stress induced by puromycin. However, in the virulent strain CLO, both *htrA*$_{1}$, and *htrA*$_{2}$ are required for thermal stress survival but not puromycin-induced stress. In addition, expression of secreted proteins was significantly reduced in both *S*. *aureus* strains only in the absence of both HtrAs (Rigoulay, Entenza et al. 2005), indicating overlapping functions between the two HtrA homologs.

S. *mutans* is commensal of the human oral cavity and is also the principal pathogen responsible for dental caries (McNeill and Hamilton 2003). *S*. *mutans* can sustain growth in the oral cavity with the help of HtrA to tolerate growth in low pH (McNeill and Hamilton 2003, Kang, Lee et al. 2010). HtrA is important for the biogenesis of cell wall-associated

glycolytic enzymes important for biofilm formation (Biswas and Biswas 2005). A *S. mutans htrA* null mutant is less tolerant to low and high temperature, low pH, oxidative stress, and DNA damaging agents (Ahn, Lemos et al. 2005, Biswas and Biswas 2005, Banerjee and Biswas 2008), and is attenuated for biofilm formation in the oral cavity (Kang, Lee et al. 2010).

In another Streptococcus species, *S. pneumoniae*, the *htrA* expression is regulated by the CiaR-CiaH TCS, which is involved in β-lactam resistance (Mascher, Heintz et al. 2006). In the *ciaRH* mutants, HtrA is the main mediator of attenuated virulence in the mouse lung and the infant rat nasopharynx, as well as incompetence inhibition (Sebert, Palmer et al. 2002). In another study, HtrA limits activation of the *blp* locus that was responsible for regulation and secretion of pneumocins and their associated immunity proteins in *S. pneumoniae* (Kochan and Dawid 2013).

2.3.2 Role of Deg proteases in *E. coli*

E. coli express three Deg proteases - DegP, DegS, and DegQ. DegP is the first HtrA protease discovered (Swamy, Chung et al. 1983), and has been best characterized in *E. coli*. The DegP monomer is composed of a serine protease domain and two PDZ domains. DegP proteases form hexamers in the resting state, and forms higher 12-, 15-, 18-, and 24-oligomeric structures upon activation. DegP performs dual functions as a protease and a chaperone (Krojer, Sawa et al. 2008). As a protease, misfolded proteins that accumulate in the periplasm are recognized by DegP via its PDZ-1 domain, which presents the misfolded substrate to its proteolytic domain for degradation (Clausen, Kaiser et al. 2011). DegP also functions as a chaperone by encapsulating folded outer membrane proteins (OMPs) and protecting them from degradation when they pass

through the periplasm (Spiess, Beil et al. 1999). The *degP* expression can be regulated by both the Cpx TCS system and the RNA polymerase sigma E (σ^E) factor (RpoE) pathway that sense extra-cytoplasmic stresses (Isaac, Pinkner et al. 2005). Details of each system will be further described in **Sections 2.3.2.1** and **2.3.2.2**.

The second *E. coli* HtrA, DegS, is a regulatory protease that is made up of a conserved serine protease domain and only one PDZ (Wilken, Kitzing et al. 2004, Kim and Kim 2005). DegS exists as a trimer during its resting state and is membrane-anchored (Wilken, Kitzing et al. 2004, Clausen, Kaiser et al. 2011). DegS switches to an active conformation only upon binding of misfolded, or mislocalized OMPs to the PDZ domain (Walsh, Alba et al. 2003). This process triggers the DegS-mediated cleavage of RseA of the σ^E pathway. Details of this DegS-mediated pathway is further described in **Section 2.3.2.2**.

The third HtrA protease, DegQ, is homologous to DegP, and is comprised of one serine protease domain and two PDZ domains. Like DegP, DegQ harbors similar substrate specificities and cleaves misfolded protein substrates (Kolmar, Waller et al. 1996). In addition, overproduction of DegQ can recover the temperature-sensitive growth defect in an *E. coli* Δ*degP* strain (Waller and Sauer 1996). A cryo-electron microscopic structure of *E. coli* DegQ predicts DegQ will change its oligomeric state from a resting hexameric form to 12- and 24-mers depending on the concentration of unfolded substrates (Malet, Canellas et al. 2012). This substrate-induced oligomer reassembly depends on the first PDZ domain (Sawa, Malet et al. 2011). DegQ is the first response to pH-mediated misfolded proteins (Sawa, Malet et al. 2011), while DegP will only be

activated when levels of misfolded proteins cannot be rapidly cleared by DegQ alone (Danese, Snyder et al. 1995, Sawa, Malet et al. 2011).

2.3.2.1 DegP and the Cpx system

In the Cpx system of *E coli*, the CpxP adaptor protein engages the CpxA sensor kinase to keep the Cpx response in its 'off' state in the absence of a stress stimulus. The presence of misfolded proteins, such as misfolded PapE pilin subunits that form the tip of the P-pilus, titrate away the CpxP adaptor protein from CpxA. The CpxP adaptor protein escorts misfolded PapE pilin subunits to the DegP protease to be degraded (Isaac, Pinkner, Hultgren, & Silhavy, 2005). Unbound CpxA leads to activation of the Cpx response regulator (CpxR), which upregulates expression of genes coding for proteins involved in trafficking and periplasmic folding, such as the CpxP adaptor protein and DegP protease. When misfolded protein damage is cleared, the CpxP adaptor protein accumulates in the periplasm and returns the system to an 'off' state by binding to CpxA (**Fig 2.8A**) (Raivio, Popkin, & Silhavy, 1999; Tschauner, Hornschemeyer, Muller, & Hunke, 2014). DegP is one of the Cpx-regulated genes directly involved in protein folding (chaperone function), or protein degradation (protease function) in the bacterial envelope of *E. coli* (Ruiz and Silhavy 2005, Price and Raivio 2009).

2.3.2.2 DegP, DegS, and the Sigma E pathway

The activity of RpoE is modulated by RseA, encoded by *rseA* which lies downstream of the *rpoE* gene (Schurr, Yu et al. 1996). At baseline, RpoE is kept in an inactive conformation by the anti-sigma factor RseA, an inner membrane protein consisting of an N-terminal cytoplasmic domain and a large coiled-coil periplasmic domain (**Fig 2.8B**). RpoE is activated in response to a signal generated by the presence

of misfolded OMPs in the periplasm (Missiakas and Raina 1997). Upon sensing misfolded protein stress, the carboxyl end of the misfolded proteins binds to DegS at the PDZ domain, triggering its activation. Activated DegS cleaves the anti-sigma factor RseA, which subsequently gets processed by RseP, ClpXP, and Lon proteases. This process releases sigma factor RpoE from the membrane, allowing activation of downstream effector genes. Once the misfolded proteins are removed from the periplasm, DegS no longer gets activated to process RseA and un-cleaved RseA binds to RpoE, returning the system to the basal condition.

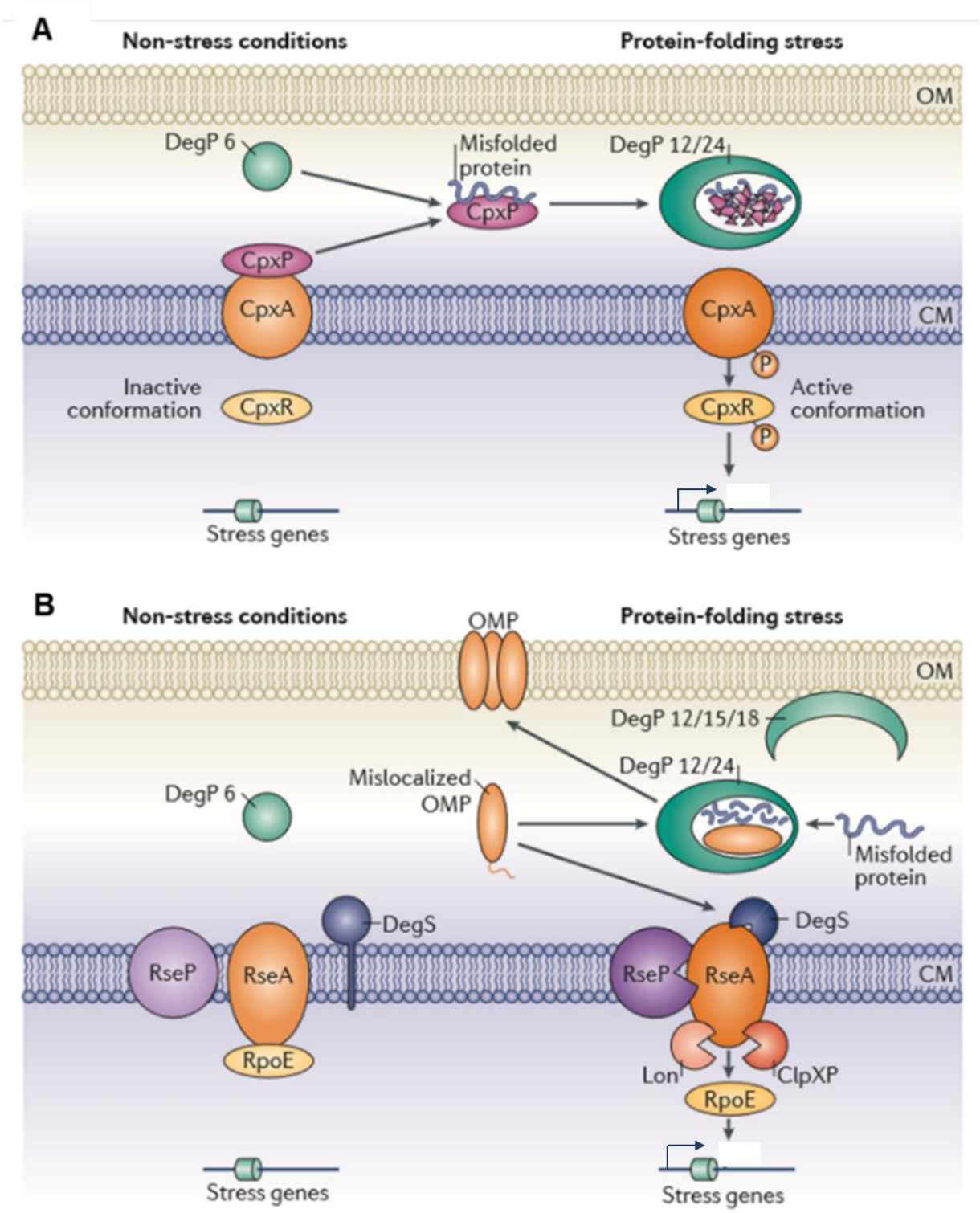

Figure 2.8 | RpoE and Cpx pathways regulate transcription of *degP* (*htrA*) expression in *E. coli*. (**A**) The Cpx system. During non-stress conditions (left), The CpxP adaptor protein binds to CpxA to keep CpxA in an inactive conformation. DegP is present in the periplasm as a hexamer. In the presence of misfolded proteins (right), such as misfolded PapE pilin subunits of the P pili, CpxP binds to the misfolded proteins and forms

a substrate-CpxP complex that is targeted by the DegP active oligomeric form (DegP 12/24) for degradation. Autophosphorylation of CpxA phosphorylates CpxR (CpxR~P) in response to envelope stress and CpxR~P is free to activate expression of stress genes. (**B**) The RNA polymerase sigma E (σ^E) factor pathway. During non-stress conditions, RseA acts as an anti-sigma factor to keep sigma factor RpoE in an inactive conformation. DegP, DegS, and RseP are also present in their inactive state. C-termini of mislocalized OMPs bind to the PDZ domain of DegS, triggering its activation. Activated DegS cleaves RseA, which is subsequently processed by RseP and the cytoplasmic proteases ClpXP and Lon, releasing the sigma factor RpoE to activate expression of downstream genes involved in stress response. The C-termini of mislocalized proteins also triggers DegP into its active oligomeric form (DegP 12/24) to activate the proteolysis pathway via DegP (Figure adapted with permission from Clausen *et al*, 2011).

2.3.3 HtrA in virulence and in anti-bacterial therapy

Bacterial HtrAs have been implicated in the establishment and the progression of several infectious diseases. Upon inactivation or deletion of HtrA, most bacteria display attenuated virulence, with the exception of *Neisseria gonorrhoeae* where the presence of HtrA is not critical for virulence (Hoy, Geppert et al. 2012). Similarly, in *Pseudomonas aeruginosa*, the presence of *algW* (*htrA* homolog) is not critical for acute sepsis and bacteremia (Boucher, Martinez-Salazar et al. 1996, Hoy, Geppert et al. 2012). A summary of the various roles of HtrA in disease models is shown in **Table 2.4**.

In addition to their role as membrane-anchored proteases, some HtrAs function as secreted proteases released into the extracellular environment, and others are released indirectly by membrane vesicles to target host cell factors. For *C*. *jejuni* and *H*. *pylori*, the route of infection is usually through the GI tract. Both *C*. *jejuni* and *H*. *pylori* must withstand the low pH in the gut and adhere strongly to epithelial cells prior to the subsequent invasion of the host cell. HtrA can be both secreted and/or released by membrane vesicles in these gut pathogens. Extracellular HtrA can disrupt the epithelial barrier by E-cadherin proteolysis, leading to paracellular bacterial transmigration (Hoy, Lower et al.

2010, Boehm, Lind et al. 2015). Some pathogenic bacteria, such as *K*. *pneumoniae* and *Salmonella typhimurium*, can infect hosts via the bloodstream. These bacteria secrete HtrA to resist oxidative and low pH environments encountered during phagocytosis by macrophages and neutrophils (Baumler, Kusters et al. 1994, Cortes, de Astorza et al. 2002, Lewis, Skovierova et al. 2009), although the specific host substrate in these systems is not yet known. Among all the studied HtrAs, *H. pylori* are the only species in which HtrA cannot be deleted, indicating its essentiality in the organism (Salama, Shepherd et al. 2004, Tegtmeyer, Moodley et al. 2016).

Given the conservation of HtrA, its expression in most bacteria, and its critical intracellular and extracellular functions in bacteria, HtrA has been considered an alternative target for future anti-bacterial therapy. Studies of *S*. *typhimurium* HtrA have proven that, despite being highly attenuated in virulence in mice, Δ*htrA* of *S*. *typhimurium* make an excellent live vaccine that protects mice against subsequent infections by WT *Salmonella* (Humphreys, Stevenson et al. 1999). In addition, with the availability of high-resolution structural models of HtrA from various pathogens available in the database, computational structure-based protein inhibitors can be designed and synthesized.

One successful example of HtrA inhibitor synthesized was against *Chlamydia trachomatis. C. trachomatis* is a human pathogen that causes sexually-transmitted infections and can lead to severe outcomes such as infertility, pelvic inflammation, and ectopic pregnancy if left untreated (Patton, Askienazy-Elbhar et al. 1994, Burton and Mabey 2009, Rekart, Gilbert et al. 2013). *C*. *trachomatis* HtrA (CtHtrA) exhibits multifunctional roles in *C*. *trachomatis* stress responses, the replication life cycle, virulence, and OMPs assembly (Huston, Theodoropoulos et al. 2008, Wyrick 2010, Wu,

Lei et al. 2011, Marsh, Wee et al. 2015). Protease inhibitor JO146 targets CtHtrA by irreversibly inhibiting the protease activity of CtHtrA, and JO146 treatment was lethal to *C*. *trachomatis* when added during the replicative stage of development (Gloeckl, Ong et al. 2013, Lawrence, Fraser et al. 2016). Despite the highly conserved HtrA protein sequences across all domains of life, JO146 is specific to *C*. *trachomatis* since JO146 was significantly less active towards *E. coli* DegP and human HTRA1, indicating that HtrA inhibitor specificity can be genus or even species-specific.

Table 2.4 | HtrA contributions to virulence in various disease models.			
Organism*	***In vivo* model**	***In vitro* model**	**References**
Bacillus anthracis Vollum	Δ*htrA* confers protection on guinea pigs against WT anthrax challenge.	Δ*htrA e*xhibits delayed proliferation in a macrophage infection assay.	(Chitlaru, Zaide et al. 2011)
Borrelia burgdorferi		HtrA is a B-cell antigen that elicits a robust antibody response.	(Coleman, Crowley et al. 2013)
Brucella abortus *Brucella melitensis*	*htrA cycL* double deletion exhibit attenuated infection in cattle Δ*htrA* exhibit attenuated virulence in goat.	Δ*htrA* exhibits less resistant to killing by cultured murine neutrophil and macrophages *in vitro.* Δ*htrA* is more sensitive to oxidative killing by cultured neutrophils.	(Elzer, Hagius et al. 1996, Elzer, Phillips et al. 1996, Phillips, Elzer et al. 1997, Phillips and Roop 2001, Dorneles, Sriranganathan et al. 2015)
Burkholderia cenocepacia	HtrA is required for survival in a rat model of chronic lung infection.		(Flannagan, Aubert et al. 2007)
Campylobacter jejuni	Δ*htrA* exhibit attenuated virulence in *Galleria mellonella* larvae.	Δ*htrA* exhibits attenuated E-cadherin cleavage, cell adherence, paracellular transmigration, and basolateral invasion.	(Champion, Karlyshev et al. 2010, Hoy, Geppert et al. 2012)
*Chlamydia trachomatis**		HtrA required for persistence infection in the human epithelial cell line (HEp-2) 44 hpi.	(Huston, Theodoropoulos et al. 2008)
Clostridium difficile	Δ*htrA* exhibit enhanced virulence in Golden Syrian hamster model.	Decreased adherence of Δ*htrA* to Caco-2 cells.	(Bakker, Buckley et al. 2014)
Escherichia coli	Δ*degP* exhibits attenuated virulence in UTI model. UPEC CFT073Δ*degS* exhibits attenuated virulence in mouse peritoneal and UTI.		(Redford, Roesch et al. 2003, Redford and Welch 2006)
Haemophilus parasuis	Δ*htrA* exhibits attenuated virulence intraperitoneal infection in mice.		(Zhang, Li et al. 2016)

Table 2.4 (*Continued*.)			
*Helicobacter pylori**	HtrA is essential to *H. pylori* as the *htrA* null mutant is lethal.	Secreted HtrA (HpHtrA) cleaves E-cadherin and fibronectin.	(Hoy, Lower et al. 2010, Tegtmeyer, Moodley et al. 2016)
Klebsiella pnuemoniae	Δ*htrA* exhibits attenuated virulence in intraperitoneal infection in mice.	Δ*htrA* is more sensitive to phagocytosis.	(Cortes, de Astorza et al. 2002)
Legionella pneumophila	Δ*htrA* exhibits attenuated virulence mice intratracheal infection.	Δ*htrA* cannot replicate within macrophages and epithelial cells.	(Pedersen, Radulic et al. 2001)
Listeria monocytogenes	Δ*htrA* exhibits attenuated virulence in mouse intravenous infection.		(Wilson, Brown et al. 2006)
*Mycobacterium tuberculosis**	Δ*htrA2* exhibits smaller lesions with fewer foam cells and survive longer in a mouse model of tuberculosis.		(Mohamedmohaideen, Palaninathan et al. 2008)
Neisseria gonorrhoeae		Δ*htrA* does not interfere with E-cadherin binding and cleavage.	(Hoy, Geppert et al. 2012)
Pseudomonas aeruginosa	Δ*algW* (*htrA* homologue) not critical for acute sepsis and bacteremia.		(Boucher, Martinez-Salazar et al. 1996)
Salmonella typhimurium	Δ*htrA* exhibits attenuated virulence in mouse intravenous or oral infection.		(Chatfield, Strahan et al. 1992)
Staphylococcus aureus	RN6390Δ$htrA_1$ and Δ$htrA_2$ exhibit attenuated virulence in the rat endocarditis model.		(Rigoulay, Entenza et al. 2005)
Streptococcus pneumoniae	Δ*htrA* exhibits attenuated virulence in the infant rat model of a nasopharyngeal model.		(Sebert, Palmer et al. 2002)
Streptococcus pyogenes	Δ*htrA* exhibits attenuated virulence in a mouse systemic infection model. Δ*htrA* was not attenuated in a murine subcutaneous infection model.		(Jones, Bolken et al. 2001, Lyon and Caparon 2004)
Shigella flexneri		Δ*htrA* exhibits smaller plaque size on Henle or Caco-2 cell monolayer.	(Purdy, Hong et al. 2002)
Yersinia enterocolitica	Δ*htrA* exhibits attenuated virulence by oral administration in mice.		(Li, Dorrell et al. 1996)

Table 2.4 (*Continued*.)			
Yersinia pestis	Δ*htrA* exhibits attenuated virulence in mouse survival assay.		(Williams, Oyston et al. 2000)
*Indicates vaccines developmental studies have been done. Red text indicates a lethal mutation.			

CHAPTER 3: CONSTRUCTION AND CHARACTERIZATION OF HIGH-TEMPERATURE REQUIREMENT A (HTRA) MUTANT IN *ENTEROCOCCUS FAECALIS*

3.1 INTRODUCTION

High-Temperature Requirement A (HtrA) is a highly conserved serine protease across all domains of life. The functions of HtrA have been widely characterized in *E. coli,* where one of the HtrAs, DegP, functions as a periplasmic protease responsible for high-temperature growth and degrades misfolded PapE pilin subunits (Danese, Snyder et al. 1995, Pallen and Wren 1997). In *S*. *pyogenes*, HtrA is important in the maturation and processing of the virulence factor, SpeB (Lyon and Caparon 2004). HtrA has also been widely characterized in *H*. *pylori* and *C*. *trachomatis* for its contribution to pathogenesis in various disease models (Huston, Theodoropoulos et al. 2008, Tegtmeyer, Moodley et al. 2016).

Even though a lot of work has been done on HtrA in other organisms, nothing is known about HtrA function(s) in *E. faecalis*. In this chapter, to characterize the function(s) of HtrA, I first generated a marker-less, in-frame deletion of *htrA* in *E*. *faecalis*. Since HtrA in other bacteria respond to various environmental stress conditions (Poquet, Saint et al. 2000, Darmon, Noone et al. 2002, Flannagan, Aubert et al. 2007, Huston, Theodoropoulos et al. 2008, Kang, Lee et al. 2010), we exposed the *E*. *faecalis* Δ*htrA* to

heat, oxidative, osmolarity, and low pH stresses. In addition, we also addressed the contribution of HtrA to *E*. *faecalis* virulence *in vivo* murine wound model.

3.2 MATERIALS AND METHODS

3.2.1 Bacterial strains and growth conditions

Bacterial strains and plasmids used in this chapter are listed in **Table 3.1**. We inoculated single *Enterococcus faecalis* from single colonies and grew it statically at 37°C in Brain Heart Infusion (BHI) (Acumedia, USA) broth or agar (1.5%, Difco, US) for all assays unless otherwise stated. We grew *Escherichia coli* in Luria Bertini (Difco, US) broth with shaking or agar at 37°C for DNA isolation and manipulation. To stimulate pilus expression in *E*. *faecalis*, we grew strains in Trypticase Soy Broth (Oxoid, UK) supplemented with 0.25% glucose (TSBG), statically at 37°C (Nallapareddy, Singh et al. 2006). We used Muller Hinton (MH) broth and 1.5% agar to perform antibiotic susceptibility assays. All inoculations were cultured for 15 to 18 h unless stated otherwise. When required, antibiotics were added at the following concentrations: for *E*. *coli*, Kanamycin (Km) 50 mg/L, Erythromycin (Em) 500 mg/L; for *E*. *faecalis* strains, Em 25 mg/L, Km 500 mg/L, Rifampicin (Rif) 25 mg/L, Streptomycin (Str) 500 mg/L. All antibiotics were purchased from Sigma-Aldrich Corporation (USA).

Table 3.1 | Bacterial Strains and Plasmids used in this study.[a]		
Strains or plasmids	Relevant characteristic(s)[b]	References or source
Strains		
Enterococcus faecalis		
OG1RF	Fus^r, Rif^r, derived from OG1	Lab stock
OG1X	Strept^r, derived from OG1	Lab stock
Δ*htrA*	OG1RF isogenic derivative of in-frame *htrA* deletion mutant	This work
Escherichia coli		
Stellar Cells	Routine cloning host when using In-fusion kit	Clontech, USA
DH5α	Routine cloning host	Lab stock
Plasmids		
pGCP123 (p*Empty*)	Expression vector, Km^r	(Paulsen, Banerjei et al. 2003)
pGCP213	Temperature sensitive allelic exchange vector, Em^r	(Paulsen, Banerjei et al. 2003)
pABG5-PhoZF	Vector for alkaline phosphatase secretion assay, Km^r	(Granok, Parsonage et al. 2000)
p*htrA*	P_{htrA} *htrA* in pGCP123	This work
p*htrA-HA*	P_{htrA} *htrA-HA* in pGCP123	This work
p*delta-htrA*	Δ*htrA* deletion allele in pGCP213	This work

Abbreviations: Fus, fusidic acid; Rif, rifampin; Km, kanamycin; Em, erythromycin; Str, streptomycin. [a]See Materials and Methods for intermediate strain and plasmid constructions. [b]Superscript "r" indicates resistance.

3.2.2 Competent cell preparation and electro-transformation of *E. coli* and *E. faecalis*

We inoculated 1 mL of an overnight *E. faecalis* culture grown in BHI into 10 mL of fresh BHI with Rif antibiotic and allowed to grow at 37°C to OD_{600} of 0.5-0.7. We harvested the bacteria by centrifugation, re-suspended the pellet in 10 mL of 10% glycerol. We added 1 mL of 25 µg/mL lysozyme in lysozyme buffer (10 mM Tris-HCl pH 8, 50 mM NaCl, 1 mM EDTA, 0.75 M sucrose) and incubated for 20 mins at 37°C. We washed the pellet four times with 10 mL of electroporation buffer (0.5 M sucrose + 10% glycerol),

resuspended in 500 μL of electroporation buffer, aliquoted 50 μL per reaction and quick freeze using ethanol-dry ice before storing at -80°C. 50 μL of cells were mixed with <300 ng of plasmid DNA harvested from *E*. *coli* and electroporated using chilled 0.1 cm cuvette (1.6-1.75 kV, 200 Ω, 25 μF) with a Bio-Rad Gene Pulser. Cells were recovered using 2 X BGYT (BHI, Glucose, Yeast extract, tryptone). After recovery at 37°C for 1 h, transformants were selected on BHI with antibiotic selective solid media. To propagate temperature-sensitive plasmid, pGCP213, we recovered electroporated *E. faecalis* cells at 30°C. Electrocompetent cells of *E*. *coli* were prepared as described previously (Tu, He et al. 2005).

3.2.3 Molecular techniques

We used the Wizard® Genomic DNA Purification Kit (Promega, USA) to isolate bacterial genomic DNA from *E*. *faecalis* and the PureLink® Quick Plasmid Miniprep Kit (Invitrogen, USA) to isolate plasmid DNA from *E*. *coli*. Genes targeted for mutation, primer design, was performed based on the annotated complete genome of *E*. *faecalis* OG1RF (NCBI accession: NC_017316.1) (Bourgogne, Garsin et al. 2008). Amplification of all gene products was performed using Phusion High-Fidelity DNA Polymerase (Thermos Scientific, USA); screening and validation of DNA sequences were performed using *Taq* DNA Polymerase (New England Biolabs, USA). T4 DNA ligase and restriction enzymes were purchased from New England Biolabs, USA. Ligations and restriction digestions were performed per respective manufacturer's protocol. Some plasmids were created by infusion cloning, where the In-fusion enzyme (Clontech, USA) fuses PCR-generated sequences containing a 15 bp overlap with linearized vectors on both ends of the insert via homologous recombination. All plasmids were sequenced for verification by standard

Sanger sequencing (AIT biotech, Singapore). All primer sequences can be found in **Table 3.2**.

3.2.4 Construction of *htrA* deletion mutant

In-frame deletion of *htrA* locus (OG1RF_12305) was created according to the previously described method (Ruiz, Wang et al. 1998). Briefly, we amplified regions approximately 450 bp upstream and downstream of the *htrA* from OG1RF using primer pair dHtrAF_PstI/RF12305_SewR for upstream region and RF12305_SewF/dHtrAR_PstI for downstream regions (**Table 3.2**). These products were sewed together and amplified using dHtrAF_PstI/dHtrAR_PstI. We cloned the 900 bp PCR amplicon into pGCP213, a temperature-sensitive Gram-positive plasmid (Nielsen, Guiton et al. 2012), at the PstI restriction site to generate deletion construct p*delta-htrA.* We transformed the deletion construct into wildtype OG1RF by electroporation and the transformants were selected at 30°C on BHI agar containing Em. Single colonies were inoculated into individual tubes of BHI broth containing Em and passaged for two days at 30°C. Chromosomal integrant of this temperature-sensitive plasmid was selected by passaging the culture at 42°C in BHI, in the presence of Em. Selection for excision of the integrated plasmid by homologous recombination was accomplished by growing the bacteria at 30°C in the absence of Em. Loss of the *htrA* locus in Em sensitive bacteria was verified by PCR using dHtrAF_PstI/dHtrAR_PstI and htrA_compF_EcoRI/dHtrAR_PstI. Loss of HtrA expression was further confirmed by immunoblotting of whole-cell lysates with HtrA antiserum.

Table 3.2 | Primers used in this study.	
Primer name	Sequence (5'→3') [a]
Complementary	
htrA_compF_EcoRI	GCTTGATACGAATTCATTCGATAGACTAAAGGAGTAG
htrA_compR_BamHI	TAGAACTAGTGGATCCTTAGAATTGCCTTTTGATGC
htrA_compR_BamHI_HA tag	AACTAGTGGATCCCTTTTACTAAGCATAATCTGGAACATCATATGGATATTGATTGCTGCGATTATTT
Deletion	
htrA_SewF	TTTATGCAACGAAAAGATGTTCGCAGCAATCAATAAAAGAAA
htrA_SewR	TTTCTTTTATTGATTGCTGCGAACATCTTTTCGTTGCATAAA
dHtrAF_PstI	AAACTGCAGATCTTGGCATAGCTATTTAAACG
dHtrAR_PstI	TCCAATGCATTGGCTGCAGAATACAGCGATTAAAGATGCG
Universal primers	
T7 Universal Promoter	TAATACGACTCACTATAGGG
T3 Universal Promoter	CAATTAACCCTCACTAAAGG
M13 (-20) F primer	GTAAAACGACGGCCAGTG
M13 (-40) R primer	CAGGAAACAGCTATGAC

[a]Restriction sites underlined. Complementary sequences to vector are in red.

3.2.5 pGPC123-*htrA* plasmid construction

We constructed *htrA* expression plasmids by amplifying the *htrA* coding sequence plus 200 bp upstream of the *htrA* start codon to include the native promoter for *htrA* with htrA_compF_EcoRI/htrAcompR_BamHI or htrAcompF_EcoRI/htrAcompR_BamHI_HA to add an HA tag at the 3' end. We digested the resultant 1.5 kb PCR product with EcoRI and BamHI and ligated into pGCP123, giving rise to p*htrA* and p*htrA-HA*. We verified the expression and stability of HtrA from the expression plasmids by immunoblot using anti-HtrA.

3.2.6 Whole genome sequencing (WGS) of WT and *htrA* deletion mutant

We used the Wizard® Genomic DNA Purification Kit (Promega, USA) to isolate bacterial genomic DNA from *E. faecalis* Wildtype OG1RF and Δ*htrA*. We measured the quality of DNA extracted using NanoDrop™ 2000/2000c Spectrophotometer (Thermos Scientific, USA) and Qubit™ dsDNA BR Assay Kit (Invitrogen, USA) prior to WGS. DNA libraries and subsequent reads mapping were performed by SCELSE sequencing facility (NTU, Singapore), where libraries were prepared using TruSeq DNA Nano Library Prep Kit (Illumina, USA) according to the manufacturer's protocol. The samples were sequenced on an Illumina MiSeq v3 platform and analyzed using CLC Genomic Workbench 8.0 software. The completed OG1RF reference genome (NCBI accession: NC_017316.1) from the NCBI database was used for mapping and annotation. Non-synonymous mutations found within the coding region were filtered out and excluded.

3.2.7 Generation of antibodies

Recombinant protein fragments were designed, expressed and purified using Protein Production Platform (NTU, Singapore) with technology and workflow of the former Biotechnology unit at the Structural Genomics Consortium at Karolinska Institute in Stockholm, Sweden (Graslund, Sagemark et al. 2008). These full length or truncated protein sequence of interest as listed in **Supplementary Table A1**. Briefly, full length or truncated DNA were amplified using a multi-construct approach and cloned in pNIC28-Bsa4 with N terminal His-Tag followed by a TEV protease cleavage site. The resultant plasmid was then transformed to BL21 (DE3) *E. coli* and recombinant protein was expressed following overnight induction with Isopropyl β-D-1thiogalactopyranoside (IPTG). Cells were lysed, and recombinant protein was purified by immobilized metal affinity chromatography (IMAC) utilizing the His-tag followed by a size exclusion

chromatography. The purity of the recombinant protein was accessed by SDS-PAGE and mass by mass spectrometry. Polyclonal antisera were generated commercially (SABio, Singapore) by immunization of hosts (**Table 3.3**) with purified recombinant proteins, except for rabbit monoclonal anti-Hemagglutinin purchase from Thermos Scientific, USA; SecA, EbpA, and EbpB immune sera were generated previously (Kline, Kau et al. 2009). Specificities of the immune sera were confirmed by a lack of signal on western blots of cell lysates from the appropriate deletion or transposon mutants. All the secondary antibodies carrying an HRP-conjugate were purchased from Thermos Scientific, USA and all the Alexa Fluor® labeled antibodies were purchased from Molecular Probe, Life Technologies, USA.

Table 3.3 | Antibodies used in this chapter.

*Antigen**	*Size (kDa)*	*Primary ab; host*	*Secondary antibody; host*
EbpA	122.7	1:3000; Rabbit	1:5000; Goat anti-rabbit HRP-conjugate
EbpB	53.4	1:3000; Rabbit	1:5000; Goat anti-rabbit HRP-conjugate
EbpC	68.2	1:3000; Guinea pig	1:5000; Goat anti-guinea pig HRP conjugate
HA		1:3000; Rabbit	1:500; Alexa Fluor® 568 labeled goat anti-guinea pig 1:5000; Goat anti-rabbit HRP-conjugate 1:500; Alexa Fluor® 488 labeled goat anti-rabbit
HtrA	45.7	1:1000; Rat	1: 5000; Goat anti-rat HRP-conjugate
SecA	97.0	1: 3000; Rabbit	1: 5000 Goat anti-rabbit HRP-conjugate
SrtA	27.1	1: 250; Mouse	1:1250; Goat anti-mouse HRP-conjugate
SrtC	32.0	1:250; Mouse	1:1250; Goat anti-mouse HRP-conjugate

*Construct sequences can be found in **Supplementary Table A1**.

3.2.8. Bacterial cell preparation for immunofluorescence staining

E. faecalis grown in TSBG to mid-log phase were washed and normalized as described above. To stain the membrane, cells were fixed with 1000 times dilution of FM4-64 dye (Thermos Fisher Scientific, Inc., USA) at a final concentration of 1 ng/µL for 30 mins on ice. The cells were fixed with fresh 3% paraformaldehyde for 10 mins and smeared on poly-L-lysine pre-coated slides (Polysciences, Inc., USA). To visualize DNA, we added DAPI stain to the fixed cells at a final concentration of 2.5 ng/µL and incubated for 15 mins at room temperature in the dark. To visualize HtrA localization on the cell membrane, we lyse cells with 10 mg/mL lysozyme for 1 h at 37°C. Cells were then blocked with filtered 2% P-BSA prior to adding 20 µL of respective primary antibody on to fixed cells and incubated overnight at 4°C, shaking. The primary antibody was paired with the respective Alexa Fluor® labeled secondary antibody and incubated at room temperature for 1 h. Finally, we mount the slide with mounting media (Vectashield®, USA) and coverslip for 30 mins before imaging or stored at 4°C in the dark prior to imaging with super-resolution structured illumination microscopy (SR-SIM) (Carl Zeiss, Germany).

3.2.9 Identification of protein localization using SR-SIM microscopy

SR-SIM images of the subcellular localization of proteins of interest were captured using LSM 780 ELYRA PS.1 system (Carl Zeiss, Germany) with a 100 x Plan-Apochromatic oil immersion objective lens (numerical aperture of 1.46). DAPI; Alexa Fluor ®488 and FM™ 4-64 Dye were excited with 405 nm HR-diode, 488 nm HR-diode and 561 nm HR-DPSS laser line respectively. The fluorescence was captured using pco. edge Scientific Complementary Metal Oxide Silicon (sCMOS) camera (pco., Germany). The

acquired images were further processed with Zen version 8 software (Carl Zeiss, Germany).

3.2.10 Growth Kinetic Assay

OG1RF WT and Δ*htrA* were grown overnight, statically in BHI or TSBG media. Starter cultures were first diluted 10-fold and grow for 1 h at 37°C. Cells were then normalized to OD_{600} of 0.003 in a final volume of 50 mL media. To test the growth kinetics of Δ*htrA* under various temperatures, we incubated each set of cultures at 30°C, 37°C, 42°C or 50°C. Cell culture was extracted hourly for measurement of OD and colony-forming unit (CFU/mL) plating on BHI plates. The plates were incubated at 37°C aerobically for 16 h.

3.2.11 Biofilm Assay

Bacteria were grown overnight, statically in 10 mL of BHI or TSBG media. Cells were then normalized to OD_{600} of 0.5-0.6. 8 µL of normalized culture were mixed with 200 µL of media in a 96-well plate (Nunc™ MicroWell™ 96-Well Microplates, Thermos Scientific™, USA). To test the effects of temperature on biofilm formation, the plates were incubated at 30°C, 37°C or 42°C statically for 24 or 48 h. to stimulate biofilm formation. Following incubation, culture media and planktonic bacteria were discarded by tipping content into a waste container. The plates were washed twice with 1 X PBS and bacteria to remove non-adherent bacteria before staining with 0.1% crystal violet for 15 mins at 4°C. The plate was then washed with PBS until negative control is clear. 200 µL of ethanol: acetone (4:1) was added per well and incubated on belly dancer for 30-60 mins with lid on to prevent evaporation. Absorbance was read at OD_{595} using the microplate

reader (Infinite M200 Pro, Tecan, Switzerland) in 96-well microplate. All biofilm assays were performed with three biological replicates, each with 12 technical replicates.

3.2.12 Environmental stress tolerance assays

For growth experiments involving stress tolerance, we prepared BHI plates containing NaCl (0.5 to 1.5 M), puromycin (0.5 to 2.0 µg/mL; Sigma-Aldrich), H_2O_2 (1.0 to 2.5 mM; Sigma-Aldrich), mitomycin C (7.5 to 15 ng/mL; Sigma Aldrich). Freshly grown overnight cultures were spun down and washed with sterile 1× PBS. Cultures were resuspended in either the same or 1/10 of the original volume in 1× PBS and measured at OD_{600} using a spectrophotometer (UVmini-1240, Shimadzu, Japan. Cells were normalized to OD_{600} of 0.5 and 10-fold serial dilutions were made. 5 µL aliquot of each dilution was spotted on the BHI agar plates containing different stressors and plates were incubated at 37°C aerobically for 48-72 h.

For growth experiments involving pH, we adjusted the initial pH of BHI agar to pH 5.5, 6.0, and 7.0 with HCl before sterilization. 50 mM citrate-phosphate buffer of the desired pH was added to media after sterilization. Cells were normalized to OD_{600} of 0.5 and 10-fold serial dilutions were made. 5 µL aliquot of each dilution was spotted on the BHI agar plates and incubated at 37°C aerobically for 48-72 h.

3.2.13 Bacterial cell fractionation

E. *faecalis* was grown to mid-log phase and an OD_{600} of 0.5, normalized to 0.6, and equivalent volumes subjected to centrifugation at 8,000 × g for 5 mins. We washed the cell pellets once in PBS and digested for 1 h. with 10 mg/mL lysozyme from chicken egg white (Sigma-Aldrich, USA) in lysozyme buffer (10 mM Tris-HCl pH8, 50 mM NaCl, 1 mM EDTA, 0.75 M Sucrose) yielding the whole cell lysate.

3.2.14 Immunoblotting

Whole cell lysates or bacterial fractions were boiled for at least 15 mins in NuPAGE® LDS Sample Buffer (4×) with dithiothreitol (DTT) and SDS-PAGE was performed with NuPAGE Novex 3 to 8% Tris-acetate gels in NuPAGE Tris-acetate SDS running buffer (Life Technologies Corp., USA) to resolve proteins >150 kDa. For smaller proteins, NuPAGE Novex 4-12% Bis-Tris gels in NuPAGE MOPS SDS running buffer were used. The iBlot® Transfer Stacks were used to transfer proteins using the iBlot® Gel Transfer Device (Life technologies Corp. USA). We blocked the membrane with 3% P-Bovine Serum Albumin (P-BSA) for one hour at room temperature or at 4°C overnight and then incubated with the indicated anti-sera for 2 h at room temperature or at 4°C overnight, with gentle shaking. Blots were washed and then incubated with Pierce™ horseradish peroxidase-conjugated secondary antibodies (Thermos Fisher Scientific, Inc., USA) and incubated with Super Signal West Femto or Pico chemiluminescent substrate (Thermos Fisher Scientific, Inc., USA). We processed the Green X-ray film (Care stream, USA) with a Kodak processor (Kodak X-OMAT processor 2000). The Page Ruler™ Pre-stained Protein Ladder, 10 to 180 kDa (Thermos Scientific, USA) was used to monitor protein sizes.

3.2.15 Murine wound infection model

The murine wound infection model was carried out as described elsewhere (Chong, Tay et al. 2017). Briefly, we grow the bacterial strains in 15 mL BHI media for 16-18 h, statically at 37°C. Cells were pelleted, resuspended in 5 mL sterile 1× PBS and the OD was normalized to 2×10^8 CFU/mL. For competitive infection, an equal volume of each strain was mixed prior to infection. Firstly, we isoflurane-anesthetized groups of four to

five male wild-type C57BL/6 mice (7-8 weeks old, 22 to 25 g; InVivos, Singapore) with their dorsal hair trimmed. Following trimming, Nair™ cream (Church and Dwight Co, Charles Ewing Boulevard, USA) was applied and the fine hair removed via shaving with a scalpel. We then disinfected the skin with 70% ethanol. A single 6-mm biopsy punch (Integra Miltex, New York, USA) was used to create a full-thickness wound per mouse and 10 µL of the bacteria inoculum applied. We sealed the wound site with a transparent dressing (Tegaderm™ 3M, St Paul Minnesota, USA). Mice were euthanized at 8 or 72 hpi and one cm by one cm squared piece of skin surrounding the wound site was excised and collected in sterile 1× PBS. We use a homogenizer (Pro200, SPD scientific, Singapore) for approximately 10 secs at high speed to homogenize the skin samples and the viable bacteria were enumerated by plating onto both BHI plates and antibiotic selection plates to ensure all recovered colony forming units corresponding to the inoculating strain.

To measure the fitness of the strains in causing infection, we calculate the competitive indices (CI) using the formula below:

$$\mathrm{CI\ (OG1RF)} = \left(\frac{\mathrm{OG1RF(output)}}{\mathrm{OG1X(output)}}\right)/\left(\frac{\mathrm{OG1RF(input)}}{\mathrm{OG1X(input)}}\right)$$

$$\mathrm{CI\ (\Delta \mathit{htrA})} = \left(\frac{\Delta \mathit{htrA}\mathrm{(output)}}{\mathrm{OG1X(output)}}\right)/\left(\frac{\Delta \mathit{htrA}\mathrm{(input)}}{\mathrm{OG1X(input)}}\right)$$

The input indicates the initial inoculum used to infect the murine wound. The output indicates the inoculum recovered from wound site after 8 or 72 hpi. As stated above, four to five mice, each with a single wound was used for each group per experiment. A P value < 0.05 was considered significant.

3.2.16 Alkaline Phosphatase (AP) Secretion assay

We grow OG1RF strains statically overnight at 37°C in BHI broth containing Km for those strains carrying pABG5 plasmid. The overnight cultures were sub-cultured at a 1:10 dilution and grown to OD_{600} of 0.5 ± 0.05. Following which, cultures were normalized to OD_{600} of 0.45. and cells were harvested by centrifugation at 6,500 rpm for five mins at 4°C. To remove bacterial cells, we filtered the supernatant through a 0.2 µm syringe filter (Sartorius, Krackeler Scientific, USA) and collected in a new tube. The AP reaction is conducted in a sterile 96-well flat bottom microtiter plate (Nunc™ MicroWell™ 96-Well Microplates, Thermos Scientific™, USA). Triplicate of 25 µL aliquots of supernatant from each sample was then added to 200 µL of AP buffer (1M Tris-HCl, pH 8.0) per well. To start the enzymatic reaction, we added 25 µL of 4 mg/mL freshly prepared *para*-nitrophenyl phosphate (pNPP) (Sigma-Aldrich, USA) to each well. For negative control, 200 µL of AP buffer and 25 µL of pNPP were added to blank BHI broth or strains without pABG5. The microtiter plate was incubated at 37°C and absorbance at 405 nm were taken with Infinite® 200 PRO spectrophotometer (Tecan Group Ltd., Switzerland) every 10 mins until the reaction time reaches 18 h.

3.2.17 Statistical analyses

Data from multiple experiments were pooled. Statistical significance for biofilm assay was determined using a two-tailed unpaired t-test. Statistical significance for *in vivo* animal experiments was determined using one-way ANOVA, Kruskal–Wallis test with Dunn's post-test to correct for multiple comparisons. Statistical analysis for secretion assay was performed using Turkey's test for two-way ANOVA. Unless otherwise stated, values represented means ± SEM derived from at least three independent experiments

and/ or three technical replicates. * $P < 0.05$; ** $P \leq 0.01$; *** $P \leq 0.001$; **** $P \leq 0.0001$; $P \geq 0.05$, differences not significant (n.s). GraphPad Prism 6 software (GraphPad Software, La Jolla, CA) was used for statistical analyses.

3.2.18 Ethics Statement

We performed all approved procedures in accordance with the Institutional Animal Care and Use Committee (IACUC) in Nanyang Technological University, School of Biological Sciences (ARFSBS/NIEA0198Z) for murine wound infection model.

3.3 RESULTS

3.3.1 Genetic organization and bioinformatics prediction of OG1RF_12305 coding for *htrA*

To gain a thorough understanding of the role of serine protease HtrA in *E. faecalis* (hereafter referred to as $HtrA_{EF}$), we looked at the genetic organization of *htrA in silico*. The *htrA* gene is flanked by a gene encoding an Alpha/beta knot family protein upstream and a gene encoding a tRNA binding domain protein downstream of *htrA* (**Fig 3.1**). The *htrA* gene encodes a 440-amino-acid protein that is predicted to be 44.8 kDa.

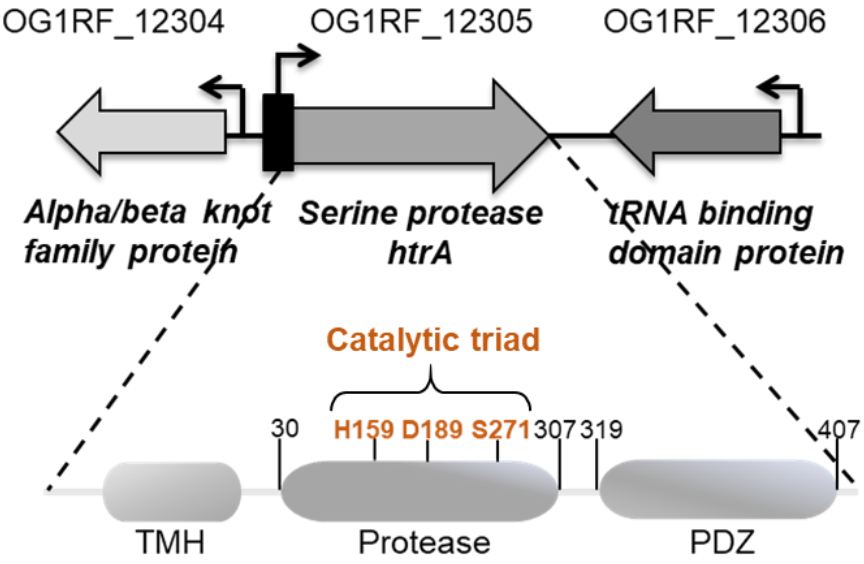

Figure 3.1 | Genomic organization of the *htrA* locus in the sequenced genome of *E. faecalis* OG1RF. Schematic representation of a *htrA* and its flanking genes in *E. faecalis* OG1RF. *E. faecalis* $HtrA_{EF}$ is made up of a transmembrane (TMH), a trypsin protease domain, and a PDZ domain. The conserved catalytic residues (orange) in the trypsin protease domain are identified based on multiple sequence alignment using Clustal Omega software and compose its catalytic triad.

To predict whether $HtrA_{EF}$ has a transmembrane domain, we used TMHMM Server V.2.0, a TM region prediction program that excludes TMs with signal peptides (Sonnhammer, von Heijne et al. 1998). $HtrA_{EF}$ is predicted to have a transmembrane helix (amino acids 20 to 42), suggesting that this protease is membrane-anchored (**Fig 3.2**). To predict $HtrA_{EF}$ membrane topology, we utilized TOPCONS computational software (Tsirigos, Peters et al. 2015). Like *S. pyogenes,* computational analyses predicted that membrane-anchored $HtrA_{EF}$ is an N-in, C-out membrane protein with the protease and PDZ domains on the extracellular side for easier substrate recognition. To identify other domains present in $HtrA_{EF}$, we used the **S**imple **M**odular **A**rchitecture **R**esearch **T**ool (SMART) that provides simple identification with annotation of protein domains and architecture (Letunic, Doerks et al. 2015, Mende, Letunic et al. 2017). Like all other HtrAs, $HtrA_{EF}$ consists of a trypsin-family serine protease domain (amino acids 30 to 307) and one PDZ domain (amino acids 319 to 407).

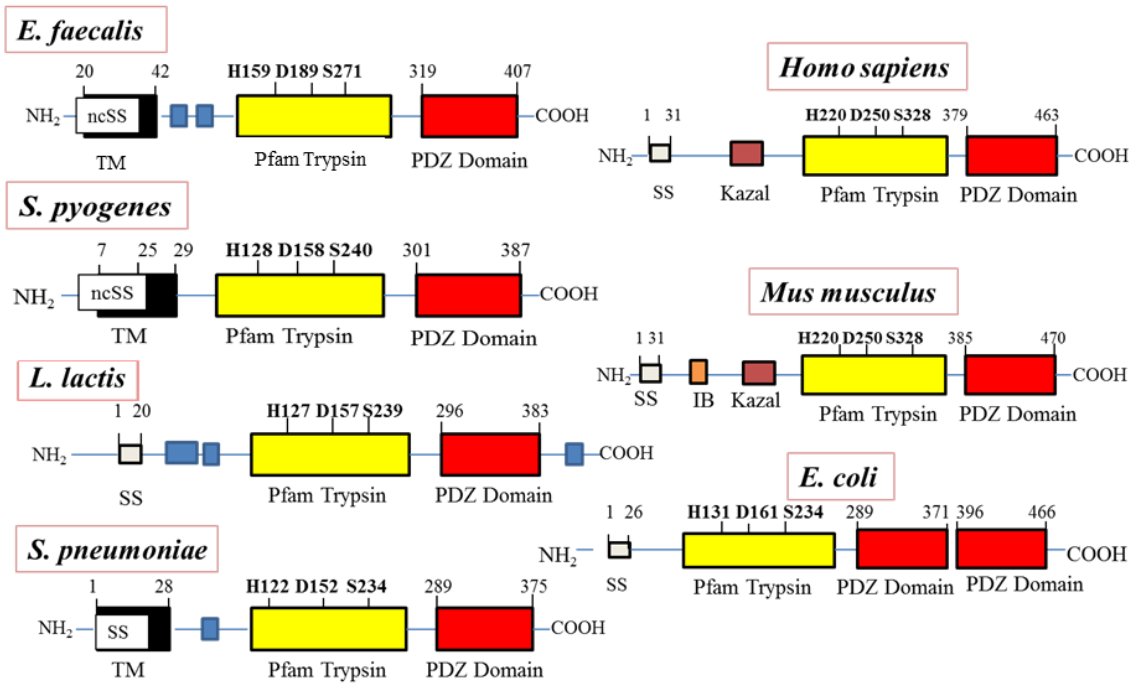

Figure 3.2 | Architecture of HtrA proteases. Each HtrA consists of a signal peptide, a trypsin serine protease domain (yellow box) and at least one PDZ domain (red box). Conserved motifs in the trypsin domain- Ser, His and Asp are in **boldface**; signal sequences, non-cleavable (ncSS) or cleavable (SS); IB, insulin-like growth factor-binding domain; Kazal, domain related to Kazal type of serpin; domains in blue indicate regions with low complexity sequences. Protease and PDZ domains predicted using the Simple Modular Architecture Research Tool (SMART). Signal sequences (SS) predicted using SignalP. Trans-membrane helix (TMH) prediction based on TMHMM Server V.2.0. Predicted catalytic residues and indicated in **boldface**. The cartoon is not drawn to scale.

Multiple sequence alignment of $HtrA_{EF}$ with characterized HtrA from *S. pyogenes* (HSC5 strain), *S. pneumoniae* (TIGR4 strain), *E. coli* (DegP protease of str. K-12 substr. MG1655 strain), *L. lactis* (subsp. lactis Il1403), *Mus musculus* (HTRA1 precursor), *Homo sapien* (HTRA1 precursor) show that $HtrA_{EF}$ is highly conserved across prokaryotes and eukaryotes. The serine protease domain contains the catalytic triad His (**H**$_{159}$), Asp (**D**$_{189}$) and Ser (**S**$_{271}$) identified using multiple sequence alignment, Clustal Omega (Sievers, Wilm et al. 2011) (**Fig 3.3**). HtrA protein sequences used for multiple sequence alignment can be found in **Supplementary Table A2.**

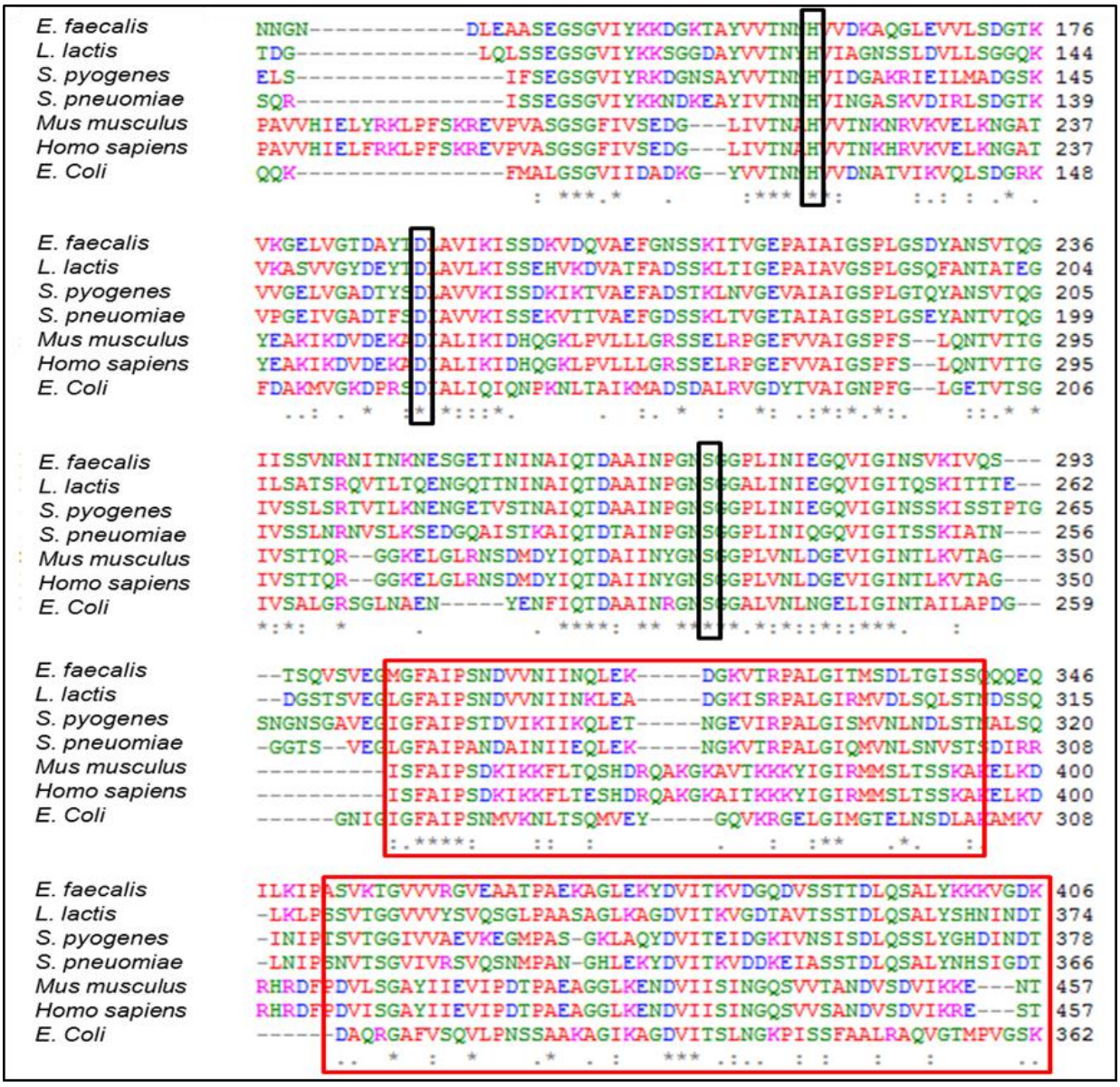

Figure 3.3 | HtrA is conserved across all domains of life. Multiple sequence alignment between $HtrA_{EF}$, with related Gram-positive strains (*L. lactis, S. pneumoniae, S. pyogenes*); *E. coli*, *Mus musculus,* and *Homo sapiens*. Identical residues are summarized as *, conserved regions summarized with a colon (:). Amino acids classes are indicated with the following colors: positively charged side chains (Pink), negatively charged side chains (Blue), polar uncharged side chain (Green), Hydrophobic side chain (Red). Catalytic triad within the three consensus motifs - Ser, His and Asp (Black boxes). Conserved regions of the PDZ domain are shown in red boxes. Alignment of *E. coli* PDZ domain sequence is only up to PDZ-1. Multiple alignments were performed using Cluster Omega.

$HtrA_{EF}$ sequence analysis using I-TASSER (**I**terative **T**hreading **ASSE**mbly **R**efinement) software to predict protein structure and function (Roy, Kucukural et al. 2010, Yang and Zhang 2015), identified proteins with the most structural similarity as *E. coli* Deg proteases (**Table 3.4**). *E. coli* has 3 Deg proteases (HtrA homologs), DegS, DegP, and DegQ; each performs different functions in contrast with *E. faecalis* which has only one HtrA. From the I-TASSER function prediction, $HtrA_{EF}$ is predicted to function more like DegS in *E. coli*, acting as a regulatory protease on the cell membrane even though it is structurally similar to DegP. Blastp analysis revealed that $HtrA_{EF}$ shares 33% identity (80% coverage) with *E. coli* DegS, 37% identity (76% coverage) with *E. coli* DegP, and 33% identity (79% coverage) with *E. coli* DegQ over the entire length of the alignment.

Table 3.4 | Function predictions of HtrA against known functions of HtrA in the database using I-TASSER.

	Homologs	Species
Template used by I-TASSER	1. DegQ +PDZ1 2. pepD Rv0983 3. DegQ + PDZ1	4. *E. coli* 5. *M. tuberculosis* 6. *E. coli*
Proteins structurally close to the target in the PDB	1. DegQ +PDZ1 2. DegP 3. DegQ	4. *E. coli* 5. *E. coli* 6. *Legionella*
Function Prediction	1. DegS 2. pepD Rv0983 3. DegS-deltaPDZ q191A mutant	4. *E. coli* 5. *M. tuberculosis* 6. *E. coli*
Predicted Gene -Ontology terms	1. pepD Rv0983 2. DegP 3. DegP1	4. *M. tuberculosis* 5. *E. coli* 6. *Arabidopsis thaliana*
Predicted Binding Site	1. DegP 2. DegP 3. DegP	4. *E. coli* 5. *E. coli* 6. *E. coli*

3.3.2 Construction of in-frame deletion of *htrA* in *E. faecalis*

To characterize the function(s) of $HtrA_{EF}$ in *E. faecalis*, we constructed an unmarked, in-frame *htrA* deletion mutant based on the genome sequence of OG1RF. We confirmed the absence of *htrA* by PCR using primer pairs dHtrAF_PstI/dHtrAR_PstI and htrA_compF_EcoRI/dHtrAR_ PstI. Pass clones that retained a wild type *htrA* locus have a 2.2 kb or a 1.8 kb when screened with the different primer pairs, respectively (**Fig 3.4A and B**). Deletion strains have a 0.9kb PCR product for primer pair dHtrAF_PstI/dHtrAR_PstI and no product for primer pair htrA_compF_EcoRI/ dHtrAR_PstI. Successful Δ*htrA* strains were subjected to immunoblotting of the whole cell *E. faecalis* lysates using an anti-$HtrA_{EF}$ antibody to validate the absence of HtrA protein (**Fig 3.4C**). Whole genome sequencing of both WT and Δ*htrA* also confirmed that no spontaneous mutations or SNPs arose during the construction of the mutant (**data not shown**).

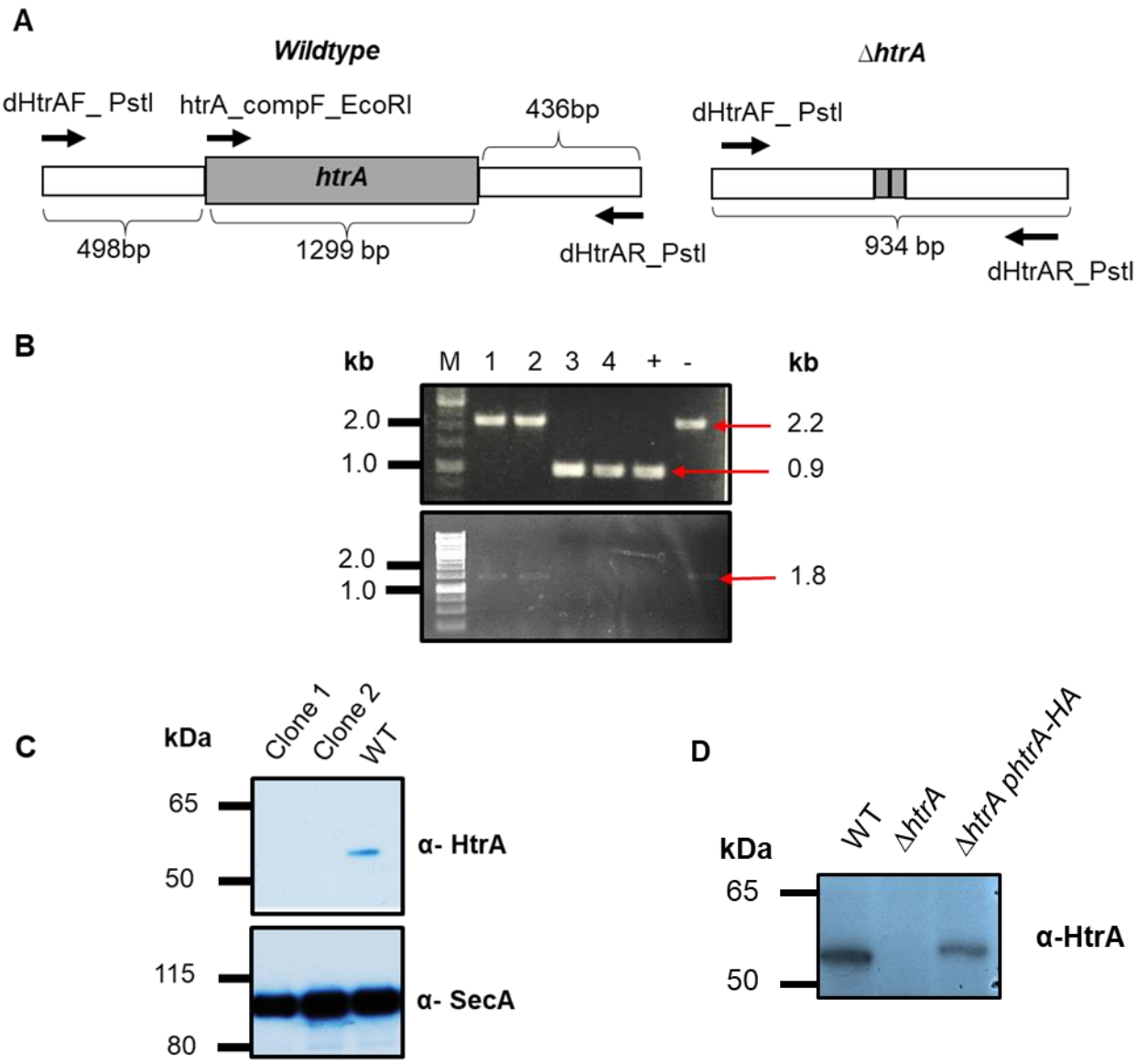

Figure 3.4 | Locus and the genetic disruption of *htrA* in *E. faecalis* OG1RF. (**A**) Schematic diagram of PCR product produced using various primer pairs combinations. (**B**) Excision of *htrA* from the chromosome was confirmed by PCR amplification using primer pairs dHtrAF_PstI/dHtrAR_PstI (Top) and htrA_compF_EcoRI/dHtrAR_PstI (Bottom). M, Gene Ruler^{TM} 1 kb DNA Ladder; lane 1 and 2 correspond to pass clones that revert to WT; Lane 3 and 4 corresponds to Δ*htrA*; +, extracted p*delta-htrA* as positive control; -, WT gDNA as a negative control. (**C**) The absence of HtrA protein expression in Δ*htrA* was validated using immunoblot with α-HtrA$_{EF}$. Lane 1 and 2, OG1RFΔ*htrA*; Lane 3, -, WT (negative control). (**D**) HtrA expression can be complemented by *htrA-HA* on a plasmid. PageRuler^{TM} pre-stained protein gel (10-250 kDa) was used as the ladder.

3.3.3 HtrA is enriched at the septum in *E. faecalis*

In *S. pyogenes*, septal focal localization of HtrA is necessary for proper targeting and the maturation of nascent SpeB (Lyon and Caparon 2004). By contrast, septal localization is absent in *S*. *pneumoniae* and localization of the Sec machinery and HtrA forms many distinct foci on the surface of the cell (Tsui, Keen et al. 2011). $HtrA_{EF}$ has a transmembrane domain in the N-terminal region, predicting $HtrA_{EF}$ to be membrane-anchored. To determine the subcellular localization of $HtrA_{EF}$, we monitored $HtrA_{EF}$ using a HtrA-HA fusion expressed on a plasmid (p*htrA-HA*), which we demonstrated to be expressed because it complements HtrA expression in the *htrA* mutant (**Fig 3.4D**) and is functional in complementing pilus biogenesis phenotypes (see **Fig 4.3**). We chose to monitor HtrA-HA using an HA antibody rather than native $HtrA_{EF}$ because the HtrA antibody detection resulted in high signal to noise ratio. We grew cells to mid-log phase, stained the cell membrane with FM 4-64 for 1 h prior to fixing, and subsequently probed them with primary rabbit anti-HA immune sera coupled with Alexa Fluor® 488 secondary antibody. Detailed localization of HtrA in *E. faecalis* was observed using SR-SIM (**Fig 3.5A**). We performed post-image analysis using Projected System of Internal Coordinates from Interpolated Contours (PSICIC), which is a modular set of MATLAB functions designed to find smooth cell borders from phase contrast microscope images and establish an internal coordinate system for each individual cell (Guberman, Fay, Dworkin, Wingreen, & Gitai, 2008). These experiments identified $HtrA_{EF}$ to be focally localized around the membrane but enriched at the cell septum (**Fig. 3.5B**).

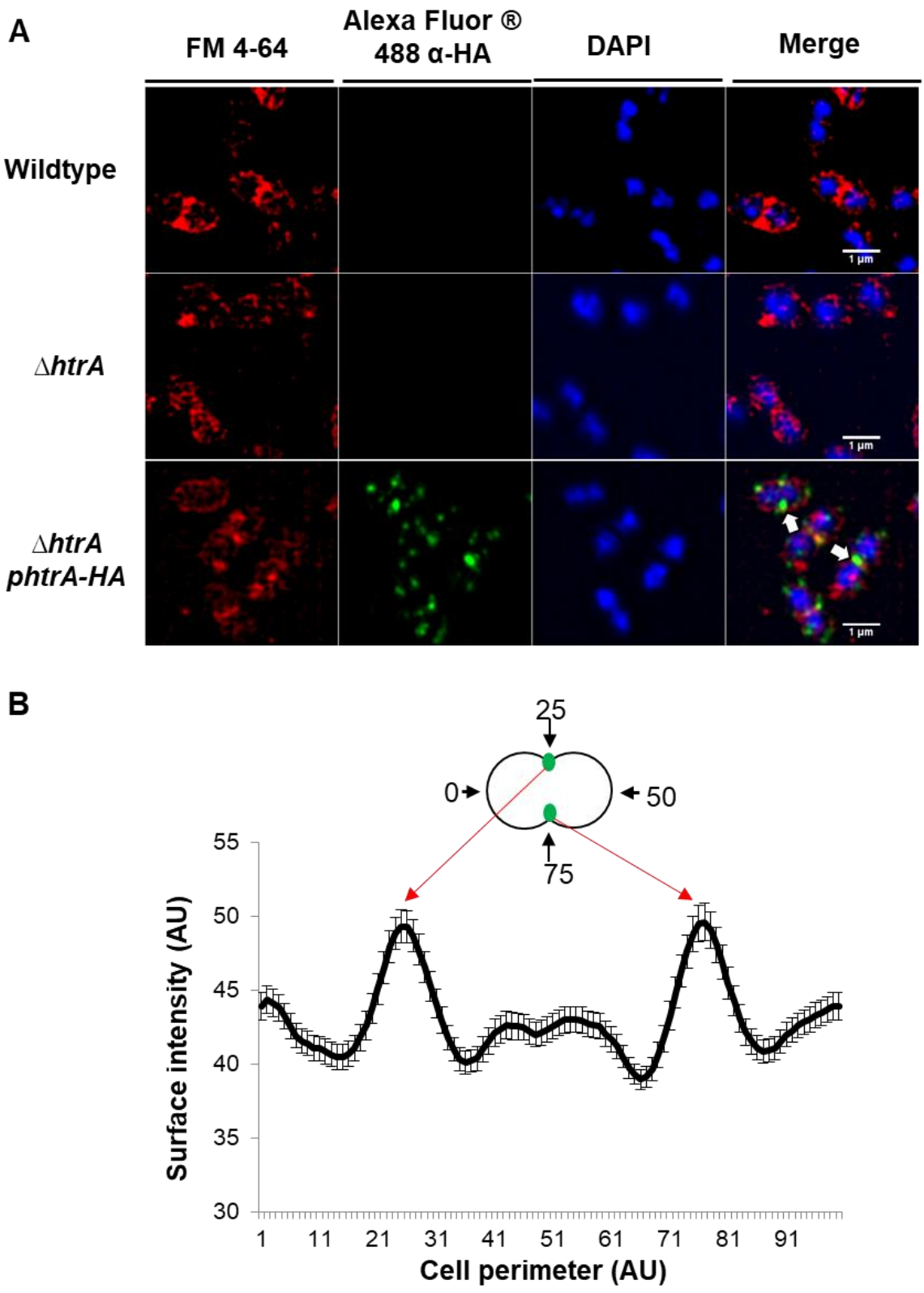

Figure 3.5 | HtrA$_{EF}$ is localized to multiple foci around the membrane but enriched at the septum. (**A**) HtrA-HA localization was analyzed using an anti-HA monoclonal

antibody coupled to Alexa Fluor® 488 antibody (green) at a 1000x magnification. The bacterial cell membrane was stained with FM 4-64 (excitation/emission maxima ~515/640 nm) (red). WT and Δ*htrA* strains served as negative controls for HA staining. Representative images of HtrA-HA localization patterns are shown. HtrA is enriched at the septum (white arrowhead) of Δ*htrA* p*htrA-HA* but not found in WT or the Δ*htrA* mutant. Scale bar represents 1 µm. (**B**) Schematic image of HtrA localization at the septum (red arrow) in Δ*htrA* p*htrA-HA* using PSICIC analysis. The result is a pooled data of three experiments, with a total of 1000 cells. The bold line indicates the mean and error bars reflect the standard error of the mean fluorescence at each point on the perimeter.

3.3.4 Characterization of HtrA functions in *E. faecalis*

3.3.4.1 Growth of *E. faecalis* is not affected by *htrA* gene disruption under high temperature

The heat shock response is an important HtrA function in many bacteria (Marsh, Ong et al. 2017) and HtrA is heat inducible in several bacteria (Lipinska, Sharma et al. 1988, Narberhaus, Weiglhofer et al. 1998, Smeds, Varmanen et al. 1998, Noone, Howell et al. 2000, Resto-Ruiz, Sweger et al. 2000, Darmon, Noone et al. 2002). To determine if $HtrA_{EF}$ is also heat inducible, we performed immunoblots of whole lysates extracted from WT *E. faecalis* grown at four temperatures (30°C, 37°C, 42°C, 50°C) and normalized for CFU. We detected less $HtrA_{EF}$ protein at 50°C compared to the other temperatures (**Fig 3.6A**). Therefore, to test the functionality of $HtrA_{EF}$ as a heat-shock response protein, we similarly grew *E. faecalis* at the same four temperatures and measured both the optical density (OD) and the colony-forming units per mL (CFU/mL). However, we observed no difference in the growth pattern of WT and Δ*htrA* at any temperature, suggesting that $HtrA_{EF}$ does not contribute to cell survival and growth at different temperatures (**Fig 3.6B**).

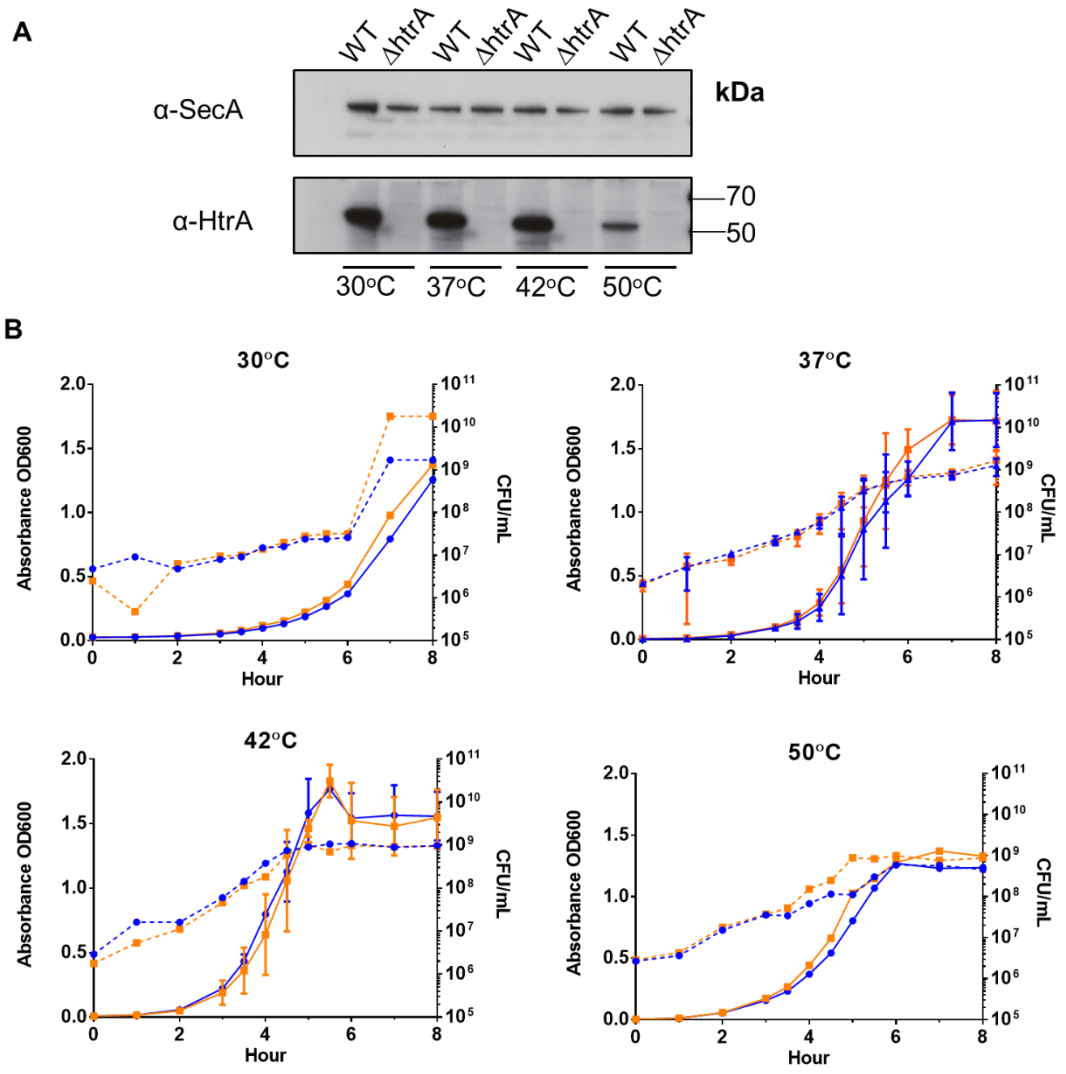

Figure 3.6 | HtrA$_{EF}$ does not play a role in high-temperature growth. (**A**) Western blots of whole cell lysates from various temperature. To detect HtrA$_{EF}$, affinity purified α-HtrA$_{EF}$ was used (Bottom). Immunoblots performed on the same samples using α-SecA membrane protein (Top) as a loading control. (**B**) Growth phenotypes of *E. faecalis* WT (**orange**) and Δ*htrA* (**blue**). Growth curves performed in BHI broth at 30°C (Top left), 37°C (Top right), 42°C (Bottom left) and 50°C (Bottom right). Representative data of three independent experiments except for growth at 50°C. CFU/mL for the growth kinetic assays were represented as dashed lines; OD reading for the growth kinetic assays was represented as bold lines. Triplicate cultures were conducted at 37°C and 42°C, with standard errors indicated by the error bars.

3.3.4.2 $HtrA_{EF}$ is not essential in biofilm formation

HtrA plays an important role in the attachment of bacterial cells to a surface during biofilm formation in *S*. *mutans* (Ahn, Lemos et al. 2005, Biswas and Biswas 2005, Kang, Lee et al. 2010). To investigate if $HtrA_{EF}$ also plays a role in biofilm formation, we grew WT and Δ*htrA* in BHI in a 96-well microtiter plate for 24 and 48 h under static growth conditions. To quantify biofilm formation, we stained biomass with crystal violet (CV) and quantified it by adding an ethanol/acetone mix and measured OD_{595}. As pili play an important role in biofilm formation (Nallapareddy, Singh et al. 2006), we grew WT and Δ*htrA* in TSB supplemented with 0.25% glucose to induce pilus production for maximal biofilm formation, and then investigated if the absence of $HtrA_{EF}$ affected biofilm formation. Regardless of the media used, no differences in biofilm biomass were observed between WT and Δ*htrA* at 24 and 48 h. Together these data suggest that $HtrA_{EF}$ is not involved in biofilm formation in *E*. *faecalis* (**Fig 3.7**).

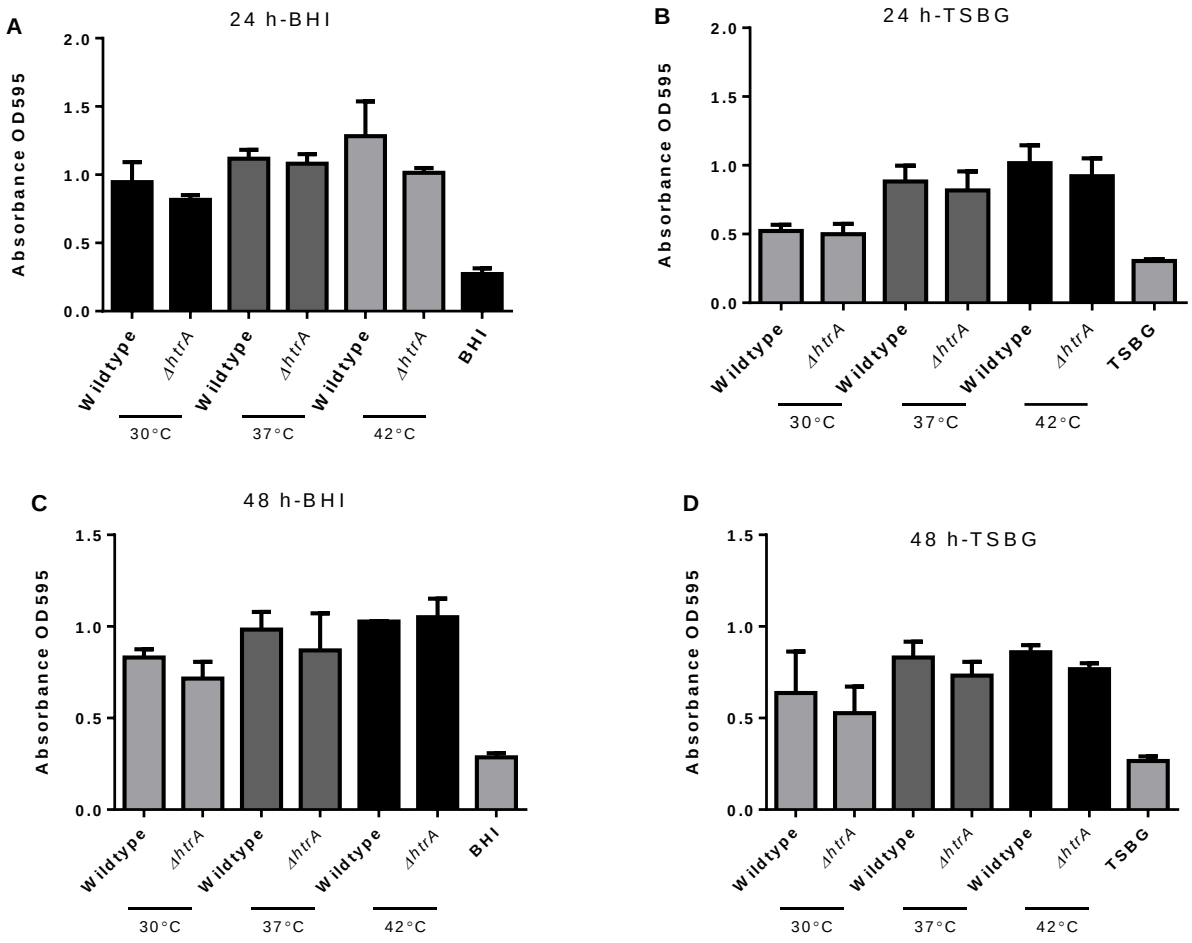

Figure 3.7 | HtrA$_{EF}$ does not play a role in biofilm formation in *E. faecalis*. Biofilms formation of WT and Δ*htrA* in either BHI (**A and C**) or TSBG for (**B and D**) 24 h and 48 h at 30°C, 37°C and 42°C. The values represent the mean values ± standard deviation obtained from three independent experiments, each with 12 technical replicates.

3.3.4.3 Growth of *E. faecalis* is not affected by *htrA* gene disruption under various environmental stresses

Although HtrA$_{EF}$ does not confer temperature-sensitive growth or play a role in biofilm formation, we postulated that HtrA$_{EF}$ may instead be involved in overcoming other environmental stresses. However, in the absence of HtrA$_{EF}$, *E. faecalis* growth in a range of pHs, high salt, and oxidative stresses did not affect its growth or its tolerance towards

these stressors (**Table 3.5**). These data indicate that $HtrA_{EF}$ does not play a primary role in coping with damage inflicted from these environmental stresses.

Table 3.5 | Characteristics of HtrA in *E. faecalis*

	Conditions tested[a]
Colony morphology	Wet mount
Temperature	30°C, 37°C, 42°C, 50°C
pH stress	pH 2-10
Osmotic stress	0.5M and 1M NaCl
Biofilm formation	30°C, 37°C, 42°C, TSBG or BHI
Oxidative	0.25-512 µg/mL H_2O_2
Mitomycin C	0.25-512 µg/mL
Puromycin	0.25-512 µg/mL

[a] Conditions for HtrA function was assessed and no differences between WT OG1RF and Δ*htrA* were identified.

3.3.5 Deletion of *htrA* does not affect pilus protein expression in *E. faecalis*

In *E. coli*, DegP (HtrA) is part of the Cpx system that plays an important role in removing misfolded pilins of the P pili (Danese, Snyder et al. 1995). In *E. faecalis*, it is not known how misfolded pilins are handled and removed because a system homologous to Cpx has not been reported in *E. faecalis*. To determine if $HtrA_{EF}$ plays a similar role in handling pilin proteins as DegP in *E. coli*, we examined pilus polymerization in Δ*htrA*. A western blot analysis of WT and Δ*htrA* cell wall fractions using α-EbpA (**Fig 3.8A, Left**), α-EbpB (**Fig 3.8A, Middle**) and α-EbpC (**Fig 3.8A, Right**) immune sera revealed high molecular weight ladder (HMWL) for both strains. This HMWL is indicative of pilus polymerization since the intermolecular isopeptide bonds between the pilus subunits do not disassociate upon boiling in SDS (Nallapareddy, Singh et al. 2006). $HtrA_{EF}$ does not affect the assembly of Ebp pilus biogenesis as we observed a similar amount of protein expressed for both strains. Consistent with the absence of an effect on Ebp proteins, expression of the sortase enzymes, SrtA and SrtC, was also unaffected in the Δ*htrA*

mutant (**Fig 3.8B**). RNA transcriptomic analysis comparing WT and the *htrA* mutant identified a total of 5 genes (including *htrA*) to be differentially regulated (**Supplementary Table A3**), further supporting our hypothesis that the absence of *htrA* does not give rise to widespread transcription changes.

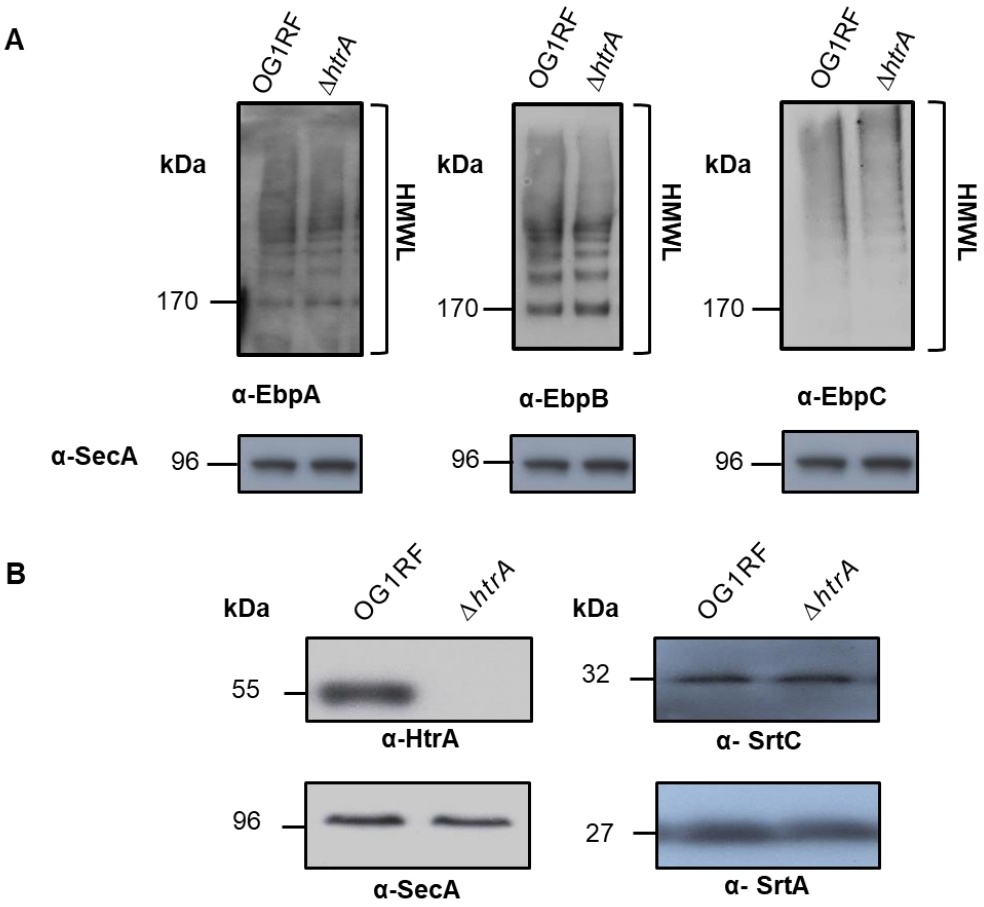

Figure 3.8 | Pili was expressed at equivalent levels in OG1RF WT and Δ*htrA*. (**A**) Whole cell lysates were assessed by western blotting with the indicated α-pilin immune sera (Top). Immunoblots performed on the same samples using α-SecA membrane protein (Bottom) as a loading control. (**B**) Whole cell lysates of WT and Δ*htrA* were also assessed by western blotting with α-HtrA$_{EF}$, α-SecA, α-SrtC, and α-SrtA immune sera.

3.3.6 HtrA$_{EF}$ contributes to colonization fitness during chronic wound infection

HtrAs have been implicated in the virulence of many bacterial pathogens, and *htrA* null mutants typically resulted in attenuated infections (Humphreys, Stevenson et al.

1999, Cortes, de Astorza et al. 2002, Heimesaat, Alutis et al. 2014, Marsh, Ong et al. 2017). Since *E*. *faecalis* has emerged as an important cause of wound infection, we investigated the fitness of the *htrA* mutant in a mouse model of wound infection. We created a 6-mm wound on each mouse and infected the wound with a 1:1 CFU mix of either OG1RF/OG1X pair or Δ*htrA*/OG1X pair, for a total of 2.0 x 10^6 CFU, for 8 h.

We chose OG1X as our comparative strain because it is highly genetically related to OG1RF, different at 76 SNPs (**data not shown**) but harbors a different antibiotic resistance profile compared to OG1RF, enabling differential growth on selective media. Fitness was quantified by the relative number of CFU recovered from the excised wounds that are homogenized and enumerated on selective agar plates. An approximate median titer of 2.0 x 10^7 CFU/mL was recovered for each strain, suggesting that HtrA is not necessary for acute wound infection (**Fig 3.9A**). However, Chong *et al* demonstrated that viable *E. faecalis* bacteria can still be recovered at 7 dpi, persisting in wounds at bacteria titer of 10^5 CFU/mL (Chong, Tay et al. 2017). Therefore, to investigate if $HtrA_{EF}$ is required for persistent wound infection, we infected as above and examined the bacterial burdens at 72 h.

Similar levels of bacteria titers were recovered from the WT OG1RF/OG1X infection. However, bacteria titers recovered from Δ*htrA* (median titer of 1.83 x 10^4 CFU/mL) were significantly ($P \leq 0.01$) lower than OG1X (median titer of 1.28 x 10^5 CFU/mL). Competitive indices (CI) calculations further confirmed that Δ*htrA* was significantly outcompeted by OG1X (**Fig 3.9C**). To investigate whether this out competition was HtrA-dependent, we co-infected OG1X with OG1RFΔ*htrA* complemented with p*htrA* or p*Empty* vectors and performed the experiment under the

same conditions. Plasmid specific selection plates (BHI+ Kanamycin) were used to select for bacteria that still retained the plasmid 72 hpi. The Δ*htrA* strain complemented with p*htrA* was no longer out-competed by OG1X unlike the Δ*htrA* strain carrying p*Empty* indicating that this out-competition is HtrA-dependent (**Fig 3.9C**).

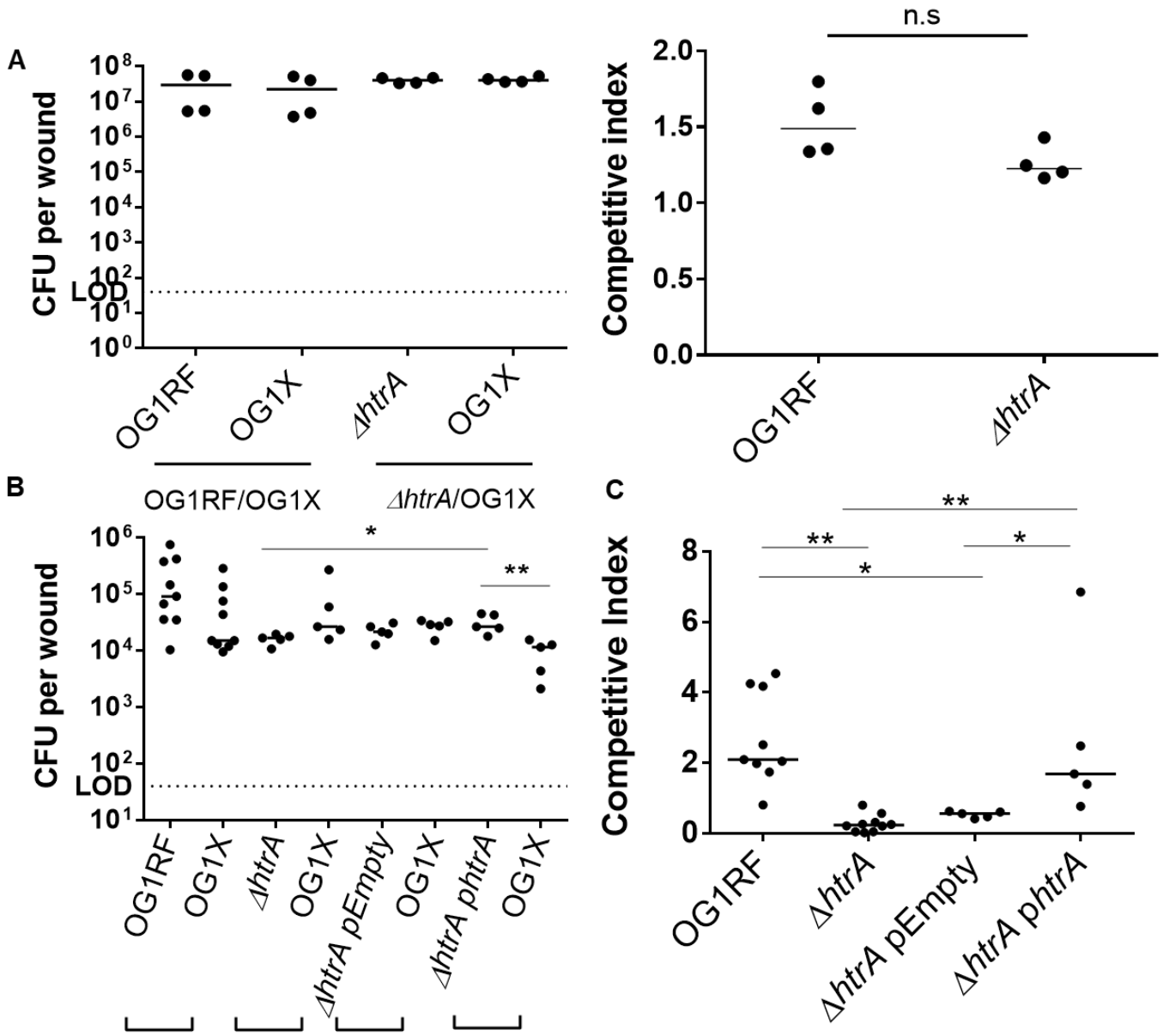

Figure 3.9 | HtrA is required for persistent wound infection. Wounds were infected with a 1:1 ratio of *E. faecalis* strains OG1X/wildtype OG1RF or OG1X/OG1RFΔ*htrA*, at 10^6 CFU per inoculum, harvested at (**A**) 8 hpi or (**B & C**) 72 hpi, and the recovered bacteria were enumerated on selective media for each strain. ⌊⌋ Represents strains that are co-infected for the competitive assay. Each dot in the graph on the left represents one mouse. Competitive index (CI) was calculated using the final CFU ratio of OG1X with OG1RF or Δ*htrA* (output) over the initial CFU ratio of OG1X with OG1RF or Δ*htrA* (input). Each dot in the graphs on the left represents one mouse, and the solid horizontal line indicates the median. The limit of detection (LOD) of 40 CFU is indicated. For 72 hpi, N=1,

n=10 for OG1RF and Δ*htrA*, n=5 for Δ*htrA* p*Empty* and Δ*htrA*p*htrA*; for 8 hpi, N=1, n=4. Statistical analysis was performed using the Kruskal–Wallis test with Dunn's post-test to correct for multiple comparisons. **** $P \leq 0.0001$; *** $P \leq 0.001$; ** $P \leq 0.01$; * $P < 0.05$. Abbreviations: N, biological replicates; n, technical replicates.

3.3.7 Attenuated fitness of the Δ*htrA* mutant *in vivo* is not due to a growth defect in mixed culture

The inability of the *htrA* null mutant to grow to the same bacteria titers as the WT *in vivo* could result either from a growth defect when co-cultured with OG1X or the observed phenotype is due to attenuated virulence. To test the former possibility, we performed a growth assay for both OG1RF/OG1X and Δ*htrA*/OG1X co-cultures under shaking and static conditions for 24 h (**Fig 3.10**). We measured the OD and recovered the CFU from various time points. CFU enumeration showed that both WT and Δ*htrA* grew to similar CFU in both conditions, indicating that the lower bacteria titers observed *in vivo* were not due to an inability to grow in co-culture.

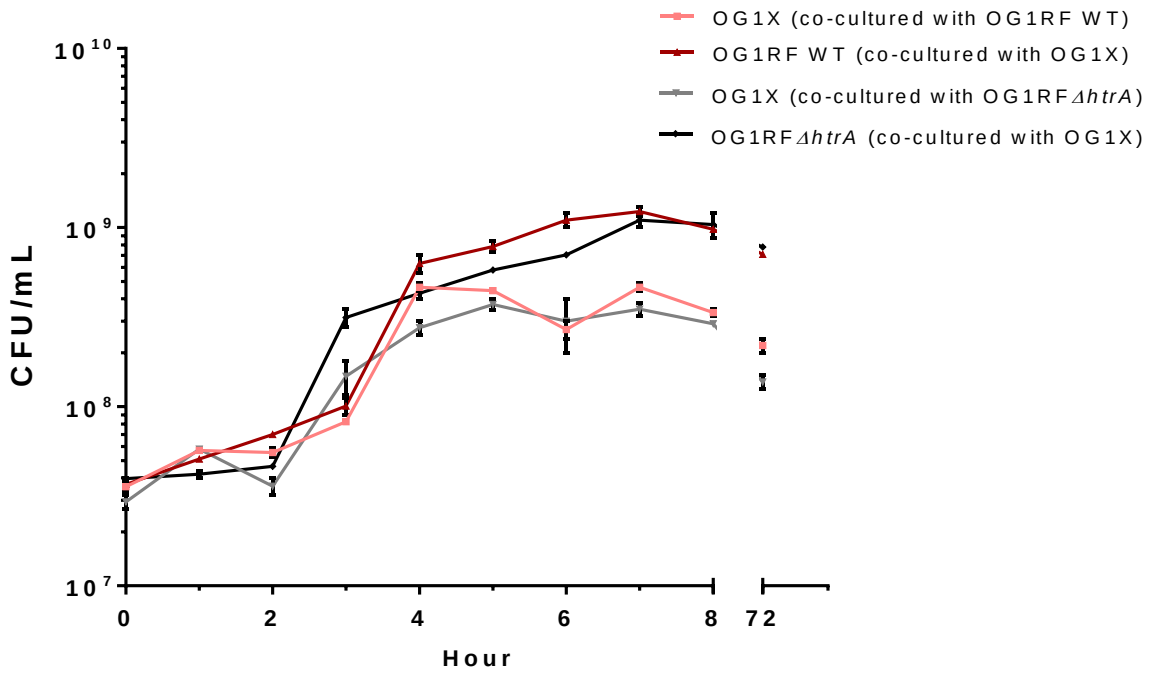

Figure 3.10 | Co-culture with OG1X does not cause slower growth of Δ*htrA*. CFU enumeration for growth kinetic performed on 1:1 ratio of *E. faecalis* strains OG1X/ OG1RF or OG1X/OG1RFΔ*htrA*, at 10^8 CFU per well. Cultures were subjected to static incubation for 72 h. Absorbance reading was recorded hourly for 8 h and at the 24th h and 72nd h.

3.3.8 The Δ*htrA* mutant exhibits a severe defect in protein maturation

In *B. subtilis,* the *htrA* expression is transcriptionally regulated by the CssR-CssS TCS, which governs secretion stress caused by overproduction of α-amylase (Hyyrylainen, Bolhuis et al. 2001, Darmon, Noone et al. 2002). The absence of CssS resulted in an accumulation of misfolded mature α-amylase on the cell envelope that is not removed in the absence of HtrA (Hyyrylainen, Bolhuis et al. 2001). To investigate if $HtrA_{EF}$ also plays a role in protein maturation, we performed alkaline phosphatase (AP) secretion assays.

AP secretion assays work by transforming into the strain of interest, a pABG5 plasmid that encodes a chimeric protein of the enzymatic domain of PhoZ and the secretion domain of protein F from *S. pyogenes* (Granok, Parsonage et al. 2000). This chimeric form of PhoZ (PhoZF) can be secreted from the cell and catalyzes hydrolysis with a chromogenic substrate, pNPP, in the media, liberating phenolate as a by-product which has maximal absorption at 405nm. The higher the absorbance reading, the more secreted pNPP in the supernatant is converted to phenolate.

We observed the linear increase of absorbance for WT harboring pABG5-PhoZF, indicating that PhoZ is being secreted and accumulating in the supernatants over time. However, Δ*htrA* mutant to exhibit a four-fold decrease in absorbance, indicating a significant defect in protein secretion ($P \leq 0.0001$) with a minimal amount of substrate converted compared to WT harboring pABG5-PhoZF (**Fig 3.11A and B**). To ensure that this observed defect is PhoZ-dependent, we performed similar experiments in parallel with WT and Δ*htrA* without pABG5 and no observable absorbance was obtained.

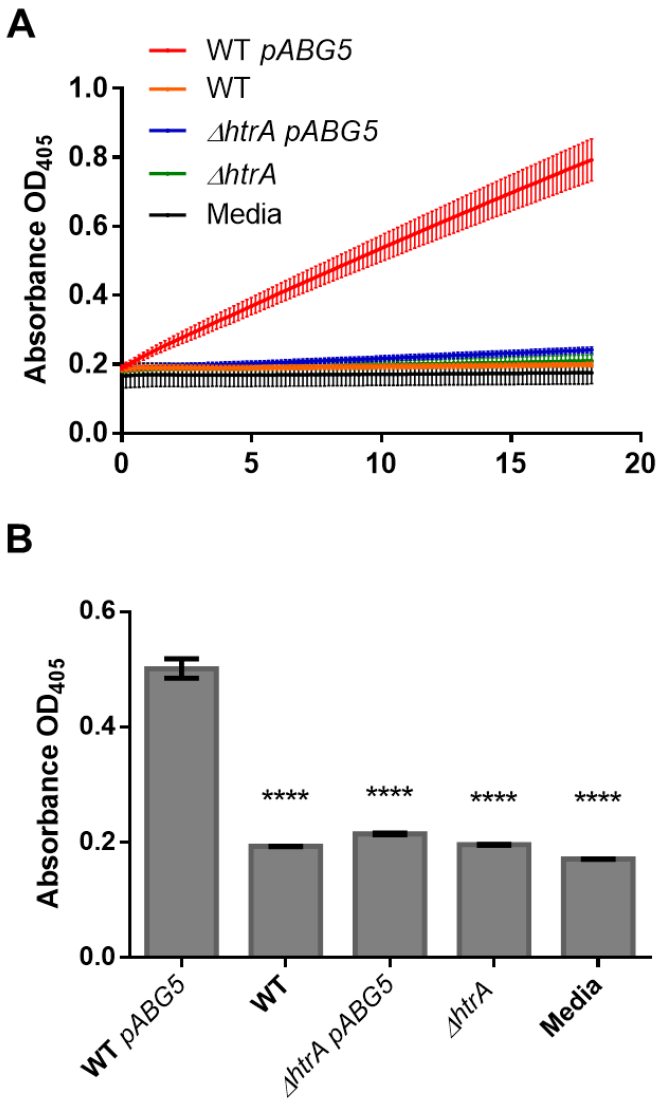

Figure 3.11 | The *E. faecalis* Δ*htrA* mutant exhibits a severe defect in protein maturation. (**A**) The rate of enzymatic pNPP conversion by WT and Δ*htrA* harboring the PhoZF-expressing pABG5 plasmid over the course of 18 h by measuring the colorimetric changes at OD_{405} every 10 mins. Reading without plasmid and blank media are used as baseline controls. Error bars represent the standard error of the mean from three biological replicates, with 12 technical replicates each. (**B**) Levels of enzymatic pNPP conversion by PhoZF at the 18th h time point in WT and Δ*htrA* harboring the PhoZF-expressing pABG5 plasmid. Statistical analysis was performed using Turkey's test for two-way ANOVA; **** $P \leq 0.0001$.

3.4 DISCUSSION

To characterize the function(s) of $HtrA_{EF}$, we first created an in-frame deletion of *htrA* (**Fig 3.4**). The Δ*htrA* mutant was subjected to a series of environmental stresses because in other bacteria, HtrA functions as an essential chaperone/protease in response to various environmental stresses such as high temperature (Darmon, Noone et al. 2002), biofilm formation (Fang, Jin et al. 2018), low pH (Kang, Lee et al. 2010, Tegtmeyer, Moodley et al. 2016), or oxidative stresses (Jones, Bolken et al. 2001) (**Fig 3.6 and 3.7**). However, both *E. faecalis* WT and Δ*htrA* responded similarly to all stress conditions tested (**Table 3.5**) suggesting that *E. faecalis* respond to these stresses by another mechanism. Despite its name, it is not necessarily surprising that *E. faecalis* HtrA is not temperature-responsive as *htrA* mutants of *H. pylori*, *C. jejuni,* and *S. typhimurium* also do not display thermo-sensitivity and show similar growth kinetics at elevated temperature as their WT parental strains (Johnson, Charles et al. 1991, Pallen and Wren 1997). Even though HtrAs are highly conserved in structure across all domains of life (**Fig 3.2**), they are functionally distinct and do not all conform to the *E. coli* DegP model. However, one of caveat the stress experiments performed is the lack of positive control strains, such as a DegP mutant from *E. coli* or a HtrA mutant from *S. pyogenes*, where stress-associated phenotypes of HtrA is characterized (Spiess, Beil et al. 1999, Jones, Bolken et al. 2001). In addition, out of the three Deg proteases expressed by *E. coli*, only the DegP mutant is temperature-sensitive. *E. faecalis* only expresses one HtrA, whose function(s) may be a combination of the three *E. coli* Deg proteases, as the I-TASSER analysis revealed $HtrA_{EF}$ to function like DegS but looks structurally like DegP (**Table 3.4**). Consistent with the functional prediction of $HtrA_{EF}$ to be like DegS, membrane-anchored HtrA proteins such as DegS and $HtrA_{EF}$ are often regulatory proteases, where activation and proteolytic

cleavage occurs separately (Wilken, Kitzing et al. 2004, Hasselblatt, Kurzbauer et al. 2007).

Using SR-SIM, we identified $HtrA_{EF}$ to be focally localized around the cell membrane but enriched at the septum (**Fig 3.5**), which we propose to be in close proximity with the Sec machinery and the sortases at the septum, in order to facilitate translocation and quality control of surface proteins moving through the Sec machinery.

We also show that Δ*htrA* exhibits attenuated fitness during chronic wound infection (**Fig 3.9**) but not acute wound infection, similar to what was observed in *C. trachomatis*, where HtrA is required only for persistent infection in human epithelial cells (HEp-2) at 44 hpi (Huston, Theodoropoulos et al. 2008). The decreased fitness of Δ*htrA* during competitive *in vivo* wound infection with OG1X is not due to slower growth of Δ*htrA* when co-cultured with OG1X in general (**Fig 3.10**), suggesting that *E. faecalis* requires HtrA to process factors that are only present *in vivo,* which could include induced bacterial substrates or host substrates required for better fitness. Future work should include other *in vivo* murine models to investigate if Δ*htrA* also exhibits attenuated fitness in general.

No studies have yet addressed the potential proteolytic activity of HtrA in *E. faecalis* nor have any potential substrates been identified. While we observed a strong secretion defect in Δ*htrA* for PhoZ, we speculate that this phenotype would arise either by $HtrA_{EF}$ activity affecting the Sec secretion machinery directly or acting on secreted Sec substrates. The Sec secretion machinery is the only secretion system present in *E. faecalis*. Disruption of the essential Sec machinery by deleting HtrA would also render the cells to be extremely sick or non-viable (Asai, Kawamura, Sadaie, & Takahashi, 1997). The fact that the loss of $HtrA_{EF}$ does give rise to a growth or viability defect, and does not

affect pilin secretion, as measured by pilus attachment on the cell wall, indicate that $HtrA_{EF}$ does not act directly on the Sec machinery, but instead acts on specific secreted proteins (**Fig 3.11**). The role of HtrA in substrate folding of extracellular proteins has been elucidated in several pathogens, such as *Chlamydia* species, *C. jejuni*, *H. pylori* and *B. subtilis* (Backert, Bernegger, Skorko-Glonek, & Wessler, 2018; Hoy et al., 2012; Huston, Theodoropoulos, Mathews, & Timms, 2008; Tjalsma et al., 2004). In *Chlamydia,* HtrA is transported out into the extracellular space and cleaves host cell-cell junction proteins, such as E-cadherins, enabling paracellular transmigration of bacteria in the host (Wu et al., 2011). In *H. pylori*, HtrA is also secreted into the cell supernatant and cleaves E-cadherin to disrupt adherence junctions of mammalian cells (Hoy et al., 2010). In *B. subtilis*, both HtrA and HtrB are found on the cell membrane as well as secreted into the supernatant where they assist in folding and degradation of misfolded secretory proteins (Tjalsma et al., 2004). Thus, the effect of $HtrA_{EF}$ deletion on PhoZ secretion is not likely due to a general secretion defect but is instead a result of defective HtrA-mediated protein stability and/or maturation.

Due to the increasing concern of the spread of antibiotic resistance pathogens, alternative treatments are urgently required. The discovery of HtrA as a virulence factor in various pathogens suggested that HtrA represents an attractive drug target for the development of anti-infective therapy (**Table 2.2**) (Lawrence et al., 2016; Marsh et al., 2017; Wessler et al., 2017). Taken together, the virulence defect observed in the *E. faecalis* HtrA mutant may also indicate that $HtrA_{EF}$ could be a good drug target for this species as well.

CHAPTER 4: HTRA MONITORS SORTASE-ASSEMBLED PILUS BIOGENESIS IN *ENTEROCOCCUS FAECALIS*

4.1 INTRODUCTION

HtrA is a conserved protease involved in protein quality control that deals with misfolded or accumulated proteins in several bacteria (Missiakas and Raina 1997, Hyyrylainen, Bolhuis et al. 2001, Walsh, Alba et al. 2003, Ehrmann and Clausen 2004). Based on our observation in **Chapter 3**, we hypothesized that $HtrA_{EF}$ is only involved in 'off-pathway' scenarios where proteins are misfolded or mislocalized. We therefore postulate that the absence of *htrA* alone does not cause protein accumulation, and thus does not drive proteins towards 'off-pathway' events. Using Ebp pili as a model sortase substrate, to mimic pilus accumulation and mislocalization, we generated an *htrA* deletion in both Δ*srtA* and Δ*srtC* mutant backgrounds, wherein Δ*srtA* cells are unable to attach polymerized Ebp onto the cell wall, and in Δ*srtC* cells where monomeric pilin subunits are not polymerized, but instead remain anchored in the cell membrane. Both mutants result in retention of pilins/pili on the cell membrane, and we term this as *E. faecalis* 'off-pathway'.

4.2 MATERIALS AND METHODS

4.2.1 Bacterial strains and growth conditions

Bacterial strains and plasmids used in this chapter are listed in **Table 4.1**. Bacteria were propagated according to **Section 3.2.1**.

Table 4.1 | Bacterial Strains and Plasmids used in this study.[a]

Strains or plasmids	Relevant characteristic(s)[b]	References or source
Strains		
Enterococcus faecalis		
OG1RF	Fus^r, Rif^r, derived from OG1	Lab stock
Δ*htrA*	OG1RF isogenic derivative of in-frame *htrA* deletion mutant	Chapter 3
Δ*srtA*	OG1RF isogenic derivative of in-frame *srtA* deletion mutant	(Kline, Kau et al. 2009)
Δ*srtA*Δ*htrA*	OG1RF isogenic derivative of in-frame *srtA* and *htrA* double deletion mutant	This work
Δ*ebpABC*	OG1RF isogenic derivative of in-frame *ebpABC* operon deletion mutant	(Nielsen, Flores-Mireles et al. 2013)
Δ*srtA*Δ*ebpABC*	OG1RF isogenic derivative of in-frame *srtA* and *ebpABC* deletion mutant	(Nielsen, Flores-Mireles et al. 2013)
Δ*srtA*Δ*ebpABC*Δ*htrA*	OG1RF isogenic derivative of in-frame *srtA*, *ebpABC* and *htrA* deletion mutant	This work
Escherichia coli		
Stellar Cells	Routine cloning host when using In-fusion kit	Clontech, USA
DH5α	Routine cloning host	Lab stock
Plasmids		
pGCP123 (p*Empty*)	Expression vector, Km^r	Paulsen, Banerjei et al. 2003
pAL1	Expression vector, Km^r	Kline *et al*, 2009
pGCP213	Temperature sensitive allelic exchange vector, Em^r	Paulsen, Banerjei et al. 2003
p*htrA*	P_{htrA} *htrA* in pGCP123	Chapter 3

Table 4.1 (*Continued*.)		
p*htrA*$_{S271A}$	P_{htrA} *htrA*$_{S271A}$ in pGCP123	This work
p*delta-htrA*	Δ*htrA* deletion allele in pGCP213	Chapter 3
p*srtA*	P_{srtA} *srtA* in pAL1	(Kline, Kau et al. 2009)
p*delta-srtA*	Δ*srtA* deletion allele in pGCP213	(Kline, Kau et al. 2009)
p*ebpABC*	P_{ebpA}*ebpABC* in pGCP123	(Nielsen, Flores-Mireles et al. 2013)
p*ebpABCsrtC*	P_{ebpA}*ebpABC-*P_{srtC} *srtC* in pGCP123	(Nielsen, Flores-Mireles et al. 2013)
p*ebpABC*$_{K186A}$*srtC*	P_{ebpA}*ebpABC*$_{K186A}$*-*P_{srtC} *srtC* in pGCP123	This work
p*ftsW/rodA*	P_{ftsW} *ftsW/rodA* in pGCP123	This work

Abbreviations: Fus, fusidic acid; Rif, rifampin; Km, kanamycin; Em, erythromycin. [a]See Materials and Methods for intermediate strain and plasmid constructions. [b]Superscript "r" indicates resistance.

4.2.2 OG1RF Δ*srtA*Δ*htrA* mutant construction

The deletion construct p*delta-htrA* obtained from **Chapter 3** was transformed into Δ*srtA* strain and screened for the absence of *htrA* according to the previously described method in **Section 3.2.2** and **Section 3.2.4**. We confirmed the absence of HtrA and SrtA expression in *E. faecalis* Δ*srtA*Δ*htrA* by immunoblotting whole cell lysate with anti-HtrA$_{EF}$ and anti-SrtA immune sera, respectively.

4.2.3 OG1RFΔ*ebpABC*Δ*srtA*Δ*htrA* mutant construction

The deletion construct p*delta-htrA* obtained from **Chapter 3** was transformed into Δ*srtA*Δ*ebpABC* strain and screened for the absence of *htrA* according to the previously described method in **Section 3.2.2** and **Section 3.2.4**. We then confirmed the absence of EbpABC, HtrA and SrtA protein expression in Δ*srtA*Δ*ebpABC*Δ*htrA* by immunoblotting whole cell lysate with anti-EbpC, anti-HtrA$_{EF}$, and anti-SrtA immune sera, respectively.

4.2.4 *pGPC123-srtA* construction

Complementation of Δ*srtA*Δ*htrA* with either *htrA* or *srtA* on a plasmid was performed by transformation according to **Section 3.2.2** and protein expression is validated by immunoblotting of whole-cell *E. faecalis* with respective antibodies.

Gene-targeted for mutations as well as designing the primers for complementation and deletion constructs were identified based on the annotated complete genome of *E. faecalis* OG1RF (NCBI accession: NC_017316.1). Molecular techniques and reagents used in this chapter follow according to **Section 3.2.3**. All constructs were confirmed by sequencing and transformed into respective *E. faecalis* mutants. All primer sequences can be found in **Table 4.2**.

4.2.5 Growth Kinetic Assay

WT OG1RF, Δ*htrA,* Δ*srtA* and Δ*srtA*Δ*htrA* were grown overnight, statically in TSB media supplemented with 0.25% glucose. Starter cultures were first diluted 10-fold and grow for 1 h at 37°C. Cells were then normalized to OD_{600} of 0.003 in a final volume of 50 mL media. Cell culture was extracted hourly for measurement of OD and CFU plating on TSBG plates. The plates were incubated at 37°C aerobically for 16 h.

Table 4.2 | Primers used in this study.	
Primer name	Sequence (5'→3')[a]
Complementation	
ftsW_infusion_F_PstI	TTGATATCGAATTCCTGCAGCAGAAATGTGAGCAACACAC AAAAATTATATAAATGTCT
rodA_HA tag	TCAAGCGTAATCTGGAACATCGTATGGGTAAGCGTAATCT GGAACATCGTATGGGTAGGTAGCGGCTTCTCTTCCTTT
rodA_infusion_R_XbaI	TGGCGGCCGCTCTAGATCAAGCGTAATCTGGAACATCGT ATGGGTAA
Deletion	
dHtrAF_ PstI	AAACTGCAGATCTTGGCATAGCTATTTAAACG
dHtrAR_PstI	TCCAATGCATTGGCTGCAGAATACAGCGATTAAAGATGC G
htrA_compF_EcoRI	GCTTGATACGAATTCATTCGATAGACTAAAGGAGTAG
Site-directed mutagenesis[b]	
S271A_F_SDM	GCCATTCAAACCGATGCTGCCATCAATCCAGGAAAC**G**CT G
S271A_R_SDM	GACTTGTCCTTCAATATTGATTAGTGGACCACCAG**C**GTTT
EbpC_K186A_F	GTTGTTCATATTTATCCT**GC**AAATGTAGTAGCCAATGATG
EbpC_K186A_R	CTACATTT**GC**AGGATAAATATGAACAACCGCTAATTCTTC
Universal/ Screening primers	
T7Universal Promoter	TAATACGACTCACTATAGGG
T3Universal Promoter	CAATTAACCCTCACTAAAGG
M13 (-20) F primer	GTAAAACGACGGCCAGTG
M13 (-40) R primer	CAGGAAACAGCTATGAC
EbpC_F	AGCGGGAAAGAAATGAGCGA
EbpC_R	AACGCCACCACCATATTCGT
qPCR primers	
ebpA_F	GGATGGTCGCTTTTACGGGA
ebpA_R	GCCATTGCCTCACCTATCGT
ebpB_F	GCTACTCGCTCTTTTCGGGT
ebpB_R	CTTCCCCTGTGTTTTGCTGC
ebpC_F	CGGTCATACCGACGACCAAA
ebpC_R	TGTCACATCGCCATCGACTT
gyrB_F	CAAGCCAAAACAGGTCGCC
gyrB_R	ACCAACACCGTGCAAGCC
croR_F	ATTTTTGAGCGTGTGTGGCAA
croR_R	TCTCCACCAGTTGCTTCTTCAA
croS_F	AGCTGTTCTCTATTGGCGCT
croS_R	CAAACGGAATGCGGTGATTGT

[a]Restriction sites underlined. Non-complementary sequences to the gene of interest are in red. [b] Site-directed mutagenesis residues are in **boldface**.

4.2.6 Biofilm assay

To induce pili formation, we grow bacteria overnight, statically in 10 mL of TSB media supplemented with 0.25% glucose. Cells were then normalized to OD_{600} of 0.5-0.6 the next day. 8 µL of normalized culture were mixed with 200 µL of media in a 96-well plate (Nunc™ MicroWell™ 96-Well Microplates, Thermo Scientific™, USA). The plates were then incubated at 37°C statically for 24 h to simulate biofilm formation. Following incubation, cells preparation of CV staining was performed according to **Section 3.2.11**. All biofilm assays were performed with three biological replicates, each with 12 technical replicates.

4.2.7 Construction of HtrA and EbpC point mutations using site-directed mutagenesis (SDM)

To construct a HtrA expression plasmid defective of protease activity, extracted p*htrA* was subjected to a single amino acid change on the conserved serine (S271) on *htrA* allele by site-directed mutagenesis (SDM) using S271A_F_SDM/S271A_R_SDM. To construct an EbpABC expression plasmid defective in pilus assembly, extracted p*ebpABCSrtC* was subjected to a single amino acid change on the conserved lysine (K186) of *ebpC* allele using primer pairs EbpC_K186A_F/EbpC_K186A_R. The parameters for the SDM cycle were shown in **Table 4.3**. The sequence was validated using Sanger sequencing and protein expression was validated using immunoblotting with the respective immune sera.

Table 4.3 | Cycling Parameters for QuikChange Site-Directed Mutagenesis.

Segment	Cycles	Temperature	Time
1	1	95°C	30 secs
2	16	95°C	30 secs
		55°C	1 min
		68°C	2.5 mins

4.2.8 Bacterial cell fractionation and Immunoblotting

To detect and measure the amount of pilin protein expressed by *E. faecalis* mutant strains, we perform bacteria cell fractionation according to **Section 3.2.13**, with the exception that whole cell lysate was further subjected to centrifugation at 20, 000 x *g* for 5 mins. The resulting supernatant containing material liberated from the cell wall digestion was designated the cell wall fraction and the pellet designated the cell-wall free fraction. All fractions were stored at -20°C until use. Immunoblotting was done according to **Section 3.2.14**.

4.2.9 Generation of antibodies

Protocol on antibodies generation for use in this chapter was done according to **Section 3.2.7**. Antibodies used in this chapter are listed in **Table 4.4**.

4.2.10 Bacterial cell preparation for immunofluorescence staining

E. faecalis grown in TSBG to mid-log phase were washed and normalized as described above. The cells were fixed with fresh 3% paraformaldehyde for 10 mins and smeared on poly-L-lysine pre-coated slides (Polysciences, Inc., USA). Cells were washed once with 1 X PBS and incubated with 100 times dilution of BODIPY® FL vancomycin (Van-FL) (Thermo Fisher Scientific, Inc., USA) at a final concentration of 5 ng/µL and incubated for 1 h at room temperature in the dark. Vancomycin binds to the terminal D-Ala-D-Ala found on PG precursors or inserted precursors that have not been incorporated at the sites of new cell wall synthesis, which is usually at the septum of the cell (Reynolds 1989). Van-FL is a fluorescent stain that targets the nascent PG. To visualize DNA, we added DAPI stain to the fixed cells at a final concentration of 2.5 ng/µL and incubated for 15 mins at room temperature in the dark. Cells were then blocked with filtered 2% P-BSA prior to adding 20 µL of respective primary antibody on to fixed cells and incubated

overnight in 4°C, shaking. The primary antibody was paired with the respective Alexa Fluor® labeled secondary antibody and incubated at room temperature for 1 h. Finally, we mount the slide with mounting media (Vectashield®, USA) and coverslip for 30 mins before imaging or stored at 4°C in the dark prior to imaging with super-resolution structured illumination microscopy (SR-SIM) (Carl Zeiss, Germany) or inverted epi-fluorescence microscope (Zeiss Axio Observer Z1, Germany). Details on imaging using LSM 780 ELYRA PS.1 system were performed according to **Section 3.2.9**.

Table 4.4 | Antibodies used in this chapter.

*Antigen**	*Size (kDa)*	*Primary ab; host*	*Secondary antibody; host*
EbpA	122.7	1:3000; Rabbit	1:5000; Goat anti-rabbit HRP-conjugate
EbpB	53.4	1:3000; Rabbit	1:5000; Goat anti-rabbit HRP-conjugate
EbpC	68.2	1:3000; Guinea pig	1:5000; Goat anti-guinea pig HRP conjugate 1:500; Alexa Fluor® 568 labeled goat anti-guinea pig
HtrA	45.7	1:1000; Rat	1: 5000; Goat anti-rat HRP-conjugate
SecA	97.0	1: 3000; Rabbit	1: 5000 Goat anti-rabbit HRP-conjugate
SrtA	27.1	1: 250; Mouse	1:1250; Goat anti-mouse HRP-conjugate
SrtC	32.0	1:250; Mouse	1:1250; Goat anti-mouse HRP-conjugate

*Construct sequence can be found in **Supplementary Table A1**.

4.2.11 Visualization of bacterial chain length with phase contrast microscopy

To visualize chain length, 5 µL of the culture was mixed with an equal volume of low melting agar (BioWorld, USA) on a glass slide before covering it with a coverslip. The slides were visualized using a phase contrast microscope (Zeiss Axio Observer Z1; Carl Zeiss GmbH) fitted with a 100X oil immersion objective with a numerical aperture 1.4

optovar 1.0 magnification changer 1.5X. Images were collected with AxioVision (Carl Zeiss Zen 8.0 and analyzed with ImageJ (http://rsb.info.nih.gov/ij/).

4.2.12 Transmission Electron Microscopy (TEM)

For ultrastructural analysis, we grow *E. faecalis* strains overnight and sub-cultured 1:10 into 20 mL TSBG media and grown to mid-log phase. We fixed the bacteria in 2% paraformaldehyde/2.5% glutaraldehyde in 100 mM phosphate buffer, pH 7.4 for 1 h at room temperature, washed in phosphate buffer, and post-fixed in 1% osmium tetroxide (Polysciences Inc.) for 1 h. Samples were then rinsed extensively in deionized water prior to en bloc staining with 1% aqueous uranyl acetate (Ted Pella Inc., Redding, CA) for 1 hr. Following several rinses in deionized water, we dehydrated the samples in a graded series of ethanol and embedded in Eponate 12 resin (Ted Pella Inc.). Sections of 95 nm were cut with a Leica Ultracut UCT ultramicrotome (Leica Microsystems Inc., Bannockburn, IL), stained with uranyl acetate and lead citrate, and viewed on a JEOL 1200 EX transmission electron microscope (JEOL USA Inc., Peabody, MA) equipped with an AMT 8-megapixel digital camera and AMT Image Capture Engine V602 software (Advanced Microscopy Techniques, Woburn, MA).

4.2.13 Quantitative analysis of fluorescent foci and cell length

Images were collected with AxioVision (Carl Zeiss Zen 8.0 and analyzed with ImageJ (Schindelin, Arganda-Carreras et al. 2012). We performed post-image analysis using **P**rojected **S**ystem of **I**nternal **C**oordinates from **I**nterpolated **C**ontours (PSICIC), which is a modular set of MATLAB functions designed to find smooth cell borders from phase contrast microscope images and establish an internal coordinate system for each individual cell (Guberman, Fay et al. 2008). Briefly, the perimeter fluorescence intensity

profiles of detected cells were calculated by sampling intensity values in pixels identified by using PSICIC at the cell border. These intensity values then were plotted against the total distance along the cell border at which they were found. Quantitative analysis was performed on at least 1000 cells per condition, from at least three independent experiments. The maximum cell width is measured using MicrobeJ, a plug-in for the open-source platform ImageJ (Ducret, Quardokus et al. 2016). Quantitative analysis was performed on at least 500 cells per condition, from at least three independent experiments.

4.2.14 RNA extraction and purification

For mRNA transcriptomic analyses, we grew the bacteria overnight, statically in TSBG media at 37°C. The next morning, cultures were diluted 1:10 and grown to an optical density (600 nm) of 0.5. Total RNA was extracted using the UltraClean® Microbial RNA Isolation Kit (MO BIO Laboratories Inc., Singapore). Extracted RNA samples were subjected to rigorous DNase treatment using TURBO DNA-free™ kit (Ambion®, Singapore) and purified DNA-free RNA samples were subjected to ribosomal depletion with Ribo-Zero™ Magnetic Kits (Epicenter®, Singapore), all according to manufacturer's protocols. Quantification of RNA and DNA were performed using the Qubit™ RNA Assay Kits and Qubit™ dsDNA HS Assay Kits (Invitrogen, Singapore), respectively. The integrity of RNA was analyzed by gel electrophoresis using Agilent RNA ScreenTape (Agilent Technologies, Singapore). RNA samples were prepared in triplicate from three independent biological samples.

4.2.15 mRNA library preparation and Illumina sequencing

To convert depleted rRNA into double-stranded cDNA for sequencing, we performed cDNA synthesis (NEBNext RNA First-Strand Synthesis Module; NEBNext Ultra Directional RNA Second Strand Synthesis Module, NEB, Singapore) and purification of cDNA (AMPure XP beads, Beckman Coulter, Singapore) as described previously. mRNA libraries for RNA sequencing were prepared using TruSeq Stranded mRNA Library Prep Kit (Illumina, USA), the quality of the library analyzed via Bioanalyzer (Agilent, USA), and sequencing performed using an Illumina Miseq V2 machine. RNA sequencing reads were mapped to the *E. faecalis* OG1RF reference genome (NCBI accession: NC_017316.1) using BWA (v0.5.9) with default parameters (Li and Durbin 2009, Nagalakshmi, Waern et al. 2010). Sequencing reads mapping to predicted open reading frames (ORFs) were quantified using HTSeq (Anders, Pyl et al. 2015). Counts for ribosomal and transfer RNA sequences were filtered out of the data set and differential expression analyses were performed in R (Version 2.15.1) using the Bioconductor package, edgeR (Robinson et al., 2010). Significantly differentially expressed genes were determined using a P-value and false discovery rate (FDR) cut off of 0.05. We annotated differentially expressed genes using a combination of KEGG annotations, as well as manual annotation using operon and other functional data from the literature.

4.2.16 pP_{ftsW}-*ftsW/rodA* construction

The expression construct of *ftsW/rodA* operon was cloned into p*Empty* using a two-step PCR amplification. We constructed a *ftsW/rodA* expression vector by amplifying the fts*W/rodA* coding sequence plus 200 bp upstream of the *ftsW* start codon to include its native promoter and two HA tags at the downstream of *rodA* with ftsW_infusion_F_PstI/rodA_HA tag. The second PCR amplification was performed using

ftsW_infusion_F_PstI/rodA_infusion_R_XbaI to include the homologous region of the vector at 5' and 3' of the PCR product for infusion cloning (Clontech, USA), where primers included homologous sequences to the vectors and insert of interest into the vector proceeds via homologous recombination. We verified the expression and stability of FtsW/RodA protein from the expression plasmid by immunoblot with anti-HA immune serum.

4.2.17 qRT-PCR

4900 ng of DNA-depleted RNA was converted to complementary DNA (cDNA) using Superscript® III First-Strand Synthesis System Kit (Invitrogen, USA). Following cDNA synthesis, 0.09 ng of cDNA per well was used in qRT-PCR with KAPA SYBP® FAST qPCR Kit MasterMix (2X) (KAPA Biosystems, USA) in StepOnePlus™ Real-Time PCR System (Applied Biosystems, USA). No amplification was observed for no-template control in qPCR reaction (Ct value above 35). To compare the differences between the target genes, the $\Delta\Delta C_T$ method was used (Livak & Schmittgen, 2001). Prior to the $\Delta\Delta C_T$ analysis, qPCR data was validated by running a standard curve for each gene as described in Applied Biosystems User Bulletin No.2 (P/N 4303859) and elsewhere (Livak & Schmittgen, 2001). The housekeeping gene gyrase B (*gyrB*) was used as an endogenous control in this study (Djoric & Kristich, 2015, 2017). Primers used in the study are listed in Table 4.2 and were generated using NCBI primer design software (Primer-BLAST) to amplify PCR products of size between 100- 150 bp.

4.2.18 Statistical analyses

Data from multiple experiments were pooled. Statistical significance for biofilm assay was determined using a two-tailed unpaired t-test. Statistical significance with the

percentage of cells expressing pilin was determined using the unpaired t-test. Statistical significance with the number of division septa per cell unit was determined using the Holm-Sidak method. Unless otherwise stated, values represented means ± SEM derived from at least three independent experiments and/ or three technical replicates. * $P < 0.05$; ** $P \leq 0.01$; *** $P \leq 0.001$; **** $P \leq 0.0001$; $P \geq 0.05$, differences not significant (n.s). GraphPad Prism 6 software (GraphPad Software, La Jolla, CA) was used for statistical analyses.

4.3 RESULTS

4.3.1 Construction of Δ*srtA*Δ*htrA* and Δ*srtC*Δ*htrA* mutations in *E. faecalis* OG1RF

To investigate if HtrA is required to remove 'off-pathway' pilus substrates, we generated Δ*srtA*Δ*htrA* and Δ*srtC*Δ*htrA*. In the Δ*srtA*Δ*htrA* strain, we expect that the polymerized pili are retained on the membrane; whereas, in Δ*srtC*Δ*htrA,* monomeric pilin subunits are expected to be retained on the membrane (**Fig 4.1A**). Successful mutants were validated by immunoblots of *E. faecalis* whole cell lysates (**Fig 4.1B**). Preliminary examination of Δ*srtC*Δ*htrA* revealed the unexpected finding that overall pilus gene expression was downregulated for reasons we did not explore in this thesis, and hence we did not proceed further with the Δ*srtC*Δ*htrA* mutant, but we will discuss it in **Section 6.2.5**. In this chapter, we solely focus on Δ*srtA*Δ*htrA*. We anticipated that in this genetic background, new insights into the mechanism of HtrA actions could be gained since pili would accumulate on the membrane in the absence of SrtA and be more amenable to study (**Fig 4.1B**).

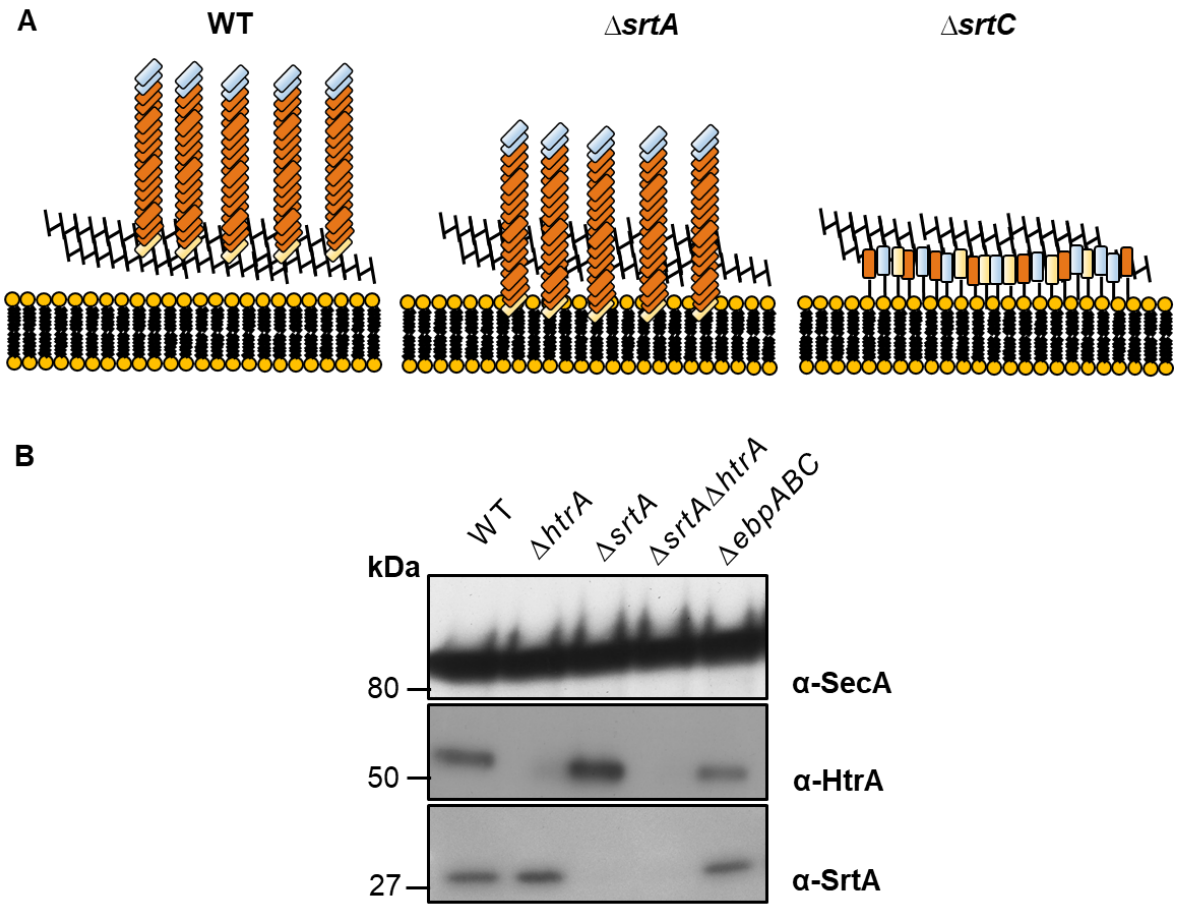

Figure 4.1 | Construction and validation of Δ*srtA*Δ*htrA* mutant. (**A**) Schematic diagram of pili localization in WT, Δ*srtA* and Δ*srtC* background. (**B**) Validation by immunoblot was performed with α-HtrA$_{EF}$ and α-SrtA immune sera on whole cell lysates of WT (positive control), Δ*htrA* (negative control), Δ*srtA* (negative control) and Δ*srtA*Δ*htrA* strains. PageRuler^{TM} pre-stained protein gel (10-250 kDa) was used as ladder.

4.3.2 Growth kinetics and biofilm formation by Δ*srtA*Δ*htrA* mutant

We compared the growth between WT and Δ*srtA*Δ*htrA*. In contrast to WT, Δ*srtA*Δ*htrA* shows higher OD readings despite having similar CFU (**Fig 4.2A and B)**, suggesting that cells aggregate and/or exhibit altered morphology in the presence of *ΔsrtA*-induced membrane stress without the HtrA protease.

Because sortase-assembled Ebp pili play a role in biofilm formation and Δ*srtA* forms poor biofilms *in vitro* (Guiton, Hung et al. 2009, Guiton, Hung et al. 2010), we examined the biofilm-forming capacity of Δ*srtA*Δ*htrA* on microtiter plates. We observed

that Δ*srtA*Δ*htrA* is slightly attenuated in the biofilm-forming capacity as compared to Δ*srtA* (**Fig 4.2C**). The significant decrease in biofilm-forming capability in Δ*srtA*Δ*htrA* suggests that the loss of $HtrA_{EF}$ may contributes to biofilm formation in the presence of membrane stress.

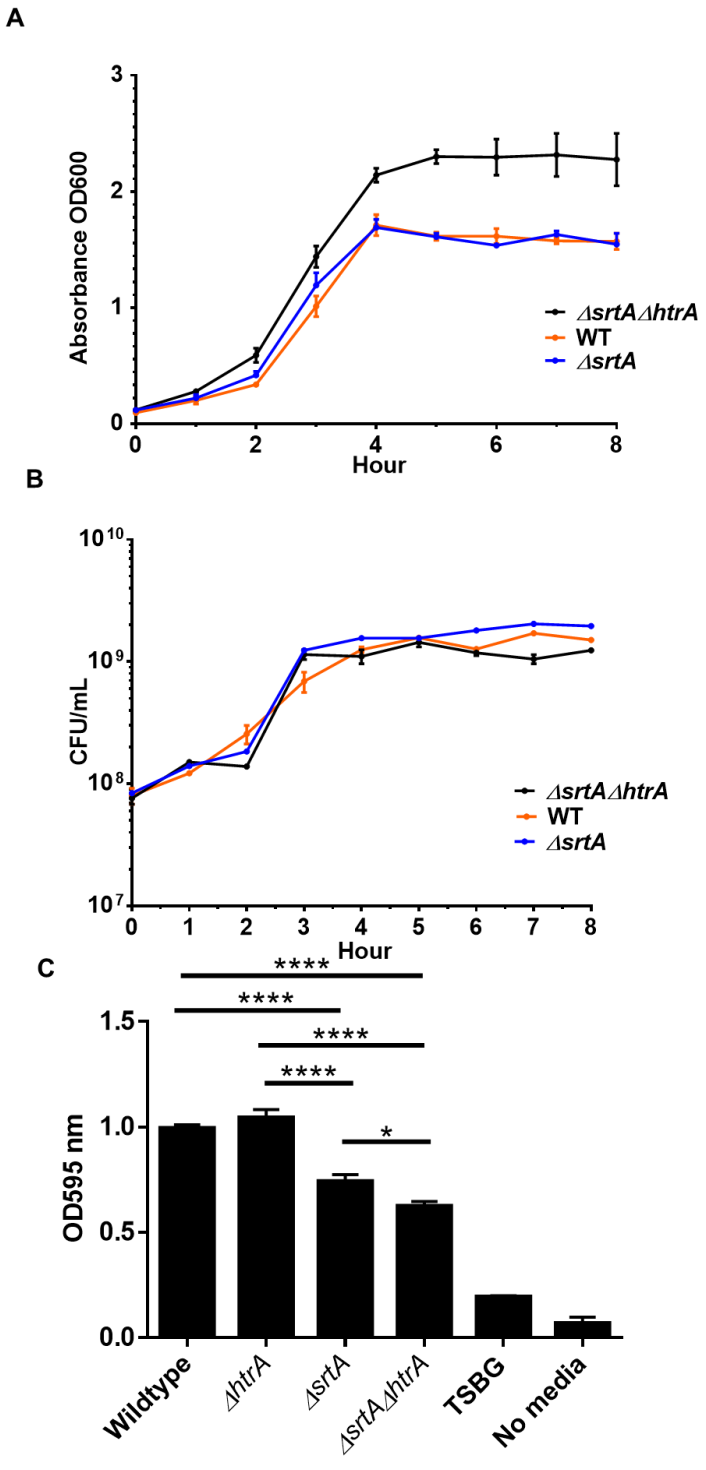

Figure 4.2 | Growth kinetics and biofilm formation by Δ*srtA*Δ*htrA*. (**A**) The OD readings and (**B**) the CFU/mL for growth kinetic assays for WT (**orange**), Δ*srtA* (**blue**) and Δ*srtA*Δ*htrA* (**black**) at 37°C. The data shown are from two independent experiments. The error bar represents the standard error of mean. (**C**) Biofilm formation of Δ*srtA* and Δ*srtA*Δ*htrA* in TSBG for 48 h at 37°C. Mean results are represented as bar graphs with a

standard error of the mean. Combined data from two independent experiments were shown. Statistical significance for biofilm assay was determined using a two-tailed unpaired t-test. **** $P \leq 0.0001$; * $P < 0.05$.

4.3.3 HtrA is needed for the removal of mistargeted Ebp pili in *E. faecalis*

DegP (HtrA) is involved in the removal of accumulated misfolded PapE pilin subunits in *E. coli* via the Cpx and σ^E systems (Jones, Danese et al. 1997). In *E. faecalis, srtA* deletion results in retention and accumulation of sortase substrates, such as mature polymerized Ebp pili, on the membrane of the cell (Nielsen, Flores-Mireles et al. 2013). If $HtrA_{EF}$ is involved in 'off-pathway' processing of mislocalized pili in *E. faecalis*, we would expect to see a greater accumulation of pili in Δ*srtA*Δ*htrA* on the membrane. To investigate if the absence of *htrA* and *srtA* affect Ebp pilus production, we performed immunoblot analysis on the protoplast fractions of WT, Δ*srtA,* Δ*htrA,* and Δ*srtA*Δ*htrA* with anti-EbpC immune serum. We found that the level of the major subunit EbpC was 4.6-fold higher in the membrane fraction of Δ*srtA*Δ*htrA* as compared to Δ*srtA*, whereas the loading control for expression of SecA was unaffected (**Fig 4.3**). This phenotype was not EbpC-specific as we observed similar trends with minor subunits, EbpA or EbpB (**Supplementary Fig B1**).

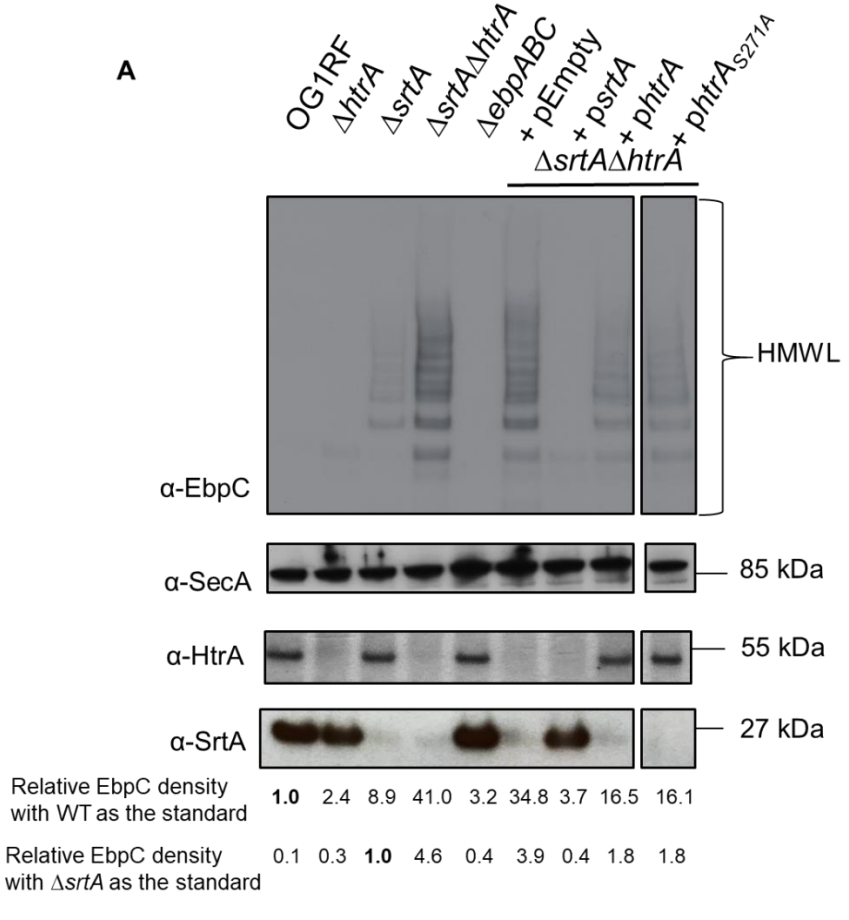
A
OG1RF
ΔhtrA
ΔsrtA
ΔsrtAΔhtrA
ΔebpABC
+ pEmpty
+ psrtA
+ phtrA
+ phtrAS271A
ΔsrtAΔhtrA
HMWL
α-EbpC
α-SecA
85 kDa
α-HtrA
55 kDa
α-SrtA
27 kDa
Relative EbpC density with WT as the standard
1.0 2.4 8.9 41.0 3.2 34.8 3.7 16.5 16.1
Relative EbpC density with ΔsrtA as the standard
0.1 0.3 1.0 4.6 0.4 3.9 0.4 1.8 1.8

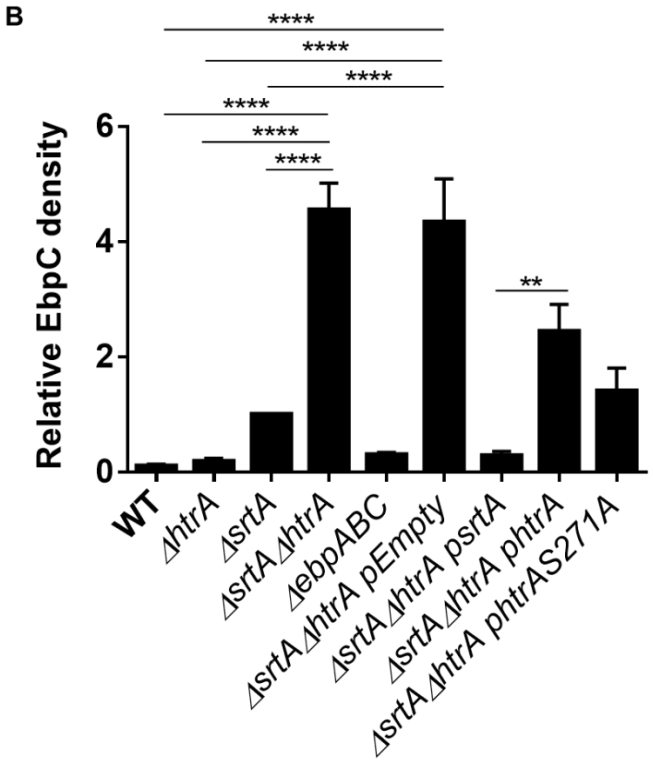
B
Relative EbpC density
0
2
4
6
****
****
****
****
****
****
**
WT
ΔhtrA
ΔsrtA
ΔsrtAΔhtrA
ΔebpABC
ΔsrtAΔhtrA pEmpty
ΔsrtAΔhtrA psrtA
ΔsrtAΔhtrA phtrA
ΔsrtAΔhtrA phtrAS271A

Figure 4.3 | Increased EbpC protein levels in Δ*srtA*Δ*htrA*. (A) Immunoblot was performed with α-EbpC immune serum on protoplast fractions of WT, Δ*htrA,* Δ*srtA,* Δ*srtA*Δ*htrA;* Δ*srtA*Δ*htrA* strains carrying p*Empty* (vector control), p*htrA,* p*srtA* or p$htrA_{S271A}$ and Δ*ebpABC* (Ebp-negative control) for EbpC staining. The top blot shows pilus HMWL (brackets) and α-SecA immune serum was used as a loading control. Both α-$HtrA_{EF}$ and α-SrtA immune sera were included as additional loading controls and for strain validation. PageRuler™ pre-stained protein gel (10-250 kDa) was used as the ladder. Relative EbpC densities differences were calculated with WT or the Δ*srtA* EbpC expression as the standard. One irrelevant lane between Δ*srtA*Δ*htrA* p*srtA* and p$htrA_{S271A}$ was omitted for clarity, and this omission is indicated by the break in the frame. (**B**) Statistical analyses of relative EbpC density from four independent experiments, using Δ*srtA* as the comparison standard, are represented as bar graphs with the standard error of the mean. ** P ≤ 0.01; **** P ≤ 0.0001; P ≥ 0.05 (n.s). Combined data from four independent experiments were shown.

Approximately 10-20% of *E. faecalis* WT cells grown under laboratory conditions typically express Ebp (Nallapareddy, Singh et al. 2006). To determine whether increased Ebp protein expression observed on the immunoblot of Δ*srtA*Δ*htrA* affects the frequency of piliation in the total cell population, we performed immunofluorescent labeling for EbpC. Eighty percent of Δ*srtA*Δ*htrA* cells expressed pili as compared to WT (15%), Δ*srtA* (60%) and Δ*htrA* (30%) (**Fig 4.4A and B**). In the absence of SrtA, accumulation of Ebp correlates with the increased population and increased pilus abundance (Kline, Kau et al. 2009, Nielsen, Flores-Mireles et al. 2013). A further increase in pilus abundance in Δ*srtA*Δ*htrA* suggests that the absence of $HtrA_{EF}$ further contributes to pilus abundance.

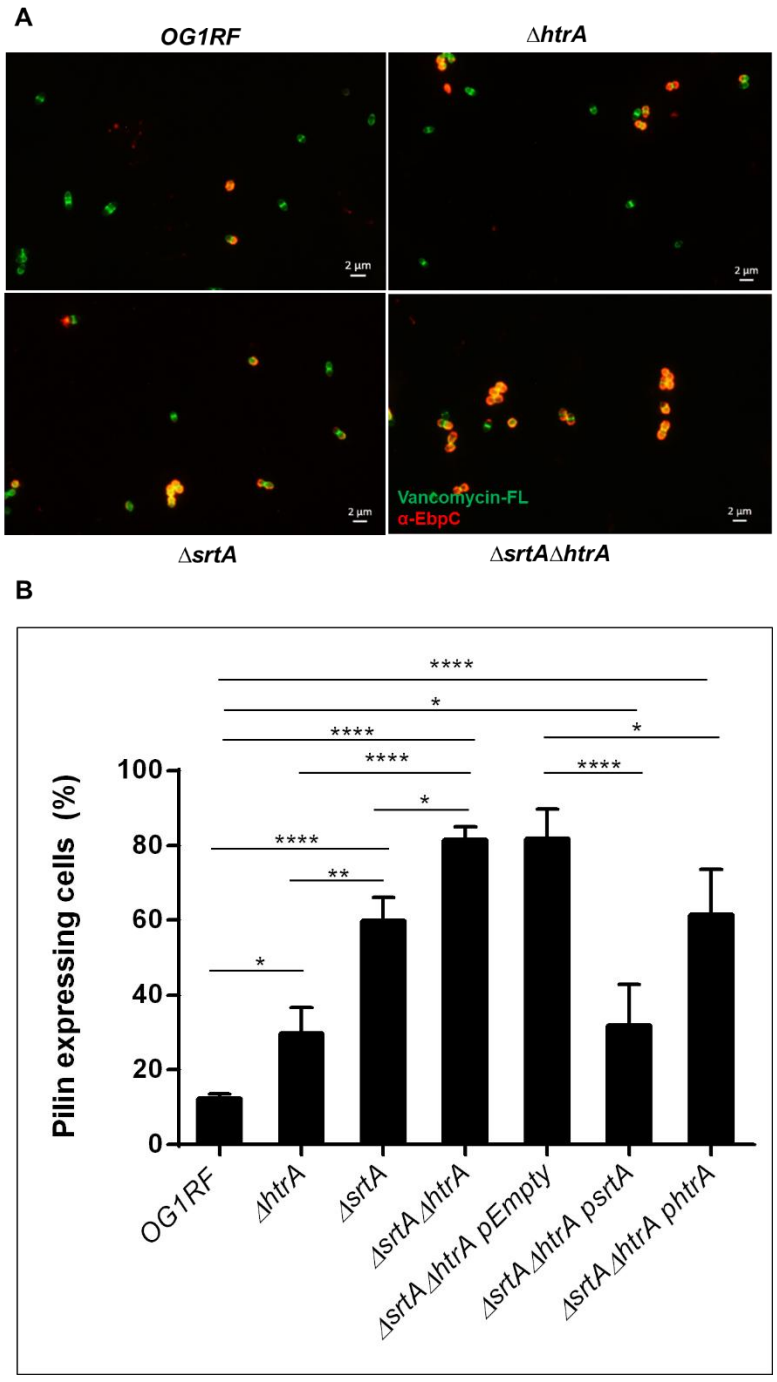

Figure 4.4 | Increased pilin expressing cells in Δ*srtA*Δ*htrA*. (**A**) Pili were visualized with α-EbpC immune serum coupled to Alexa Fluor® 568 secondary antibody (red). Cells were stained with vancomycin-FL that targets the nascent PG. Scale bar represents 2 µm. (**B**) Statistical analyses of pilus-expressing cells of WT, Δ*htrA,* Δ*srtA,* Δ*srtA*Δ*htrA;* Δ*srtA*Δ*htrA* strains carrying p*Empty* (vector control), p*srtA* or p*htrA,* labeled with anti-EbpC immune serum and Alexa Fluor® 568 secondary antibody. Mean results are represented as bar graphs with standard deviation. * $P < 0.05$; ** $P \leq 0.01$; $P \geq 0.05$,

differences not significant (n.s). Combined data from three independent experiments were shown.

4.3.4 HtrA chaperone function is sufficient to restore Ebp pilus expression

Most HtrAs possess dual functions as a protease and a chaperone. However, it is not necessary for HtrA to perform both functions for its role in virulence. In *C. jejuni,* HtrA chaperone plays a major role in host cell binding, while the protease function plays a minor role in host cell interactions (Baek, Vegge et al. 2011). On the other hand, *S. typhimurium* requires both proteolytic and chaperone function of HtrA to survive in the murine liver and spleen (Lewis, Skovierova et al. 2009). To investigate which of these activities are important for regulation of pilus biogenesis during 'off-pathway' conditions, we designed an expression plasmid of $HtrA_{EF}$ with a single amino-acid change at the conserved serine (S271A) in the proteolytic active site causing the protein to lack protease activity but retaining chaperone activity. Immunoblot analysis revealed a decrease in the total pilus levels in the membrane fraction of Δ*srtA*Δ*htrA* complemented with p$htrA_{S271A}$ (**Lane 9**), similar to Δ*srtA*Δ*htrA* complemented with WT *phtrA* (**Lane 8**) (**Fig 4.3**) suggesting that HtrA protease activity does not significantly contribute to the increased piliation phenotype of the double mutant, and instead suggest that HtrA chaperone activity may be sufficient to alleviate membrane stress.

4.3.5 HtrA interacts with EbpC, DnaK, and SrtA

In *E. coli*, under normal laboratory conditions, assembly of P pilin subunits is dependent on the PapD-like periplasmic chaperone (Jones, Danese et al. 1997). In the absence of the PapD chaperone, these pilin subunits accumulate and are driven 'off-pathway' via non-productive interactions involving Deg proteases, Cpx, and σ^E systems (Danese, Snyder et al. 1995, Danese and Silhavy 1997, Jones, Danese et al. 1997).

Similarly, in *E. faecalis* in the absence of SrtA, pilus assembly goes 'off-pathway' and $HtrA_{EF}$ may function similarly under these conditions. We sought further evidence to support an interaction between HtrA and Ebp pili using a bacterial two-hybrid (BacTH) system. This system detects protein-protein interactions by the means of activation of a reporter-gene expression. Two putative interacting proteins are genetically fused to the DNA-binding domain of a transcription factor and to a transcriptional activation domain, respectively. A productive interaction between the two proteins of interest will bring the transcriptional activation domain in the proximity of the DNA-binding domain and will trigger the transcription of *lacZ* reporter gene, giving rise to blue colonies (**Fig 4.5**). In addition, we observe that $HtrA_{EF}$ also interacts with DnaK and SrtA, and EbpC also interacts with DnaK (**Fig 4.5**) (Mitra, S., and Afonina, I., unpublished data). These data might suggest that DnaK functions as a chaperone in pilus biogenesis, perhaps analogous to PapD in *E. coli* P pilus biogenesis.

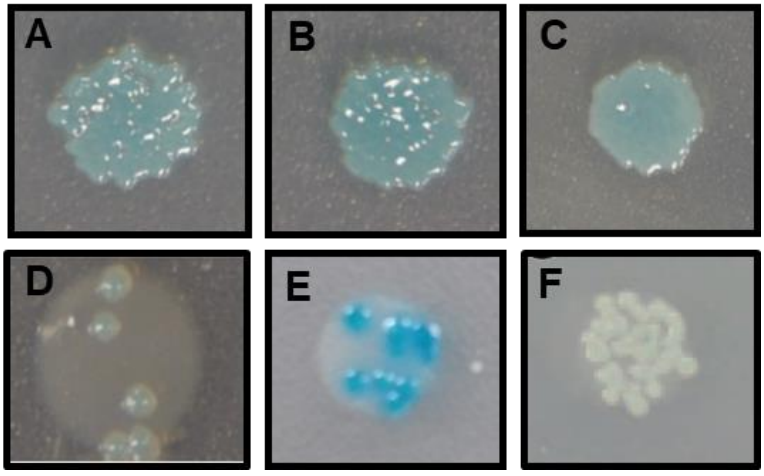

Figure 4.5 | HtrA interacts with EbpC, DnaK, and SrtA. (**A**) Bacterial two-hybrid showing interaction between T18-HtrA and T25-DnaK, (**B**) T18-HtrA and T25-EbpC, (**C**) T18-DnaK and T25-EbpC, (**D**) T18-HtrA and T25-SrtA, (**E**) T25-zip and T18-zip (positive control) and (**F**) T18-HtrA and T25-zip (negative control). Blue colonies indicate a positive interaction.

4.3.6 Localization of Ebp pili is not affected in a Δ*srtA*Δ*htrA* mutant

To investigate if the upregulation of *ebp* expression and increased surface deposition of Ebp pili in *E. faecalis* lacking SrtA and HtrA affects its subcellular localization, we employed immunofluorescence analysis (IFA) on WT, Δ*srtA,* Δ*htrA* and Δ*srtA*Δ*htrA* using α-EbpC polyclonal antibody coupled with Alexa Fluor® 568 secondary antibody. In the WT cells, once the pilin subunits get polymerized by SrtC, SrtA attaches the mature Ebp pilus onto the cell wall before it gets distributed throughout the cell surface (Kline, Kau et al. 2009). In mature WT and Δ*htrA* cells*,* EbpC is found in a hemispherical pattern at the poles of the cells and is excluded from the septum (**Fig 4.6**)*.* When SrtA is absent, pilin subunits get polymerized by SrtC but the Ebp pili never get attached to the cell wall and are instead retained on the cell membrane. We, therefore, postulate that visible EbpC staining in Δ*srtA* and Δ*srtA*Δ*htrA* are due to the membrane-anchored pili that protrude out of the cell wall. IFA of Δ*srtA* and Δ*srtA*Δ*htrA* revealed a similar EbpC localization pattern as WT and Δ*htrA.* To distinguish the cell wall, we visualized peptidoglycan (PG) using a vancomycin-fluorescein (Van-FL) dye. Vancomycin binds to the terminal D-Ala-D-Ala found on PG precursors or inserted precursors that have not been incorporated at the sites of new cell wall synthesis, which is usually at the septum of the cell (Reynolds 1989).

To discern protein localization features at sub-pixel scales, we implemented the PSICIC computational approach for the quantitative, high-throughput analysis of cellular images (Guberman, Fay et al. 2008). In the WT OG1RF, PSICIC analyses discern the hemispherical localization and septal exclusion of Ebp pili, as indicated by the 2 distinct peaks at cell perimeter between 21-41 and 61-81 of the PSICIC graph (**Fig 4.7**). Even

though Δ*srtA*, Δ*htrA*, and Δ*srtA*Δ*htrA* also exhibit hemispherical localization and septal exclusion of Ebp pili as shown in **Fig 4.6**, the PSICIC analysis revealed less distinct peaks for the three mutant strains (**Fig 4.7**). This may suggest that distribution of the Ebp pili is mildly affected in the absence of *srtA* and/or *htrA*, which can only be quantified using PSICIC analysis. PSICIC analysis may also suggest that the amount the Ebp pili produced in these mutant strains is not enough to be distributed at the poles causing the intensity of the fluorescent at the peaks to be lower than that in the WT strain.

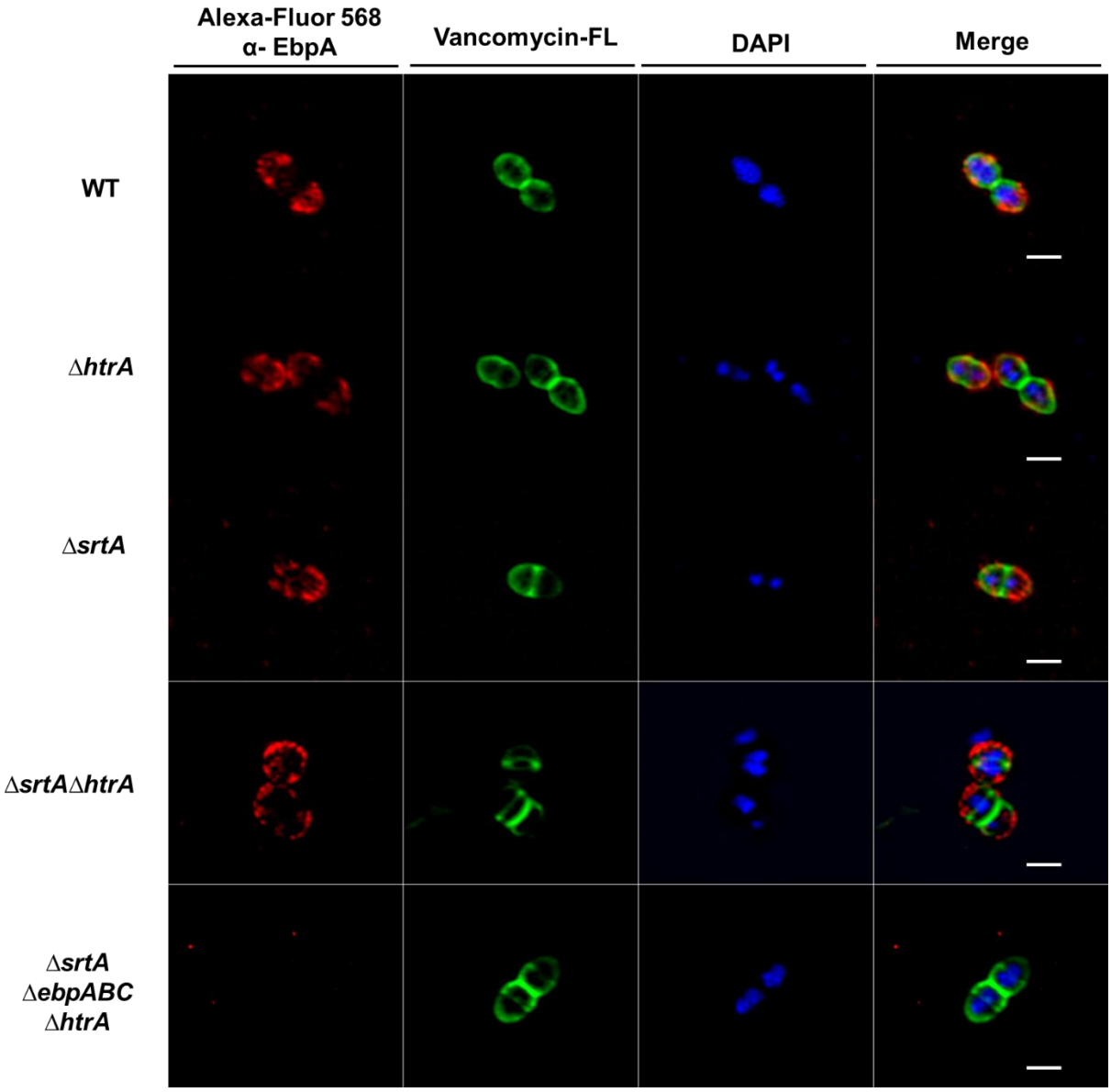

Figure 4.6 | Localization pattern of Ebp pili on Δ*srtA*Δ*htrA*. The cell wall was stained with Van- FL conjugate (green), blocked and incubated with anti-EbpC immune serum coupled to Alexa Fluor® 568 antibody (red). DAPI (blue) was used to visualize DNA. Δ*ebpABC* strain served as a negative control for EbpC staining. Representative images were shown. The scale bar represents 2 µm. A total of at least 200 cells were sampled per strain.

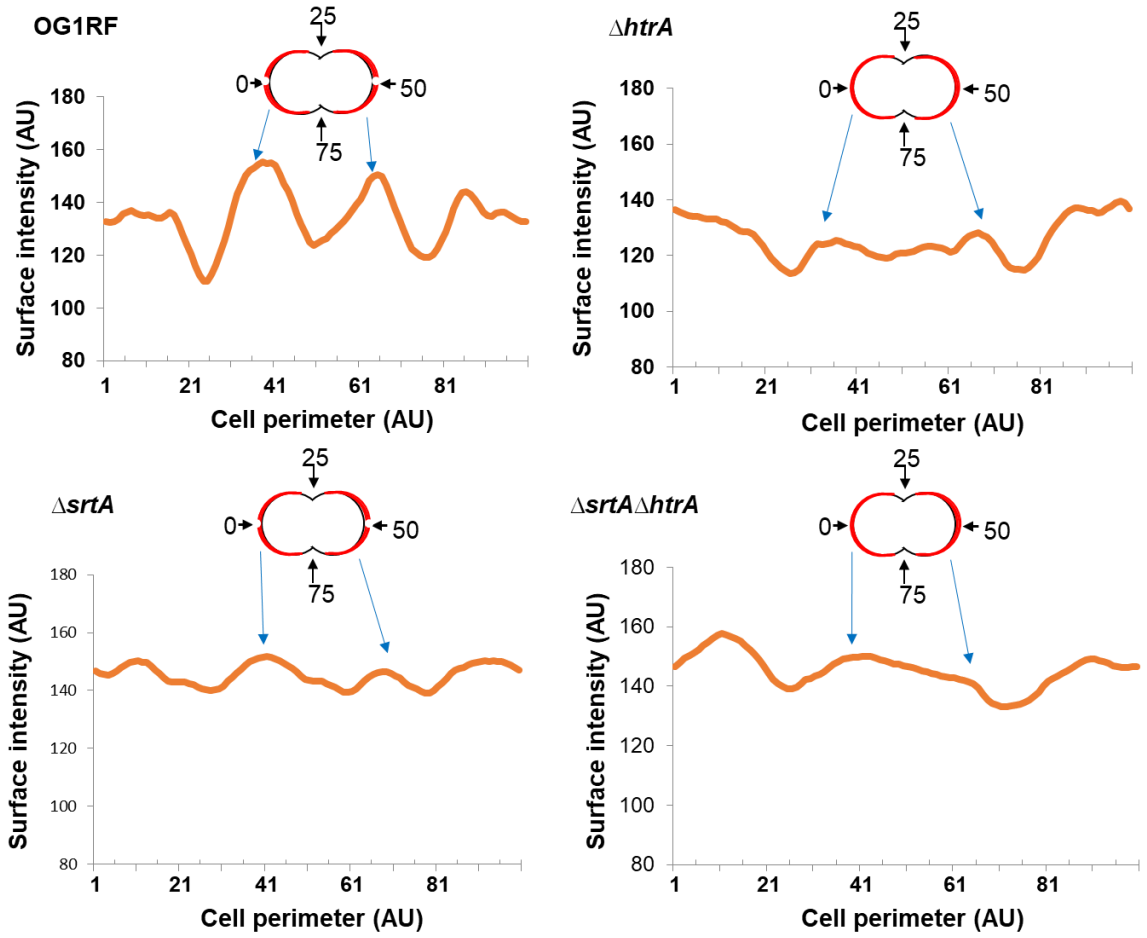

Figure 4.7 | Localization pattern of Ebp pili on Δ*srtA*Δ*htrA* using PSICIC. Graphs depict predominant sites of EbpC localization in WT, Δ*htrA,* Δ*srtA* and Δ*srtA*Δ*htrA* strains. Cells in which no fluorescence was detected were excluded from the analyses. Intensity analysis performed in PSICIC (MATLAB). The coordinates of the perimeter that correspond with the X-axes were also shown. The line indicated the mean fluorescence at each point on the perimeter of at least 500 mid-log cells.

4.3.7 Absence of *srtA* and *htrA* results in chaining of cells

While examining Δ*srtA*Δ*htrA* for pilus expression, we noticed a striking phenotype characterized by the presence of chains containing about 4-8 tightly joined cells in a subset of the population (**Fig 4.8A**). The chaining phenotype of Δ*srtA*Δ*htrA* could be complemented with p*htrA* or p*srtA,* but not with the empty vector control, p*Empty* resulting in a reversion to a diplo-ovococcal shape similar to WT (**Fig 4.8A**).

Analysis of cell length confirmed the chaining phenotype and showed that WT and strains that lack either *htrA* or *srtA*, but not both, have most cells with chain length between 1.5- 2.0 µm, while Δ*srtA*Δ*htrA* strain has cells with chain length more than 4 µm and can span to 23 µm due to the chaining phenotype (**Fig 4.8B**). These data suggest that HtrA is required for *E. faecalis* to clear the accumulated pilin proteins, and if not, excess pili accumulation could result in growth deformities, that will, in turn, affects the cell viability as shown in **Fig 4.2**.

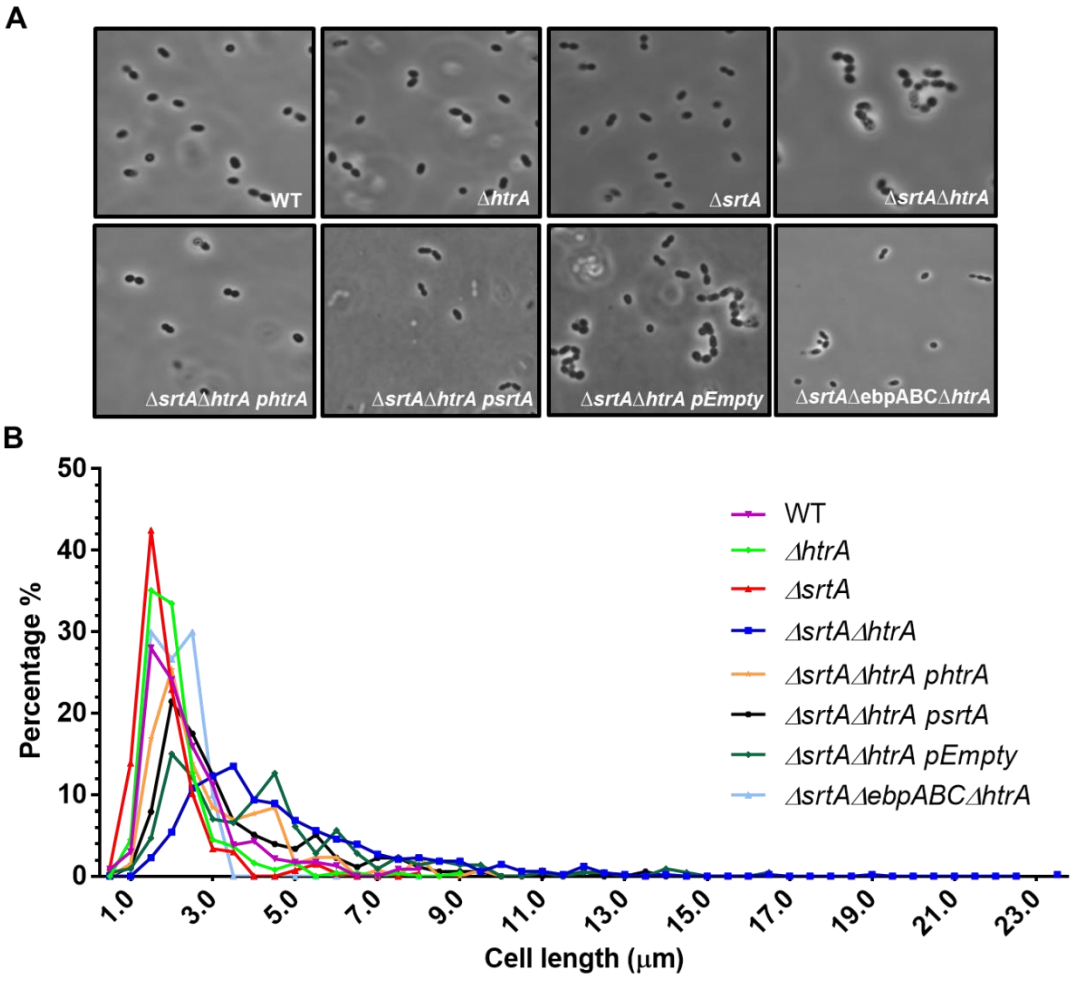

Figure 4.8 | Chaining morphology observed in Δ*srtA*Δ*htrA*. (**A**) Morphology of indicated *E. faecalis* strains was visualized at a magnification of 100X with a phase contrast microscope. Representative images were shown. Chaining morphology diminished upon complementation of Δ*srtA*Δ*htrA* with p*htrA or* p*srtA,* but not with p*Empty*.

(**B**) The relative cell length of the bacterial population was determined by measuring the mid-length of the cells using PSICIC and ImageJ. Cells that were not in-phase were excluded from the analysis. A total of at least 200 cells were sampled per strains.

4.3.8 Deletion of *E. faecalis srtA* and *htrA* results in aberrant cell morphology

To gain more insight into the morphology defects observed in Δ*srtA*Δ*htrA*, which were suggestive of a defect in cell division or cell elongation mechanisms at the peptidoglycan (PG) level, we visualized PG using a vancomycin-fluorescein (Van-FL) dye. Vancomycin binds to the terminal D-Ala-D-Ala found on PG precursors or inserted precursors that have not been incorporated at the sites of new cell wall synthesis, which is usually at the septum of the cell (Reynolds 1989). Apart from the chained cells, individual Δ*srtA*Δ*htrA* cells appear fatter, shorter and rounder than WT (**Fig 4.9A**), suggesting a defect in cell elongation mechanism as well. In addition, Van-FL labeling of Δ*srtA*Δ*htrA* cells revealed aberrant placement of septa across 30% of the cell population that was not apparent for Δ*srtA* or Δ*htrA* (**Fig 4.9B**) indicating that cell separation may also be affected. As a control, we checked that Van-FL labeled a single band at the division plane in WT cells as previously described using fluorescent vancomycin in *B. subtilis* (Daniel and Errington 2003) (**Fig 4.9A, WT**).

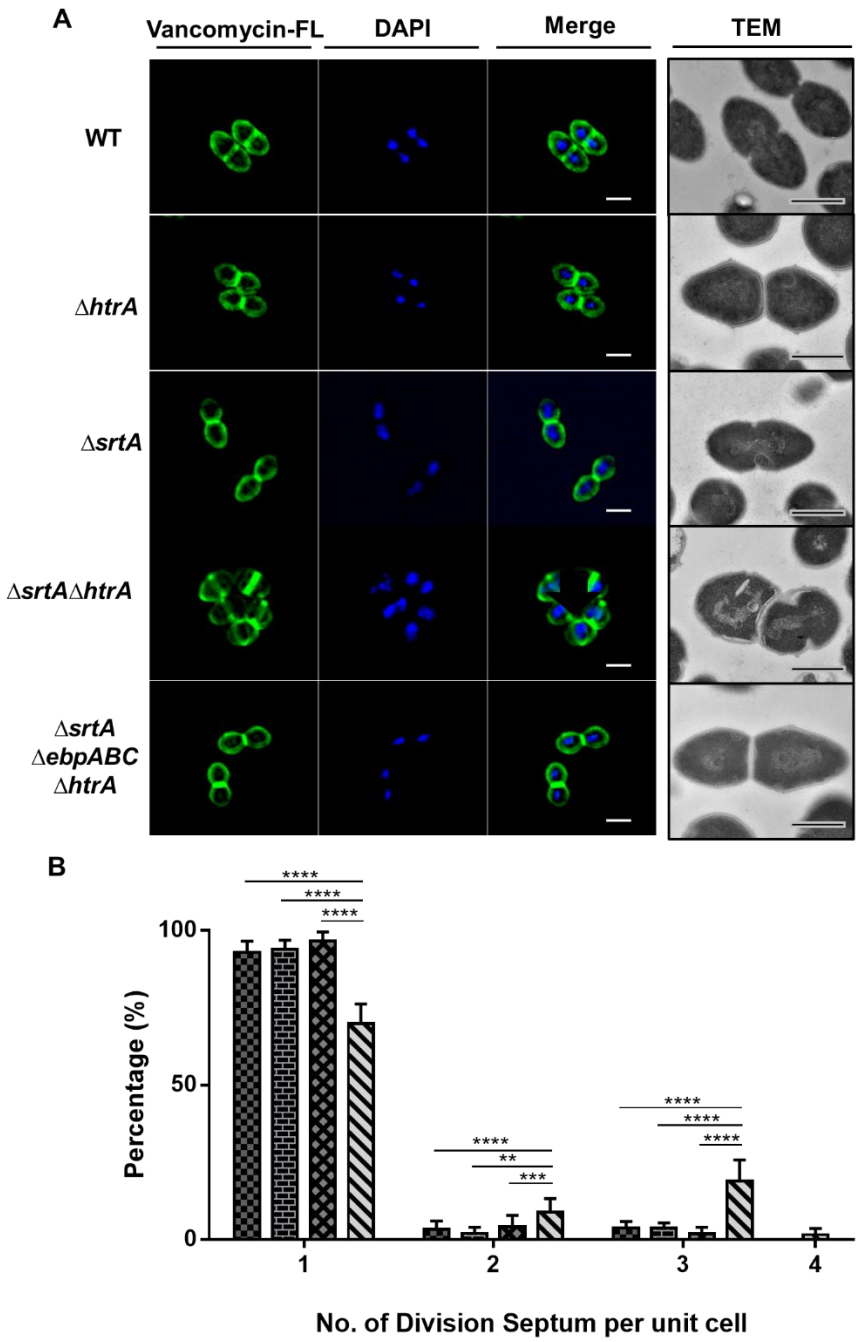

Figure 4.9 | Absence of SrtA and HtrA resulted in aberrant fluorescent-vancomycin staining. (A) The cell wall was stained with Van-FL conjugate (green). DAPI (blue) was used to visualize DNA. Representative images were shown. Scale bars for TEM represent 500 nm; scale bars for IFM represent 1 µm. (**B**) Δ*srtA*Δ*htrA* (▨); OG1RF wildtype (■); Δ*htrA* (▦) and Δ*srtA* (▩). Results are represented as bar graphs. **P < 0.01; ****P < 0.0001. A total of at least 500 cells were sampled per strain.

To quantify these observations, we measured the maximum cell width of 200 cells from each strain and plotted a histogram to identify the distribution of cell width. The majority of Δ*srtA*Δ*htrA* cells had maximum cell widths of ~0.8 µm as compared to WT, Δ*srtA* or Δ*htrA* (all approximately 0.7 µm) indicating that Δ*srtA*Δ*htrA* has a wider cell width (**Fig 4.10**). Together, these findings suggest that pilus accumulation hampers the ability of the cell to elongate and divide.

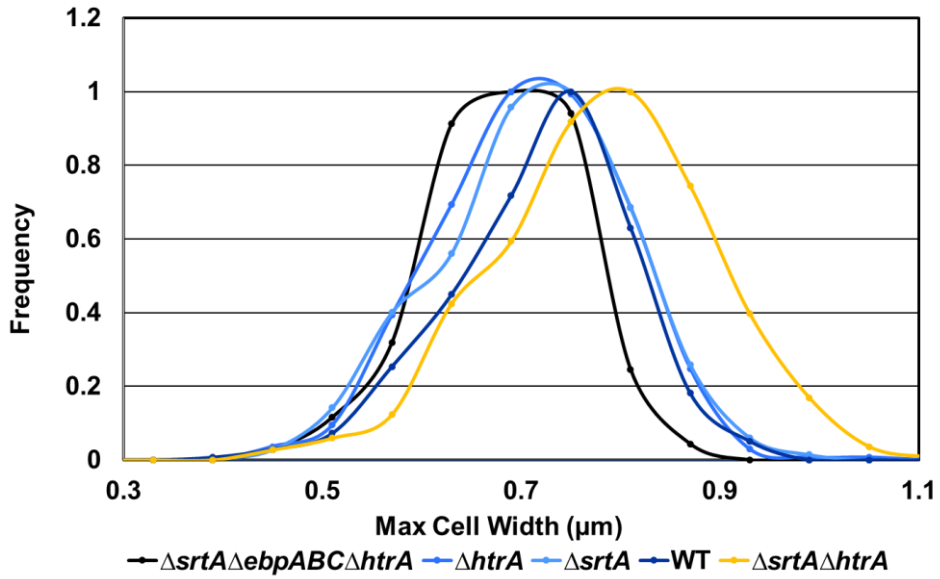

Figure 4.10 | Δ*srtA*Δ*htrA* exhibits cells with wider cell width. The relative cell width of the indicated bacterial population was determined by measuring the mid-width of the cells and quantified using MicrobeJ plugin in ImageJ. Cells that were not in-phase were excluded from the analysis. A total of at least 200 cells were sampled per strain.

To investigate the cell constriction in these cells, the ultrastructure of division septa was analyzed using transmission electron microscopy (TEM). TEM further revealed some Δ*srtA*Δ*htrA* cells to have severely deformed septa (**Fig 4.11**). These cells were clearly not ovoid like the WT strain but instead exhibited a spherical morphology. Forty percent of the total cell population also had excessive white patches within the cells which may be attributed to processing artifacts or may also reflect excessive nucleoid accumulation in

the cells. Altogether, these data suggest that cell septa constriction and separation were hampered in Δ*srtA*Δ*htrA*, affecting the last step of cell division that allows the final separation of daughter cells.

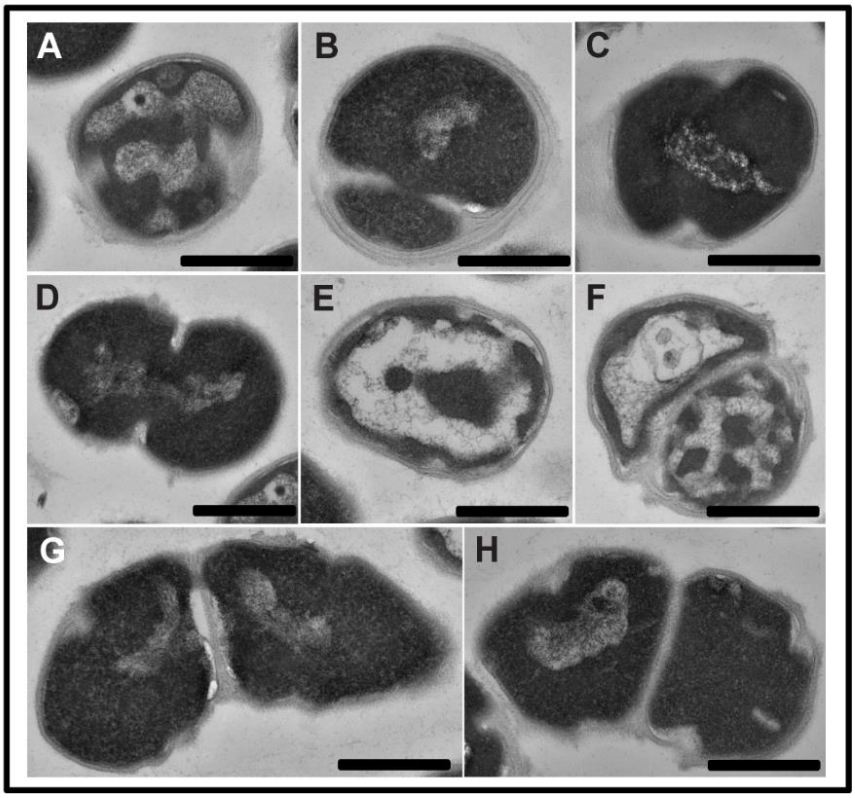

Figure 4.11 | TEM revealed cells morphology defects in Δ*srtA*Δ*htrA*. The cells were processed for TEM as described in the materials and methods section. Image representations of Δ*srtA*Δ*htrA* cell structures. Scale bar represents 500 nm.

4.3.9 Aberrant cell morphology in Δ*srtA*Δ*htrA* mutant is pilus-dependent

To investigate if the morphological defect is pilus-dependent, we constructed a quintuple mutant, Δ*srtA*Δ*ebpABC*Δ*htrA that* did not express pili in the Δ*srtA*Δ*htrA* background. As shown in **Fig 4.8-4.10**, Δ*srtA*Δ*ebpABC*Δ*htrA* does not exhibit chaining phenotypes or multiple septations; consistent with the hypothesis that mislocalized 'off-pathway' Ebp pili on the membrane gives rise to aberrant cell morphology.

4.3.10 Accumulated monomeric or polymerized pili in the membrane can lead to aberrant cell morphology

Since we observed that accumulation of pili on the cell membrane induces cellular defects, we next investigated whether monomeric pilin subunits or polymerized pili induced the cell shape defect. We designed an expression plasmid with a single amino-acid change in the EbpC subunit in the pilin-like motif (K186A) that is necessary for pilus fiber polymerization (Nielsen, Flores-Mireles et al. 2013). IFA showed that complementation of the quintuple mutant with either monomeric pilin subunits (p*ebpABC*$_{K186A}$*srtC*) or polymerized pili (p*ebpABCsrtC*) can induce morphology defects (**Fig 4.12**). These data suggest that in the absence of *srtA* and *htrA*, cell septa separation or elongation can be affected in the presence of either form of Ebp (pilin or pili) accumulation on the membrane.

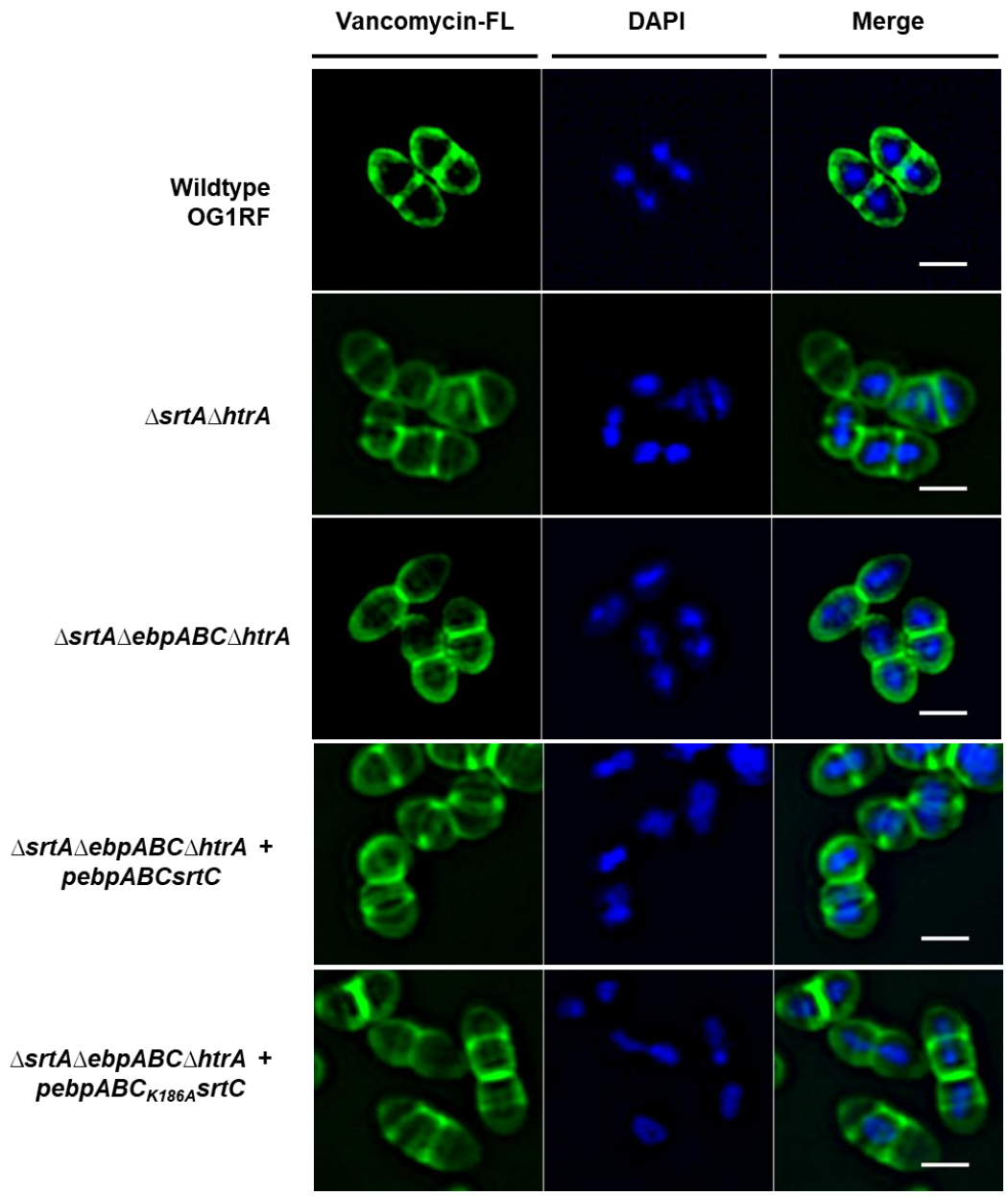

Figure 4.12 | Ebp effects on cell morphology in the absence of *srtA* and *htrA*. The cell wall was stained with Van-FL conjugate (green). DAPI (blue) was used to visualize DNA. Representative images were shown. Scale bars represent 1 µm.

4.3.11 Transcriptomic analysis reveals differential expression of *ebp* genes in Δ*srtA*Δ*htrA* mutant

To investigate whether the increased Ebp protein levels and total cell population piliation levels observed in Δ*srtA*Δ*htrA* occurred transcriptionally or post-transcriptionally,

we performed RNA sequencing on WT, Δ*htrA*, Δ*srtA,* and Δ***srtA***Δ*htrA.* We observed that transcription of the pilin genes, *ebpA, ebpB* and *ebpC* encoding the three pilin subunits EbpA, EbpB, and EbpC, respectively, was significantly higher in Δ***srtA***Δ*htrA* compared to WT (**Fig 4.13**). Unlike Δ*srtA*Δ*htrA,* the increased pilus abundance in the *srtA* mutant was not a result of increased *ebp* transcript as we did not observe significant induction of *ebp* expression in Δ*srtA* relative to WT (**Supplementary Table C7**). The induction of *ebp* expression in Δ*srtA*Δ*htrA* likely contributes to the further increased piliation relative to Δ*srtA*. However, we noticed that the primary regulator that controls *ebp* expression, *ebpR* was not transcriptionally affected (**Fig 4.13**), nor were *rnjB* or *ahrC* genes suggesting the regulation of *ebp* is controlled by another pathway (Bourgogne, Singh et al. 2007, Gao, Pinkston et al. 2010, Manias and Dunny 2018).

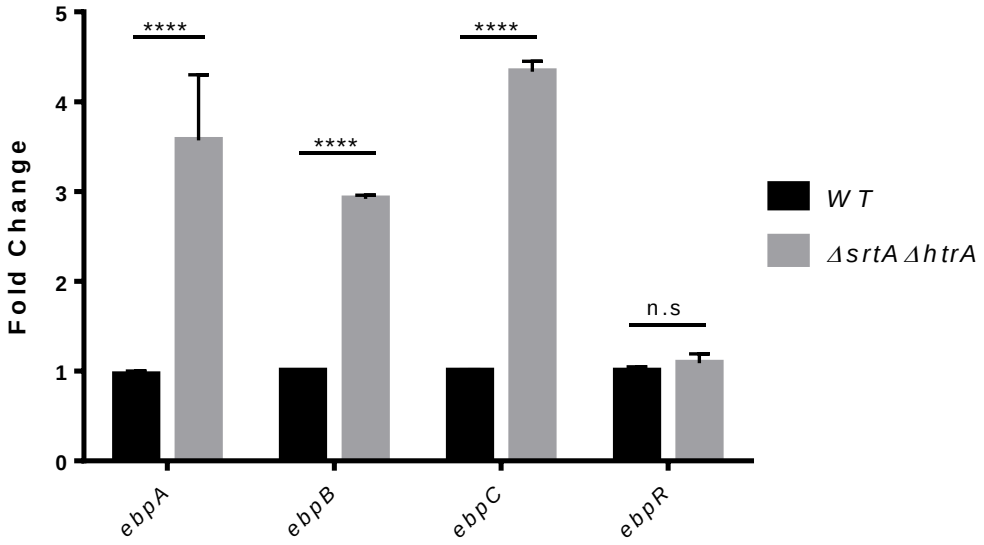

Figure 4.13 | *ebpABC* transcription is higher in Δ*srtA*Δ*htrA*. qRT-PCR analysis of *ebpABC* expression in the OG1RF WT (black bars) and Δ*srtA*Δ*htrA* (grey bars). qRT-PCR was performed in biological triplicate and analyzed by the $\Delta\Delta C_T$ method, using *gyrB* as a housekeeping gene. Fold change indicates the change in *ebpA, ebpB,* and *ebpC* transcription, compared to control (WT). Statistical analysis was performed by the 2-way ANOVA; Turkey's multiple comparison tests using GraphPad. **** $P \leq 0.0001$, $P \geq 0.05$ differences not significant (n.s).

4.3.12 Identification of genes induced in the presence of membrane stress

To gain mechanistic insights into the role of *htrA* in pilus biogenesis and these 'off-pathway' morphology defects, we performed transcriptomic analyses to shed light on what might be happening in the Δ*srtA*Δ*htrA*. We compared the transcriptional data of Δ*srtA*Δ*htrA* with Δ*srtA,* Δ*htrA* or WT to identify genes that were differentially regulated specifically during membrane stress. Genes with significant differences in abundance of mRNAs were determined using a P value and false discovery rate (FDR) cut-off of 0.05. We identified differentially expressed genes common in all pairwise comparisons between each genetic background. We found 164 genes that are differentially regulated in all transcriptome comparisons, suggesting that these differentially expressed genes may regulate/facilitate/respond to the absence of *srtA* and/or *htrA* (**Supplementary Table C5, Fig 4.14A**).

We further characterized these 164 consensus genes into various categories by manual classifications based on known functions or predictions from literature and *E. faecalis* OG1RF database available on Biocyc (https://biocyc.org/). Otherwise, they were grouped as 'unclassified'. The $\log_2$ fold change in mRNA levels in Δ*srtA*Δ*htrA* are displayed relative to Δ*srtA* and shown as a dot plot (**Fig 4.14B**).

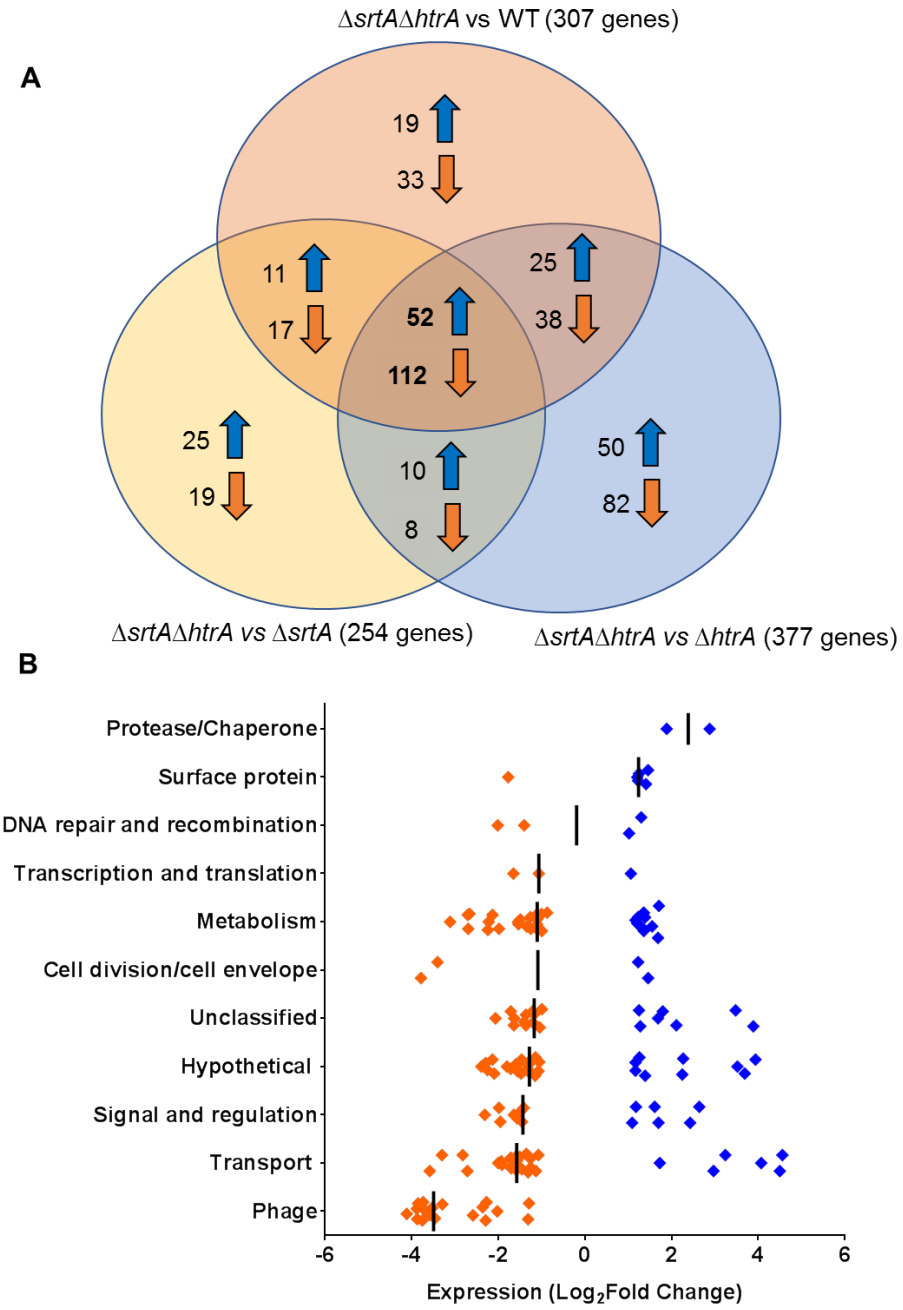

Figure 4.14 | Transcriptional gene expression profile of Δ*srtA*Δ*htrA*. (**A**) Significant genes from the respective comparisons were grouped based on genes presence/absence in each group. Venn diagram showing a total of 164 genes found to be differentially regulated specifically during membrane stress. Genes only uniquely found in the indicated groups are in the non-overlapping region. The total number of differentially expressed genes in each comparison is indicated beside each group. (**B**) The $\log_2$ fold change in mRNA levels of these 164 genes in Δ*srtA*Δ*htrA* relative to Δ*srtA* is displayed as a dot plot. Significant genes were determined by the Bioconductor package EdgeR ($P < 0.05$; FDR < 0.05). Genes with negative $\log_2$ fold change are colored orange; genes with positive $\log_2$ fold change are colored blue.

4.3.12.1 Differential expression of several cell division/separation genes

Since we observed a morphological defect in Δ*srtA*Δ*htrA*, we first looked at the genes classified as “cell division and cell envelope”. The four differentially expressed genes, namely *ftsH,* OG1RF_11070, OG1RF_11071, and *penA* were associated with Δ*srtA*Δ*htrA* (**Table 4.5**). Based on Blastp searches, OG1RF_11070 and OG1RF_11071 were annotated as FtsW/RodA/SpovE family cell division proteins that were also annotated as *ftsW* in *S. agalactiae* and *rodA* in *S. oralis,* respectively, and we will refer to them as *ftsW* and *rodA* from here on. In *E. faecalis, ftsW* and *rodA* are predicted to be co-transcribed in a single operon. Since we observed morphological defects in Δ*srtA*Δ*htrA*, and it is easier to perform complementation with transcriptionally down-regulated genes, we designed an expression plasmid (p*ftsW/rodA*) containing both genes expressed in *trans* in Δ*srtA*Δ*htrA.* As shown in **Fig 4.15**, the morphological defect (as measured by multiple septa) was only partially alleviated in Δ*srtA*Δ*htrA* p*ftsW/rodA*, with 9.5 ± 3% of the 500 cells analyzed still exhibiting the morphology defect, as compared to 19.3 ± 0.7 % in Δ*srtA*Δ*htrA.* These data indicate that the morphology defect is multi-factorial and there may be other effectors (e.g. PenA) involved in regulating cell morphology.

FtsH is an ATP-dependent metalloprotease involved in quality control of misfolded or incorrectly inserted membrane proteins and acts as either a chaperone to help refold or as a protease to degrade them (Narberhaus, Obrist et al. 2009). FtsH directly interacts with flotillin-like proteins, FloA and FloT, to regulate membrane lipid raft homeostasis in *B. subtilis* (Mielich-Suss, Schneider et al. 2013). Even though FtsH is annotated as a gene involved in cell division, it performs more of a role as a regulatory protease with critical

functions in proteins and membrane lipid homeostasis; hence we did not analyze it as a cell division protein here.

Table 4.5 | Expression of several cell envelope proteins are differentially regulated.

Locus Tag	Gene	Log_2FC[a]	P-value	Annotation
OG1RF_11070	*ftsW*	**-3.79**	**4.64E-09**	FtsW/RodA/SpovE family cell division protein
OG1RF_11071	*rodA*	**-3.40**	**9.83E-10**	FtsW/RodA/SpovE family cell division protein
OG1RF_10209	*ftsH*	**1.23**	**4.69E-04**	Cell division protein FtsH
OG1RF_12158	*penA*	**1.46**	**1.90E-03**	Penicillin-binding protein 2B

[a] The LogFC represents the log_2 change between biological triplicates of Δ*srtA*Δ*htrA* compared to *ΔsrtA* when grown to mid-log phase in TSB supplemented with 0.25% glucose.

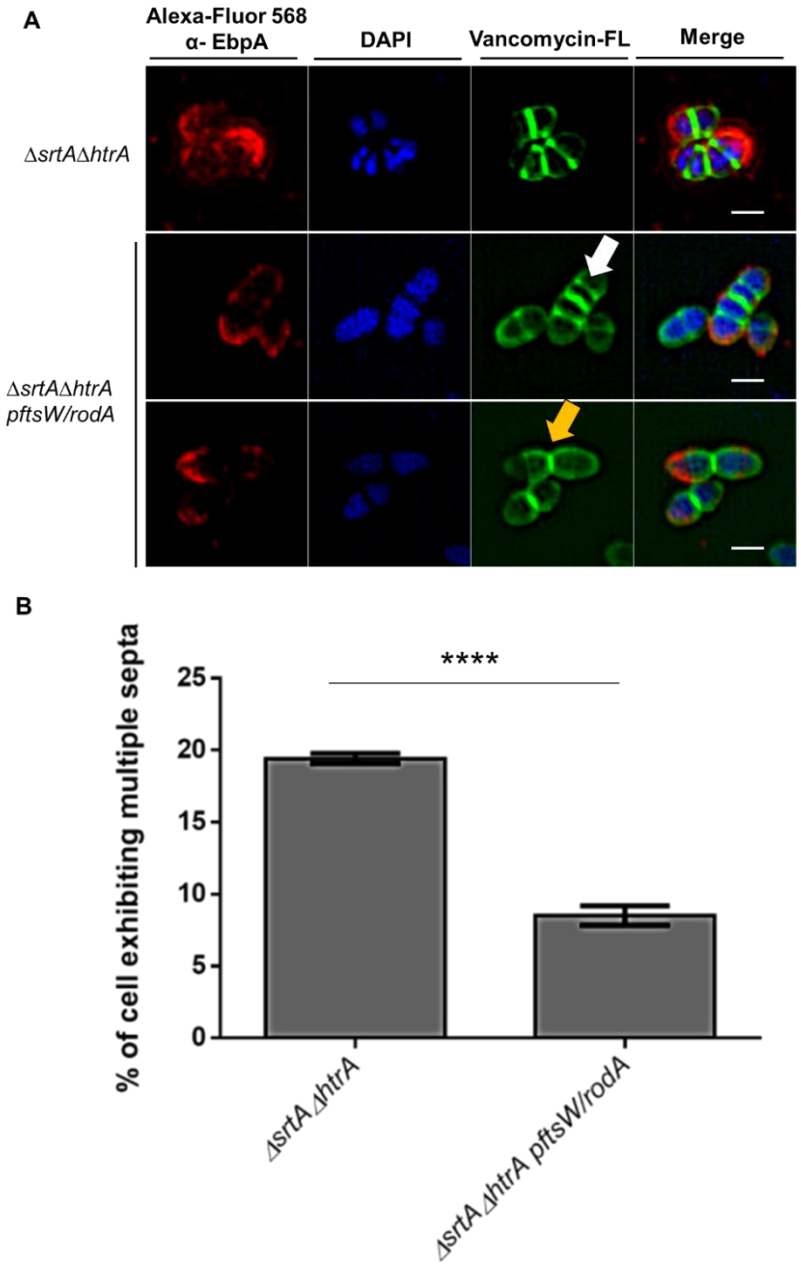

Figure 4.15 | Complementation of Δ*srtA*Δ*htrA* with p*ftsW/rodA* partially alleviates the morphology defect. The cell wall was stained with Van-FL conjugate (green), blocked and incubated with anti-EbpC immune serum coupled to Alexa Fluor® 568 antibody (red). DAPI (blue) was used to visualize DNA. Cell morphology was partially alleviated in Δ*srtA*Δ*htrA* p*ftsW/rodA* to WT morphology (yellow arrow). 9.5 ± 3% of the cells still exhibit the morphology defect (white arrow), as compared to 19.3 ± 0.7 % in Δ*srtA*Δ*htrA*. Representative images were shown. A total of 500 cells were analyzed per strain. Scale bars represent 1 µm. Statistical analysis was performed by the unpaired parametric T-test using GraphPad. **** P ≤ 0.0001.

4.3.12.2 Differential expression of genes involved in signal transduction pathways

TCSs are known to regulate numerous processes such as cell morphology, housekeeping functions, virulence, and response to environmental stresses (Hancock and Perego 2002, Stephenson and Hoch 2002, Okada, Gotoh et al. 2007). Since we hypothesized that a Cpx-like system may be important in clearing these 'off-pathway' pili in *E. faecalis*, we looked for TCSs and regulators that are differentially regulated in Δ*srtA*Δ*htrA,* just like in *E. coli*. **Table 4.6** shows a list of genes involved in signaling and regulation that were differentially regulated among the 164 genes. Based on predicted TCS in *E. faecalis* strain V583 (**Chapter 2**, **Table 2.2 and 2.3**), we identified homologous TCSs in OG1RF that were differentially regulated in Δ*srtA*Δ*htrA*. Among all the genes listed under signaling and regulation, only one TCS, CroR-CroS was upregulated in Δ*srtA*Δ*htrA* relative to WT (**Fig 4.16**). CroR-CroS is involved in ceftriaxone antibiotic resistance (Comenge, Quintiliani et al. 2003, Kellogg and Kristich 2016, Kellogg, Little et al. 2017), oxidative-induced cell envelope stress (Djoric and Kristich 2015) and modulates expression of a secreted stress-induced SalB protein in *E. faecalis* (Muller, Le Breton et al. 2006). Upregulation of this TCS suggests that cells probably undergo a CroRS-mediated stress response during 'off-pathway' pilus biogenesis. We did not observe differential expression of the *fsr* system that indirectly affects *ebp* transcription through *ebpR* regulation (Bourgogne, Hilsenbeck et al. 2006).

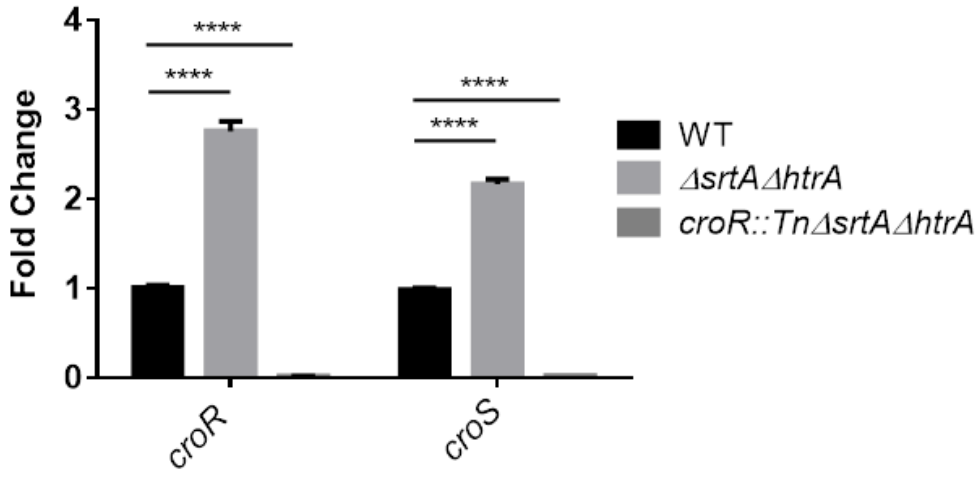

Figure 4.16 | *croRS* transcription is higher in Δ*srtA*Δ*htrA*. qRT-PCR analysis of *croRS* expression in the OG1RF WT (black bars), and Δ*srtA*Δ*htrA* (grey bars), and *croR::Tn*Δ*srtA*Δ*htrA* (dark grey bars). qRT-PCR was performed in biological triplicate and analyzed by the $\Delta\Delta C_T$ method, using *gyrB* as a housekeeping gene. Fold change indicates the change in *croR* and *croS* transcription, compared to control (WT). The *croR::Tn*Δ*srtA*Δ*htrA* mutant strain was used as the negative control for *croRS* transcription. Statistical analysis was performed by the 2-way ANOVA; Sidak's comparisons test using GraphPad. **** $P \leq 0.0001$.

Among the rest of the genes displayed in **Table 4.6**, the LytSR-regulated dicistronic operon *lrgA/lrgB* is also of interest. LrgA/LrgB murein hydrolases negatively control hydrolytic activities of specific components of the peptidoglycan, presumably playing a role in the biosynthesis and processing of the bacterial cell wall (Groicher, Firek et al. 2000). However, LytSR, the TCS that regulates *lrgA/lrgB* expression is not transcriptionally affected, possibly suggesting an alternative route of activation via other pathways yet to be identified.

Table 4.6 | List of genes classified under signaling and regulation.

Locus Tag	Log_2FC^a	P value	Gene	Annotation
OG1RF_10820	**-1.95**	**2.85E-06**		LytR family response regulator
OG1RF_11067	**-1.64**	**1.33E-03**		PadR family transcriptional regulator
OG1RF_11069	**-1.41**	**4.39E-04**		Putative transcriptional regulator
OG1RF_11157	**-1.56**	**2.07E-03**		Cro/CI family transcriptional regulator
OG1RF_11230	**-1.98**	**2.48E-03**	*sacT*	SacPA operon antiterminator
OG1RF_11523	**-1.45**	**6.92E-04**		LysR family transcriptional regulator
OG1RF_11656	**2.43**	**5.90E-12**		ABC superfamily ATP binding cassette transporter, permease protein
OG1RF_11657	**2.64**	**3.98E-16**		ABC superfamily ATP binding cassette transporter, ABC protein
OG1RF_11922	**-1.48**	**3.22E-05**		M protein trans-acting positive regulator
OG1RF_11926	**-2.31**	**1.05E-11**		Cro/CI family transcriptional regulator
OG1RF_12460	**1.70**	**3.36E-05**	*lrgB*	Murein hydrolase regulator LrgB
OG1RF_12461	**1.61**	**2.14E-05**	*lrgA*	Murein hydrolase regulator LrgA
OG1RF_12535	**1.18**	**8.53E-04**	*croR*	Response regulator
OG1RF_12536	**1.09**	**8.16E-04**	*croS*	Sensor histidine kinase

a The LogFC represents the log_2 change between biological triplicates of Δ*srtA*Δ*htrA* compared to *ΔsrtA* when grown to mid-log phase in TSB supplemented with 0.25% glucose.

4.4 DISCUSSION

Sortase-assembled Ebp pili are one of the major virulence factors commonly associated with enterococcal nosocomial infections. These pili are essential for adherence to human platelets, as well as host extracellular matrix proteins fibrinogen and collagen, for subsequent infection (Nallapareddy, Sillanpaa et al. 2011, Nallapareddy, Singh et al. 2011, Nielsen, Guiton et al. 2012). However, during host infections, bacteria face a plethora of stress factors that can lead to the formation of protein aggregates which can potentially be toxic to the bacterial cell. *E. faecalis* must overcome these stress factors to survive and infect the host. How *E. faecalis* modulates the removal of these protein aggregates is currently not known. It is therefore essential to uncover the regulations behind efficient pilus biogenesis.

In **Chapter 3**, we showed that absence of *htrA* alone does not affect pilus biogenesis and we proposed $HtrA_{EF}$ only functions in the event when proteins accumulate on the membrane and are driven via 'off-pathway' interactions. In *E. coli*, DegP is activated in the presence of misfolded proteins (Danese and Silhavy 1997, Jones, Danese et al. 1997). We created an in-frame double deletion of *srtA* and *htrA* to mimic protein accumulation on the membrane, using Ebp as the model sortase substrate to test HtrA's role during 'off-pathway' events (**Fig 4.1**). Immunoblot and IFA revealed an increased level of pili in the membrane fraction of Δ*srtA*Δ*htrA* as compared to WT, Δ*srtA* or Δ*htrA* (**Fig 4.3 and 4.4**). This hyper-piliation phenotype can be turned down by complementing with WT HtrA or a protease-defective HtrA on an expression plasmid, suggesting that HtrA chaperone function helps with the folding of these accumulated pili probably to ensure they do not form toxic aggregates (**Fig 4.3**). HtrA interacts strongly

with EbpC from the BacTH system in **Chapter 3** and this data reaffirms our hypothesis that HtrA may play a role in processing accumulated pilins. In *E. coli,* it is thought that a pilin subunit in a membrane-associated state is most likely not in the native or stable conformation and usually subjected to proteolytic degradation (Kolmar, Waller et al. 1996). In the absence of the PapD chaperone, P pilin subunits are more susceptible to proteolysis by DegP protease, which acts on partially unfolded or denatured proteins (Kolmar, Waller et al. 1996, Jones, Danese et al. 1997). As we have yet to prove the necessity of HtrA protease function, we cannot rule out the fact that HtrA protease may also be important to process these pili.

Both the Cpx system and modulation of σ^E respond to these off-pathway interactions to monitor the assembly state of extra-cytoplasmic proteins (Missiakas and Raina 1997). The absence of pili on the cell wall in Δ*srtA*Δ*htrA* or the accumulation of pili on the membrane may mediate stress signals sensed by a yet-unknown pathway that monitors the assembly state of cell surface proteins in *E. faecalis.* Ebp can indirectly be regulated by the *fsr* quorum-sensing system, where it negatively regulates pilus expression through the regulation of EbpR (Bourgogne, Hilsenbeck et al. 2006). While we did not observe differential expression of the *ebpR* regulator (**Fig 4.13**), it is possible that EbpR activity is changed in the Δ*srtA*Δ*htrA* mutant background giving rise to altered pilus expression. In parallel with this, we did not observe any transcriptional differences in other *ebp* regulators, *rnjB* or *ahrC/argR2* suggesting a novel regulatory mechanism that may be installed for pilus biogenesis.

While performing these experiments, we noticed a growth defect in the growth kinetic assay between Δ*srtA*Δ*htrA* and WT (**Fig 4.2A**). The growth defect in the absence

of HtrA suggested that the toxic effect may originate from the over-production and accumulation of pili on the membrane. The formation of chained cells and aberrant displacement of septa in some Δ*srtA*Δ*htrA* cells which disappeared in quintuple mutant Δ*srtA*Δ*ebpABC*Δ*htrA,* suggested that this morphology is pilus-dependent (**Fig 4.8 and 4.9)**. Furthermore, complementation of Δ*srtA*Δ*ebpABC*Δ*htrA* with either monomeric or polymerized pili in *trans* restored pleiotropic cell morphology hinting that overcrowding on the membrane may have caused membrane instability or deleterious 'jamming' of the Sec secretion machinery. These possibilities may interfere with essential processes such as protein translocation via the Sec machinery or the folding and activity of essential cell wall proteins, resulting in cell envelope biogenesis inhibition (Snyder and Silhavy 1992) (**Fig 4.12**). Even though we observed more than a three-fold reduction in *ftsW* and *rodA,* complementation of these two genes in *trans* only partially complements the phenotype in the Δ*srtA*Δ*htrA*, suggesting that the morphology defect is multi-factorial (**Table 4.5 and Fig 4.15**).

In principle, bacterial cells can prevent detrimental accumulation of misfolded proteins by increasing the levels of proteases and foldases (Danese and Silhavy 1997). We observed an increased expression of metalloprotease FtsH (1.23-$\log_2$ fold change) (**Table 4.5**) and a ubiquitous protein folding factor, a peptidyl-prolyl isomerase, PrsA (2.88-$\log_2$ fold change) in Δ*srtA*Δ*htrA* relative to the single mutants or WT (**Supplementary Table C5**), which may facilitate the folding or clearance of extracellular proteins. In *S. aureus*, PrsA plays a role in the post-transcriptional maturation of penicillin-binding protein 2A (PBP2A), possibly in the export and/ or folding of newly synthesized PBP2A (Jousselin, Manzano et al. 2016). PBP2A is a high molecular-weight

transpeptidase enzyme involved in lateral cell wall synthesis and rod-shape determination (Popham and Young 2003). In *B*. *subtilis*, PrsA is essential for growth and secretion of α-amylase (Hyyrylainen, Marciniak et al. 2010). Furthermore, PBPA and PBPB were identified as putative PrsA substrates in *L*. *monocytogenes* (Alonzo, Xayarath et al. 2011). Even though the function of PrsA in *E*. *faecalis* is currently uncharacterized, we postulate that PrsA may be important for cell wall synthesis, secretion, and interaction with PBP2A as we also observed 1.08-$\log_2$ fold change in PBP2A expression. These findings emphasize that some form of cell checkpoint is in place to sense these off-pathway processes and cells use this information to modulate the synthesis of proteases and foldase.

Among all the genes that are differentially downregulated, we noticed all the phage genes (locus tags OG1RF_11046-OG1RF_11063) coding for prophage 2 (pp2) are transcriptionally downregulated. We observed at least a 1.31-$\log_2$ fold change reduction of all the phage genes, suggesting that the accumulation of proteins on membrane turn down the phage expression (**Supplementary Table A4**). pp2 is the first phage to be associated with the core genome of *E. faecalis* (McBride, Fischetti et al. 2007). A recent study on *E. faecalis* V583 prophages identified pp2 to be a remnant prophage not able to excise out of the chromosome and does not respond to fluoroquinolone to form active phage progeny (Matos, Lapaque et al. 2013). The natural selection to allow the bacteria to retain this region is still not clear. In OG1RF, genetic organization reveals that even though pp2 lacks a capsid (**Supplementary Fig B2**), a pp2 tail fiber can be assembled and expressed in WT OG1RF (Afonina. I. and Mark Veleba, unpublished data). This indicates that pp2 can be expressed during normal laboratory growth conditions. Under

certain stress conditions such as the SOS response to DNA damage, integrated phages may also be induced to excise out of the chromosome and enter the lytic replication cycle (Fogg, Rigden et al. 2011). It is therefore surprising that we see down-regulation of pp2 under membrane stress conditions in Δ*srtA*Δ*htrA*. Whether pp2 represents a functional phage or a remnant of a once-operative bacteriophage in OG1RF requires more investigation.

In many bacteria such as *B. subtilis, E. coli*, *S. aureus,* and *S. pneumoniae*, *htrA* expression is regulated by a TCS (Danese and Silhavy 1997, Pallen and Wren 1997, Darmon, Noone et al. 2002, Sebert, Palmer et al. 2002, Rigoulay, Entenza et al. 2005). This knowledge led us to postulate whether a TCS is recruited to regulate *htrA* expression. To identify possible signal transduction pathways that may be involved in pilus biogenesis, we examined transcriptomic data and looked at genes categorized under signaling and regulation. Among all the genes, only one TCS, CroRS, was induced in Δ*srtA*Δ*htrA* (**Table 4.6**). CroRS is the key determinant to ceftriaxone-resistance in *E. faecalis* (Comenge, Quintiliani et al. 2003, Kellogg, Little et al. 2017). CroRS is only studied in the context of sensing and responding to cell-wall targeting antimicrobial agents. Virulence defects have been reported for CroRS mutants but the reasons for such defects are not known. Transcriptomic analyses of daptomycin-treated OG1RF relative to untreated WT cells also revealed induction of *croRS* expression, suggesting that CroRS responds to membrane perturbation as well as cell wall perturbation (Iris H. Gao, unpublished data).

In addition to *croRS* expression, genes that are involved in murein hydrolase activity, *lrgAB,* were also induced in Δ*srtA*Δ*htrA*. *lrgAB* is a LytSR-regulated dicistronic

operon located downstream of LytSR (Brunskill and Bayles 1996, Groicher, Firek et al. 2000). LrgAB controls gene products that possess murein hydrolase activity and play a role in cell wall metabolism in *S. aureus* (Groicher, Firek et al. 2000). Deletion of *lrgAB* in *S. aureus* increases extracellular murein hydrolases activity, causing more cellular autolysis. We observed a 1.61- and 1.70- $\log_2$ fold change induction for *lrgA* and *lrgB* in Δ*srtA*Δ*htrA* relative to Δ*srtA*, suggesting that murein hydrolases activities are turned down. However, it is not known how *lrgAB* is regulated. Upregulation of these murein hydrolases suggests that its processed substrates involved in PG hydrolysis may be turned down, arresting daughter cell separation leading to the formation of chained cells.

Altogether, our findings in this chapter suggest that Δ*srtA*Δ*htrA* 'off-pathway' interactions drive a hyper-piliation phenotype in cells that require HtrA to process to prevent accumulation of toxic aggregates. When HtrA is not present to offset the accumulation, overcrowding on the membrane likely occurs and clutters the Sec machinery, blocking translocation of proteins involved in cell wall turnover, leading to aberrant cell wall biosynthesis. This membrane perturbation causes cells to undergo CroRS-mediated stress responses as a feedback mechanism by governing cell cycle checkpoint and pilus biogenesis in *E. faecalis* during membrane stress. Induction of *lrgAB* may utilize alternative pathways or possible cross-talk between CroRS and LytSR may exist and this should be investigated further. This is the first report that links the normal cellular process of virulence factor assembly to antibiotic resistance through the common CroRS signaling node. Identification of additional CroR targets and binding sites would provide a better understanding of CroRS function. Work on CroRS in **Chapter 5** will shed light on the possible interactions between HtrA, CroRS, and pilus biogenesis and inform

how the opportunistic pathogen *E. faecalis* adapts to stressful conditions to modulate its virulence.

CHAPTER 5: POTENTIAL ROLE OF CRORS IN GOVERNING CELL CYCLE CHECKPOINT DURING MEMBRANE STRESS IN *ENTEROCOCCUS FAECALIS*

5.1 INTRODUCTION

In **Chapter 4**, our findings suggest the morphological defects displayed in Δ*srtA*Δ*htrA* are attributed to pilus accumulation on the cell membrane. We took a holistic approach by performing transcriptomic analysis to shed light on the mechanisms for *htrA* in 'off-pathway' pilus biogenesis and identified a TCS, CroR-CroS, induced in the presence of this membrane perturbation.

Bacteria contain dozens of TCSs that play important roles in sensing and responding to their environment. CroRS is activated in response to cell wall-targeting antibiotics, initiating a transcriptional response that mediates resistance to the same antimicrobials (Comenge, Quintiliani et al. 2003, Kellogg and Kristich 2016, Kellogg, Little et al. 2017). However, neither the activating signal for CroS, nor the direct CroR regulon has been described. Prior to this work, a role for CroRS in cell wall-associated virulence factor biogenesis or monitoring has not been reported.

We propose that the accumulation of pili on the membrane cause cells to undergo alternative signal transduction cascade through a CroRS-mediated stress response by governing cell cycle checkpoints and pilus biogenesis. We will address this hypothesis in this chapter by creating in-frame deletions of *srtA* and *htrA* in transposon mutants of *croR::Tn* and *croS::Tn* to investigate phenotypic and transcriptomic changes in these triple mutants.

5.2 MATERIALS AND METHODS

5.2.1 Bacterial strains and growth conditions

Bacteria strains and plasmids used in this chapter are listed in **Table 5.1**. The bacterial cell was propagated according to **Section 3.2.1**, with the additional use of chloramphenicol (Cm) 10 mg/L in *E. faecalis* carrying transposon cassette.

Table 5.1 | Bacterial Strains and Plasmids used in this study.[a]

Strains or plasmids	Relevant characteristic(s)[b]	References or source
Strains		
Enterococcus faecalis		
OG1RF	Fus^r, Rif^r, derived from OG1	Lab stock
Δ*srtA*Δ*htrA*	OG1RF isogenic derivative of in-frame *srtA* and *htrA* double deletion mutant	Chapter 4
croR::Tn	TA nucleotides insertion at map position 2692439, Cm^r	(Kristich, Nguyen et al. 2008)
croS::Tn	TA nucleotides insertion at map position 2694115, Cm^r	(Kristich, Nguyen et al. 2008)
*croR::Tn*Δ*srtA*Δ*htrA*	In-frame *srtA* and *htrA* double deletion in *croR::Tn,* Cm^r	This work
*croS::Tn*Δ*srtA*Δ*htrA*	In-frame *srtA* and *htrA* double deletions in *croS::Tn,* Cm^r	This work
Escherichia coli		
Stellar Cells	Routine cloning host when using In-fusion kit	Clontech, USA
DH5α	Routine cloning host	Lab stock
Plasmids		
pGCP123 (p*Empty*)	Expression vector, Km^r	(Paulsen, Banerjei et al. 2003)
pGCP213	Temperature sensitive allelic exchange vector, Em^r	(Paulsen, Banerjei et al. 2003)
p*delta-htrA*	Δ*htrA* deletion allele in pGCP213	Chapter 3
p*delta-srtA*	Δ*srtA* deletion allele in pGCP213	(Kline, Kau et al. 2009)
p*croRS-2xHA*	P_{croR} *croRS-2XHA* in pGCP123	This work

Abbreviations: Fus, fusidic acid; Rif, rifampin; Km, kanamycin; Em, erythromycin; Str, streptomycin; Cm, chloramphenicol. [a]See Materials and Methods for intermediate strain and plasmid constructions. [b]Superscript "r" indicates resistance.

5.2.2 Validation of *croR::Tn* and *croS::Tn*

To validate that the *croR* and *croS* transposon insertion mutants (a gift from Gary Dunny) harbor only one transposon element, EfaMarTN (2.1 kb) in the indicated gene locus, we screened *croR::Tn* and *croS::Tn* with croRcmScreen_F/croRcmScreen_R and croScmScreen_F/croScmScreen_R respectively (**Table 5.2**).

5.2.3 Construction of *E. faecalis croR::Tn*Δ*srtA*Δ*htrA* and *croS::Tn*Δ*srtA*Δ*htrA* mutants in OG1RF

The deletion constructs p*delta-htrA* obtained from **Chapter 3** and p*delta-srtA* obtained from Kline, Kau et al. 2009 were transformed into *croR::Tn* and *croS::Tn* strains according to methods described in **Section 3.2.2** and **Section 3.2.4**. Loss of *srtA* locus in Em-sensitive bacteria was demonstrated by PCR using dsrtA_F IFD Screen/dsrtA_R IFD Screen and dsrtA_F IFD internal/dsrtA_R IFD Screen. We confirmed the absence of HtrA and SrtA protein expression immunoblotting whole cell lysates of *croR::Tn*Δ*srtA*Δ*htrA* and *croS::Tn*Δ*srtA*Δ*htrA* with anti-$HtrA_{EF}$ and anti-SrtA immune sera, respectively.

5.2.4 p*CroR*$_{promoter}$-*croRS* plasmid construction

The expression construct of *croR/croS* operon was cloned into pGCP123 using a two-step PCR amplification. We constructed a *croR/croS* expression vector by amplifying the *croR/croS* coding sequence plus 200 bp upstream of the *croR* start codon to include its native promoter and two HA tags at the downstream of *croS* with croR_infusion_F_EcoRI/croS_HA tag. The second PCR amplification was performed using croR_infusion_F_EcoRI/croS_infusion_R_PstI to include the homologous region of the vector at 5' and 3' of the PCR product for infusion cloning (Clontech, USA), where primers included homologous sequences to the vectors and insert of interest into the

vector proceeds via homologous recombination. We verified the expression and stability of CroRS from the expression plasmid by immunoblot with anti-HA_{EF} immune serum.

Gene-targeted for mutations as well as designing the primers for complementation and deletion constructs were identified based on the annotated complete genome of *E. faecalis* OG1RF (NCBI accession: NC_017316.1). Molecular techniques and reagents used in this chapter follow according to **Section 3.2.3**. All constructs were confirmed by sequencing and transformed into respective *E. faecalis* mutants. All primer sequences can be found in **Table 5.2**.

Table 5.2 | Primers used in this study.	
Primer name	Sequence (5'→3') [a]
Complementation	
croR_infusion_F_EcoRI	GCTTGATATCGAATTCGATTGGTATAGGTATTTTCGTTCGTTTTTTACCC
croS_HA tag	TTAAGCGTAATCTGGAACATCGTATGGGTAAGCGTAATCTGGAACATCGTATGGGTAACTCTCTGATTTCTTGTTG
croS_infusion_R_PstI	GTGGATCCCCCGGGCTGCAGTTAAGCGTAATCTGGAACATCGTATGGGTAAG
Deletion	
dHtrAF_PstI	AAACTGCAGATCTTGGCATAGCTATTTAAACG
dHtrAR_PstI	TCCAATGCATTGGCTGCAGAATACAGCGATTAAAGATGCG
htrA_compF_EcoRI	GCTTGATACGAATTCATTCGATAGACTAAAGGAGTAG
dsrtA_F IFD Screen	CGATTGACGCTTTCTTCTCC
dsrtA_R IFD Screen	GAAACAGCAAGAACGCCAAG
dsrtA_F IFD internal	CGGTGATGAAAGCCCAAT
dsrtA_R IFD internal	TCTAAAGGTGAAAATAAGGAAACG
Universal/ Screening primers	
T7 Universal Promoter	TAATACGACTCACTATAGGG
T3 Universal Promoter	CAATTAACCCTCACTAAAGG
M13 (-20) F primer	GTAAAACGACGGCCAGTG
M13 (-40) R primer	CAGGAAACAGCTATGAC
croRcmScreen_F	TTTACCCCCTTTCATCCTTTTT
croRcmScreen_R	CGACCGCATCCTTAGTGG
croScmScreen_F	CCAAAGAAGAACCCGATGAA
croScmScreen_R	GCTGGACACCTGGAAGAGAC
croR screen_F	ATTTCGTTCGAAGGAACTACA
croR screen_R	TATAGGGAGACCGGCCTCGAG

[a]Restriction sites underlined. Complementary sequences to vector are in red. [b] Site-directed mutagenesis residues are in **bold**.

5.2.5 Generation of antibodies

Protocol on antibodies generation for use in this chapter was done according to **Section 3.2.7**. Antibodies used in this chapter are listed in **Table 5.3**.

Table 5.3 | Antibodies used in this chapter.

*Antigen**	*Size (kDa)*	*Primary ab; host*	*Secondary antibody; host*
CroR	25.9	1:5000; Guinea Pig	1:5000; Goat anti-guinea pig HRP conjugate
CroS-HA	44.6	*See HA description*	*See HA description*
EbpA	122.7	1:3000; Rabbit	1:5000; Goat anti-rabbit HRP-conjugate
EbpB	53.4	1:3000; Rabbit	1:5000; Goat anti-rabbit HRP-conjugate
EbpC	68.2	1:3000; Guinea pig	1:5000; Goat anti-guinea pig HRP conjugate
HA		1:3000; Rabbit	1:500; Alexa Fluor® 568 labeled goat anti-guinea pig 1:5000; Goat anti-rabbit HRP-conjugate 1:500; Alexa Fluor® 488 labeled goat anti-rabbit
HtrA	45.7	1:1000; Rat	1: 5000; Goat anti-rat HRP-conjugate
SecA	97.0	1: 3000; Rabbit	1: 5000 Goat anti-rabbit HRP-conjugate
SrtA	27.1	1: 250; Mouse	1:1250; Goat anti-mouse HRP-conjugate
SrtC	32.0	1:250; Mouse	1:1250; Goat anti-mouse HRP-conjugate

*Construct sequences can be found in **Supplementary table A1**.

5.2.6 Growth Kinetic Assay

E. faecalis strains used to perform growth kinetic assay were grown overnight, statically in TSB media supplemented with 0.25% glucose and Cm for strains carrying the transposon cassette. Starter cultures were first diluted 10-fold and grow for one hour at 37°C. Cells were then normalized to OD_{600} of 0.003 in a final volume of 200 µL per well in a 96-well microtiter plate (Nunc™ MicroWell™ 96-Well Microplates, Thermo

Scientific™, USA). The microtiter plate was incubated at 37°C and absorbance were taken at OD_{600} with Infinite® 200 PRO spectrophotometer (Tecan Group Ltd., Switzerland) every 15 mins until the reaction time reached 24 h. All growth kinetic assays were performed with three biological replicates, each with three technical replicates.

5.2.7 Bacterial cell fractionation

To detect and measure the amount of pilin protein expressed by *E. faecalis* mutant strains, we perform bacteria cell fractionation according to **Section 3.2.13**, with the exception that whole cell lysate was further subjected to centrifugation at 20, 000 x *g* for 5 mins. The resulting supernatant containing material liberated from the cell wall digestion was designated the cell wall fraction and the pellet designated the cell-wall free fraction. All fractions were stored at -20^{o}C until use. Immunoblotting was done according to **Section 3.2.14**.

5.2.8 Bacterial cell preparation for TEM, immunofluorescence staining and visualization

To visualize bacterial cell morphology and pili localization on *E. faecalis* mutant strains, we grow bacterial cells and prepared them according to **Section 4.2.10**. Antibodies used against the different antigens of interest can be found in **Table 5.3**. We visualized pili localization and cell morphology using SR-SIM microscopy. Details on imaging using LSM 780 ELYRA PS.1 system was performed according to **Section 3.2.9**.

5.2.9 Quantitative analysis of cell length

Images were collected with AxioVision (Carl Zeiss Zen 8.0 and analyzed with ImageJ (Schindelin, Arganda-Carreras et al. 2012). The maximum cell width is measured using MicrobeJ, a plug-in for the open-source platform ImageJ (Ducret, Quardokus et al.

2016). Quantitative analysis was performed on at least 500 cells per condition, from at least three independent experiments.

5.2.10 Antibiotic susceptibility determinations

E-test (ETEST®, BioMérieux, USA) MICs were determined with 1.5% MH agar using the incubation condition as described in **Section 3.2.1**. Briefly, bacteria from stationary phase cultures in MHB media were washed and normalized visually in 1 X PBS to McFarland standard 1.0. E-test inoculum preparation, plating, strip application, and MIC determinations were carried out according to the manufacturer's protocol (Jorgensen, Ferraro et al. 1997). The antibiotics tested were vancomycin, daptomycin, ceftriaxone, and cefotaxime. Insufficient growth of bacteria on the agar plate to form a bacteria lawn for accurate MIC determination after 18 h incubation will be given an additional incubation time of not more than 24 h.

5.2.11 RNA extraction, purification, and sequencing

For mRNA transcriptomic analyses, we grew the bacteria overnight, statically in TSBG media at 37°C. The next morning, cultures were diluted 1:10 and grown to an optical density (600 nm) of 0.5. Total RNA was extracted using the UltraClean® Microbial RNA Isolation Kit (MO BIO Laboratories Inc., Singapore). Extracted RNA samples were subjected to rigorous DNase treatment using TURBO DNA-free™ kit (Ambion®, Singapore) and purified DNA-free RNA samples were subjected to ribosomal depletion with Ribo-Zero™ Magnetic Kits (Epicenter®, Singapore), all according to manufacturer's protocols. Quantification of RNA and DNA were performed using the Qubit™ RNA Assay Kits and Qubit™ dsDNA HS Assay Kits (Invitrogen, Singapore), respectively. The integrity of RNA was analyzed by gel electrophoresis using Agilent RNA ScreenTape (Agilent

Technologies, Singapore). RNA samples were prepared in triplicate from three independent biological samples.

5.2.12 mRNA library preparation and Illumina sequencing

To convert depleted rRNA into double-stranded cDNA for sequencing, we performed cDNA synthesis (NEBNext RNA First-Strand Synthesis Module; NEBNext Ultra Directional RNA Second Strand Synthesis Module, NEB, Singapore) and purification of cDNA (AMPure XP beads, Beckman Coulter, Singapore) as described previously. mRNA libraries for RNA sequencing were prepared using TruSeq Stranded mRNA Library Prep Kit (Illumina, USA), the quality of the library analyzed via Bioanalyzer (Agilent, USA), and sequencing performed using an Illumina Miseq V2 machine. RNA sequencing reads were mapped to the *E. faecalis* OG1RF reference genome (NCBI accession: NC_017316.1) using BWA (v0.5.9) with default parameters (Li and Durbin 2009, Nagalakshmi, Waern et al. 2010). Sequencing reads mapping to predicted open reading frames (ORFs) were quantified using HTSeq (Anders, Pyl et al. 2015). Counts for ribosomal and transfer RNA sequences were filtered out of the data set and differential expression analyses were performed in R (Version 2.15.1) using the Bioconductor package, edgeR (Robinson et al., 2010). Significantly differentially expressed genes were determined using a P-value and FDR cut off of 0.05. We annotated differentially expressed genes using a combination of KEGG annotations, as well as manual annotation using operon and other functional data from the literature.

5.2.13 Statistical analysis

Data from multiple experiments were pooled. Statistical significance with the percentage of cells expressing pilin was determined using the unpaired t-test. Statistical significance with the number of division septa per cell unit was determined using the Holm-Sidak method. Unless otherwise stated, values represented means ± SEM derived from at least three independent experiments and/ or three technical replicates. * $P < 0.05$; ** $P \leq 0.01$; *** $P \leq 0.001$; **** $P \leq 0.0001$; $P \geq 0.05$, differences not significant (n.s). GraphPad Prism 6 software (GraphPad Software, La Jolla, CA) was used for statistical analyses.

5.3 RESULTS

5.3.1 CroR confers resistance to cell wall antibiotics

CroR-CroS TCS plays a critical role in intrinsic resistance to β-lactams antibiotics, such as ceftriaxone and cefotaxime (Djoric and Kristich 2015, Kellogg and Kristich 2016, Kellogg, Little et al. 2017). Deletion of the gene locus *croRS* leads to a 4000-fold reduction in MIC against ceftriaxone (Comenge, Quintiliani et al. 2003, Kellogg, Little et al. 2017, Muller, Massier et al. 2018). Phosphorylated CroR drives enhanced cephalosporin resistance, and absence of CroS phosphatase activity causes hyper-resistance to ceftriaxone and cefotaxime because *croR* transcription can be regulated by a non-cognate HK, CisS, leading to constitutive expression and phosphorylation of CroR (Kellogg and Kristich 2016). To investigate if the *croR::Tn* and *croS::Tn* respond similarly to *croR* and *croS* null mutants used in previous studies (Djoric and Kristich 2015, Kellogg and Kristich 2016, Kellogg, Little et al. 2017) towards ceftriaxone and cefotaxime, we performed the same antibiotic susceptibility test on *croR::Tn* and *croS::Tn*. As shown in **Table 5.4**, both mutants responded similarly towards ceftriaxone and cefotaxime, validating the loss of function in *croR::Tn* and *croS::Tn*.

Table 5.4 | MICs of various antibiotics for *E. faecalis* mutants.

Strains	Median MIC (µg/mL) [#]			
	Vancomycin	Daptomycin	Ceftriaxone	Cefotaxime
ATCC 29212	2.0	0.75	>256	>32
WT OG1RF	2.0	0.75	>256	>32
Δ*srtA*Δ*htrA*	2.0	0.50	16.0	4.0
croR::Tn	1.0	0.38	3.0	1.0
*croR::Tn*Δ*srtA*Δ*htrA*	0.75	0.25	6.0	3.0
croS::Tn	2.0	0.50	>256	>32
*croS::Tn*Δ*srtA*Δ*htrA*	1.0	0.032	4.0	2.0

[#] Median MICs are reported from 2 biological replicates. ATCC 29212 is the positive control strain that fit the standard MIC of gentamicin (4-16 µg/mL).

5.3.2 Construction of *E. faecalis croR::Tn*Δ*srtA*Δ*htrA* and *croS::Tn*Δ*srtA*Δ*htrA* mutants in OG1RF

To characterize the functions of CroR-CroS TCS in 'off-pathway' pilus biogenesis, we constructed an unmarked, in-frame deletion of *srtA* and *htrA* in *croR::Tn* and *croS::Tn* mutants, based on the genome sequence of OG1RF (NCBI accession: NC_017316.1). We performed stepwise gene deletion by homologous recombination. We confirmed the absence of *srtA* in these mutant constructs by PCR screen using primer pairs dsrtA_F IFD screen/dsrtA_R IFD screen and dsrtA_F IFD screen/dsrtA_R IFD internal (**Fig 5.1A**). *croR::Tn*Δ*srtA* and *croS::Tn*Δ*srtA* clones were subjected to immunoblotting of whole-cell lysates using anti-SrtA immune serum to validate the absence of SrtA expression (**Fig 5.1B**). *croR::Tn*Δ*srtA* and *croS::Tn*Δ*srtA* were subjected to deletion of *htrA* using homologous recombination. We confirmed the absence of *htrA* in this mutant construct

by PCR screen using primer pairs dHtrAF_ PstI/dHtrAR_PstI and htrA_compF_EcoRI /dHtrAR_PstI. *croR::Tn*Δ***srtA***Δ*htrA* and *croS::Tn*Δ***srtA***Δ*htrA* were subjected to immunoblotting of *E. faecalis* whole-cell lysates using anti-$HtrA_{EF}$ immune serum to validate the absence of HtrA protein expression (**Fig 5.1C**). Validated *croR::Tn*Δ***srtA***Δ*htrA* and *croS::Tn*Δ***srtA***Δ*htrA* strains are used for subsequent experiments to investigate how CroR or CroS loss-of-function affect signaling cascades in 'off-pathway' pilus biogenesis.

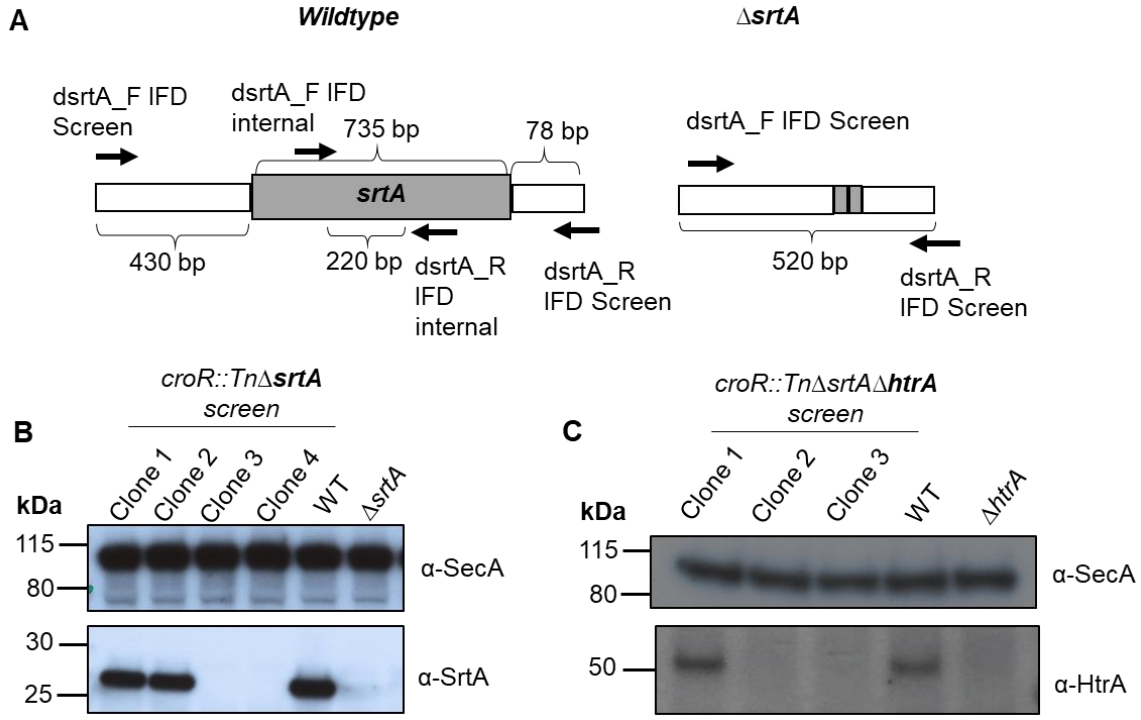

Figure 5.1 | Locus and genetic disruption of *srtA* and *htrA* in *croR::Tn* and *croS::Tn* transposon mutants. (**A**) Schematic diagram of PCR product sizes produced using various primer pairs combination. (**B**) Representative blot showing the absence of SrtA protein expression in *croR::Tn*Δ*srtA* validated by immunoblot with α-SrtA immune serum. (**C**) Representative blot showing the absence of HtrA protein expression in *croR::Tn*Δ***srtA***Δ*htrA* validated by immunoblot with α-$HtrA_{EF}$ immune serum. Immunoblots performed on the same samples using the α-SecA immune serum as a loading control. PageRuler™ pre-stained protein gel (10-250 kDa) was used as ladder.

5.3.3 Absence of *croR* restores piliation levels during membrane stress

In **Chapter 4**, we showed that hyper-piliation drives upregulation of *croRS* operon expression and we hypothesize that hyper-piliation is a CroR-mediated stress response. To investigate if CroR influences surface pilus expression, we performed immunofluorescent labeling of *croR::Tn*Δ*srtA*Δ*htrA* with anti-EbpC immune serum. The absence of *croR* exhibits a significant decrease in the number of cells expressing pili (36%), as compared to Δ*srtA*Δ*htrA* (57%). Complementation of *croR::Tn*Δ*srtA*Δ*htrA* with *croRS* on an expression plasmid (p*croRS-2xHA*) restores the number of cells expressing pili on the surface to 62%, showing that CroR can indeed influence surface pilus expression. To investigate if the absence of CroS also affects surface pilus expression, we performed a similar test on *croS::Tn*Δ*srtA*Δ*htrA* but we did not observe a significant drop in the number of cells expressing pili in *croS::Tn*Δ*srtA*Δ*htrA* (47%), as compared to Δ*srtA*Δ*htrA* (**Fig 5.2B**). This phenotype is probably linked to the influence of a non-cognate HK, CisS (Kellogg and Kristich 2016), that can regulate *croR* expression in the absence of CroS. This will be further discussed in **Section 5.4**.

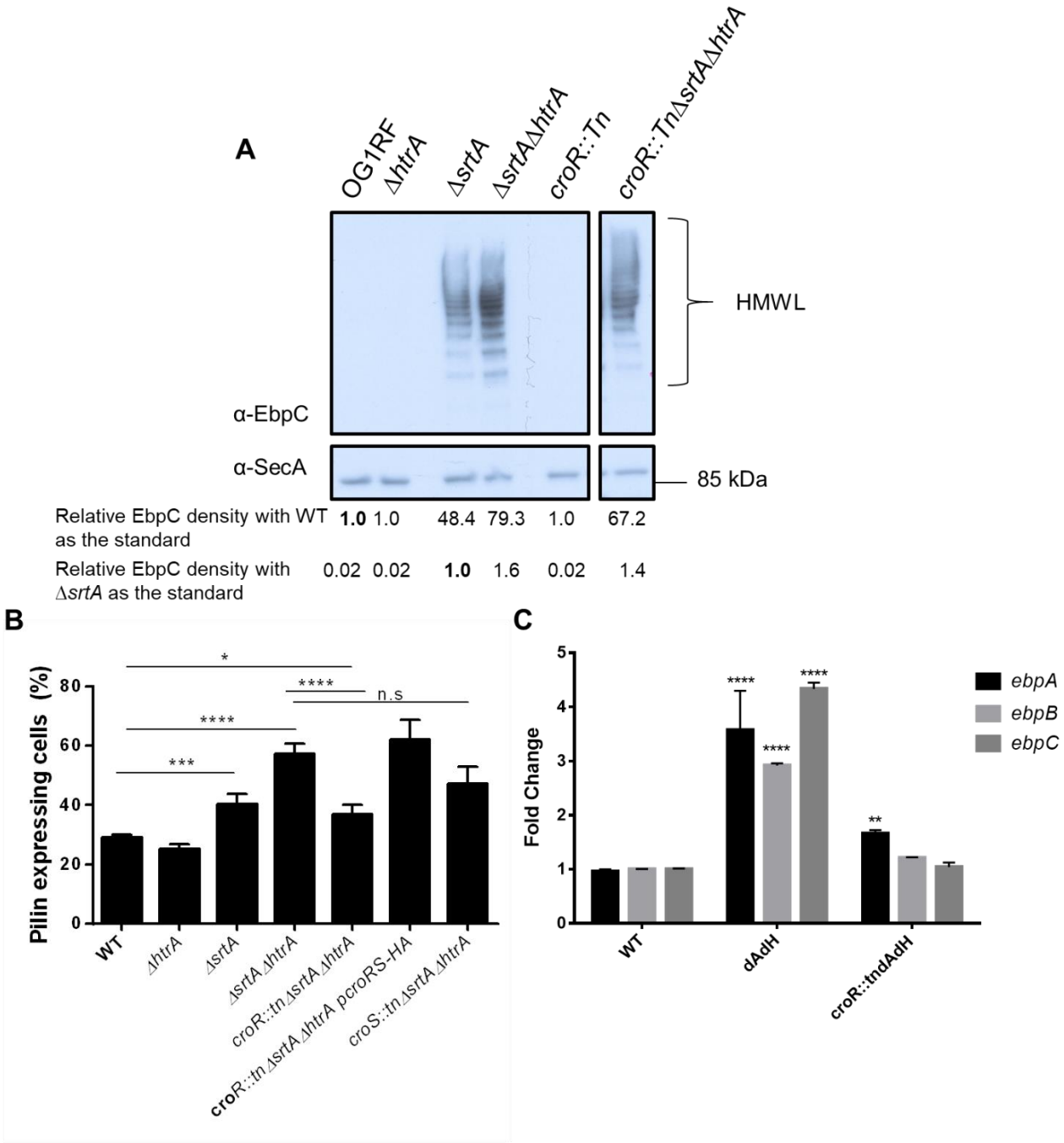

Figure 5.2 | *croR* is responsible for Ebp pili expression. (A) Immunoblot was performed with α-EbpC immune serum on protoplast fractions of WT, Δ*htrA,* Δ*srtA,* Δ*srtA*Δ*htrA; croR::Tn,* and *croR::Tn*Δ*srtA*Δ*htrA*. The top blot shows pilus HMWL (brackets) and α-SecA immune serum was used as a loading control. PageRuler™ pre-stained protein gel (10-250 kDa) was used as ladder. Relative EbpC densities were calculated with WT or the Δ*srtA* strain as the standard. Two irrelevant lanes between *croR::Tn* and *croR::Tn*Δ*srtA*Δ*htrA* were omitted for clarity, and this omission is indicated

by the break in the frame. (**B**) Statistical analysis of pili expressing cells labeled with α-EbpC immune serum and Alexa Fluor® 568 secondary antibody determined using the unpaired t-test. Results are represented as bar graphs. * $P < 0.05$; *** $P \leq 0.001$; **** $P \leq 0.0001$; $P \geq 0.05$, differences not significant (n.s). Combined data from three independent experiments were shown. (**C**) qRT-PCR analysis of *ebpA* (black bars)*, ebpB* (light gray bars) and *ebpC* (dark gray bars) expression in the OG1RF WT, Δ*srtA*Δ*htrA* and *croR::Tn*Δ*srtA*Δ*htrA*. qRT-PCR was performed in biological triplicate and analyzed by the $\Delta\Delta C_T$ -method, using *gyrB* as a housekeeping gene. Fold change indicates the change in *ebp* genes transcription, compared to control (WT). Statistical analysis was performed by the 2-way ANOVA; Sidak's comparisons test using GraphPad. **** $P \leq 0.0001$.

5.3.4 CroR induction correlates with cell morphology

Since CroR influences Ebp pilus expression, and we have previously determined that hyper-piliation induces morphology defects, to visualize the cell morphology of *croR::Tn*Δ*srtA*Δ*htrA,* we performed IFA using vancomycin-fluorescein (Van-FL) to stain the nascent PG of the cell. Observations by SR-SIM showed that *croR::Tn*Δ*srtA*Δ*htrA* exhibits morphology similar to WT, further supporting the data in **Chapter 4** that the cell morphology is CroR and pilus-dependent. Since *croS::Tn*Δ*srtA*Δ*htrA* does not restore piliation to WT levels, we expected that *croS::Tn*Δ*srtA*Δ*htrA* still exhibits abnormally-shaped cells. Indeed, *croS::Tn*Δ*srtA*Δ*htrA* cells appeared shorter than the WT strain (**Fig 5.3**).

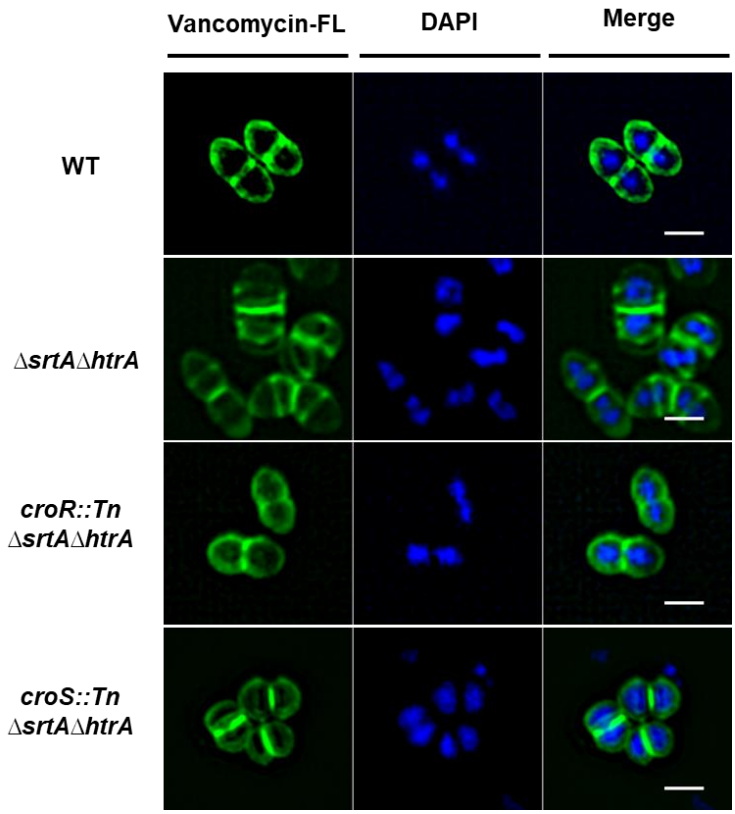

Figure 5.3 | CroR induction correlates with cell morphology. The cell wall was stained with Van-FL conjugate (green). DAPI (blue) was used to visualize DNA. Representative images were shown. Scale bars represent 1 µm.

To quantify our observation, we measured the maximum cell width of 200 cells from each strain and plotted a histogram to identify the distributions of cell width of each strain (**Fig 5.4A**). *croS::Tn*Δ*srtA*Δ*htrA* and Δ*srtA*Δ*htrA* have maximum cell width that are approximately ~0.85 µm, as compared to *croR::Tn*Δ*srtA*Δ*htrA* or WT (~0.7-0.75 µm). Even though both *croS::Tn*Δ*srtA*Δ*htrA* and Δ*srtA*Δ*htrA* share similar cell width, individual *croS::Tn*Δ*srtA*Δ*htrA* cells appear shorter in length as compared to Δ*srtA*Δ*htrA* (**Fig 5.4B**).

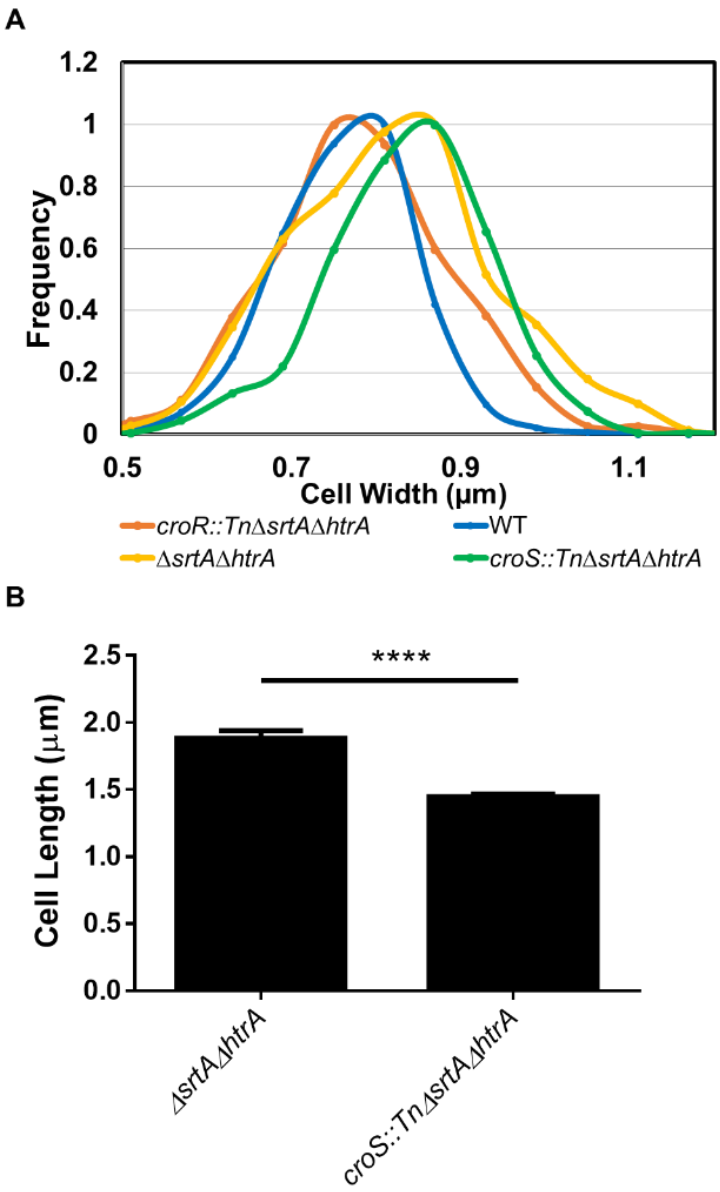

Figure 5.4 | *croS::TnΔsrtAΔhtrA* cells are wider in cell width and shorter in length. (**A**) The relative cell width of indicated strains of bacterial populations was determined by measuring the mid-width of the cells. (**B**) The relative cell length of Δ*srtA*Δ*htrA* and *croS::TnΔsrtAΔhtrA* bacterial populations was determined by measuring the mid-length that runs from one cell pole to the other. The cell width and length of cells are quantified using MicrobeJ plugin in ImageJ. Cells that were not in-phase were excluded from both analyses. A total of at least 200 cells were sampled per strains. Statistical significance for cell length was determined using a two-tailed unpaired Mann-Whitney test. **** P ≤ 0.0001. The error bars reflect the standard error of the mean.

To investigate if the cell shape abnormalities observed in *croS::Tn*Δ***srtA***Δ***htrA*** affected growth, we performed growth kinetics assays. The growth profile of *croS::Tn*Δ***srtA***Δ***htrA*** shows both an extended lag phase and a slight depression in the growth rate (**Fig 5.5**). The growth retardation in *croS::Tn*Δ***srtA***Δ***htrA*** could be attributed to the decreased cell size that halted cell growth.

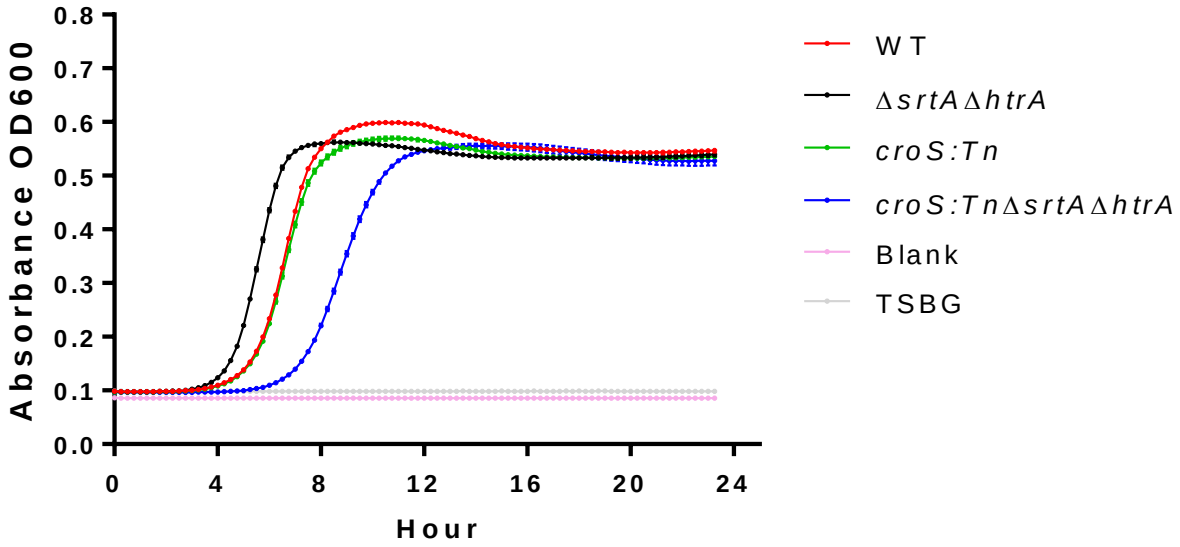

Figure 5.5 | Growth kinetic profiles of *croS* mutant variants. Growth phenotypes of indicated *E. faecalis* strains in TSBG at 37°C without shaking. OD reading for the growth kinetic assays was represented for *croS* mutant variants. The data shown are from three independent experiments. The standard error of mean bars is smaller than the symbols.

5.2.5 croS*::Tn*Δ***srtA***Δ***htrA*** exhibits sensitivity to cell wall and membrane-targeting antibiotics

To investigate if the MIC of *croR::Tn* and *croS::Tn* mutant derivatives towards β-lactam antibiotics are affected in the presence of membrane stress, we performed antibiotic susceptibility tests on *croR::Tn*Δ***srtA***Δ***htrA*** and *croS::Tn*Δ***srtA***Δ***htrA.*** *croR::Tn*Δ***srtA***Δ***htrA*** shows similar susceptibility phenotype as *croR::Tn* towards

ceftriaxone and cefotaxime. Unlike *croS::Tn*, *croS*::*Tn*Δ***srtA***Δ*htrA* exhibits sensitivity towards ceftriaxone and cefotaxime (**Table 5.4**).

In addition, we performed vancomycin susceptibility tests on *croR::Tn*Δ***srtA***Δ*htrA* and *croS::Tn*Δ***srtA***Δ*htrA* to determine if CroR-CroS TCS is responsive to other classes of cell wall-targeting antibiotics. Both strains were modestly more sensitive to vancomycin, similar to previous studies performed in *E. faecium* Δ*croRS* mutant (Kellogg, Little et al. 2017), suggesting that CroR-CroS plays a major role specifically towards β-lactam antibiotics.

We postulate that in *croS::Tn*Δ***srtA***Δ*htrA,* membrane stress and the absence of phosphorylated CroR can affect cells' ability to resist to β-lactam antibiotics. We asked if the presence of membrane stress (in addition to cell wall stress) can cause Δ***srtA***Δ*htrA,* c*roR::Tn*Δ***srtA***Δ*htrA* and *croS::Tn*Δ***srtA***Δ*htrA* to be more susceptible to cell membrane-targeting antibiotics as well. Δ***srtA***Δ*htrA* cells were mildly more sensitive to daptomycin, similar to *croS::Tn* (0.50 µg/mL, WT-0.75 µg/mL). This mild effect may be due to CroR induction in Δ***srtA***Δ*htrA*, as observed by RNA sequencing (**Fig 4.16, Table 4.6**). We observed a three-fold decrease in the median MIC for daptomycin of c*roR::Tn*Δ***srtA***Δ*htrA* (0.25 µg/mL) compared to WT (0.75 µg/mL), providing a correlation between Dap sensitivity and *croR* transcript levels (**Fig 4.16** and **Table 5.4**). It is interesting to note that *croR::Tn* also shows decreased resistance to daptomycin (0.38 µg/mL), but the presence of membrane stress makes c*roR::Tn*Δ***srtA***Δ*htrA* more sensitive to daptomycin. A drastic drop in MIC towards daptomycin was observed in *croS::Tn*Δ***srtA***Δ*htrA* (0.032 µg/mL) as compared to *croS::Tn* (0.5 µg/mL). These findings indicate that CroR is required to mediate a stress response towards membrane perturbation, as well as cell wall disruption.

5.3.5 Identification of potential CroR targets by RNA sequencing

In addition to its role in intrinsic β-lactam resistance, the CroR-CroS TCS in *E. faecalis* is also required during exponential growth as a pleiotropic regulator of genes involved in the stress response (Le Breton, Boel et al. 2003, Muller, Le Breton et al. 2006), cell shape maintenance (Muller, Le Breton et al. 2006), biofilm formation (Mohamed, Teng et al. 2006), cell adherence (Mohamed, Teng et al. 2006), and glutamine/glutamate transport (Le Breton, Muller et al. 2007).

Based on the above results, CroR influences surface pilus expression, cell morphology, and resistance to cell wall and membrane-targeting antibiotics. However, we do not know if CroR directly or indirectly regulates genes involved in these events. To identify genes differentially regulated in the absence of CroR-CroS TCS, we performed transcriptomic analysis on total RNA extracted from *croR::Tn*Δ*srtA*Δ*htrA*, Δ*srtA*Δ*htrA,* and Δ*srtA.* Genes with significant differences in the abundance of mRNAs were determined using a P value and FDR cut-off of 0.05. Read mapping and differential analyses revealed a total of 282 genes statistically significantly different between *croR::Tn*Δ*srtA*Δ*htrA* relative to Δ*srtA*Δ*htrA* (summarized in **Supplementary table C4**).

To identify genes that are differentially regulated due to *croR* transposon insertion and not due to the absence of *htrA* and *srtA,* we identified 282 genes that are common between *croR::Tn*Δ*srtA*Δ*htrA* in comparison with Δ*srtA*Δ*htrA*. Because we are interested to identify genes common between *htrA* and *croR*, we further filtered the 282 genes against the Δ*srtA*Δ*htrA* in comparison with Δ*srtA* to get the contribution of *htrA*. For example, *glnP*, a known CroR target, is suppressed (1.93 $\log_2$ fold reduction) when *croR* expression is induced in Δ*srtA*Δ*htrA* relative to Δ*srtA.* (**Table 5.5**). In *croR::Tn*Δ*srtA*Δ*htrA*

when *croR* expression is absent, *glnP* expression will not be suppressed but is induced (1.71 $\log_2$ fold induction) in *croR::Tn*Δ*srtA*Δ*htrA* relative to Δ*srtA*Δ*htrA*. Based on this method, we identified 81 potential CroR targets involved in multiple cellular functions, such as cell envelope homeostasis, ABC transport systems, cell metabolism, and gene signaling and regulation (**Supplementary Table C6**). The $\log_2$ fold change distribution of the 81 genes is displayed using transcriptomic data comparing between *croR::Tn*Δ*srtA*Δ*htrA* relative to Δ*srtA*Δ*htrA* and shown as a dot plot (**Fig 5.6B**). Among these 81 genes, 29 genes were downregulated in the absence of *croR* (CroR-activated genes) and 52 were upregulated in the presence of *croR* (CroR-repressed genes).

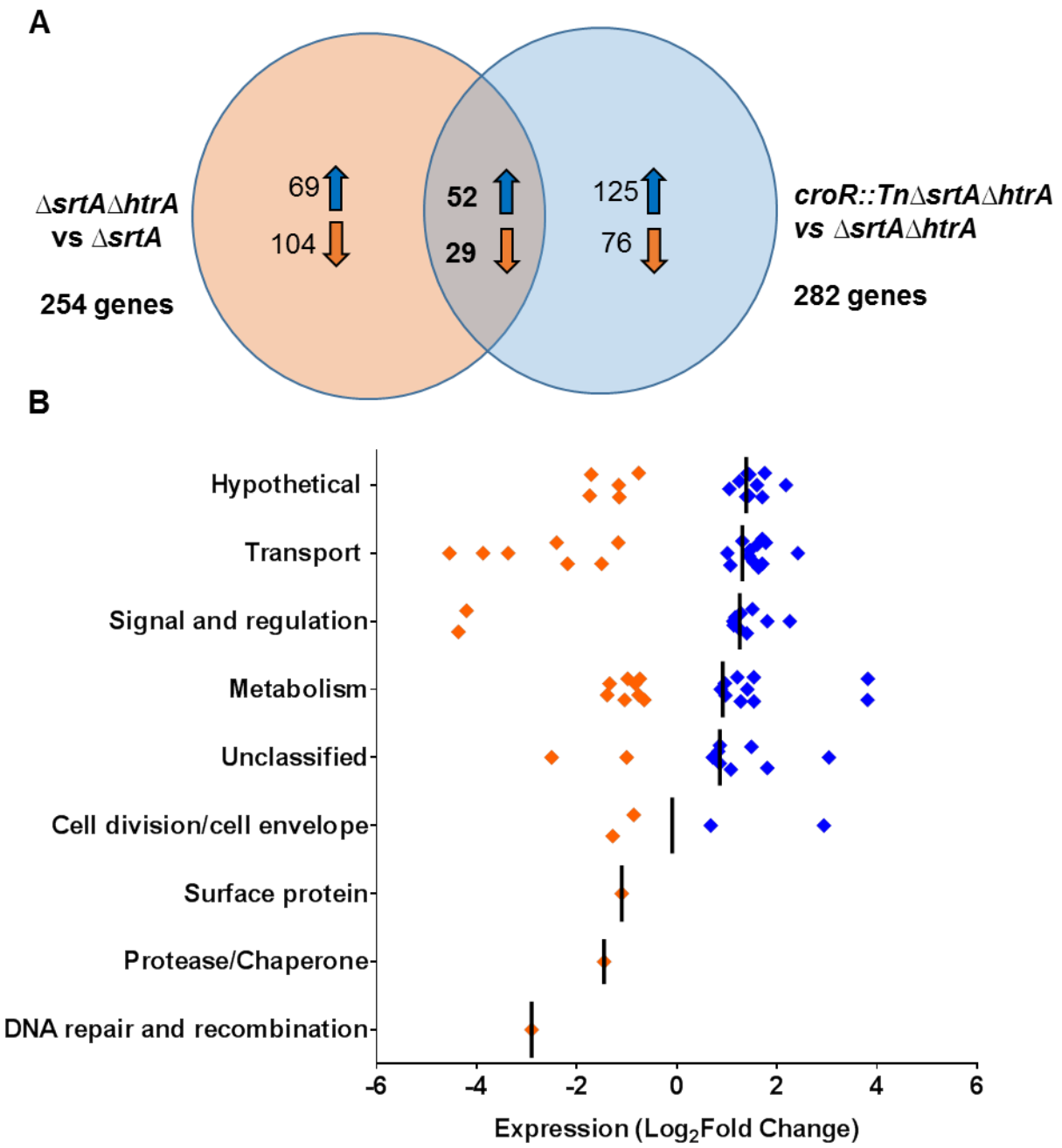

Figure 5.6 | Transcriptional gene expression profile of predicted CroR-regulated genes. (**A**) Venn diagram showing 81 potential genes to be CroR regulated specifically during membrane stress. (**B**) The $\log_2$ fold change in mRNA levels of these 81 genes is displayed as a dot plot. Gene expression differences were significant ($P < 0.05$).

CroR regulates *croRS* expression (Le Breton, Muller et al. 2007) and among the 81 genes, we observed *croRS* operon expression to be downregulated (*croR* -4.36 log_2 fold change; *croS* -4.20 log_2 fold change) in *croR::Tn*Δ*srtA*Δ*htrA*, validating its absence. In addition to the *croRS* operon, seven additional genes that are known to be direct CroR targets (Muller, Massier et al. 2018) were also differentially regulated (**Table 5.5**). Among these seven genes, three genes code for hypothetical proteins of unknown functions. The *glnQHMP* operon is involved in glutamine/glutamate transport (Le Breton, Muller et al. 2007) and *telA* codes for a tellurite resistance protein not known to affect virulence factor assembly or play a part in cell morphology.

Table 5.5 | Known CroR-targets differently regulated during membrane stress.

Locus Tag	*croR::Tn*Δ*srtA*Δ*htrA* vs Δ*srtA*Δ*htrA*[#]	Δ*srtA*Δ*htrA* vs Δ*srtA*[#]	Gene	Annotation
OG1RF_10895	**1.71**	**-1.93**	*glnP*	glutamine ABC superfamily ATP binding cassette transporter, membrane protein
OG1RF_10897	**1.44**	**-1.71**	*glnH*	glutamine ABC superfamily ATP binding cassette transporter, binding protein
OG1RF_10898	**1.78**	**-1.45**	*glnQ*	ABC superfamily ATP binding cassette transporter, ABC protein
OG1RF_11464	**-1.16**	**3.69**		hypothetical protein
OG1RF_12066	**-1.15**	**2.25**		hypothetical protein
OG1RF_12067	**-1.00**	**1.69**	*telA*	tellurite resistance protein
OG1RF_12152	**1.60**	**-1.15**		hypothetical protein
OG1RF_12535	**-4.36**	**1.18**	*croR*	response regulator
OG1RF_12536	**-4.20**	**1.09**	*croS*	sensor histidine kinase

Manual annotation in red. [#]Values are in Log_2 fold change.

5.3.6 Genes of the *fsr* system and cell wall synthesis and elongation are potential CroR targets

We next looked for other genes that may contribute to CroR-dependent piliation phenotypes. Among the genes involved in signaling and regulation, we identified genes of the *fsr* system (*fsrB* and *fsrC*) to be potentially repressed by CroR (**Table 5.6**). The *fsr* system negatively regulates *ebpR* expression leading to decreased Ebp expression (Bourgogne, Thomson et al. 2010) which may explain the increased piliation phenotype in *ΔsrtAΔhtrA*.

Table 5.6 | Potential CroR-regulated genes of interest.

Locus Tag	*croR::TnΔsrtAΔhtrA* vs *ΔsrtAΔhtrA*[#]	*ΔsrtAΔhtrA* vs *ΔsrtA*[#]	Gene	Annotation
OG1RF_11526	**1.13**	**-2.38**	*gelE*	Gelatinase
OG1RF_11525	**1.28**	**-2.40**	*sprE*	SprE protein
OG1RF_11528	**1.51**	**-1.57**	*fsrB*	FsrB protein
OG1RF_11527	**1.81**	**-1.72**	*fsrC*	Sensor histidine kinase FsrC
OG1RF_12158	**-1.28**	**1.46**	*penA*	Penicillin-binding protein 2B
OG1RF_12333	**-0.86**	**0.98**	*mreC*	Rod shape-determining protein MreC
OG1RF_11573	**0.68**	**-1.48**	*murC*	UDP-N-acetylmuramate--L-alanine ligase
OG1RF_11071	**2.94**	**-3.40**	*rodA*	FtsW/RodA/SpovE family cell division protein

[#]Values are in Log_2 fold change.

As we observed a restoration of cell morphology to the WT phenotype in *croR::Tn∆srtA∆htrA,* we looked at genes classified under “cell division and cell envelope”. We identified four genes, namely *penA, mreC, rodA, murC* to be differentially expressed. MurC is the UDP-N-Acetylmuramic acid l-alanine ligase positioned as the third enzyme in the Mur pathway that catalyzes the first stepwise addition of pentapeptide to UDP-N-acetyl-muramic acid (UNAM) required for lipid I biosynthesis (Humnabadkar, Prabhakar et al. 2014, Laddomada, Miyachiro et al. 2016). *penA* codes for penicillin-binding protein 2 (PBP2) that exhibits transpeptidase activity during PG biosynthesis (Popham and Young 2003). MreC is a structural protein that serves as a platform during cell wall elongation, scaffolding other essential peptidoglycan biosynthesis macromolecules, such as PBPs (Contreras-Martel, Martins et al. 2017). RodA is the FtsW/RodA/SpovE family cell division protein that controls cell shape and is required for viability (Bendezu and de Boer 2008). The last three genes are part of the Rod system that catalyzes the addition of newly synthesized PG material along the cell body to promote cell elongation (Typas, Banzhaf et al. 2011). These findings suggest that CroR might mediate stress responses through the regulation of genes involved in cell elongation.

5.4 Discussion

In **Chapter 4**, we showed that HtrA is required for processing 'off-pathway' pilins. In the absence of HtrA, mislocalized pili on the cell membrane are not cleared, giving rise to a hyper-piliation-induced morphology defect. *E. faecalis* need strategies to cope with such stress. How *E. faecalis* handles this is currently unknown. Bacteria often involve TCSs to sense and response to environmental stimuli, by quickly activating downstream signaling cascades that help cells to survive better during stressful conditions. We identified the CroR-CroS TCS that was induced in the presence of pilus accumulation in **Chapter 4** and we think that the CroR-CroS TCS senses the membrane perturbation to mediate a stress response in Δ*srtA*Δ*htrA.*

To determine if CroR-CroS TCS is required to respond to 'off-pathway' pilin accumulation, we examined piliation levels in *croR::Tn*Δ*srtA*Δ*htrA* and *croS::Tn*Δ*srtA*Δ*htrA* and observed that *croR::Tn*Δ*srtA*Δ*htrA* no longer exhibits morphology defects (**Fig 5.3**), suggesting that CroR can influence Ebp pili expression and morphology defects are dependent on the accumulation of 'off-pathway' pilins as well as the presence of CroR.

Receiver (REC) domains of the response regulators (RRs) participate in the catalysis of phosphoryl transfer from the HK to itself and regulate the activity of the effector domain in a phosphorylation-dependent manner (Gao and Stock 2009). Based on NMR dynamic studies, REC domains of RRs are primarily in the unphosphorylated, inactive conformation and can be phosphorylated within microseconds to stabilize the active conformations of the REC domain controlling the effector domain activity (Gardino

and Kern 2007). For *E. faecalis* to be resistant against β-lactam antibiotics, CroR must be phosphorylated by CroS to drive cephalosporin resistance (Kellogg and Kristich 2016). We think that CroR in Δ*srtA*Δ*htrA* is in the phosphorylated form to mediate stress responses to 'off-pathway' pilus accumulation just like how phosphorylated CroR is required to promote cephalosporin resistance.

However, tight regulation of CroR phosphorylation is necessary as an increase in phosphorylated CroR leads to impaired growth (Kellogg and Kristich 2016). CroS exhibits both kinase and phosphatase activities to control CroR phosphorylation *in vivo* in response to cephalosporin antibiotics to prevent unnecessary cross-talk with a non-cognate HK (Kellogg and Kristich 2016). *croS::Tn* exhibits hyper-resistance towards these β-lactam antibiotics due to constitutive CroR phosphorylation by the non-cognate HK, CisS (Kellogg and Kristich 2016). Decreased resistance towards ceftriaxone and cefotaxime in *croS::Tn*Δ*srtA*Δ*htrA* suggests that the presence of membrane stress in this mutant prevents phosphorylation of CroR by the non-cognate CisS or aberrant cell morphology caused by membrane stress make these cells more prone to β-lactam antibiotic killing (**Table 5.4**). Even though *cisRS* expression is not transcriptionally affected in *croS::Tn*Δ*srtA*Δ*htrA* (**Supplementary Table C8**), we speculate that a minute amount of activated CisS may be enough to drive phosphorylation of CroR in the absence of CroS (personal communication with Christopher J. Kristich).

An interesting finding from antibiotic susceptibility tests revealed that *croS::Tn*Δ*srtA*Δ*htrA* and Δ*srtA*Δ*htrA,* despite our predictions that CroR is phosphorylated in these two strains, are still sensitive to cell wall-targeting and membrane-targeting antibiotics suggesting that membrane stress may contribute to increased sensitivity to cell

wall and membrane-targeting antibiotics (**Table 5.4**). Furthermore, *croR::Tn*Δ*srtA*Δ*htrA* is more sensitive to daptomycin than *croR::Tn* revealing for the first time that CroR plays a potential role in sensing membrane stress (as opposed to cell wall stress).

Why are we seeing an aberrant phenotype in Δ*srtA*Δ*htrA* when induced CroRS is supposed to help clear the stress? A slight imbalance in PG synthesis and degradation on the cell wall could be perceived by CroRS as cell wall stress, leading to kinase activation and phosphorylation (Kellogg, Little et al. 2017). Since CroR may also sense membrane stress, we think that a slight perturbation on the membrane leads to kinase activation and phosphorylation and that 'off-pathway' Ebp pili signals drive constitutive CroR phosphorylation and override CroS phosphatase activity leading to an imbalance in the kinase: phosphatase activity ratios, resulting in an Ebp-dependent morphological defect.

As these are speculations based on previous studies, the phosphorylation state of both the CroR-CroS and CisR-CisS TCSs should be examined, in addition to transcriptomic analyses of these mutants, to determine their involvement in Δ*srtA*Δ*htrA*. To determine if phosphorylated CroR responds to pilus-mediated stress, we can perform alanine site-directed mutagenesis on the conserved aspartic acid residue on CroR (D52) to prevent phosphorylation and investigate the flow of phosphoryl groups from CroS to CroR in influencing piliation. This will be discussed further in **Chapter 6.2.1**.

In this study, we have identified 81 potential CroR-targets, with most of the genes involved in metabolic activities and substrate transport. Eleven of the gene targets encode proteins with regulatory functions, suggesting that CroR plays a central role in controlling members of secondary regulation pathways (**Supplementary Table C6**). These potential

targets set as the stepping stone for a possible continuation of the project (see **Chapter 6, Section 6.2.3**).

We identified genes coding for cell elongation proteins to be CroR-regulated. The proteins that are involved in cell elongation are MreB, MreC, MreD, RodA and PBP2 (Cho, Uehara et al. 2014, Laddomada, Miyachiro et al. 2016, Contreras-Martel, Martins et al. 2017). Tight orchestration of the cell elongation system is important, as inhibition or dysregulation of these genes can lead to defects in cell shape, impaired growth, and often cell wall lysis and death (Holtje 1998, den Blaauwen, de Pedro et al. 2008). Among the three genes (MreC, RodA, and PBP2) that are involved in cell elongation, *rodA* transcription is highly repressed (log_2 fold change -3.40) by CroR. Even though *penA* and *mreC* are CroR-induced, transcription of both genes is less affected than that of *rodA* (1.46 and 0.98-log_2 fold change); hence, we postulate that dysregulation of *rodA* is enough to inhibit cell elongation. This may explain why Δ*srtA*Δ*htrA* and *croS::Tn*Δ*srtA*Δ*htrA* are fatter and shorter than WT (**Fig 5.3 and 5.4**).

In addition, we identified genes of the *fsr* system as CroR-regulated genes. The *fsr* locus consists of four genes, namely, *fsrA, fsrB, fsrC* and *fsrD* (**Table 5.6 and Fig 5.7**). The *fsrA* gene encodes the response regulator FsrA, that autoregulates its own expression (Bourgogne, Hilsenbeck et al. 2006). Activated FsrA regulates expression of *fsrB*, *fsrC, gelE,* and *sprE*, which are located downstream of the *fsr* system (Qin, Singh et al. 2001). FsrB is a transmembrane protein responsible for processing the auto-inducing pro-peptide FsrD to generate gelatinase biosynthesis-activating pheromone (GBAP) (Bourgogne, Hilsenbeck et al. 2006). GBAP is a quorum-sensing signal sensed by the FsrC HK to activate the FsrA-FsrC TCS. Apart from the regulation of *fsr* gene expression

by the FsrA response regulator, *fsrB, fsrC, gelE*, and *sprE* expression are also *fsrB*-dependent (Bourgogne, Hilsenbeck et al. 2006). Deletion of either *fsrA*, *fsrB* or *fsrC* affects *gelE* and *sprE* expression (Qin, Singh et al. 2000), consistent with our data where we observe decreased *gelE* and *sprE* expression when *fsrB* and *fsrC* expression is suppressed in *croR::Tn*Δ*srtA*Δ*htrA.* Since *fsrB* and *fsrC* are co-transcribed and both *fsrA* and *fsrD* autoregulate their own expression, we postulate that the downregulation of *fsrB* causes the subsequent suppression of *fsrC*, *gelE* and *sprE* expression in *croR::Tn*Δ*srtA*Δ*htrA*. The *fsr* system also negatively regulates *ebpR* expression leading to decreased Ebp expression (Bourgogne, Hilsenbeck et al. 2006, Bourgogne, Thomson et al. 2010). We do not observe a significant change in *ebpR* expression in *croR::Tn*Δ*srtA*Δ*htrA* relative to Δ*srtA*Δ*htrA* suggesting a novel pathway that negatively regulates Ebp expression involving both the FsrA-FsrC and CroR-CroS TCSs. We postulate that the observed decreased pili on the surface of *croR::Tn*Δ*srtA*Δ*htrA* is attributed to the upregulation of *fsrB* when CroR is gone, leading to activation of the *fsr* system and a novel pathway via the CroR-CroS TCS to suppress *ebpABC* operon expression.

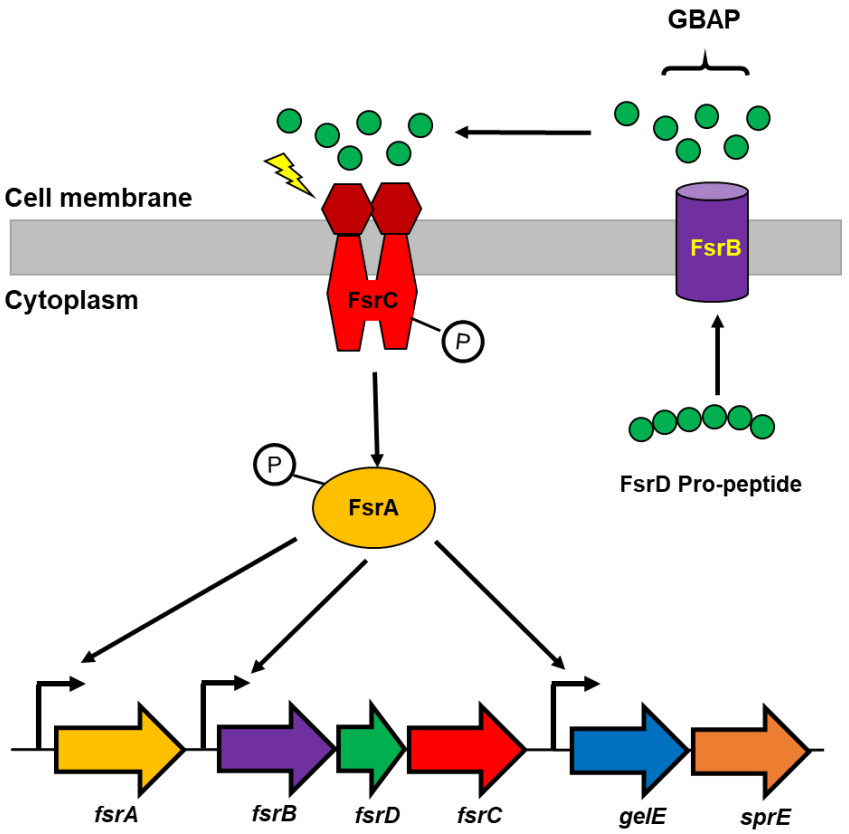

Figure 5.7 | A simplified cartoon of the *fsr* quorum-sensing system and its regulation in *E. faecalis*. FsrA autoregulates its own gene, *fsrA*, as well as *fsrB* (co-transcribed with *fsrD* and *fsrC*) and *gelE* (co-transcribed with *sprE*). *fsrB* encodes a transmembrane protein responsible for processing FsrD pro-peptide to generate gelatinase biosynthesis-activating pheromone (GBAP). Accumulated quorum-sensing molecule GBAP in the extracellular environment is sensed by FsrC sensor kinase, leading to activation of the FsrA-FsrC TCS and downstream signaling cascade.

In addition, we compared the 81 potential CroR targets with previously published work where they identified a set of genes that were *croR*-dependent in the context of antibiotic insults (Muller, Massier et al. 2018). Out of the 81 genes we identified, only nine genes were found to be differentially regulated in both sets of data, suggesting that different environmental stimuli can also lead to activation of a different subset of genes (**Supplementary Fig B3**). We hypothesize that the CroR-mediated stress response is

dependent on environmental stimuli and this results in the activation of specific mechanisms to recover from that stress response.

This work describes novel findings that suggest that the CroR-CroS TCS senses membrane perturbation and mediates a stress response by activating genes involved in cell wall synthesis and pilus expression. We propose that the CroR-CroS TCS is a 'Cpx-like system' of *E. faecalis* where in the event of certain types of membrane stress, including aberrant pilus biogenesis in the absence of HtrA and SrtA, a cell separation checkpoint is triggered, which we postulate may potentially provide a window for cells to respond to and recover from the membrane stress events. However, careful regulation of CroR phosphorylation must be in place as there is a potential fitness cost if constitutive CroR phosphorylation occurs, overriding CroS phosphatase activity, leading to Ebp-dependent morphological defects and a futile effort to eradicate the stress.

CHAPTER 6: CONCLUSION AND FUTURE RECOMMENDATIONS

6.1 CONCLUSIONS

With the emergence of *E. faecalis* and many other bacterial strains resistant to most of the antibiotics currently available in the market, the challenge to identify novel drug targets is high. Since we now understand the conservation and importance of pili among the Gram-positive bacteria to establish an infection, identifying and understanding the factors that govern their expression, assembly, and deposition on the cell surface is of our top interest. Since bacteria are often bombarded with various kinds of stresses during infection, understanding the mechanism underlying pilus biogenesis in *E. faecalis* during stress conditions may enable us to identify additional factors that may be important for pilus biogenesis under less than ideal, stressful, and/or infection-associated conditions. We hope that the identification of these novel factors may enable the development of new bacterial targets and inhibitors that may possibly have broad implications for pilus biogenesis in other Gram-positive bacteria.

A novel role for *E. faecalis* HtrA in handling 'off-pathway' proteins

In **Chapter 3**, we characterized the highly conserved serine protease, HtrA, in *E. faecalis*. Unlike HtrA in other bacteria, $HtrA_{EF}$ does not play a role in responding to high temperature, oxidative stress, pH stresses, or biofilm formation (**Fig 3.6, 3.7 and Table 3.5**). Despite showing indifferent sensitivity towards these environmental stress conditions *in vitro*, HtrA plays an important role in virulence as Δ*htrA* exhibits decreased fitness for colonization during competitive chronic wound infection (**Fig 3.9**). However,

nothing is known about what regulates HtrA expression and what its substrate(s) are during infection. In **Chapter 4**, we uncovered a novel role for HtrA in *E. faecalis* pilus regulation. HtrA interacts with Ebp pilin subunits and is required to process 'off-pathway' pili that are mislocalized on the membrane (**Fig 4.5**). The absence of this protease to offset membrane-anchored pili in the *srtA* null mutant leads to hyper-piliation (**Fig 4.3 and 4.4**). This hyper-piliation condition in *ΔsrtAΔhtrA* is likely due to transcriptional upregulation of *ebp* suggesting that 'off-pathway' pili in the membrane induce a transcriptional response leading to increased *ebp* expression (**Fig 4.13**).

CroRS-mediated stress response

A transcriptomic analysis comparing *ΔsrtAΔhtrA* with WT, *ΔsrtA,* and *ΔhtrA* identified a TCS, CroRS, previously known to initiate a transcriptional response to mediate resistance to β-lactam cell-wall targeting antibiotics (Comenge, Quintiliani et al. 2003). The absence of HtrA to offset the accumulated pili induces a CroRS-mediated stress response (**Table 4.6**). Global gene expression studies identified 81 potential CroR-targets (**Supplementary Table C6**). We discovered three genes, *mreC*, *rodA* and *penA* that are involved in cell elongation and *murC* that is involved in peptidoglycan synthesis among the 81 potential CroR targets (**Table 5.6**). In addition to genes involved in cell elongation and synthesis, our data suggest that *croR* negatively regulates *fsrB* and *fsrC* expression which we think leads to an increased piliation in *ΔsrtAΔhtrA*. We hypothesize that a tight regulation of CroR phosphorylation is required to prevent potential fitness cost as 'off-pathway' Ebp pili signals may drive constitutive CroR phosphorylation and override CroS phosphatase activity leading to Ebp-dependent morphological defects that can be harmful to the cell (**Fig 5.3 and 5.4**) and resulting in a futile effort to eradicate the stress.

Additional studies will be necessary to further dissect the pathways under the control of CroRS in the context of pilus biogenesis and cell cycle checkpoint in *E. faecalis.*

With all the findings from this thesis, we proposed a model for the CroR-mediated stress response to 'off-pathway' pilus-induced stress (**Fig 6.1**). In the event when pilus proteins go 'off-pathway', for example when pili accumulate and are mislocalized in the membrane, HtrA is activated to process these 'off-pathway' proteins. The absence of HtrA to clear mislocalized pili leads to overcrowding of proteins on the membrane. Either of these could activate the membrane-anchored metalloprotease, FtsH, and foldase, PrsA to facilitate the folding or clearance of extracellular proteins. Accumulation of pili on the membrane can be sensed by CroS of the CroR-CroS TCS, leading to phosphorylation of CroR, and regulation of CroR effector genes, such as genes involved in cell elongation and peptidoglycan synthesis. Activated CroR can suppress *fsrB*, leading to suppression of the *fsr* system, which we postulate increases pilus expression via a novel pathway involving the CroR-CroS TCS. A more drastic cellular defect observed in *croS::TnΔsrtAΔhtrA* suggests the involvement of CisS that can phosphorylate CroR in the absence of CroS phosphatase activity. Therefore, tight regulation of CroR phosphorylation must be in place as constitutive CroR phosphorylation may result in potential fitness cost by overriding CroS phosphatase activity leading to Ebp-dependent morphological defects, resulting in a futile effort to eradicate the stress.

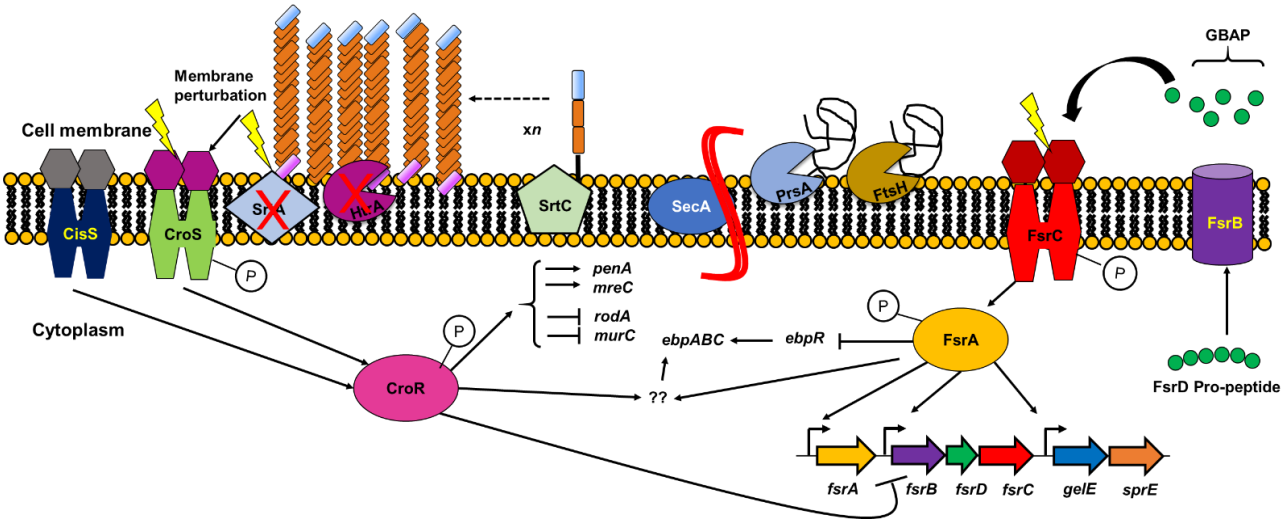

Figure 6.1 | A model for CroR-regulated hyper-piliation induced stress response. During 'off-pathway' event, the absence of HtrA to offset the accumulated pili, leading to membrane overcrowding that induces synthesis of metalloprotease FtsH and foldase PrsA to facilitate with the folding or clearance of extracellular proteins. Accumulation of pili on the membrane induces a CroR-mediated stress response, triggering a cell separation checkpoint potentially to provide a window for cells to respond to and recover from membrane stress events. However, careful regulation of CroR phosphorylation must be in place as there is a potential fitness cost that can drive constitutive CroR phosphorylation and override CroS phosphatase activity leading to Ebp-dependent morphological defects via *fsr* system, resulting in a futile effort to eradicate the stress.

Even though HtrA is conserved across all domains of life, and despite having a similar overall fold, it has been shown that differences in the number of polar residues surrounding the active sites of human HtrA as compared to, for example, *H. pylori* HtrA, results in different target specificity (Lu, Yamaoka et al. 2005, Hoy, Lower et al. 2010, Hoy, Geppert et al. 2012). Therefore, substrate specificities may render bacteria HtrA a reasonable drug target for antimicrobial compounds. Given the widespread occurrence of TCS and conservation HtrA in bacteria, this may represent a general mechanism by which bacteria regulate surface protein expression with a variety of sensory responses to extracellular stimuli.

6.2 FUTURE RECOMMENDATIONS

We have shown that $HtrA_{EF}$ and CroRS participate in novel roles in pilus biogenesis and sensing membrane perturbations, and data presented in this thesis have laid out many possible continuations of this project. Below is the list of suggestions where we can continue.

6.2.1 Investigation of the phosphorylation state of CroRS

One of the fundamental questions in TCS studies is to identify the percentage of protein molecules that are phosphorylated in the presence or absence of stimuli. This disruption of the balance between phosphatase and kinase activities can affect the output response. To investigate the phosphorylation state of CroR in Δ*srtA*Δ*htrA*, we can implement the use of Phos-tag SDS-PAGE to monitor signaling through CroR as the gel allows separation of phosphorylated CroR and non-phosphorylated CroR, which has been done for other RRs. (Barbieri and Stock 2008, Kellogg and Kristich 2016). Next, to determine if the levels of CroR phosphorylation affect phenotypes observed in Δ*srtA*Δ*htrA*, we can construct expression plasmids of CroR and CroS with substitutions at the predicted phosphoryl- accepting residues shown in **Fig 2.9B**. For example, to genetically decrease phosphorylated CroR, we can design a construct of *croR* with a substitution of the aspartic acid residue (D52) to alanine. To constitutively phosphorylate CroR, we can design a construct of *croR* with a substitution of aspartic acid residue to glutamate (D52E). In **Chapter 5**, we predict that phosphorylated CroR affects piliation and if this hypothesis is true, we will not observe hyper-piliation in *croR::Tn*Δ*srtA*Δ*htrA* complemented with *croR* defective in phosphor-transfer (*pcroR*$_{D52A}$*croS*) but will with the constitutively phosphorylated CroR (D52E) expression plasmid.

Preliminary data on the complementation studies of *croR::Tn*∆*srtA*∆*htrA* revealed that expression plasmids of p*croR,* p*croR(D52E)* or p*croR(D52A)* showed similar piliation levels as the empty vector suggesting that these plasmids may not be complementing properly (**Supplementary Fig B4**). As this has only been done once, additional replicates will have to be carried out to validate the data. Furthermore, CroR expression from these plasmids should be validated using immunoblot with anti-CroR antiserum prior to IFA to determine piliation levels. In previous studies, *croR* expression plasmids were created together with *croS* as they are co-transcribed in the same operon (Kellogg and Kristich 2016, Kellogg, Little et al. 2017). Therefore, the absence of *croS* on the complementation plasmids may influence *croR* expression. The work to create an expression plasmid with the *croRS* operon is currently in progress.

6.2.2 Investigation of the interaction between CroRS and non-cognate CisRS

As the phenotype of *croS::Tn*∆*srtA*∆*htrA* exhibits a similar phenotype as ∆*srtA*∆*htrA,* we predict that deletion of *croS* leads to *croS*-independent CroR phosphorylation by the non-cognate kinase CisS. To test this prediction, we should determine levels of phosphorylated CroR in *croS::Tn*∆*srtA*∆*htrA* using Phos-tag SDS-PAGE. To determine if CisS also plays a role in piliation, knocking out *cisS* in *croS::Tn*∆*srtA*∆*htrA* background should remove the cross-talk between CisS and CroR and thus restore piliation and morphology to WT.

6.2.3 Identification of the CroR regulon

Apart from the work done on the CroRS system with cephalosporin antibiotic, no work has been done on the CroR regulon in the context of sensing membrane stress. In **Chapter 5**, we identified 81 possible gene targets that CroR regulates, and we can select

candidate targets, such as the *fsr* system, *penA, rodA, murC* and *mreC* to validate their interaction with CroR using EMSA. To directly determine the CroR-regulon, **C**hromatic **I**mmuno**P**recipitation (ChIP) sequencing can be performed on Δ*srtA*Δ*htrA pcroR*-HIS controlled by a nisin-inducible promoter to define DNA binding regions of genes that CroR binds during the 'off-pathway' scenario. Preliminary data showed the successful construction of the nisin-inducible p*croR*-6XHIS and we are currently optimizing the concentration of nisin to activate CroR-HIS expression in Δ*srtA*Δ*htrA* (**Supplementary Fig B5**). However, since we concurrently realized that this construct not does phenotypically complement a *croR* mutation, additional work must be conducted to create a functional His-tagged CroR.

6.2.4 Involvement of FsrA-FsrC two-component systems in membrane stress response in *Enterococcus faecalis*

In **Chapter 5,** we proposed that *fsrB* expression is repressed in the presence of CroR activation during membrane stress (**Table 5.6**), leading to hyper-piliation in the Δ*srtA*Δ*htrA* since the *fsr* system negatively regulates pili expression. To study the loss of the *fsr* system in the context of piliation, we can perform IFA measuring the percentage of cells expressing surface pili in *fsrA* and *fsrC* knockouts in a Δ*srtA*Δ*htrA* background to determine if the number of pili expressing cells is influenced by the absence of FsrA-FsrC TCS. Preliminary data shows that all strains that lack both *srtA* and *htrA* expression exhibit hyper-piliation regardless in the absence of *fsrA* or *fsrC* (**Supplementary Fig B6**), which is consistent with our prediction, since the Fsr system is already downregulated in Δ*srtA*Δ*htrA,* and the removal of *fsrA* or *fsrC* genes in Δ*srtA*Δ*htrA* does not further affect piliation levels. Next, we should complement the Δ*srtA*Δ*htrA* strain with plasmids encoding *fsrABC*.

To investigate if the loss of *fsrA* or *fsrC* affects *croRS* expression during 'off-pathway' events, mRNA transcriptomic analysis can be performed comparing expression profiles of *fsrA::Tn*Δ*srtA*Δ*htrA*, *fsrC::Tn*Δ*srtA*Δ*htrA* against Δ*srtA*Δ*htrA.* Preliminary data show that loss of *fsrA* or *fsrC* downregulates expression of *croRS* (**data not shown**) suggesting that the FsrA-FsrC TCS can also influence *croRS* expression.

6.2.5 Investigating the role of HtrA in processing pilin monomers

Our work in **Chapter 4** revealed that HtrA is required for the removal of excess polymerized pili from the membrane during 'off-pathway' events. To investigate if HtrA functions similarly in the presence of accumulated pilin subunits on the membrane, future work should include studies on Δ*srtC* and Δ*srtC*Δ*htrA* that do not polymerize pili but accumulate monomers in the cell envelope (Nielsen, Flores-Mireles et al. 2013). Preliminary data showed that, unlike Δ*srtA*Δ*htrA,* we observed reduced pilin expression in Δ*srtC*Δ*htrA* on the immunoblot (**Supplementary Fig B7**).

IFA findings show that a total number of cells expressing pilin monomers on the surface are also significantly reduced (**Supplementary Fig B8**). RNA transcriptomic analyses revealed that the reduced pilin on the immunoblot is due to reduced transcription (**Supplementary Fig B9**). We know that HtrA interacts with EbpC from the BacTH system, but we do not know if HtrA interacts with polymerized or monomeric forms of pili. To investigate, we will compare co-IPs for HtrA and EbpC from WT cells and *ΔsrtC* cells. *ΔhtrA* and *ΔebpC* will serve as negative controls for co-IP experiments. Preliminary transcriptomic analysis between Δ*srtC*Δ*htrA* and Δ*srtC* revealed insignificant differences in *croRS* expression levels, indicating that even though both Δ*srtC*Δ*htrA* and Δ*srtA*Δ*htrA*

results in accumulation of proteins on the membrane, it appears that cells can respond differently towards accumulated polymerized pili and monomeric pilin subunits.

6.2.6 *E. faecalis* HtrA roles in virulence

In **Chapter 3**, we observed an attenuated infection in the *htrA* mutant during competitive wound infections. However, the substrates that HtrA targets in *E. faecalis* are not known. In some bacterial species and also in *E. faecalis*, HtrA is released from the cell into the supernatant (Hoy, Lower et al. 2010, Wu, Lei et al. 2011, Tegtmeyer, Moodley et al. 2016) (**Supplementary Fig B10**). One of the highest priorities for future work in this section would include identification of both bacterial and host substrates for HtrA involved in host-pathogen interactions. **Table 2.2** presented in **Chapter 2** provides a starting point to investigate the possible targets of *E. faecalis* HtrA based on HtrA functions in other pathogens. Future work includes performing *in vitro* cell adherence assays in epithelial cells with Δ*htrA* to investigate if E-cadherin and fibronectin are a substrate for HtrA. If E-cadherin and fibronectin are true substrates of HtrA, Δ*htrA* cells may exhibit attenuated E-cadherin cleavage as compared to WT. To investigate if HtrA is required for survival in macrophages, future work can include macrophage survival assays with Δ*htrA*. If HtrA is required, Δ*htrA* would exhibit less resistance to killing by cultured macrophages *in vitro*.

With the emergence of multi-drug resistant bacteria, many have considered creating inhibitors targeting proteases and virulence factors involved in infection. Small HtrA inhibitors have been designed to block HtrA action in *H*. *pylori* and *C*. *trachomatis* (Hoy, Lower et al. 2010, Marsh, Ong et al. 2017, Wessler, Schneider et al. 2017). However, given the conservation of HtrA domain structures, most HtrA proteases binding site inhibitors identified to date have been of low selectivity (Clausen, Kaiser et al. 2011).

Importantly, HtrA activity relies not only upon catalytic activity, but also conformational changes upon activation, multimer formation, and allosteric activation (Clausen, Kaiser et al. 2011). We, therefore, hypothesize that, based on these multiple points for potential function perturbation, higher selectivity inhibitors may be identified to limit the activity of *E*. *faecalis* HtrA during infection that may not bind to human HtrA. In addition, vaccines against several pathogens, such as *S*. *typhimurium* and *Y*. *enterocolitica*, have made use of *htrA* null mutants in protecting mice against subsequent challenge with virulent WT strains (Chatfield, Strahan et al. 1992, Li, Dorrell et al. 1996, Lu, Yamaoka et al. 2005). Thus, future work could either screen for small molecules or examine a vaccine approach to inhibit HtrA activity in *E. faecalis* which can be promising targets to create for future therapeutic intervention.

PERMISSIONS

Figure 2.1 was adapted with permission from an open-access article (Goh, Yong *et al*, 2017) distributed under the terms of Creative Commons Attribution-Non-Commercial License. **Figure 2.4A and B** was adapted with permission from (Kline *et al*, 2009) distributed under Rightslink® by Copyright Clearance Center. **Figure 2.4C** was adapted and modified with permission from an open-access article (Kandaswamy *et al,* 2013) distributed under the terms of CC-BY-NC-ND or CC-BY license. **Figure 2.5** was adapted with permission from an open-access article (Ali *et al*, 2017) distributed under the terms of MDPI Open Access Information and Policy. **Figure 2.6A** was adapted with permission from (Rosch and Caparon, 2005) under license number 4505170197819. **Figure 2.6B** was adapted with permission from an open-access article (Tsui *et al*, 2011) distributed under Rightslink® by Copyright Clearance Center. **Figure 2.7** was adapted with permission from (Clausen *et al*, 2011) under license number 4505170441463.

CHAPTER 7: APPENDICES

APPENDIX A

Supplementary Table A1 | Protein sequences used to raise antibodies in animals.

Antigens	Protein sequence[#]
ClpP	MHHHHHHHSSGVDLGTENLYFQSMRAYDIYSRLLKDRIIMLSGPIDDNVANSVIAQLLFLD AQDSEKDIYLYINSPGGSVSAGLAIFDTMNFVKADVQTIVLGMAASMGSFLLTAGQKGKR FALPNAEIMIHQPLGGAQGQATEIEIAARHILDTRQRLNSILAERTGQPIEVIERDTDRDNY MTAEQAKEYGLIDEVME-
CroR	MHHHHHHSSGVDLGTENLYFQSMMKILVADDDKEIVELLSIYIHNEGYEVVKAYDGKEAL SKLHTTPDIDLLILDIMMPIMDGMEVVKELRKESQIPIIMLTAKTTDMDKIKGLVAGADDYVT KPFNPLEVMARVKSILRRSQMQLTKEEPDELEVGPLMINKDSHEVKTIEGKEIQLTALEFG ILYLLASHPNRVFSADEIFERVWQQESIVSAKTVMVHVSHLRDKIEEATGGEKVIQTVWG VGYKIDAR-
EbpA	MITDENDKTNINIELNLLNQTEQPLQREIQLKNAQFMDTAVIEKDGYSYQVTNGTLYLTLD AQVKKPVQLSLAVEQSSLQTAQPPKLLYENNEYDVSVTSEKITVEDSAKESTEPEKITVP ENTKETNKNDSAPEKTEQPTATEEVTNPFAEARMAPATLRANLALPLIAPQYTTDNSGTY PTANWQPTGNQNVLNHQGNKDGGAQWDGQTSWNGDPTNRTNSYTEYGGTGDQADY AIRKYARETTTPGLFDVYLNVRGNVQKEITPLDLVLVVDWSGSMNENNRIGEVQKGVNR FVDTLADSGITNNINMGYVGYSSDGYNNNAIQMGPFDTVKNPIKNITPSSTRGGTFTQKA LRDAGDMLATPNGHKKVIVLLTDGVPTFSYKVSRVQTEADGRFYGTQFTNRQDQPGST SYISGSYNAPDQNNISKRINSTFIATIGEAMALKQRGIEIHGLGIQLQSDPRANLSKQQVED KMREMVSADENGDLYYESADYAPDISDYLAKKAVQISGTVVNGKVVDPIAEPFKYEPNTL SMKSVGPVQVQTLPEVSLTGATINSNEIYLGKGQEIQIHYQVRIQTESENFKPDFWYQMN GRTTFQPLATAPEKVDFGVPSGKAPGVKLNVKKIWEEYDQDPTSRPDNVIYEISRKQVT DTANWQTGYIKLSKPENDTSNSWERKNVTQLSKTADESYQEVLGLPQYNNQGQAFNYQ TTRELAVPGYSQEKIDDTTWKNTKQFKPLDLKVIKNSSSGEKNLVGAVFELSGKNVQTTL VDNKDGSYSLPKDVRLQKGERYTLTEVKAPAGHELGKKTTWQIEVNEQGKVSIDGQEVT TTNQVIPLEIENKFSSLPIRIRKYTMQNGKQVNLAEATFALQRKNAQGSYQTVATQKTDTA GLSYFKISEPGEYRMVEQSGPLGYDTLAGNYEFTVDKYGEIHYAGKNIEENAPEWTLTH QNHLKPFDLTVHKKADNQTPLKGAKFRLTGPDTDIELPKDGKETDTFVFENLKPGKYVLT ETFTPEGYQGLKEPIELIIREDGSVTIDGEKVADVLISGEKNNQITLDVTNQAKVPLPETGG IGRLWFYLIAISTFVIAGVYLFIRRPEGSV-
EbpB	MKNARWLSICVMLLALFGFSQQALAEASQASVQVTLHKLLFPDGQLPEQQQNTGEEGTL LQNYRGLNDVTYQVYDVTDPFYQLRSEGKTVQEAQRQLAETGAMNRKPIAEDKTQTING EDGVVSFSLASKDSQQRDKAYLFVEAEAPEVVKEKASNLVMILPVQDPQGQSLTHIHLYP KNEENAYDLPPLEKTVLDKQQGFNQGEHINYLTTQIPANILGYQEFRLSDKADTTLTLLPE SIEVKVAGKTVTTGYTLTTQKHGFTLDFSIKDLQNFANQTMTVSYQMRLEKTAEPDTAIN NEGQLVTDKHTLTKRAAVRTGGKSFVKVDSENAKITLPEAVFIVKNQAGEYLNETANGYR WQKEKALAKKITSNQAGEFSVKGLKDGQYFLEEISAPKGYLLNQTEIPFTVEKNSYATNG QRTAPLHVINKKVKESGFLPKTNEERSIWLTIAGLLIIGMVVIWLFYQKQKRGERK-

Supplementary Table A1 (*Continued.*)

EbpC	MKQLKKVWYTISTLLLILPLFTSVLGTTTAFAEENGESAQLVIHKKKMTDLPDPLIQNSGKE MSEFDKYQGLADVTFSIYNVTSEFYEQRAAGASVDAAKQAVQSLTPGKPVAQGTTDAN GNVTVQLPKKQNGKDAVYTIKEEPKEGVVAATNMVVAFPVYEMIKQADGSYKYGTEELA VVHIYPKNVVANDGSLHVKKVGTAENEGLNGAEFVISKSEGSPGTVKYIQGVKDGLYTW TTDKEQAKRFITGKSYEIGENDFTEAENGTGELTVKNLEVGSYILEEVKAPNNAELIENQT KTPFTIEANNQTPVEKTVKNDTSKVDKTTPSLDGKDVAIGEKIKYQISVNIPLGIADKEGDA NKYVKFNLVDKHDAALTFDNVTSGEYAYALYDGDTVIAPENYQVTEQANGFTVAVNPAYI PTLTPGGTLKFVYFMHLNEKADPTKGFKNEANVDNGHTDDQTPPTVEVVTGGKRFIKVD GDVTATQALAGASFVVRDQNSDTANYLKIDETTKAATWVKTKAEATTFTTTADGLVDITG LKYGTYYLEETVAPDDYVLLTNRIEFVVNEQSYGTTENLVSPEKVPNKHKGTLPSTGGKG IYVYLGSGAVLLLIAGVYFARRRKENA-
FtsH	MHHHHHHSSGVDLGTENLYFQSMGKSKAKEADKKANRVRFSDVAGAEEEKQELVEVV EFLKDPRRFAELGARIPAGVLLEGPPGTGKTLLAKAVAGEAGVPFYSISGSDFVEMFVGV GASRVRDLFETAKKNAPAIIFIDEIDAVGRQRGAGMGGGHDEREQTLNQLLVEMDGFDG NEGVIVIAATNRSDVLDPALLRPGFDRQILVGRPDVKGREAILRVHAKNKPLADDVDLKVV AQQTPGFAGADLENVLNEAALVAARRNKKKIDASDVDEAEDRVIAGPAKKDRVINKKERE MVAYHEAGHTIVGLVLSRARVVHKVTIIPRGRAGGYMIALPKEDQFLMTKEDMFEQIVGL LGGRTAEEIIFGVQSTGASNDFEQATGIARSMVTEYGMSDKLGPVQYEGNHQVFVGRD YGQTKAYSEQVAFEIDQEVRRILMDAHTKAHEIIEAHREQHKLIAEKLLEYETLDAKAIKSL FETGKMPEGAD-
HtrA	MHHHHHHSSGVDLGTENLYFQSMAASEGSGVIYKKDGKTAYVVTNNHVVDKAQGLEVV LSDGTKVKGELVGTDAYTDLAVIKISSDKVDQVAEFGNSSKITVGEPAIAIGSPLGSDYAN SVTQGIISSVNRNITNKNESGETININAIQTDAAINPGNSGGPLINIEGQVIGINSVKIVQSTS QVSVEGMGFAIPSNDVVNIINQLEKDGKVTRPALGITMSDLTGISSQQQEQILKIPASVKT GVVVRGVEAATPAEKAGLEKYDVITKVDGQDVSSTTDLQSALYKKKVGDKMEVTYYRGS KEMKATIDLTIDKSALTQQNNRSN-
SecA	MKGTQIPMANFLKKMIENDKKELRRLEKIADKIDAHASAMEQLSDEQLREKTDEFKARYQ KGETLDELLPEAFAVVREAAKRVLGLFPYRVQLMGGIVLHDGNIPEMRTGEGKTLTATMP VYLNALSGEGVHVVTVNEYLATRDSNEMGELYNFLGLSVGLNINSKSSDEKREAYNCDIT YSTNNELGFDYLRDNMVVYRSQMVQRPLNYAIVDEVDSILIDEARTPLIISGQAEKSTALY TRADNFVKRLKEDEDYKIDIQSKTIGLTEAGIEKAEQTFGLDNLYDIENTALTHHLDQALRA NYIMLLDIDYVVQDNKVLIVDQFTGRIMDGRRYSDGLHAIEAKEGVEIEDETKTMATITFQ NYFRMYKKLAGMTGTAKTEEEFREIYNIQVIQIPTNRPIIRDDRPDLLYPTLESKFNAVVED IKERYHKGQPVLVGTVAVETSELLSDKLNAAKIPHEVLNAKNHFKEAEIIMNAGQKGAVTI ATNMAGRGTDIKLGLGVLELGGLAVIGTERHESRRIDNQLRGRAGRQGDPGVSQFYLSL EDDLMKRFGSERIKTFLERMNVQEEDAVIQSKMFTRQVESAQKRVEGNNYDTRKNVLQ YDDVMREQREVIYAQRQEVIMEENDLSDVLMGMVKRTIGRVVDSHTQLEKEEWNLDGIV DFAASTLVHEDTISKKDLENKSAEEIKDYLVARAQEVFEEKSQQLNGQEQLLEFEKVVILR VVDTKWTDHIDAMDQLRQSVGLRAYGQNNPLVEYQTEGYSMYNNMVGSIEYEVTRLFM KSEIRQNVQREQVAQGQAEHPETEQDAAARSNTSAKRQPVRVDKKVGRNDLCPCGSG KKFKNCHGRNA-
SrtA	MHHHHHHSSGVDLGTENLYFQSMMRPKEKKRGKNWLINSLLVLLFIIGLALIFNNQIRSW VVQQNSRSYAVSKLKPADVKKNMARETTFDFDSVESLSTEAVMKAQFENKNLPVIGAIAI PSVEINLPIFKGLSNVALLTGAGTMKEDQVMGKNNYALASHRTEDGVSLFSPLERTKKDE LIYITDLSTVYTYKITSVEKIEPTRVELIDDVPGQNMITLITCGDLQATTRIAVQGTLAATTPIK DANDDMLKAFQLEQKTLADWVA-
SrtC	MHHHHHHSSGVDLGTENLYFQSMENTKEMAELQEKMEKKNQELAKKGSNPGLDPFSE TQKTTKKPDKSYFESHTIGVLTIPKINVRLPIFDKTNALLLEKGSSLLEGTSYPTGGANTHA VISGHRGLPQAKLFTDLPELKKGDEFYIEVNGKTLAYQVDQIKTVEPTDTKDLHIESGQDL VTLLTCTPYMINSHRLLVRGHRIPY-

[#]Cleavable N-terminal His-tag with TEV-protease cleavage site in blue.

Supplementary Table A2 | HtrA DNA sequences used for sequence alignment.

>***Enterococcus faecalis*** **OG1RF**

MHLLGGYFMQRKDVTPNSDKKSLLQKFGIGLAGGLLGGALILGGAYSGIIPTPNGGNNAATTT
STNHGDTKVSNVSYNVSSDVTKAVKKVQNSVVSVINMQSASNNSSADDPFGGLFGGNEGT
QDSSGNNGNDLEAASEGSGVIYKKDGKTAYVVTNNHVVDKAQGLEVVLSDGTKVKGELVGT
DAYTDLAVIKISSDKVDQVAEFGNSSKITVGEPAIAIGSPLGSDYANSVTQGIISSVNRNITNKN
ESGETININAIQTDAAINPGNSGGPLINIEGQVIGINSVKIVQSTSQVSVEGMGFAIPSNDVVNII
NQLEKDGKVTRPALGITMSDLTGISSQQQEQILKIPASVKTGVVVRGVEAATPAEKAGLEKYD
VITKVDGQDVSSTTDLQSALYKKKVGDKMEVTYYRGSKEMKATIDLTIDKSALTQQNNRSNQ

>***Lactococcus lactis*** **subsp. lactis Il1403**

MAKANIGKLLLTGVVGGAIALGGSAIYQSTTNQSANNSRSNTTSTKVSNVSVNVNTDVTSAIK
KVSNSVVSVMNYQKDNSQSSDFSSIFGGNSGSSSSTDGLQLSSEGSGVIYKKSGGDAYVVT
NYHVIAGNSSLDVLLSGGQKVKASVVGYDEYTDLAVLKISSEHVKDVATFADSSKLTIGEPAIA
VGSPLGSQFANTATEGILSATSRQVTLTQENGQTTNINAIQTDAAINPGNSGGALINIEGQVIGI
TQSKITTTEDGSTSVEGLGFAIPSNDVVNIINKLEADGKISRPALGIRMVDLSQLSTNDSSQLKL
PSSVTGGVVVYSVQSGLPAASAGLKAGDVITKVGDTAVTSSTDLQSALYSHNINDTVKVTYY
RDGKSNTADVKLSKSTSDLETSSPSSSN

>***Escherichia coli*** **str. K-12 substr. MG1655**

MKKTTLALSALALSLGLALSPLSATAAETSSATTAQQMPSLAPMLEKVMPSVVSINVEGSTTV
NTPRMPRNFQQFFGDDSPFCQEGSPFQSSPFCQGGPGGNGGGQQQKFMALGSGVIIDAD
KGYVVTNNHVVDNATVIKVQLSDGRKFDAKMVGKDPRSDIALIQIQNPKNLTAIKMADSDALR
VGDYTVAIGNPFGLGETVTSGIVSALGRSGLNAENYENFIQTDAAINRGNSGGALVNLNGELI
GINTAILAPDGGNIGIGFAIPSNMVKNLTSQMVEYGQVKRGELGIMGTELNSDLAKAMKVDAQ
RGAFVSQVLPNSSAAKAGIKAGDVITSLNGKPISSFAALRAQVGTMPVGSKLTLGLLRDGKQ
VNVNLELQQSSQNQVDSSTIFNGIEGAEMSNKGKDQGVVVNNVKTGTPAAQIGLKKGDVIIG
ANQQAVKNIAELRKVLDSKPSVLALNIQRGDSTIYLLMQ

>***Streptococcus pyogenes*** **HSC5**

MPSMKHILKSLSILLIGFLGGLIAIITFNNLYPHSPSKINSGKATTSNMVFNNTTNTTKAVKAVQ
NAVVSVINYQDNPSSSLSNPYTKLFGEGRSKENKDAELSIFSEGSGVIYRKDGNSAYVVTNN
HVIDGAKRIEILMADGSKVVGELVGADTYSDLAVVKISSDKIKTVAEFADSTKLNVGEVAIAIGS
PLGTQYANSVTQGIVSSLSRTVTLKNENGETVSTNAIQTDAAINPGNSGGPLINIEGQVIGINS
SKISSTPTGSNGNSGAVEGIGFAIPSTDVIKIIKQLETNGEVIRPALGISMVNLNDLSTNALSQIN
IPTSVTGGIVVAEVKEGMPASGKLAQYDVITEIDGKTVNSISDLQSSLYGHDINDTIKVTFYRGT
TKKKADIKLTKTTQDLTKTQ

>***Mus musculus*** **HTRA1 precursor**

MQSLRTTLLSLLLLLLAAPSLALPSGTGRSAPAATVCPEHCDPTRCAPPPTDCEGGRVRDAC
GCCEVCGALEGAACGLQEGPCGEGLQCVVPFGVPASATVRRRAQAGLCVCASSEPVCGS
DAKTYTNLCQLRAASRRSEKLRQPPVIVLQRGACGQGQEDPNSLRHKYNFIADVVEKIAPAV
VHIELYRKLPFSKREVPVASGSGFIVSEDGLIVTNAHVVTNKNRVKVELKNGATYEAKIKDVDE
KADIALIKIDHQGKLPVLLLGRSSELRPGEFVVAIGSPFSLQNTVTTGIVSTTQRGGKELGLRN
SDMDYIQTDAIINYGNSGGPLVNLDGEVIGINTLKVTAGISFAIPSDKIKKFLTESHDRQAKGKA
VTKKKYIGIRMMSLTSSKAKELKDRHRDFPDVLSGAYIIEVIPDTPAEAGGLKENDVIISINGQS
VVTANDVSDVIKKENTLNMVVRRGNEDIVITVIPEEIDP

Supplementary Table A2 (*Continued.*)

>***Homo sapiens***

MQIPRAALLPLLLLLLAAPASAQLSRAGRSAPLAAGCPDRCEPARCPPQPEHCEGGRARDA
CGCCEVCGAPEGAACGLQEGPCGEGLQCVVPFGVPASATVRRRAQAGLCVCASSEPVCG
SDANTYANLCQLRAASRRSERLHRPPVIVLQRGACGQGQEDPNSLRHKYNFIADVVEKIAPA
VVHIELFRKLPFSKREVPVASGSGFIVSEDGLIVTNAHVVTNKHRVKVELKNGATYEAKIKDVD
EKADIALIKIDHQGKLPVLLLGRSSELRPGEFVVAIGSPFSLQNTVTTGIVSTTQRGGKELGLR
NSDMDYIQTDAIINYGNSGGPLVNLDGEVIGINTLKVTAGISFAIPSDKIKKFLTESHDRQAKGK
AITKKKYIGIRMMSLTSSKAKELKDRHRDFPDVISGAYIIEVIPDTPAEAGGLKENDVIISINGQS
VVSANDVSDVIKRESTLNMVVRRGNEDIMITVIPEEIDP

>***Streptococcus pneumoniae*** *TIGR4*

MKHLKTFYKKWFQLLVVIVISFFSGALGSFSITQLTQKSSVNNSNNNSTITQTAYKNENSTTQA
VNKVKDAVVSVITYSANRQNSVFGNDDTDTDSQRISSEGSGVIYKKNDKEAYIVTNNHVINGA
SKVDIRLSDGTKVPGEIVGADTFSDIAVVKISSEKVTTVAEFGDSSKLTVGETAIAIGSPLGSEY
ANTVTQGIVSSLNRNVSLKSEDGQAISTKAIQTDTAINPGNSGGPLINIQGQVIGITSSKIATNG
GTSVEGLGFAIPANDAINIIEQLEKNGKVTRPALGIQMVNLSNVSTSDIRRLNIPSNVTSGVIVR
SVQSNMPANGHLEKYDVITKVDDKEIASSTDLQSALYNHSIGDTIKITYYRNGKEETTSIKLNK
SSGDLES

Supplementary Table A3 | mRNA transcriptomics profile between WT and ∆*htrA*. Genes with significant differences in abundance of mRNAs were determined using a P-Value and false discovery rate (FDR) cutoff of 0.05.

Locus tag	WT vs ∆*htrA*	Gene	Annotation
OG1RF_11031	3.07		hypothetical protein
OG1RF_11032	2.80		hypothetical protein
OG1RF_11938	-1.52		fumarate reductase
OG1RF_12441	-1.52		hypothetical protein
OG1RF_12305	-8.89	*htrA*	serine protease HtrA

Supplementary Table A4 | List of genes classified under phages.			
Locus tag	***ΔsrtAΔhtrA* vs *ΔsrtA***	**Gene**	**Annotation**
OG1RF_11046	-1.31		hypothetical protein
OG1RF_11047	-1.29		cro/CI family transcriptional regulator
OG1RF_11048	-2.02		hypothetical protein
OG1RF_11049	-2.36		DNA replication protein
OG1RF_11050	-2.27		DNA replication protein
OG1RF_11051	-2.29		hypothetical protein
OG1RF_11052	-2.58		RinA family transcriptional regulator
OG1RF_11053	-3.29		Transposase
OG1RF_11054	-3.58		hypothetical protein
OG1RF_11055	-3.52		TP901-1 family phage major tail protein
OG1RF_11056	-3.46		hypothetical protein
OG1RF_11057	-3.67		hypothetical protein
OG1RF_11058	-3.73		ABC superfamily ATP binding cassette transporter permease subunit
OG1RF_11059	-3.85		phage tail protein
OG1RF_11060	-3.88		phage structural protein
OG1RF_11061	-3.87		hypothetical protein
OG1RF_11062	-3.75		Holing
OG1RF_11063	-4.11	*amiD2*	N-acetylmuramoyl-L-alanine amidase

APPENDIX B

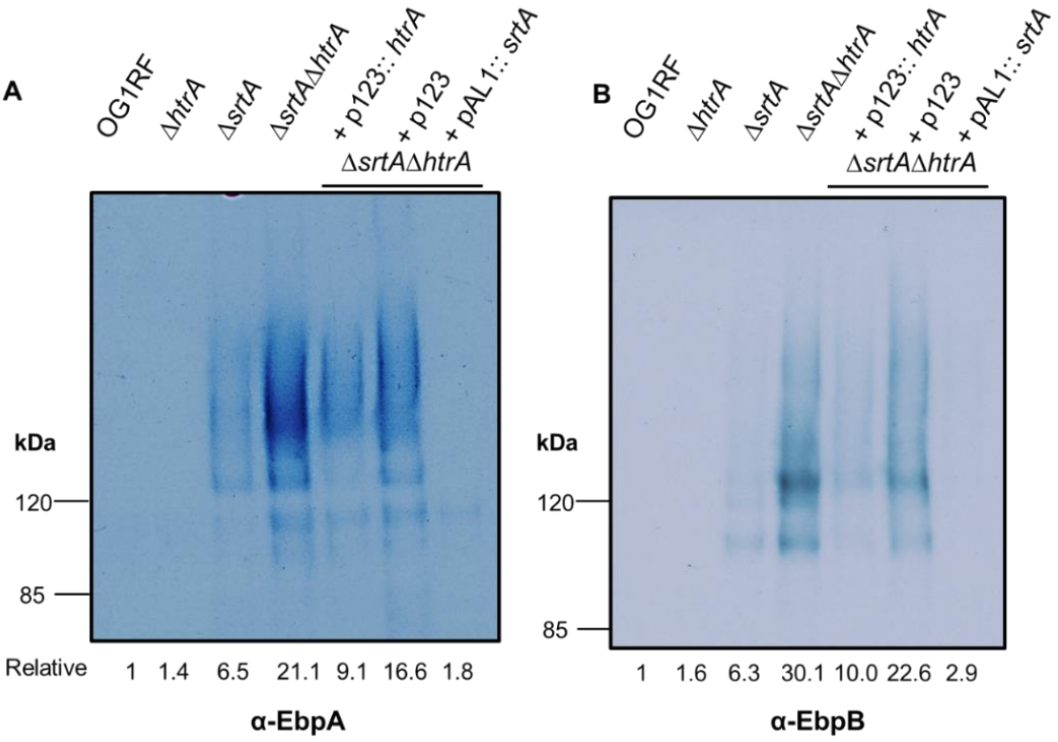

Supplementary Figure B1 | Increased Ebp pilus expression in Δ*srtA*Δ*htrA*. Immunoblot was performed with (**A**) anti-EbpA and (**B**) anti-EbpB immune sera on protoplast fractions of WT, Δ*htrA,* Δ*srtA,* Δ*srtA*Δ*htrA* strains and Δ*srtA*Δ*htrA* carrying p*123* (vector control), p*htrA* or p*srtA*. Relative density differences were calculated using WT as the standard.

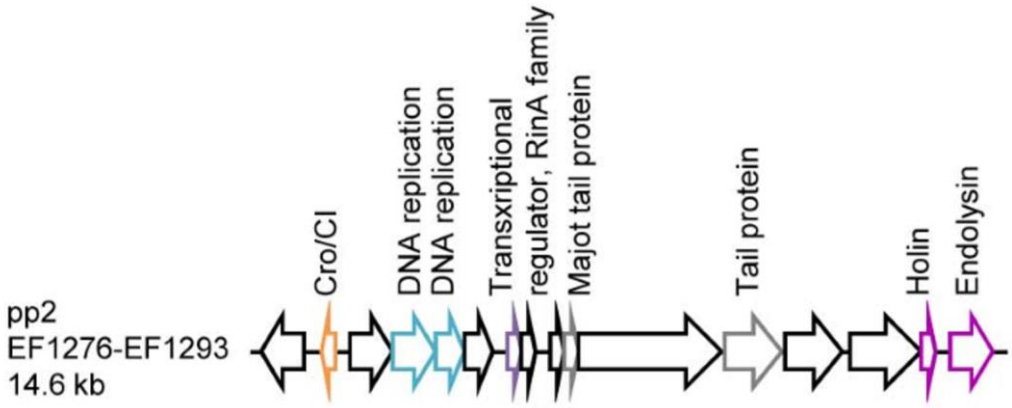

Supplementary Figure B2 | Genetic organization of pp2 phage in V583. The locus tag corresponding to pp2 in OG1RF is OG1RF_11046 to OG1RF_11063. Colors of gene locus correspond to the genes listed in **Supplementary Table A4** (Schematic diagram adapted from Matos, R.C *et al*, 2013).

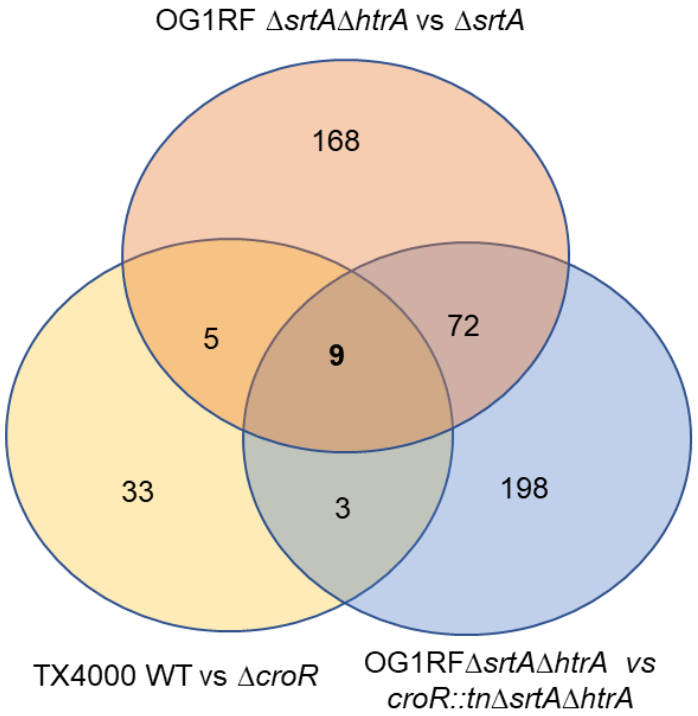

Supplementary Figure B3 | Different subset of genes regulated in the presence of different stress stimulus. Differential gene expression that was dependent on *croR* from this study was also compared with differential expression in TX4000 WT with Δ*croR* when treated with ceftriaxone antibiotics (Muller, Massier et al. 2018).

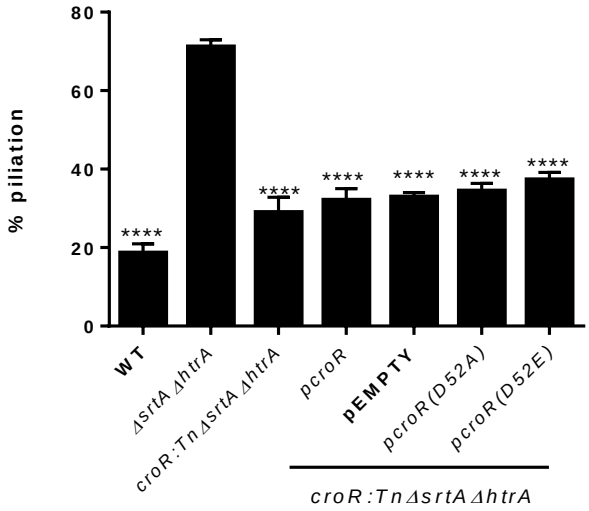

Supplementary Figure B4 | Complementation of *croR:Tn*Δ*srtA*Δ*htrA* p*croR(D52A)* does not phenocopy Δ*srtA*Δ*htrA*. Statistical analysis of pili expressing cells of indicated strains labeled with anti-EbpC immune serum and Alexa Fluor® 568 secondary antibody. Results are represented as bar graphs. **** P ≤ 0.0001. The result is from one experiment.

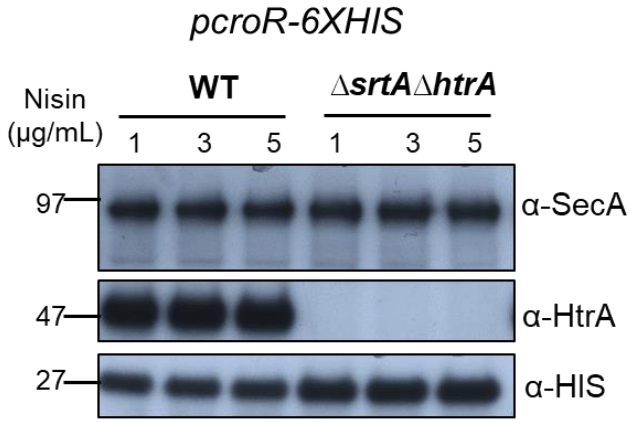

Supplementary Figure B5 | Optimization of nisin concentration for CroR expression. Immunoblot was performed with α-His immune sera on whole cell lysate of WT, and Δ*srtA*Δ*htrA* strains carrying p*croR-6xHIS*.1, 3, 5 μg/mL of Nisin were used for initial optimization of CroR expression. α-SecA immune serum was used as a loading control. α-HtrA immune serum was used for strain validation. PageRuler™ pre-stained protein gel (10-250 kDa) was used as ladder.

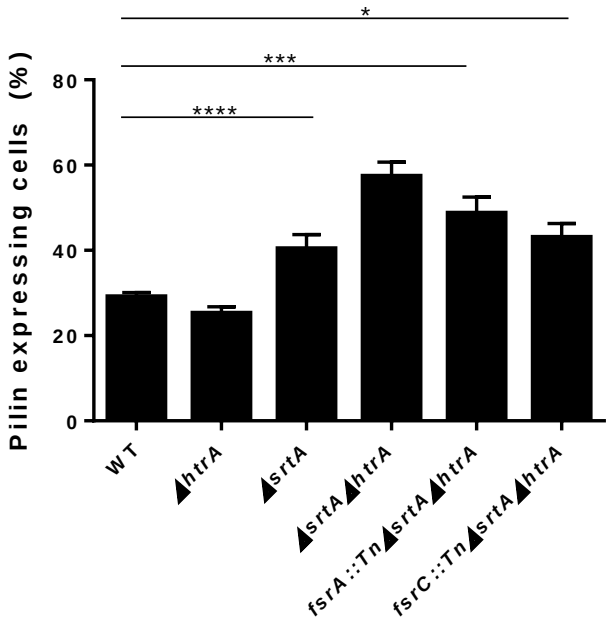

Supplementary Figure B6 | Hyper-piliation observed in strains that lack both SrtA and HtrA. Statistical analysis of pili expressing cells of indicated strains labeled with α-EbpC immune serum and Alexa Fluor® 568 secondary antibody. Results are represented as bar graphs. **** P ≤ 0.0001; *** P ≤ 0.001; ** P ≤ 0.01; * P < 0.05. Combined data from two independent experiments were shown.

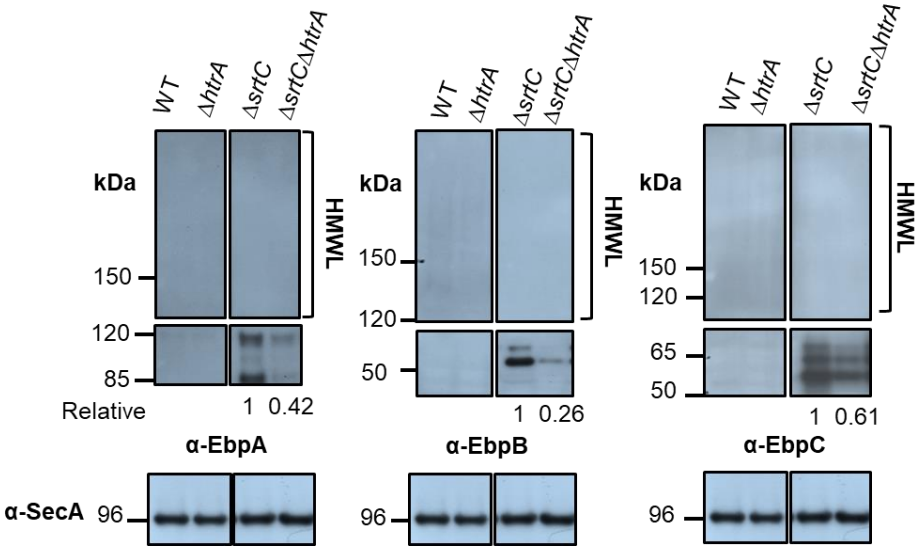

Supplementary Figure B7 | Decreased Ebp pili protein expression in Δ*srtC*Δ*htrA*. Immunoblot was performed with indicated α-pilin immune sera on protoplast fractions of WT, Δ*htrA,* Δ*srtC,* Δ*srtC*Δ*htrA* strains. Top blots show pilus HMWL (brackets), middle blots show monomeric pilin subunits and bottom blots show α-SecA used as a loading control. Relative density differences between Δ*srtC* and Δ*srtC*Δ*htrA* were calculated with Δ*srtC* as the standard. PageRuler™ pre-stained protein gel (10-250 kDa) was used as ladder.

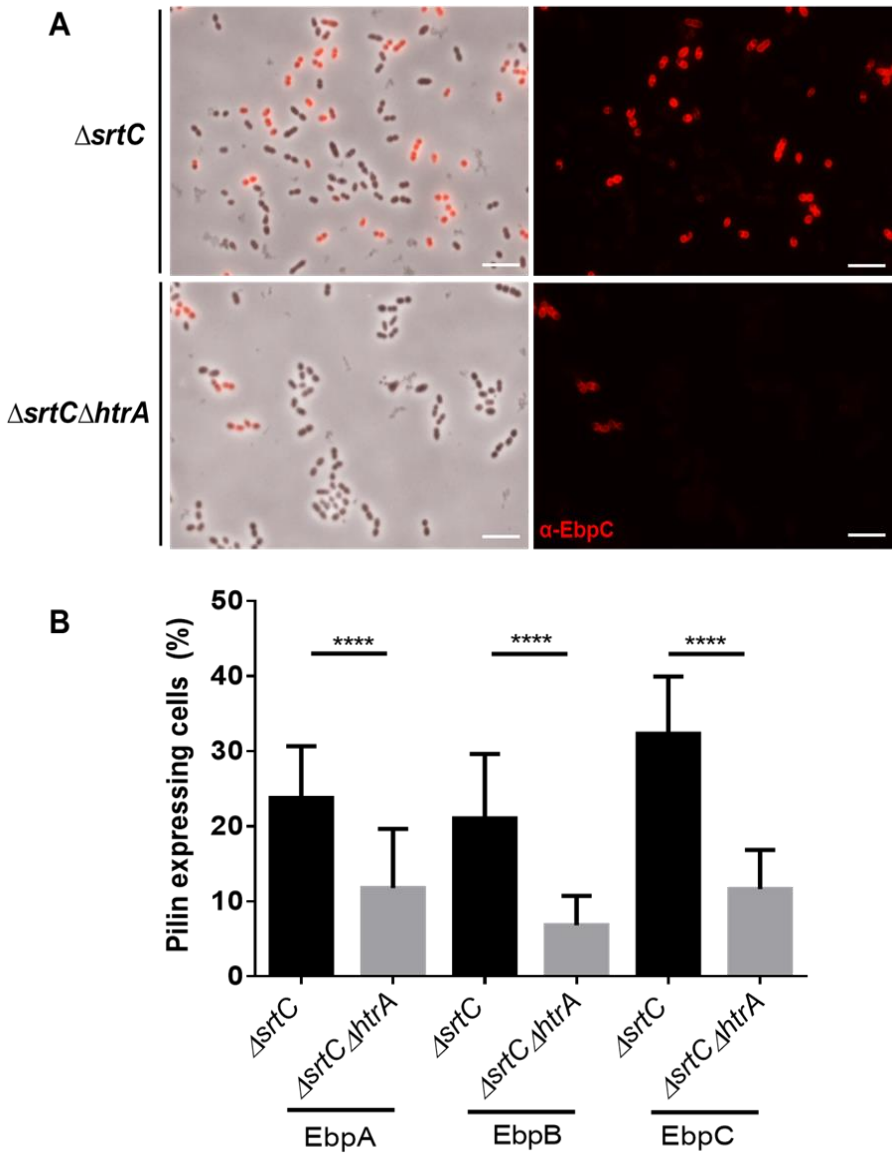

Supplementary Figure B8 | Decrease in pili monomers expressed in Δ*srtC*Δ*htrA*. (**A**) Pili were revealed with α-EbpC coupled to Alexa Fluor® 568 secondary antibody (red). The scale bar represents 5 µm. (**B**) Statistical analysis of pili expressing cells of Δ*srtC* and Δ*srtC*Δ*htrA* strains. Results are represented as bar graphs. **** P ≤ 0.0001. The data shown were from a single experiment representative of three independent experiments.

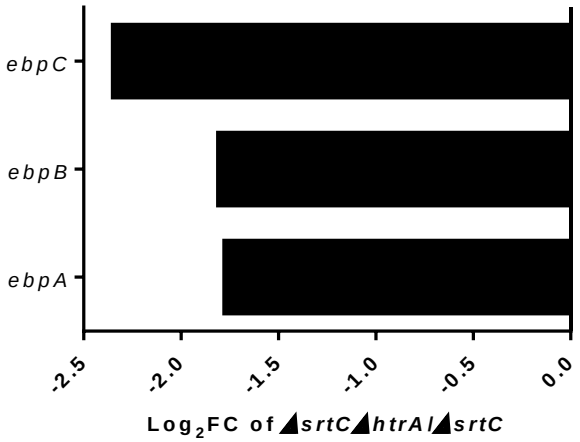

Supplementary Figure B9 | Ebp pilus expression in Δ*srtC*Δ*htrA* was transcriptionally affected. Log_2 fold change in mRNA levels in Δ*srtC*Δ*htrA* relative to Δ*srtC*, when grown to mid-log phase in TSB, supplemented with 0.25% glucose. Gene expression differences were significant ($P < 0.05$).

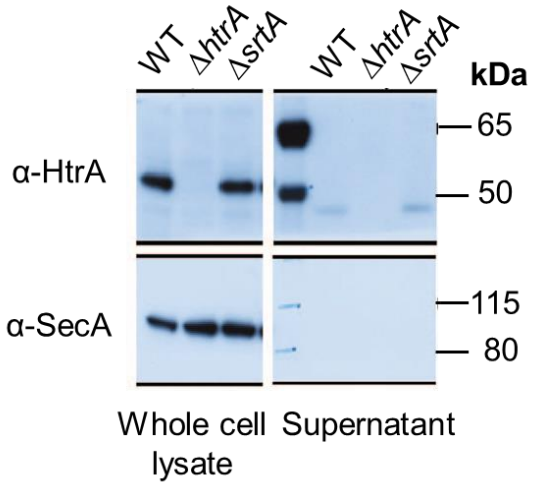

Supplementary Figure B10 | $HtrA_{EF}$ is released from cells in the absence of lysis. *E. faecalis* lysates or supernatants probed with α-$HtrA_{EF}$ or α-SecA immune sera (a cytoplasmic protein which serves as a lysis control) in the strains indicated.

APPENDIX C

Supplementary Table C1 | RNA-Seq results comparing WT and *ΔsrtAΔhtrA*.

Genes with significant differences in abundance of mRNAs were determined using a P-value and false discovery rate (FDR) cutoff of 0.05. The LogFC represents the log2 change between biological triplicates of Δ*srtA*Δ*htrA* compared to WT OG1RF when grown to mid-log phase in TSB supplemented with 0.25% glucose.

Locus Tag	LogFC	Gene[#]	Annotation	Manual classification
OG1RF_10024	1.71	-	hypothetical protein	Hypothetical
OG1RF_10040	1.17	-	PIN domain-containing protein	Unclassified
OG1RF_10041	1.09	*IspF*	2-C-methyl-D-erythritol 2,4-cyclo diphosphate synthase	Metabolism
OG1RF_10057	-1.22	-	oligopeptide ABC superfamily ATP binding cassette transporter, binding protein	Transport
OG1RF_10060	-1.37	*ruvA*	crossover junction ATP-dependent DNA helicase RuvA	Transcription and translation
OG1RF_10061	-1.11	*ruvB*	crossover junction ATP-dependent DNA helicase RuvB	Transcription and translation
OG1RF_10082	-1.16	-	M protein trans-acting positive regulator	Signaling and regulation
OG1RF_10098	1.75	*argR*	arginine repressor	Transcription and translation
OG1RF_10099	3.71	*arcA*	arginine deiminase	Unclassified
OG1RF_10100	3.51	*arcB*	ornithine carbamoyltransferase	Unclassified
OG1RF_10101	2.30	*arcC*	carbamate kinase	Unclassified
OG1RF_10102	1.66	*ntcA*	global nitrogen regulator NtcA	Transcription and translation
OG1RF_10113	-1.19	-	cob(I)yrinic acid a,c-diamide adenosyltransferase	Unclassified
OG1RF_10136	-1.97	-	iron (Fe3+) ABC superfamily ATP binding cassette transporter, binding protein	Transport
OG1RF_10180	-1.66	-	hypothetical protein	Hypothetical
OG1RF_10181	-1.72	-	M20D family peptidase	Unclassified
OG1RF_10182	-1.45	-	ABC superfamily ATP binding cassette transporter, ABC protein	Transport
OG1RF_10197	1.36	*amiD*	N-acetylmuramoyl-L-alanine amidase	Cell division/cell envelope
OG1RF_10198	-1.44	*aldA*	aldehyde dehydrogenase	Metabolism
OG1RF_10208	1.11	*hpt*	hypoxanthine phosphoribosyltransferase	Unclassified
OG1RF_10209	1.21	*ftsH*	cell division protein FtsH	Cell division/cell envelope
OG1RF_10218	-0.95	-	thioesterase	Unclassified
OG1RF_10222	-1.34	-	HD domain-containing protein	Unclassified
OG1RF_10223	-2.08	-	hypothetical protein	Hypothetical
OG1RF_10224	-1.58	-	hypothetical protein	Hypothetical
OG1RF_10228	-1.17	*pyrDA*	dihydroorotate oxidase	Metabolism
OG1RF_10235	-1.12	*celB*	PTS family lactose-N, N'-diacetylchitobiose-beta-glucoside (lac) porter component IIBC	Transport
OG1RF_10278	-1.35	*atzC*	N-isopropylammelide isopropylaminohydrolase	Unclassified
OG1RF_10282	-1.53	-	vitamin-B12 independent methionine synthase	Metabolism
OG1RF_10289	-0.97	-	MarR family transcriptional regulator	Signaling and regulation
OG1RF_10292	-1.04	*mtlA*	PTS family mannitol porter, EIICB component	Transport
OG1RF_10293	-1.04	-	mannitol operon transcriptional antiterminator	Unclassified
OG1RF_10294	-1.15	*mltF*	PTS family fructose/mannitol porter component IIA	Transport
OG1RF_10305	-1.07	-	hypothetical protein	Hypothetical
OG1RF_10349	-1.26	*dapF*	diaminopimelate epimerase	Unclassified

Supplementary table C1 (*continued.*)				
OG1RF_10353	3.39	-	LemA family protein	Unclassified
OG1RF_10354	3.54	-	hypothetical protein	Hypothetical
OG1RF_10355	-0.95	*nrdF*	ribonucleotide-diphosphate reductase subunit beta	Metabolism
OG1RF_10356	-0.99	*nrdE*	ribonucleotide-diphosphate reductase subunit alpha	Metabolism
OG1RF_10357	-1.01	*nrdI*	ribonucleotide-diphosphate reductase subunit gamma	Metabolism
OG1RF_10373	-1.17	*ldh2*	L-lactate dehydrogenase	Metabolism
OG1RF_10379	-1.32	-	phage integrase family site-specific recombinase	DNA repair and recombination
OG1RF_10417	1.30	*pbp2A*	penicillin-binding protein 2A	Cell division/cell envelope
OG1RF_10423	3.35	*prsA*	peptidyl-prolyl cis-trans isomerase	Protease/ Chaperone
OG1RF_10424	1.25	-	hypothetical protein	Hypothetical
OG1RF_10425	1.32	*hit*	Hisitidine Triad (HIT) family protein	Unclassified
OG1RF_10457	-1.30	-	voltage-gated chloride channel family protein	Metabolism
OG1RF_10475	-1.15	-	deoxynucleoside kinase	Unclassified
OG1RF_10476	-1.49	-	hypothetical protein	Hypothetical
OG1RF_10481	1.47	*pbp5*	beta-lactamase	Cell division/cell envelope
OG1RF_10499	-1.93	-	hypothetical protein	Hypothetical
OG1RF_10528	-1.29	-	rRNA methylase	Transcription and translation
OG1RF_10529	-1.48	-	radical SAM protein	Unclassified
OG1RF_10588	1.08	*pip*	phage infection protein	Transport
OG1RF_10589	-1.04	-	cation efflux family protein	Transport
OG1RF_10590	-1.12	-	APC family amino acid-polyamine-organocation transporter	Transport
OG1RF_10599	1.35	-	cro/CI family transcriptional regulator	Signaling and regulation
OG1RF_10613	-1.13	-	hypothetical protein	Hypothetical
OG1RF_10614	-2.00	-	hypothetical protein	Hypothetical
OG1RF_10615	-1.90	-	group 2 glycosyl transferase	Metabolism
OG1RF_10616	-1.80	-	cellulose synthase catalytic subunit	Metabolism
OG1RF_10617	-2.00	-	hypothetical protein	Hypothetical
OG1RF_10618	-1.89	-	hypothetical protein	Hypothetical
OG1RF_10626	-1.98	-	hypothetical protein	Hypothetical
OG1RF_10659	1.16	-	hypothetical protein	Hypothetical
OG1RF_10661	1.04	-	TatD family hydrolase	DNA repair and recombination
OG1RF_10672	-1.08	-	GNAT family acetyltransferase	Unclassified
OG1RF_10697	1.42	-	hypothetical protein	Hypothetical
OG1RF_10707	2.05	-	DNA repair exonuclease	DNA repair and recombination
OG1RF_10755	1.18	-	hypothetical protein	Hypothetical
OG1RF_10817	-1.64	*malR*	phage integrase family site-specific recombinase	DNA repair and recombination
OG1RF_10818	-1.47	-	nitroreductase	Metabolism
OG1RF_10820	-1.21	-	LytR family response regulator	Signaling and regulation
OG1RF_10838	-2.58	-	NRAMP family Mn2+/Fe2+ transporter	Transport
OG1RF_10839	-2.48	-	universal stress protein	Unclassified
OG1RF_10853	-1.10	-	hypothetical protein	Hypothetical
OG1RF_10858	-1.48	-	MFS family major facilitator transporter	Transport
OG1RF_10869	1.72	*ebpA*	von Willebrand factor type A domain-containing protein	Surface protein
OG1RF_10870	1.81	*ebpB*	cell wall surface anchor family protein	Surface protein
OG1RF_10871	1.86	*ebpC*	cell wall surface anchor family protein	Surface protein
OG1RF_10873	1.26	-	hypothetical protein	Hypothetical
OG1RF_10874	1.17	-	hypothetical protein	Hypothetical
OG1RF_10875	-1.69	-	hypothetical protein	Hypothetical

Supplementary table C1 (*continued.*)				
OG1RF_10876	-1.65	-	hypothetical protein	Hypothetical
OG1RF_10878	1.73	*ace*	collagen adhesin protein	Surface protein
OG1RF_10881	1.86	-	hypothetical protein	Hypothetical
OG1RF_10895	-1.69	*glnP*	glutamine ABC superfamily ATP binding cassette transporter, membrane protein	Transport
OG1RF_10896	-1.38	*glnM*	amino acid ABC superfamily ATP binding cassette transporter, membrane protein	Transport
OG1RF_10897	-1.47	*glnH*	glutamine ABC superfamily ATP binding cassette transporter, binding protein	Transport
OG1RF_10898	-1.27	*glnQ*	ABC superfamily ATP binding cassette transporter, ABC protein	Transport
OG1RF_10922	-1.29	-	hypothetical protein	Hypothetical
OG1RF_10949	-1.30	-	hypothetical protein	Hypothetical
OG1RF_10952	1.64	-	hypothetical protein	Hypothetical
OG1RF_10966	1.06	-	sensor histidine kinase	Signaling and regulation
OG1RF_10974	0.89	-	hypothetical protein	Hypothetical
OG1RF_10975	0.98	-	crossover junction endodeoxyribonuclease	DNA repair and recombination
OG1RF_10992	-1.68	-	ABC superfamily ATP binding cassette transporter, ABC protein	Transport
OG1RF_10993	-1.83	-	spermidine/putrescine ABC superfamily ATP binding cassette transporter	Transport
OG1RF_10994	-2.10	*ade*	adenine deaminase	Unclassified
OG1RF_10995	-2.42	*mtaD*	putative S-adenosylhomocysteine deaminase	Unclassified
OG1RF_11012	-1.27	-	hypothetical protein	Hypothetical
OG1RF_11029	0.89	*yclJ*	response regulator	Signaling and regulation
OG1RF_11030	0.87	*yclK*	sensor histidine kinase	Signaling and regulation
OG1RF_11031	3.69	-	hypothetical protein	Hypothetical
OG1RF_11032	3.39	-	hypothetical protein	Hypothetical
OG1RF_11033	0.93	-	sulfatase	Unclassified
OG1RF_11044	1.19	*rbfA*	ribosome-binding factor A	Unclassified
OG1RF_11045	-1.85	-	hypothetical protein	Hypothetical
OG1RF_11046	-1.50	-	hypothetical protein	Phage
OG1RF_11047	-1.58	-	cro/CI family transcriptional regulator	Phage
OG1RF_11048	-1.83	-	hypothetical protein	Phage
OG1RF_11049	-2.35	-	DNA replication protein	Phage
OG1RF_11050	-2.21	-	DNA replication protein	Phage
OG1RF_11051	-2.18	-	hypothetical protein	Phage
OG1RF_11052	-2.54	-	RinA family transcriptional regulator	Phage
OG1RF_11053	-3.23	-	transposase	Phage
OG1RF_11054	-3.66	-	hypothetical protein	Phage
OG1RF_11055	-3.49	-	TP901-1 family phage major tail protein	Phage
OG1RF_11056	-3.55	-	hypothetical protein	Phage
OG1RF_11057	-3.74	-	hypothetical protein	Phage
OG1RF_11058	-3.56	-	ABC superfamily ATP binding cassette transporter permease subunit	Phage
OG1RF_11059	-3.68	-	phage tail protein	Phage
OG1RF_11060	-3.83	-	phage structural protein	Phage
OG1RF_11061	-3.81	-	hypothetical protein	Phage
OG1RF_11062	-3.59	-	holin	Phage
OG1RF_11063	-4.15	*amiD2*	N-acetylmuramoyl-L-alanine amidase	Phage
OG1RF_11064	-1.17	*truB*	tRNA pseudouridine synthase B	Metabolism
OG1RF_11065	-1.23	*ribF*	riboflavin biosynthesis protein RibF	Metabolism
OG1RF_11066	-1.29	-	GNAT family acetyltransferase	Unclassified
OG1RF_11067	-2.29	-	PadR family transcriptional regulator	Signaling and regulation
OG1RF_11068	-2.93	-	hypothetical protein	Hypothetical
OG1RF_11069	-2.12	-	putative transcriptional regulator	Signaling and regulation

Supplementary table C1 (*continued.*)				
OG1RF_11070	-4.41	*ftsW*	FtsW/RodA/SpovE family cell division protein	Cell division/cell envelope
OG1RF_11071	-3.85	*rodA*	FtsW/RodA/SpovE family cell division protein	Cell division/cell envelope
OG1RF_11075	-1.06	*hemN*	coproporphyrinogen dehydrogenase	Metabolism
OG1RF_11086	-1.23	-	hypothetical protein	Hypothetical
OG1RF_11131	1.07	-	ABC superfamily ATP binding cassette transporter, ABC protein	Transport
OG1RF_11157	-1.71	-	cro/CI family transcriptional regulator	Signaling and regulation
OG1RF_11191	0.92	*cvpA*	colicin V production protein CvpA family protein	Unclassified
OG1RF_11193	0.99	*trxA*	thioredoxin	Unclassified
OG1RF_11200	1.21	-	hypothetical protein	Hypothetical
OG1RF_11207	1.94	*atpF1*	V-type ATPase, subunit F	Metabolism
OG1RF_11208	2.21	*atpI*	proton (H+) or sodium (Na+) translocating V-type ATPase (V-ATPase), subunit I	Metabolism
OG1RF_11209	2.00	*atpK*	proton (H+) or sodium (Na+) translocating V-type ATPase (V-ATPase), subunit K	Metabolism
OG1RF_11210	1.83	*atpE*	proton (H+) or sodium (Na+) translocating V-type ATPase (V-ATPase), subunit E	Metabolism
OG1RF_11211	1.94	*atpC*	proton (H+) or sodium (Na+) translocating V-type ATPase (V-ATPase), subunit C	Metabolism
OG1RF_11212	1.95	*atpF2*	V-type ATP synthase subunit F	Metabolism
OG1RF_11213	1.75	*atpA*	ATP synthase F1 subcomplex subunit alpha	Metabolism
OG1RF_11214	1.58	*atpB*	proton (H+) or sodium (Na+) translocating V-type ATPase (V-ATPase), subunit B	Metabolism
OG1RF_11215	1.64	*atpD*	V-type ATP synthase subunit D	Metabolism
OG1RF_11216	1.59	-	hypothetical protein	Hypothetical
OG1RF_11219	-0.97	-	beta-lactamase	Cell division/cell envelope
OG1RF_11223	-1.25	-	hypothetical protein	Hypothetical
OG1RF_11230	-2.20	*sacT*	SacPA operon anti-terminator	Signaling and regulation
OG1RF_11231	-1.93	*ptsG*	PTS family glucose porter, IICBA component	Transport
OG1RF_11239	1.15	-	transposon family protein	Unclassified
OG1RF_11250	-2.79	-	TetR family transcriptional regulator	Signaling and regulation
OG1RF_11260	-3.40	-	brp/Blh family beta-carotene 15,15'-monooxygenase	Metabolism
OG1RF_11261	-2.20	-	hypothetical protein	Hypothetical
OG1RF_11301	-1.42	-	major facilitator family transporter	Transport
OG1RF_11308	-2.44	-	N-acetyltransferase	Unclassified
OG1RF_11310	-1.80	-	multidrug ABC superfamily ATP binding cassette transporter, ABC protein	Transport
OG1RF_11311	-1.12	-	ABC superfamily ATP binding cassette transporter, ABC/membrane protein	Transport
OG1RF_11326	-1.19	-	hypothetical protein	Hypothetical
OG1RF_11348	-1.80	*pduU*	propanediol utilization protein PduU	Unclassified
OG1RF_11355	-1.01	*plsY*	acyl-phosphate glycerol 3-phosphate acyltransferase	Unclassified
OG1RF_11358	1.33	*hslU*	ATP-dependent hsl protease ATP-binding subunit HslU	Protease/Chaperone
OG1RF_11359	1.43	*hslV*	ATP-dependent protease HslVU	Protease/Chaperone
OG1RF_11360	1.58	*xerC*	tyrosine recombinase XerC	DNA repair and recombination
OG1RF_11384	1.64	-	permease protein	Transport
OG1RF_11385	2.12	-	ABC superfamily ATP binding cassette transporter, ABC protein	Transport
OG1RF_11442	-1.83	*mdlB*	multidrug ABC superfamily ATP binding cassette transporter, ABC protein	Transport

Supplementary table C1 (*continued.*)				
OG1RF_11443	-1.40	*mdlA*	multidrug ABC superfamily ATP binding cassette transporter, ABC protein	Transport
OG1RF_11461	0.92	-	endo/excinuclease amino domain-containing protein	Transcription and translation
OG1RF_11462	3.31	-	hypothetical protein	Hypothetical
OG1RF_11463	3.30	-	PspC domain-containing protein	Unclassified
OG1RF_11464	3.75	-	hypothetical protein	Hypothetical
OG1RF_11485	-1.29	*fabG2*	3-oxoacyl-ACP reductase	Metabolism
OG1RF_11488	-2.06	-	hypothetical protein	Hypothetical
OG1RF_11490	-1.48	*purH*	bifunctional purine biosynthesis protein PurH	Metabolism
OG1RF_11493	-1.39	*purF*	amidophosphoribosyltransferase	Metabolism
OG1RF_11494	-1.30	*purL*	phosphoribosylformylglycinamidine synthase	Metabolism
OG1RF_11495	-1.88	*purL2*	phosphoribosylformylglycinamidine synthase	Metabolism
OG1RF_11497	-1.39	*purC*	phosphoribosylaminoimidazolesuccinocarboxamide synthase	Metabolism
OG1RF_11498	-1.27	*purK*	phosphoribosylaminoimidazole carboxylase ATPase subunit PurK	Metabolism
OG1RF_11523	-1.67	-	LysR family transcriptional regulator	Signaling and regulation
OG1RF_11524	-1.08	-	hypothetical protein	Hypothetical
OG1RF_11525	-1.31	*sprE*	SprE protein	Signaling and regulation
OG1RF_11526	-1.33	*gelE*	gelatinase	Signaling and regulation
OG1RF_11569	1.93	-	integral membrane protein	Unclassified
OG1RF_11580	-1.28	*ysxC*	ribosome biogenesis GTP-binding protein YsxC	Transcription and translation
OG1RF_11599	-0.98	-	GntR family transcriptional regulator	Signaling and regulation
OG1RF_11604	-1.28	-	cyclic AMP receptor protein	Transcription and translation
OG1RF_11607	-0.88	-	membrane-oligosaccharide glycerophosphotransferase	Metabolism
OG1RF_11642	-1.69	-	hypothetical protein	Hypothetical
OG1RF_11656	3.20	-	ABC superfamily ATP binding cassette transporter, permease protein	Transport
OG1RF_11657	3.26	-	ABC superfamily ATP binding cassette transporter, ABC protein	Transport
OG1RF_11663	-1.80	-	ABC superfamily ATP binding cassette transporter, ABC/membrane protein	Transport
OG1RF_11664	-2.06	-	ABC superfamily ATP binding cassette transporter, ABC/membrane protein	Transport
OG1RF_11666	-1.62	*cydA*	cytochrome D ubiquinol oxidase subunit I	Transport
OG1RF_11671	-1.03	-	hypothetical protein	Hypothetical
OG1RF_11672	-1.11	-	major facilitator family transporter	Transport
OG1RF_11673	-1.63	*MnmA*	tRNA (5-methyl aminomethyl-2-thiouridylate)-methyltransferase	Unclassified
OG1RF_11677	-2.15	-	ABC superfamily ATP binding cassette transporter, ABC protein	Transport
OG1RF_11678	-2.12	-	ABC superfamily ATP binding cassette transporter, membrane protein	Transport
OG1RF_11679	-2.13	-	ABC superfamily ATP binding cassette transporter, binding protein	Transport
OG1RF_11680	-1.25	-	ABC superfamily ATP binding cassette transporter, ABC protein	Transport
OG1RF_11681	-1.32	*hipO2*	aminoacylase	Unclassified
OG1RF_11683	-2.03	-	ABC superfamily ATP binding cassette transporter, membrane protein	Transport
OG1RF_11684	-1.77	-	ABC superfamily ATP binding cassette transporter, binding protein	Transport

Supplementary table C1 (*continued.*)				
OG1RF_11693	-1.60	-	cobalt (Co2+) ABC superfamily ATP binding cassette transporter, membrane protein	Transport
OG1RF_11694	-1.75	-	ABC superfamily ATP binding cassette transporter, ABC protein	Transport
OG1RF_11695	-1.32	-	hypothetical protein	Hypothetical
OG1RF_11696	0.93	*glmM*	phosphoglucosamine mutase	Unclassified
OG1RF_11697	0.91	-	hypothetical protein	Hypothetical
OG1RF_11698	0.97	-	hypothetical protein	Hypothetical
OG1RF_11719	-1.54	*licD*	LicD-like protein	Unclassified
OG1RF_11720	-1.85	-	group 2 glycosyl transferase	Metabolism
OG1RF_11733	0.90	*rfbC*	dTDP-4-dehydrorhamnose 3,5-epimerase	Unclassified
OG1RF_11751	2.78	-	hypothetical protein	Hypothetical
OG1RF_11766	2.90	-	multidrug ABC superfamily ATP binding cassette transporter, ABC protein	Transport
OG1RF_11767	2.99	-	ABC superfamily ATP binding cassette transporter, membrane protein	Transport
OG1RF_11793	1.58	*clpB*	chaperone protein ClpB	Protease/ Chaperone
OG1RF_11797	-2.69	*pbuX*	xanthine permease	Metabolism
OG1RF_11798	-3.23	*xpt*	xanthine phosphoribosyltransferase	Metabolism
OG1RF_11860	-1.39	*guaC*	GMP reductase	Unclassified
OG1RF_11861	-1.54	-	NCS2 family xanthine/uracil permease	Transport
OG1RF_11862	-1.41	*guaD*	guanine deaminase	Unclassified
OG1RF_11875	-1.85	-	acyl-CoA thioester hydrolase	Metabolism
OG1RF_11878	-1.01	*comEC*	competence protein ComEC	Unclassified
OG1RF_11896	-0.98	-	hypothetical protein	Hypothetical
OG1RF_11903	-0.92	*gcp*	O-sialoglycoprotein endopeptidase	Unclassified
OG1RF_11904	-0.97	*rimI*	ribosomal-protein-alanine acetyltransferase	Unclassified
OG1RF_11905	-1.05	*rimI2*	ribosomal-protein-alanine acetyltransferase	Unclassified
OG1RF_11907	1.46	*pbp4*	penicillin-binding protein 4	Cell division/cell envelope
OG1RF_11922	-1.60	-	M protein trans-acting positive regulator	Signaling and regulation
OG1RF_11923	-1.61	-	hypothetical protein	Hypothetical
OG1RF_11925	-2.05	-	hypothetical protein	Hypothetical
OG1RF_11926	-1.88	-	cro/CI family transcriptional regulator	Signaling and regulation
OG1RF_11927	-2.85	*azlC*	LIV-E family branched-chain amino acid exporter AzlC	Transport
OG1RF_11928	-3.02	*azlD*	LIV-E family branched-chain amino acid exporter AzlD	Transport
OG1RF_11938	-1.42	-	fumarate reductase	Unclassified
OG1RF_11977	-1.37	*licT2*	transcription anti-terminator LicT	Unclassified
OG1RF_11979	-1.02	-	FMN-dependent NADH-azoreductase	Unclassified
OG1RF_12013	0.95	*opuAA 2*	glycine betaine/L-proline ABC superfamily ATP binding cassette transporter, ABC protein	Transport
OG1RF_12014	1.06	-	glycine betaine/carnitine/choline ABC superfamily ATP binding cassette transporter	Transport
OG1RF_12031	-1.67	-	integral membrane protein	Unclassified
OG1RF_12045	-1.10	-	competence protein ComA	Unclassified
OG1RF_12049	-1.38	*lmrA*	multidrug resistance ABC transporter ATP-binding and permease	Transport
OG1RF_12063	1.35	*mtnN*	MTA/SAH nucleosidase	Metabolism
OG1RF_12064	1.21	-	hypothetical protein	Hypothetical
OG1RF_12065	1.33	*nudF*	ADP-ribose diphosphatase	Metabolism
OG1RF_12066	2.75	-	hypothetical protein	Hypothetical
OG1RF_12067	2.20	*telA*	tellurite resistance protein	Unclassified

Supplementary table C1 (*continued.*)				
OG1RF_12098	1.09	*mviM*	gfo/Idh/MocA family oxidoreductase	Unclassified
OG1RF_12111	1.05	*dltB*	D-alanine transfer protein DltB	Cell division/cell envelope
OG1RF_12112	1.10	*dltA*	D-alanine--D-alanine ligase	Cell division/cell envelope
OG1RF_12127	-1.76	*tenA*	thiaminase	Metabolism
OG1RF_12128	-1.33	-	cobalt transporter	Transport
OG1RF_12129	-1.62	-	ABC superfamily ATP binding cassette transporter, ABC protein	Transport
OG1RF_12130	-0.95	-	ABC superfamily ATP binding cassette transporter, membrane protein	Transport
OG1RF_12138	-2.02	*thiW*	Energy coupling factor transporter S componet ThiW protein	Transport
OG1RF_12152	-1.63	-	hypothetical protein	Hypothetical
OG1RF_12158	1.67	*penA*	penicillin-binding protein 2B	Cell division/cell envelope
OG1RF_12163	1.35	*cisR*	response regulator	Signaling and regulation
OG1RF_12164	1.57	-	ErfK/YbiS/YcfS/YnhG family protein	Unclassified
OG1RF_12186	-1.21	*fabK*	enoyl-ACP reductase	Unclassified
OG1RF_12187	-1.01	*acpP*	acyl carrier protein	Unclassified
OG1RF_12188	-1.00	*fabH*	beta-ketoacyl-acyl-carrier-protein synthase III	Unclassified
OG1RF_12189	-0.98	-	MarR family transcriptional regulator	Signaling and regulation
OG1RF_12193	-1.18	-	group 1 glycosyl transferase	Unclassified
OG1RF_12225	-0.92	*cspA3*	cold shock protein CspA	Unclassified
OG1RF_12235	-1.80	-	S1 family extracellular protease	Unclassified
OG1RF_12266	1.83	-	transcriptional regulator	Signaling and regulation
OG1RF_12267	5.23	-	permease protein	Transport
OG1RF_12268	5.21	-	ABC superfamily ATP binding cassette transporter, ABC protein	Transport
OG1RF_12269	5.18	-	RND transporter	Transport
OG1RF_12294	-1.09	*pmr1*	P-ATPase superfamily P-type ATPase cation transporter	Transport
OG1RF_12305	-8.53	*htrA*	serine protease HtrA	Protease/Chaperone
OG1RF_12325	-1.18	-	putative lipoprotein	Unclassified
OG1RF_12327	-11.97	*srtA*	sortase SrtA	Unclassified
OG1RF_12352	-1.25	-	ABC superfamily ATP binding cassette transporter, ABC protein	Transport
OG1RF_12380	1.27	*rpmB2*	50S ribosomal protein L28	Transcription and translation
OG1RF_12391	-1.18	*gmk2*	guanylate kinase	Unclassified
OG1RF_12406	-1.13	-	RpiR family phosphosugar-binding transcriptional regulator	Signaling and regulation
OG1RF_12421	-1.88	-	S-layer protein	Surface protein
OG1RF_12425	-1.95	*trePP*	glycosyl hydrolase	Metabolism
OG1RF_12426	-1.88	*yvdM*	beta-phosphoglucomutase	Metabolism
OG1RF_12441	-1.17	-	hypothetical protein	Hypothetical
OG1RF_12451	1.49	-	cell wall surface anchor family protein	Surface protein
OG1RF_12452	1.94	*ubiD*	UbiD family decarboxylase	Surface protein
OG1RF_12453	2.16	-	WxL domain surface protein	Surface protein
OG1RF_12454	2.06	-	hypothetical protein	Surface protein
OG1RF_12455	2.09	-	hypothetical protein	Hypothetical
OG1RF_12456	1.97	-	WxL domain surface protein	Surface protein
OG1RF_12460	1.68	*lrgB*	murein hydrolase regulator LrgB	Signaling and regulation
OG1RF_12461	1.68	*lrgA*	murein hydrolase regulator LrgA	Signaling and regulation
OG1RF_12476	-1.14	-	PTS family fructose/mannitol (fru) porter component IIA	Transport
OG1RF_12478	-1.32	-	PTS family fructose/mannitol (fru) porter component IIC	Transport
OG1RF_12480	-1.14	-	DEAH-box family ATP-dependent helicase	Transcription and translation
OG1RF_12484	-1.28	-	hypothetical protein	Hypothetical

Supplementary table C1 (*continued.*)				
OG1RF_12500	1.24	-	cell-envelope associated acid phosphatase	Signaling and regulation
OG1RF_12523	-1.37	-	hydantoinase/oxoprolinase	Metabolism
OG1RF_12532	-1.07	*mdeA*	putative methionine gamma-lyase	Unclassified
OG1RF_12533	-1.49	-	PTS family oligomeric beta-glucoside porter component IIC	Transport
OG1RF_12535	1.44	*croR*	response regulator	Signaling and regulation
OG1RF_12536	1.41	*croS*	sensor histidine kinase	Signaling and regulation
[#]Manual annotation in red.				

Supplementary Table C2 | RNA-Seq results comparing *ΔhtrA* and *ΔsrtAΔhtrA*.

Genes with significant differences in abundance of mRNAs were determined using a P value and false discovery rate (FDR) cutoff of 0.05. The LogFC represents the log2 change between biological triplicates of Δ*srtA*Δ*htrA* compared to *ΔhtrA* when grown to mid-log phase in TSB supplemented with 0.25% glucose.

Locus Tag	logFC	Gene[#]	Annotation	Manual classification
OG1RF_10005	1.09	*gyrB*	DNA topoisomerase subunit B	Transcription and translation
OG1RF_10006	1.10	*gyrA*	DNA topoisomerase subunit A	Transcription and translation
OG1RF_10022	-1.06	-	hypothetical protein	Hypothetical
OG1RF_10040	1.38	-	PIN domain-containing protein	Unclassified
OG1RF_10041	1.32	*ispF*	2-C-methyl-D-erythritol 2,4-cyclo diphosphate synthase	Metabolism
OG1RF_10045	1.02	*cysS2*	cysteine--tRNA ligase	Unclassified
OG1RF_10047	0.90	-	hypothetical protein	Hypothetical
OG1RF_10049	1.21	*veg*	Veg protein	Unclassified
OG1RF_10057	-1.47	-	oligopeptide ABC superfamily ATP binding cassette transporter, binding protein	Transport
OG1RF_10063	-0.93	-	N-acylglucosamine-6-phosphate 2-epimerase	Unclassified
OG1RF_10096	-1.22	-	alpha/beta hydrolase fold family hydrolase	Unclassified
OG1RF_10099	2.95	*arcA*	arginine deiminase	Unclassified
OG1RF_10100	3.02	*arcB*	ornithine carbamoyltransferase	Unclassified
OG1RF_10101	1.65	*arcC*	carbamate kinase	Unclassified
OG1RF_10102	1.42	*ntcA*	global nitrogen regulator NtcA	Transcription and translation
OG1RF_10113	-1.20	-	cob(I)yrinic acid a,c-diamide adenosyltransferase	Unclassified
OG1RF_10136	-1.59	-	iron (Fe3+) ABC superfamily ATP binding cassette transporter, binding protein	Transport
OG1RF_10148	-1.24	*thiD*	phosphomethylpyrimidine kinase	Unclassified
OG1RF_10152	1.08	*rplD*	50S ribosomal protein L4/L1 family protein	Transcription and translation
OG1RF_10154	1.17	*rplB*	50S ribosomal protein L2	Transcription and translation
OG1RF_10155	1.08	*rpsS*	30S ribosomal protein S19	Transcription and translation
OG1RF_10157	1.12	*rpsC*	30S ribosomal protein S3	Transcription and translation
OG1RF_10164	1.08	*rpsN*	30S ribosomal protein S14	Transcription and translation
OG1RF_10165	1.11	*rpsH*	30S ribosomal protein S8	Transcription and translation
OG1RF_10166	1.08	*rplF*	50S ribosomal protein L6	Transcription and translation
OG1RF_10167	1.00	*rplR*	50S ribosomal protein L18	Transcription and translation
OG1RF_10170	0.97	*rplO*	50S ribosomal protein L15	Transcription and translation
OG1RF_10178	0.97	*rplQ*	50S ribosomal protein L17	Transcription and translation
OG1RF_10180	-1.77	-	hypothetical protein	Hypothetical
OG1RF_10181	-1.53	-	M20D family peptidase	Unclassified
OG1RF_10182	-1.30	-	ABC superfamily ATP binding cassette transporter, ABC protein	Transport
OG1RF_10186	-1.03	-	hypothetical protein	Hypothetical
OG1RF_10208	1.21	*hpt*	hypoxanthine phosphoribosyltransferase	Unclassified
OG1RF_10209	1.30	*ftsH*	cell division protein FtsH	Cell division/cell envelope
OG1RF_10210	-1.23	*hslO*	chaperonin HslO	Protease/Chaperone
OG1RF_10211	-1.25	*dus*	tRNA-dihydrouridine synthase	Unclassified
OG1RF_10219	-1.19	-	methylphosphotriester-DNA alkyltransferase	Unclassified
OG1RF_10223	-1.91	-	hypothetical protein	Hypothetical
OG1RF_10224	-1.61	-	hypothetical protein	Hypothetical

Supplementary table C2 (*continued*.)				
OG1RF_10225	-1.32	*fabI*	enoyl-ACP reductase	Unclassified
OG1RF_10228	-1.16	*pyrDA*	dihydroorotate oxidase	Metabolism
OG1RF_10235	-1.38	*celB*	PTS family lactose-N, N'-diacetylchitobiose-beta-glucoside (lac) porter component IIBC	Transport
OG1RF_10246	-1.61	-	flavin reductase domain-containing FMN-binding protein	Unclassified
OG1RF_10265	-1.29	-	ankyrin repeat family protein	Unclassified
OG1RF_10266	-1.12	-	amidohydrolase	Unclassified
OG1RF_10278	-1.41	*atzC*	N-isopropylammelide isopropylaminohydrolase	Unclassified
OG1RF_10306	-1.05	-	hypothetical protein	Hypothetical
OG1RF_10307	-1.20	*lmrB*	MFS family lincomycin resistance protein LmrB	Unclassified
OG1RF_10349	-1.48	*dapF*	diaminopimelate epimerase	Unclassified
OG1RF_10353	2.90	-	LemA family protein	Unclassified
OG1RF_10354	2.90	-	hypothetical protein	Hypothetical
OG1RF_10355	-1.04	*nrdF*	ribonucleotide-diphosphate reductase subunit beta	Metabolism
OG1RF_10356	-1.04	*nrdE*	ribonucleotide-diphosphate reductase subunit alpha	Metabolism
OG1RF_10357	-1.10	*nrdI*	ribonucleotide-diphosphate reductase subunit gamma	Metabolism
OG1RF_10373	-1.08	*ldh2*	L-lactate dehydrogenase	Metabolism
OG1RF_10379	-1.29	-	phage integrase family site-specific recombinase	DNA repair and recombination
OG1RF_10410	-1.39	-	putative acetyltransferase	Unclassified
OG1RF_10423	2.02	*prsA*	peptidyl-prolyl cis-trans isomerase	Protease/ Chaperone
OG1RF_10432	1.24	-	PTS family fructose porter component IIBC	Transport
OG1RF_10440	-1.37	-	hypothetical protein	Hypothetical
OG1RF_10446	1.38	-	hypothetical protein	Hypothetical
OG1RF_10449	-1.40	-	hypothetical protein	Hypothetical
OG1RF_10452	0.94	*tig*	trigger factor	Unclassified
OG1RF_10476	-1.47	-	hypothetical protein	Hypothetical
OG1RF_10481	1.95	*pbp5*	beta-lactamase	Cell division/cell envelope
OG1RF_10482	1.26	-	hypothetical protein	Hypothetical
OG1RF_10528	-1.42	-	rRNA methylase	Transcription and translation
OG1RF_10529	-1.50	-	radical SAM protein	Unclassified
OG1RF_10556	-1.09	*udk*	uridine kinase	Unclassified
OG1RF_10559	1.11	-	BglG family transcriptional anti-terminator	Unclassified
OG1RF_10589	-1.12	-	cation efflux family protein	Transport
OG1RF_10590	-1.30	-	APC family amino acid-polyamine-organocation transporter	Transport
OG1RF_10596	-1.10	-	hypothetical protein	Hypothetical
OG1RF_10599	1.43	-	cro/CI family transcriptional regulator	Signaling and regulation
OG1RF_10613	-1.12	-	hypothetical protein	Hypothetical
OG1RF_10614	-1.50	-	hypothetical protein	Hypothetical
OG1RF_10615	-1.26	-	group 2 glycosyl transferase	Metabolism
OG1RF_10616	-1.29	-	cellulose synthase catalytic subunit	Metabolism
OG1RF_10617	-1.32	-	hypothetical protein	Hypothetical
OG1RF_10618	-1.28	-	hypothetical protein	Hypothetical
OG1RF_10626	-2.13	-	hypothetical protein	Hypothetical
OG1RF_10648	-1.06	-	sulfate transporter	Transport
OG1RF_10661	1.12	-	TatD family hydrolase	DNA repair and recombination
OG1RF_10662	0.94	-	primase-like protein	Unclassified

Supplementary table C2 (*continued*.)				
OG1RF_10672	-1.27	-	GNAT family acetyltransferase	Unclassified
OG1RF_10677	-1.50	-	ATP/GTP hydrolase	Metabolism
OG1RF_10681	-1.26	-	aldose 1-epimerase	Unclassified
OG1RF_10682	-1.73	*pgmB*	beta-phosphoglucomutase	Unclassified
OG1RF_10683	-2.00	*map*	family 65 glycosyl hydrolase	Unclassified
OG1RF_10684	-2.19	*exp5*	PTS family porter component IIABC	Transport
OG1RF_10685	-2.00	*rgfB*	endonuclease/exonuclease/phosphata se family protein RgfB	Unclassified
OG1RF_10688	1.40	-	hypothetical protein	Hypothetical
OG1RF_10707	1.59	-	DNA repair exonuclease	DNA repair and recombination
OG1RF_10721	1.59	*mraZ*	cell division protein MraZ	Cell division/cell envelope
OG1RF_10722	1.54	*mraW*	S-adenosyl-methyltransferase MraW	Unclassified
OG1RF_10723	1.76	-	cell division protein	Cell division/cell envelope
OG1RF_10724	0.99	*pbpC*	penicillin-binding protein C	Cell division/cell envelope
OG1RF_10725	0.91	*mraY*	phospho-N-acetylmuramoyl-pentapeptide-transferase	Unclassified
OG1RF_10733	0.91	*ylmG*	hypothetical protein	Hypothetical
OG1RF_10739	1.41	-	hypothetical protein	Hypothetical
OG1RF_10740	1.00	*sfsA*	sugar fermentation stimulation protein	Unclassified
OG1RF_10754	0.86	-	GNAT family acetyltransferase	Unclassified
OG1RF_10764	1.25	-	phosphorylase	Unclassified
OG1RF_10784	-1.04	*csrS*	sensor histidine kinase CsrS	Signaling and regulation
OG1RF_10808	-1.25	-	M protein trans-acting positive regulator	Signaling and regulation
OG1RF_10817	-1.86	*malR*	phage integrase family site-specific recombinase	DNA repair and recombination
OG1RF_10818	-1.95	-	nitroreductase	Metabolism
OG1RF_10819	-1.98	-	membrane protein	Unclassified
OG1RF_10820	-1.74	-	LytR family response regulator	Signaling and regulation
OG1RF_10838	-2.00	-	NRAMP family Mn2+/Fe2+ transporter	Transport
OG1RF_10853	-1.18	-	hypothetical protein	Hypothetical
OG1RF_10858	-1.70	-	MFS family major facilitator transporter	Transport
OG1RF_10859	-1.16	*dinB2*	Y family DNA-directed DNA polymerase	Transcription and translation
OG1RF_10866	-1.53	-	hypothetical protein	Hypothetical
OG1RF_10869	1.60	*ebpA*	von Willebrand factor type A domain-containing protein	Surface protein
OG1RF_10870	1.83	*ebpB*	cell wall surface anchor family protein	Surface protein
OG1RF_10871	1.87	*ebpC*	cell wall surface anchor family protein	Surface protein
OG1RF_10874	1.20	-	hypothetical protein	Hypothetical
OG1RF_10877	-1.71	-	hypothetical protein	Hypothetical
OG1RF_10890	1.04	*rexB*	exonuclease RexB	DNA repair and recombination
OG1RF_10895	-1.79	*glnP*	glutamine ABC superfamily ATP binding cassette transporter, membrane protein	Transport
OG1RF_10896	-1.37	*glnM*	amino acid ABC superfamily ATP binding cassette transporter, membrane protein	Transport
OG1RF_10897	-1.45	*glnH*	glutamine ABC superfamily ATP binding cassette transporter, binding protein	Transport
OG1RF_10916	-1.21	*puuD*	putative gamma-glutamyl-gamma-aminobutyrate hydrolase	Unclassified
OG1RF_10922	-1.66	-	hypothetical protein	Hypothetical
OG1RF_10952	1.42	-	hypothetical protein	Hypothetical
OG1RF_10953	-1.49	-	oxygen-insensitive NADPH nitroreductase	Metabolism

Supplementary table C2 (*continued*.)				
OG1RF_10965	1.09	-	response regulator	Signaling and regulation
OG1RF_10966	1.21	-	sensor histidine kinase	Signaling and regulation
OG1RF_10969	1.09	-	beta-lactamase	Cell division/cell envelope
OG1RF_10975	1.01	-	crossover junction endodeoxyribonuclease	DNA repair and recombination
OG1RF_10984	1.11	-	transcriptional regulator	Signaling and regulation
OG1RF_10985	-1.30	*alsS*	acetolactate synthase	Unclassified
OG1RF_10986	-1.34	*budA*	alpha-acetolactate decarboxylase	Unclassified
OG1RF_10987	-1.51	-	hypothetical protein	Hypothetical
OG1RF_10988	-1.59	-	extracellular protein	Unclassified
OG1RF_10991	-1.76	-	spermidine/putrescine ABC superfamily ATP binding cassette transporter, permease protein	Transport
OG1RF_10992	-2.16	-	ABC superfamily ATP binding cassette transporter, ABC protein	Transport
OG1RF_10993	-2.09	-	spermidine/putrescine ABC superfamily ATP binding cassette transporter	Transport
OG1RF_10994	-2.48	*ade*	adenine deaminase	Unclassified
OG1RF_10995	-2.52	*mtaD*	putative S-adenosylhomocysteine deaminase	Unclassified
OG1RF_11033	1.21	-	sulfatase	Unclassified
OG1RF_11037	-1.06	-	cell wall surface anchor family protein	Surface protein
OG1RF_11038	1.44	-	hypothetical protein	Hypothetical
OG1RF_11044	1.32	*rbfA*	ribosome-binding factor A	Unclassified
OG1RF_11045	-2.24	-	hypothetical protein	Hypothetical
OG1RF_11046	-1.66	-	hypothetical protein	Phage
OG1RF_11047	-1.60	-	cro/CI family transcriptional regulator	Phage
OG1RF_11048	-2.95	-	hypothetical protein	Phage
OG1RF_11049	-3.33	-	DNA replication protein	Phage
OG1RF_11050	-3.32	-	DNA replication protein	Phage
OG1RF_11051	-3.30	-	hypothetical protein	Phage
OG1RF_11052	-3.66	-	RinA family transcriptional regulator	Phage
OG1RF_11053	-3.58	-	transposase	Phage
OG1RF_11054	-4.16	-	hypothetical protein	Phage
OG1RF_11055	-3.89	-	TP901-1 family phage major tail protein	Phage
OG1RF_11056	-3.84	-	hypothetical protein	Phage
OG1RF_11057	-4.26	-	hypothetical protein	Phage
OG1RF_11058	-4.04	-	ABC superfamily ATP binding cassette transporter permease subunit	Phage
OG1RF_11059	-4.24	-	phage tail protein	Phage
OG1RF_11060	-4.22	-	phage structural protein	Phage
OG1RF_11061	-4.21	-	hypothetical protein	Phage
OG1RF_11062	-4.11	-	holin	Phage
OG1RF_11063	-4.57	*amiD2*	N-acetylmuramoyl-L-alanine amidase	Phage
OG1RF_11064	-1.34	*truB*	tRNA pseudouridine synthase B	Metabolism
OG1RF_11065	-1.41	*ribF*	riboflavin biosynthesis protein RibF	Metabolism
OG1RF_11066	-1.42	-	GNAT family acetyltransferase	Unclassified
OG1RF_11067	-2.94	-	PadR family transcriptional regulator	Signaling and regulation
OG1RF_11068	-3.39	-	hypothetical protein	Hypothetical
OG1RF_11069	-2.58	-	putative transcriptional regulator	Signaling and regulation
OG1RF_11070	-4.72	*ftsW*	FtsW/RodA/SpovE family cell division protein	Cell division/cell envelope
OG1RF_11071	-4.15	*rodA*	FtsW/RodA/SpovE family cell division protein	Cell division/cell envelope
OG1RF_11074	-1.31	*mgtA*	magnesium-importing ATPase	Metabolism
OG1RF_11075	-1.25	*hemN*	coproporphyrinogen dehydrogenase	Metabolism

Supplementary table C2 (*continued*.)				
OG1RF_11084	0.95	-	SprT family protein	Unclassified
OG1RF_11086	-1.20	-	hypothetical protein	Hypothetical
OG1RF_11096	-1.07	-	hypothetical protein	Hypothetical
OG1RF_11133	-2.36	-	sugar ABC transporter ATP-binding protein	Transport
OG1RF_11134	-2.48	-	sugar ABC transporter ATP-binding protein	Transport
OG1RF_11135	-1.57	-	sugar ABC superfamily ATP binding cassette transporter, sugar-binding protein	Transport
OG1RF_11137	-1.46	*dexB*	glucan 1,6-alpha-glucosidase	Unclassified
OG1RF_11140	1.75	*mgtA2*	magnesium-importing ATPase	Unclassified
OG1RF_11145	-0.90	-	AraC family transcriptional regulator	Signaling and regulation
OG1RF_11157	-1.54	-	cro/CI family transcriptional regulator	Signaling and regulation
OG1RF_11164	-1.04	-	VanZ/RDD domain protein	Unclassified
OG1RF_11190	1.09	-	hypothetical protein	Hypothetical
OG1RF_11191	1.09	*cvpA*	colicin V production protein CvpA family protein	Unclassified
OG1RF_11193	1.20	*trxA*	thioredoxin	Unclassified
OG1RF_11201	-1.44	*msrA*	ABC superfamily ATP binding cassette transporter, ABC protein	Transport
OG1RF_11207	1.97	*atpF1*	V-type ATPase, subunit F	Metabolism
OG1RF_11208	1.91	*atpI*	proton (H+) or sodium (Na+) translocating V-type ATPase (V-ATPase), subunit I	Metabolism
OG1RF_11209	1.76	*atpK*	proton (H+) or sodium (Na+) translocating V-type ATPase (V-ATPase), subunit K	Metabolism
OG1RF_11210	1.63	*atpE*	proton (H+) or sodium (Na+) translocating V-type ATPase (V-ATPase), subunit E	Metabolism
OG1RF_11211	1.62	*atpC*	proton (H+) or sodium (Na+) translocating V-type ATPase (V-ATPase), subunit C	Metabolism
OG1RF_11212	1.72	*atpF2*	V-type ATP synthase subunit F	Metabolism
OG1RF_11213	1.55	*atpA*	ATP synthase F1 subcomplex subunit alpha	Metabolism
OG1RF_11214	1.39	*atpB*	proton (H+) or sodium (Na+) translocating V-type ATPase (V-ATPase), subunit B	Metabolism
OG1RF_11215	1.54	*atpD*	V-type ATP synthase subunit D	Metabolism
OG1RF_11216	1.34	-	hypothetical protein	Hypothetical
OG1RF_11219	-1.01	-	beta-lactamase	Cell division/cell envelope
OG1RF_11221	-1.34	*lysA*	diaminopimelate decarboxylase	Metabolism
OG1RF_11223	-1.70	-	hypothetical protein	Hypothetical
OG1RF_11230	-2.39	*sacT*	SacPA operon antiterminator	Signaling and regulation
OG1RF_11231	-2.23	*ptsG*	PTS family glucose porter, IICBA component	Transport
OG1RF_11239	2.03	-	transposon family protein	Unclassified
OG1RF_11250	-2.87	-	TetR family transcriptional regulator	Signaling and regulation
OG1RF_11260	-3.22	-	brp/Blh family beta-carotene 15,15'-monooxygenase	Metabolism
OG1RF_11261	-2.45	-	hypothetical protein	Hypothetical
OG1RF_11266	-1.10	*cmk*	cytidylate kinase	Unclassified
OG1RF_11267	-1.16	*rpsA*	30S ribosomal protein S1	Transcription and translation
OG1RF_11288	1.15	*psr*	transcriptional regulator	Signaling and regulation
OG1RF_11290	1.16	-	hypothetical protein	Hypothetical
OG1RF_11291	1.00	-	hypothetical protein	Hypothetical

Supplementary table C2 (*continued*.)				
OG1RF_11298	0.94	*lexA*	repressor lexA	Unclassified
OG1RF_11308	-3.25	-	N-acetyltransferase	Unclassified
OG1RF_11310	-2.00	-	multidrug ABC superfamily ATP binding cassette transporter, ABC protein	Transport
OG1RF_11311	-1.32	-	ABC superfamily ATP binding cassette transporter, ABC/membrane protein	Transport
OG1RF_11314	-2.14	*katA*	catalase	Unclassified
OG1RF_11318	-1.09	*malL2*	oligo-1,6-glucosidase	Unclassified
OG1RF_11322	-1.67	*yckE2*	beta-glucosidase	Unclassified
OG1RF_11323	-1.66	*bglP2*	phosphotransferase system (PTS) beta-glucoside-specific enzyme IIBCA component	Transport
OG1RF_11326	-1.02	-	hypothetical protein	Hypothetical
OG1RF_11329	1.04	*pflB*	formate acetyltransferase	Unclassified
OG1RF_11355	-1.22	*plsY*	acyl-phosphate glycerol 3-phosphate acyltransferase	Unclassified
OG1RF_11384	1.10	-	permease protein	Transport
OG1RF_11400	0.94	*apt*	adenine phosphoribosyltransferase	Unclassified
OG1RF_11442	-2.18	*mdlB*	multidrug ABC superfamily ATP binding cassette transporter, ABC protein	Transport
OG1RF_11443	-1.82	*mdlA*	multidrug ABC superfamily ATP binding cassette transporter, ABC protein	Transport
OG1RF_11457	0.98	*cap4C*	UTP--glucose-1-phosphate uridylyltransferase	Unclassified
OG1RF_11462	2.37	-	hypothetical protein	Hypothetical
OG1RF_11463	2.27	-	PspC domain-containing protein	Unclassified
OG1RF_11464	2.42	-	hypothetical protein	Hypothetical
OG1RF_11485	-1.25	*fabG2*	3-oxoacyl-ACP reductase	Metabolism
OG1RF_11486	-1.00	-	hypothetical protein	Hypothetical
OG1RF_11490	-1.17	*purH*	bifunctional purine biosynthesis protein PurH	Metabolism
OG1RF_11491	-1.45	*purN*	phosphoribosylglycinamide formyltransferase	Metabolism
OG1RF_11493	-1.52	*purF*	amidophosphoribosyltransferase	Metabolism
OG1RF_11494	-1.40	*purL*	phosphoribosylformylglycinamidine synthase	Metabolism
OG1RF_11497	-1.72	*purC*	phosphoribosylaminoimidazolesuccino carboxamide synthase	Metabolism
OG1RF_11498	-1.51	*purK*	phosphoribosylaminoimidazole carboxylase ATPase subunit PurK	Metabolism
OG1RF_11499	-1.67	*purE*	phosphoribosylaminoimidazole carboxylase catalytic subunit PurE	Metabolism
OG1RF_11507	-1.43	-	hypothetical protein	Hypothetical
OG1RF_11523	-1.40	-	LysR family transcriptional regulator	Signaling and regulation
OG1RF_11539	-0.99	-	membrane protein	Unclassified
OG1RF_11542	-1.12	-	ABC superfamily ATP binding cassette transporter, membrane protein	Transport
OG1RF_11562	1.55	-	HD domain-containing protein	Unclassified
OG1RF_11569	1.87	-	integral membrane protein	Unclassified
OG1RF_11573	-1.38	*murC*	UDP-N-acetylmuramate--L-alanine ligase	Cell division/cell envelope
OG1RF_11580	-1.25	*ysxC*	ribosome biogenesis GTP-binding protein YsxC	Transcription and translation
OG1RF_11595	-1.29	-	hypothetical protein	Hypothetical
OG1RF_11599	-1.06	-	GntR family transcriptional regulator	Signaling and regulation

Supplementary table C2 (*continued*.)				
OG1RF_11606	-1.43	-	bicyclomycin resistance protein	Unclassified
OG1RF_11607	-1.06	-	membrane-oligosaccharide glycerophosphotransferase	Metabolism
OG1RF_11631	-1.56	-	putative phosphomethylpyrimidine kinase	Unclassified
OG1RF_11637	0.98	-	RsmE family RNA methyltransferase	Unclassified
OG1RF_11638	1.07	*prmA*	50S ribosomal protein L11 methyltransferase	Transcription and translation
OG1RF_11642	-1.92	-	hypothetical protein	Hypothetical
OG1RF_11656	2.79	-	ABC superfamily ATP binding cassette transporter, permease protein	Transport
OG1RF_11657	2.97	-	ABC superfamily ATP binding cassette transporter, ABC protein	Transport
OG1RF_11660	-1.55	*ndh2*	NADH dehydrogenase	Metabolism
OG1RF_11661	-1.47	*ubiA*	1,4-dihydroxy-2-naphthoate octaprenyltransferase	Unclassified
OG1RF_11662	-0.90	-	putative trans-hexaprenyltranstransferase	Unclassified
OG1RF_11663	-1.93	-	ABC superfamily ATP binding cassette transporter, ABC/membrane protein	Transport
OG1RF_11664	-2.30	-	ABC superfamily ATP binding cassette transporter, ABC/membrane protein	Transport
OG1RF_11665	-1.64	*cydB*	cytochrome D ubiquinol oxidase subunit II	Transport
OG1RF_11666	-1.82	*cydA*	cytochrome D ubiquinol oxidase subunit I	Transport
OG1RF_11671	-1.01	-	hypothetical protein	Hypothetical
OG1RF_11672	-1.09	-	major facilitator family transporter	Transport
OG1RF_11673	-1.87	*trmU*	tRNA (5-methyl aminomethyl-2-thiouridylate)-methyltransferase	Unclassified
OG1RF_11680	-1.36	-	ABC superfamily ATP binding cassette transporter, ABC protein	Transport
OG1RF_11681	-1.38	*hipO2*	aminoacylase	Unclassified
OG1RF_11682	-1.62	-	ABC superfamily ATP binding cassette transporter, binding protein	Transport
OG1RF_11683	-2.15	-	ABC superfamily ATP binding cassette transporter, membrane protein	Transport
OG1RF_11684	-1.91	-	ABC superfamily ATP binding cassette transporter, binding protein	Transport
OG1RF_11694	-1.85	-	ABC superfamily ATP binding cassette transporter, ABC protein	Transport
OG1RF_11695	-1.50	-	hypothetical protein	Hypothetical
OG1RF_11696	1.18	*glmM*	phosphoglucosamine mutase	Unclassified
OG1RF_11697	1.19	-	hypothetical protein	Hypothetical
OG1RF_11698	1.27	-	hypothetical protein	Hypothetical
OG1RF_11717	-1.50	-	transposase	Unclassified
OG1RF_11719	-1.79	*licD*	LicD-like protein	Unclassified
OG1RF_11720	-1.90	-	group 2 glycosyl transferase	Metabolism
OG1RF_11733	1.09	*rfbC*	dTDP-4-dehydrorhamnose 3,5-epimerase	Unclassified
OG1RF_11741	-1.21	-	flavodoxin	Unclassified
OG1RF_11751	2.61	-	hypothetical protein	Hypothetical
OG1RF_11766	2.95	-	multidrug ABC superfamily ATP binding cassette transporter, ABC protein	Transport
OG1RF_11767	3.18	-	ABC superfamily ATP binding cassette transporter, membrane protein	Transport
OG1RF_11793	1.49	*clpB*	chaperone protein ClpB	Protease/ Chaperone
OG1RF_11797	-2.87	*pbuX*	xanthine permease	Metabolism

Supplementary table C2 (*continued*.)				
OG1RF_11798	-3.59	*xpt*	xanthine phosphoribosyltransferase	Metabolism
OG1RF_11803	-3.16	*bolA*	regulator of penicillin-binding proteins and beta-lactamase transcription	Signaling and regulation
OG1RF_11856	0.99	*pgcA*	bifunctional phosphoglucomutase/phosphomanno mutase	Unclassified
OG1RF_11861	-1.64	-	NCS2 family xanthine/uracil permease	Transport
OG1RF_11862	-1.28	*guaD*	guanine deaminase	Unclassified
OG1RF_11875	-1.69	-	acyl-CoA thioester hydrolase	Metabolism
OG1RF_11878	-0.99	*comEC*	competence protein ComEC	Unclassified
OG1RF_11892	1.01	*typA*	GTP-binding protein TypA/BipA	Unclassified
OG1RF_11896	-1.12	-	hypothetical protein	Hypothetical
OG1RF_11903	-1.00	*gcp*	O-sialoglycoprotein endopeptidase	Unclassified
OG1RF_11904	-1.24	*rimI*	ribosomal-protein-alanine acetyltransferase	Unclassified
OG1RF_11905	-1.11	*rimI2*	ribosomal-protein-alanine acetyltransferase	Unclassified
OG1RF_11907	1.40	*pbp4*	penicillin-binding protein 4	Cell division/cell envelope
OG1RF_11922	-1.97	-	M protein trans-acting positive regulator	Signaling and regulation
OG1RF_11923	-1.99	-	hypothetical protein	Hypothetical
OG1RF_11925	-2.24	-	hypothetical protein	Hypothetical
OG1RF_11926	-2.15	-	cro/CI family transcriptional regulator	Signaling and regulation
OG1RF_11927	-2.96	*azlC*	LIV-E family branched-chain amino acid exporter AzlC	Transport
OG1RF_11928	-3.19	*azlD*	LIV-E family branched-chain amino acid exporter AzlD	Transport
OG1RF_11929	1.91	-	hypothetical protein	Hypothetical
OG1RF_11957	1.21	*ygeW*	carbamoyltransferase YgeW	Unclassified
OG1RF_11977	-1.63	*licT2*	transcription antiterminator LicT	Unclassified
OG1RF_11997	1.16	-	GNAT family acetyltransferase	Unclassified
OG1RF_12013	1.29	*opuAA 2*	glycine betaine/L-proline ABC superfamily ATP binding cassette transporter, ABC protein	Transport
OG1RF_12014	1.49	-	glycine betaine/carnitine/choline ABC superfamily ATP binding cassette transporter	Transport
OG1RF_12017	-1.02	-	hypothetical protein	Hypothetical
OG1RF_12018	-1.42	*glxK*	glycerate kinase	Unclassified
OG1RF_12019	-1.49	-	gluconate:H+ symporter family transporter GntP	Transport
OG1RF_12031	-1.75	-	integral membrane protein	Unclassified
OG1RF_12032	-1.18	-	diacylglycerol kinase catalytic domain protein	Unclassified
OG1RF_12049	-1.24	*lmrA*	multidrug resistance ABC transporter ATP-binding and permease	Transport
OG1RF_12063	1.52	*mtnN*	MTA/SAH nucleosidase	Metabolism
OG1RF_12064	1.54	-	hypothetical protein	Hypothetical
OG1RF_12065	1.40	*nudF*	ADP-ribose diphosphatase	Metabolism
OG1RF_12066	1.97	-	hypothetical protein	Hypothetical
OG1RF_12067	1.56	*telA*	tellurite resistance protein	Unclassified
OG1RF_12098	1.04	*mviM*	gfo/Idh/MocA family oxidoreductase	Unclassified
OG1RF_12127	-1.64	*tenA*	thiaminase	Metabolism
OG1RF_12128	-1.42	-	cobalt transporter	Transport
OG1RF_12129	-1.71	-	ABC superfamily ATP binding cassette transporter, ABC protein	Transport
OG1RF_12130	-1.14	-	ABC superfamily ATP binding cassette transporter, membrane protein	Transport
OG1RF_12135	-2.35	*thiD2*	phosphomethylpyrimidine kinase	Unclassified

Supplementary table C2 (*continued*.)				
OG1RF_12136	-1.38	*thiE*	thiamine-phosphate diphosphorylase	Unclassified
OG1RF_12138	-2.19	*thiW*	ThiW protein	Transport
OG1RF_12152	-1.62	-	hypothetical protein	Hypothetical
OG1RF_12158	2.11	*penA*	penicillin-binding protein 2B	Cell division/cell envelope
OG1RF_12184	-1.02	*fabG3*	3-oxoacyl-ACP reductase	Metabolism
OG1RF_12185	-1.17	*fabD*	malonyl-CoA-[acyl-carrier-protein] transacylase	Metabolism
OG1RF_12186	-1.36	*fabK*	enoyl-ACP reductase	Metabolism
OG1RF_12266	1.29	-	transcriptional regulator	Signaling and regulation
OG1RF_12267	4.95	-	permease protein	Transport
OG1RF_12268	5.15	-	ABC superfamily ATP binding cassette transporter, ABC protein	Transport
OG1RF_12269	5.32	-	RND transporter	Transport
OG1RF_12294	-1.22	*pmr1*	P-ATPase superfamily P-type ATPase cation transporter	Transport
OG1RF_12325	-1.04	-	putative lipoprotein	Unclassified
OG1RF_12327	-11.83	*srtA*	sortase SrtA	Unclassified
OG1RF_12332	0.95	*mreD*	rod shape-determining protein MreD	Cell division/cell envelope
OG1RF_12362	1.17	*ftsY*	cell division protein FtsY	Cell division/cell envelope
OG1RF_12380	1.11	*rpmB2*	50S ribosomal protein L28	Transcription and translation
OG1RF_12393	1.19	-	hypothetical protein	Hypothetical
OG1RF_12394	0.86	-	YicC like protein	Unclassified
OG1RF_12395	1.09	-	hypothetical protein	Hypothetical
OG1RF_12420	-1.40	*mscL*	large conductance mechanosensitive channel protein	Transport
OG1RF_12421	-2.39	-	S-layer protein	Surface protein
OG1RF_12422	-1.52	-	S-layer protein	Surface protein
OG1RF_12425	-2.07	*trePP*	glycosyl hydrolase	Metabolism
OG1RF_12426	-1.86	*yvdM*	beta-phosphoglucomutase	Metabolism
OG1RF_12428	-1.58	-	hypothetical protein	Hypothetical
OG1RF_12452	1.76	*ubiD*	UbiD family decarboxylase	Surface protein
OG1RF_12453	1.89	-	WxL domain surface protein	Surface protein
OG1RF_12454	1.74	*ubiD2*	UbiD family decarboxylase	Surface protein
OG1RF_12455	1.73	-	hypothetical protein	Hypothetical
OG1RF_12456	1.78	-	WxL domain surface protein	Surface protein
OG1RF_12460	2.03	*lrgB*	murein hydrolase regulator LrgB	Signaling and regulation
OG1RF_12461	1.61	*lrgA*	murein hydrolase regulator LrgA	Signaling and regulation
OG1RF_12462	-1.11	*lytR*	response regulator	Signaling and regulation
OG1RF_12473	-1.64	-	dihydrouridine synthase	Unclassified
OG1RF_12476	-1.38	-	PTS family fructose/mannitol (fru) porter component IIA	Transport
OG1RF_12478	-1.22	-	PTS family fructose/mannitol (fru) porter component IIC	Transport
OG1RF_12479	-1.23	-	PTS family porter component II	Transport
OG1RF_12480	-1.15	-	DEAH-box family ATP-dependent helicase	Transcription and translation
OG1RF_12484	-1.40	-	hypothetical protein	Hypothetical
OG1RF_12500	1.32	-	cell-envelope associated acid phosphatase	Signaling and regulation
OG1RF_12501	-1.49	-	hypothetical protein	Hypothetical
OG1RF_12523	-1.11	-	hydantoinase/oxoprolinase	Metabolism
OG1RF_12535	1.88	*croR*	response regulator	Signaling and regulation
OG1RF_12536	1.80	*croS*	sensor histidine kinase	Signaling and regulation
OG1RF_12573	-1.52	-	GntR family transcriptional regulator	Signaling and regulation
[#]Manual annotation in red.				

Supplementary Table C3 | RNA-Seq results comparing *ΔsrtA* and *ΔsrtAΔhtrA.*

Genes with significant differences in abundance of mRNAs were determined using a PValue and false discovery rate (FDR) cutoff of 0.05. The LogFC represents the log2 change between biological triplicates of ΔsrtAΔhtrA compared to ΔsrtA when grown to mid-log phase in TSB supplemented with 0.25% glucose.

Locus Tag	LogFC	Gene[#]	Annotation	Manual classification
OG1RF_10024	1.82	-	Hypothetical protein	Hypothetical
OG1RF_10027	1.74	*malY*	Cystathionine beta-lyase	Unclassified
OG1RF_10038	1.17	*dut*	Dutp diphosphatase	Transcription and translation
OG1RF_10039	0.99	*radA*	DNA repair protein rada	DNA repair and recombination
OG1RF_10040	1.25	-	PIN domain-containing protein	Unclassified
OG1RF_10041	1.17	*ispF*	2-C-methyl-D-erythritol 2,4-cyclo diphosphate synthase	Metabolism
OG1RF_10049	1.01	*veg*	Veg protein	Unclassified
OG1RF_10096	-1.17	-	Alpha/beta hydrolase fold family hydrolase	Unclassified
OG1RF_10113	-1.20	-	Cob(I)yrinic acid a,c-diamide adenosyltransferase	Unclassified
OG1RF_10136	-2.71	-	Iron (Fe3+) ABC superfamily ATP binding cassette transporter, binding protein	Transport
OG1RF_10180	-1.80	-	Hypothetical protein	Hypothetical
OG1RF_10181	-1.64	-	M20D family peptidase	Unclassified
OG1RF_10182	-1.45	-	ABC superfamily ATP binding cassette transporter, ABC protein	Transport
OG1RF_10197	1.22	*amiD*	N-acetylmuramoyl-L-alanine amidase	Cell division/cell envelope
OG1RF_10208	1.28	*hpt*	Hypoxanthine phosphoribosyltransferase	Unclassified
OG1RF_10209	1.23	*ftsH*	Cell division protein ftsh	Cell division/cell envelope
OG1RF_10223	-1.30	-	Hypothetical protein	Hypothetical
OG1RF_10224	-1.26	-	Hypothetical protein	Hypothetical
OG1RF_10228	-1.49	*pyrDA*	Dihydroorotate oxidase	Metabolism
OG1RF_10255	-1.21	*lysC*	Aspartate kinase	Unclassified
OG1RF_10317	1.53	*dctM*	TRAP-T family tripartite ATP-independent periplasmic transporter, membrane protein	Transport
OG1RF_10320	1.10	*rhaA*	L-rhamnose isomerase	Unclassified
OG1RF_10353	3.89	-	Lema family protein	Unclassified
OG1RF_10354	3.94	-	Hypothetical protein	Hypothetical
OG1RF_10356	-0.87	*nrdE*	Ribonucleotide-diphosphate reductase subunit alpha	Metabolism
OG1RF_10357	-1.10	*nrdI*	Ribonucleotide-diphosphate reductase subunit gamma	Metabolism
OG1RF_10379	-1.40	-	Phage integrase family site-specific recombinase	DNA repair and recombination
OG1RF_10417	1.08	*pbp2A*	Penicillin-binding protein 2A	Cell division/cell envelope
OG1RF_10423	2.88	*prsA*	Peptidyl-prolyl cis-trans isomerase	Protease/ Chaperone
OG1RF_10432	1.19	-	PTS family fructose porter component IIBC	Transport
OG1RF_10475	-1.27	-	Deoxynucleoside kinase	Unclassified
OG1RF_10476	-1.80	-	Hypothetical protein	Hypothetical
OG1RF_10479	1.03	-	Sodium/dicarboxylate symporter family protein	Transport
OG1RF_10528	-1.65	-	Rrna methylase	Transcription and translation
OG1RF_10529	-1.71	-	Radical SAM protein	Unclassified
OG1RF_10533	-1.22	*lyzl6*	Cell wall lysis protein	Cell division/cell envelope
OG1RF_10589	-1.26	-	Cation efflux family protein	Transport
OG1RF_10590	-1.57	-	APC family amino acid-polyamine-organocation transporter	Transport
OG1RF_10591	-1.17	-	GNAT family acetyltransferase	Unclassified

Supplementary table C3 (*continued*.)				
OG1RF_10596	-1.31	-	Hypothetical protein	Hypothetical
OG1RF_10613	-1.07	-	Hypothetical protein	Hypothetical
OG1RF_10614	-2.25	-	Hypothetical protein	Hypothetical
OG1RF_10615	-2.22	-	Group 2 glycosyl transferase	Metabolism
OG1RF_10616	-2.24	-	Cellulose synthase catalytic subunit	Metabolism
OG1RF_10617	-2.36	-	Hypothetical protein	Hypothetical
OG1RF_10618	-2.29	-	Hypothetical protein	Hypothetical
OG1RF_10626	-2.45	-	Hypothetical protein	Hypothetical
OG1RF_10659	1.37	-	Hypothetical protein	Hypothetical
OG1RF_10672	-1.17	-	GNAT family acetyltransferase	Unclassified
OG1RF_10697	1.42	-	Hypothetical protein	Hypothetical
OG1RF_10707	1.30	-	DNA repair exonuclease	DNA repair and recombination
OG1RF_10721	1.37	*mraZ*	Cell division protein mraz	Cell division/cell envelope
OG1RF_10739	1.14	-	Hypothetical protein	Hypothetical
OG1RF_10764	1.10	-	Phosphorylase	Unclassified
OG1RF_10784	-0.87	*csrS*	Sensor histidine kinase csrs	Signaling and regulation
OG1RF_10792	1.53	-	Cro/CI family transcriptional regulator	Signaling and regulation
OG1RF_10817	-2.01	*malR*	Phage integrase family site-specific recombinase	DNA repair and recombination
OG1RF_10818	-1.98	-	Nitroreductase	Metabolism
OG1RF_10819	-2.15	-	Membrane protein	Unclassified
OG1RF_10820	-1.95	-	Lytr family response regulator	Signaling and regulation
OG1RF_10838	-2.82	-	NRAMP family Mn2+/Fe2+ transporter	Transport
OG1RF_10839	-2.76	-	Universal stress protein	Unclassified
OG1RF_10870	1.46	-	Cell wall surface anchor family protein	Surface protein
OG1RF_10871	1.41	-	Cell wall surface anchor family protein	Surface protein
OG1RF_10875	-2.48	-	Hypothetical protein	Hypothetical
OG1RF_10876	-2.19	-	Hypothetical protein	Hypothetical
OG1RF_10878	1.74	*ace*	Collagen adhesin protein	Surface protein
OG1RF_10881	1.79	-	Hypothetical protein	Hypothetical
OG1RF_10889	1.13	*lepB*	Signal peptidase I lepb	Signaling and regulation
OG1RF_10895	-1.93	*glnP*	Glutamine ABC superfamily ATP binding cassette transporter, membrane protein	Transport
OG1RF_10896	-1.71	*glnM*	Amino acid ABC superfamily ATP binding cassette transporter, membrane protein	Transport
OG1RF_10897	-1.71	*glnH*	Glutamine ABC superfamily ATP binding cassette transporter, binding protein	Transport
OG1RF_10898	-1.45	*glnQ*	ABC superfamily ATP binding cassette transporter, ABC protein	Transport
OG1RF_10922	-1.71	-	Hypothetical protein	Hypothetical
OG1RF_10949	-1.33	-	Hypothetical protein	Hypothetical
OG1RF_10952	1.39	-	Hypothetical protein	Hypothetical
OG1RF_10953	-1.36	-	Oxygen-insensitive NADPH nitroreductase	Metabolism
OG1RF_10975	1.02	-	Crossover junction endodeoxyribonuclease	DNA repair and recombination
OG1RF_10976	0.95	-	Hypothetical protein	Hypothetical
OG1RF_11000	1.68	-	M protein trans-acting positive regulator	Signaling and regulation
OG1RF_11001	1.81	-	Hypothetical protein	Hypothetical
OG1RF_11005	1.07	-	ABC superfamily ATP binding cassette transporter, substrate-binding protein	Transport
OG1RF_11031	3.34	-	Hypothetical protein	Hypothetical
OG1RF_11032	3.45	-	Hypothetical protein	Hypothetical
OG1RF_11045	-1.55	-	Hypothetical protein	Hypothetical
OG1RF_11046	-1.31	-	Hypothetical protein	Phage
OG1RF_11047	-1.29	-	Cro/CI family transcriptional regulator	Phage
OG1RF_11048	-2.02	-	Hypothetical protein	Phage

Supplementary table C3 (*continued*.)				
OG1RF_11049	-2.36	-	DNA replication protein	Phage
OG1RF_11050	-2.27	-	DNA replication protein	Phage
OG1RF_11051	-2.29	-	Hypothetical protein	Phage
OG1RF_11052	-2.58	-	Rina family transcriptional regulator	Phage
OG1RF_11053	-3.29	-	Transposase	Phage
OG1RF_11054	-3.58	-	Hypothetical protein	Phage
OG1RF_11055	-3.52	-	TP901-1 family phage major tail protein	Phage
OG1RF_11056	-3.46	-	Hypothetical protein	Phage
OG1RF_11057	-3.67	-	Hypothetical protein	Phage
OG1RF_11058	-3.73	-	ABC superfamily ATP binding cassette transporter permease subunit	Phage
OG1RF_11059	-3.85	-	Phage tail protein	Phage
OG1RF_11060	-3.88	-	Phage structural protein	Phage
OG1RF_11061	-3.87	-	Hypothetical protein	Phage
OG1RF_11062	-3.75	-	Holin	Phage
OG1RF_11063	-4.11	*amiD2*	N-acetylmuramoyl-L-alanine amidase	Phage
OG1RF_11064	-1.00	*truB*	Trna pseudouridine synthase B	Metabolism
OG1RF_11065	-1.09	*ribF*	Riboflavin biosynthesis protein ribf	Metabolism
OG1RF_11066	-0.99	-	GNAT family acetyltransferase	Unclassified
OG1RF_11067	-1.64	-	Padr family transcriptional regulator	Signaling and regulation
OG1RF_11068	-2.29	-	Hypothetical protein	Hypothetical
OG1RF_11069	-1.41	-	Putative transcriptional regulator	Signaling and regulation
OG1RF_11070	-3.78	*ftsW*	Ftsw/roda/spove family cell division protein	Cell division/cell envelope
OG1RF_11071	-3.40	*rodA*	Ftsw/roda/spove family cell division protein	Cell division/cell envelope
OG1RF_11075	-0.99	*hemN*	Coproporphyrinogen dehydrogenase	Metabolism
OG1RF_11076	1.38	*hrcA*	Heat-inducible transcription repressor hrca	Unclassified
OG1RF_11077	1.21	*grpE*	Co-chaperone grpe	Unclassified
OG1RF_11078	1.21	*dnaK*	Chaperone dnak	Unclassified
OG1RF_11086	-1.48	-	Hypothetical protein	Hypothetical
OG1RF_11150	-1.17	-	Hypothetical protein	Hypothetical
OG1RF_11157	-1.56	-	Cro/CI family transcriptional regulator	Signaling and regulation
OG1RF_11200	1.85	-	Hypothetical protein	Hypothetical
OG1RF_11207	1.71	*atpF1*	V-type atpase, subunit F	Metabolism
OG1RF_11208	1.69	*atpI*	Proton (H+) or sodium (Na+) translocating V-type atpase (V-atpase), subunit I	Metabolism
OG1RF_11209	1.55	*atpK*	Proton (H+) or sodium (Na+) translocating V-type atpase (V-atpase), subunit K	Metabolism
OG1RF_11210	1.36	*atpE*	Proton (H+) or sodium (Na+) translocating V-type atpase (V-atpase), subunit E	Metabolism
OG1RF_11211	1.39	*atpC*	Proton (H+) or sodium (Na+) translocating V-type atpase (V-atpase), subunit C	Metabolism
OG1RF_11212	1.36	*atpF2*	V-type ATP synthase subunit F	Metabolism
OG1RF_11213	1.34	*atpA*	ATP synthase F1 subcomplex subunit alpha	Metabolism
OG1RF_11214	1.21	*atpB*	Proton (H+) or sodium (Na+) translocating V-type atpase (V-atpase), subunit B	Metabolism
OG1RF_11215	1.23	*atpD*	V-type ATP synthase subunit D	Metabolism
OG1RF_11216	1.17	-	Hypothetical protein	Hypothetical
OG1RF_11219	-1.05	-	Beta-lactamase	Cell division/cell envelope
OG1RF_11221	-1.58	*lysA*	Diaminopimelate decarboxylase	Metabolism
OG1RF_11230	-1.98	*sacT*	Sacpa operon anti-terminator	Signaling and regulation
OG1RF_11231	-1.91	*ptsG*	PTS family glucose porter, IICBA component	Transport

Supplementary table C3 (*continued*.)				
OG1RF_11236	1.36	-	PTS system transporter subunit IIC	Transport
OG1RF_11239	1.80	-	Transposon family protein	Unclassified
OG1RF_11260	-3.11	-	Brp/Blh family beta-carotene 15,15'-monooxygenase	Metabolism
OG1RF_11261	-2.09	-	Hypothetical protein	Hypothetical
OG1RF_11308	-1.63	-	N-acetyltransferase	Unclassified
OG1RF_11329	1.13	*pflB*	Formate acetyltransferase	Unclassified
OG1RF_11373	1.92	*lpd2*	Dihydrolipoyl dehydrogenase	Unclassified
OG1RF_11384	1.73	-	Permease protein	Transport
OG1RF_11385	1.96	-	ABC superfamily ATP binding cassette transporter, ABC protein	Transport
OG1RF_11442	-1.57	*mdlB*	Multidrug ABC superfamily ATP binding cassette transporter, ABC protein	Transport
OG1RF_11443	-1.25	*mdlA*	Multidrug ABC superfamily ATP binding cassette transporter, ABC protein	Transport
OG1RF_11462	3.52	-	Hypothetical protein	Hypothetical
OG1RF_11463	3.48	-	Pspc domain-containing protein	Unclassified
OG1RF_11464	3.69	-	Hypothetical protein	Hypothetical
OG1RF_11485	-1.25	*fabG2*	3-oxoacyl-ACP reductase	Metabolism
OG1RF_11488	-1.54	-	Hypothetical protein	Hypothetical
OG1RF_11490	-1.12	*purH*	Bifunctional purine biosynthesis protein purh	Metabolism
OG1RF_11511	1.65	-	PTS system mannose/fructose/sorbose transporter subunit IID	Transport
OG1RF_11523	-1.45	-	Lysr family transcriptional regulator	Signaling and regulation
OG1RF_11524	-1.03	-	Hypothetical protein	Hypothetical
OG1RF_11525	-2.40	*sprE*	Spre protein	Signaling and regulation
OG1RF_11526	-2.38	*gelE*	Gelatinase	Signaling and regulation
OG1RF_11527	-1.72	*fsrC*	Sensor histidine kinase fsrc	Signaling and regulation
OG1RF_11528	-1.57	*fsrB*	Fsrb protein	Signaling and regulation
OG1RF_11529	-1.85	*fsrA*	Fsra response regulator	Signaling and regulation
OG1RF_11569	2.11	-	Integral membrane protein	Unclassified
OG1RF_11573	-1.48	*murC*	UDP-N-acetylmuramate--L-alanine ligase	Cell division/cell envelope
OG1RF_11586	-1.03	-	Transcriptional regulator	Signaling and regulation
OG1RF_11593	-0.97	-	M protein trans-acting positive regulator	Signaling and regulation
OG1RF_11594	-1.06	-	Pyridine nucleotide-disulfide family oxidoreductase	Unclassified
OG1RF_11601	-1.15	-	GNAT family acetyltransferase	Unclassified
OG1RF_11606	-1.14	-	Bicyclomycin resistance protein	Unclassified
OG1RF_11607	-1.26	-	Membrane-oligosaccharide glycerophosphotransferase	Metabolism
OG1RF_11656	2.43	-	ABC superfamily ATP binding cassette transporter, permease protein	Transport
OG1RF_11657	2.64	-	ABC superfamily ATP binding cassette transporter, ABC protein	Transport
OG1RF_11663	-1.71	-	ABC superfamily ATP binding cassette transporter, ABC/membrane protein	Transport
OG1RF_11664	-2.00	-	ABC superfamily ATP binding cassette transporter, ABC/membrane protein	Transport
OG1RF_11671	-1.02	-	Hypothetical protein	Hypothetical
OG1RF_11672	-0.97	-	Major facilitator family transporter	Transport
OG1RF_11677	-2.14	-	ABC superfamily ATP binding cassette transporter, ABC protein	Transport
OG1RF_11678	-2.62	-	ABC superfamily ATP binding cassette transporter, membrane protein	Transport

Supplementary table C3 (*continued*.)				
OG1RF_11679	-2.82	-	ABC superfamily ATP binding cassette transporter, binding protein	Transport
OG1RF_11680	-0.98	-	ABC superfamily ATP binding cassette transporter, ABC protein	Transport
OG1RF_11681	-1.21	*hipO2*	Aminoacylase	Unclassified
OG1RF_11683	-1.58	-	ABC superfamily ATP binding cassette transporter, membrane protein	Transport
OG1RF_11684	-1.50	-	ABC superfamily ATP binding cassette transporter, binding protein	Transport
OG1RF_11694	-1.70	-	ABC superfamily ATP binding cassette transporter, ABC protein	Transport
OG1RF_11695	-1.46	-	Hypothetical protein	Hypothetical
OG1RF_11720	-1.34	-	Group 2 glycosyl transferase	Metabolism
OG1RF_11751	2.27	-	Hypothetical protein	Hypothetical
OG1RF_11752	-1.29	-	Hypothetical protein	Hypothetical
OG1RF_11766	2.97	-	Multidrug ABC superfamily ATP binding cassette transporter, ABC protein	Transport
OG1RF_11767	3.24	-	ABC superfamily ATP binding cassette transporter, membrane protein	Transport
OG1RF_11782	1.43	*iolE*	Myo-inositol catabolism protein iole	Unclassified
OG1RF_11793	1.89	*clpB*	Chaperone protein clpb	Protease/ Chaperone
OG1RF_11797	-2.13	*pbuX*	Xanthine permease	Metabolism
OG1RF_11798	-2.66	*xpt*	Xanthine phosphoribosyltransferase	Metabolism
OG1RF_11861	-1.31	-	NCS2 family xanthine/uracil permease	Transport
OG1RF_11875	-1.54	-	Acyl-coa thioester hydrolase	Metabolism
OG1RF_11903	-1.04	*gcp*	O-sialoglycoprotein endopeptidase	Unclassified
OG1RF_11904	-1.36	*rimI*	Ribosomal-protein-alanine acetyltransferase	Unclassified
OG1RF_11905	-1.36	*rimI2*	Ribosomal-protein-alanine acetyltransferase	Unclassified
OG1RF_11922	-1.48	-	M protein trans-acting positive regulator	Signaling and regulation
OG1RF_11923	-1.59	-	Hypothetical protein	Hypothetical
OG1RF_11925	-2.39	-	Hypothetical protein	Hypothetical
OG1RF_11926	-2.31	-	Cro/CI family transcriptional regulator	Signaling and regulation
OG1RF_11927	-3.30	*azlC*	LIV-E family branched-chain amino acid exporter azlc	Transport
OG1RF_11928	-3.58	*azlD*	LIV-E family branched-chain amino acid exporter azld	Transport
OG1RF_11929	1.42	-	Hypothetical protein	Hypothetical
OG1RF_11949	1.37	-	Putative cysteine desulfurase	Unclassified
OG1RF_11957	1.40	*ygeW*	Carbamoyltransferase ygew	Unclassified
OG1RF_11969	-1.28	*ampC*	Beta-lactamase	Cell division/cell envelope
OG1RF_11970	-1.32	-	Glyoxalase	Unclassified
OG1RF_11997	1.35	-	GNAT family acetyltransferase	Unclassified
OG1RF_11999	1.38	-	P-atpase superfamily P-type atpase cadmium transporter	Transport
OG1RF_12031	-2.06	-	Integral membrane protein	Unclassified
OG1RF_12063	1.36	*mtnN*	MTA/SAH nucleosidase	Metabolism
OG1RF_12064	1.17	-	Hypothetical protein	Hypothetical
OG1RF_12065	1.30	*nudF*	ADP-ribose diphosphatase	Metabolism
OG1RF_12066	2.25	-	Hypothetical protein	Hypothetical
OG1RF_12067	1.69	*telA*	Tellurite resistance protein	Unclassified
OG1RF_12102	1.25	*trxB2*	Thioredoxin-disulfide reductase	Unclassified
OG1RF_12127	-1.53	*tenA*	Thiaminase	Metabolism
OG1RF_12128	-1.35	-	Cobalt transporter	Transport

Supplementary table C3 (*continued*.)				
OG1RF_12129	-1.58	-	ABC superfamily ATP binding cassette transporter, ABC protein	Transport
OG1RF_12130	-1.07	-	ABC superfamily ATP binding cassette transporter, membrane protein	Transport
OG1RF_12152	-1.15	-	hypothetical protein	Hypothetical
OG1RF_12158	1.46	*penA*	penicillin-binding protein 2B	Cell division/cell envelope
OG1RF_12225	-1.13	*cspA3*	cold shock protein CspA	Unclassified
OG1RF_12267	4.07	-	permease protein	Transport
OG1RF_12268	4.50	-	ABC superfamily ATP binding cassette transporter, ABC protein	Transport
OG1RF_12269	4.56	-	RND transporter	Transport
OG1RF_12289	2.00	-	hypothetical protein	Hypothetical
OG1RF_12294	-1.13	*pmr1*	P-ATPase superfamily P-type ATPase cation transporter	Transport
OG1RF_12305	-8.19	*htrA*	serine protease HtrA	Unclassified
OG1RF_12325	-1.40	-	putative lipoprotein	Unclassified
OG1RF_12328	1.14	-	hypothetical protein	Hypothetical
OG1RF_12332	1.04	*mreD*	rod shape-determining protein MreD	Cell division/cell envelope
OG1RF_12333	0.98	*mreC*	rod shape-determining protein MreC	Cell division/cell envelope
OG1RF_12350	-1.17	-	oligopeptide ABC superfamily ATP binding cassette transporter, binding protein	Transport
OG1RF_12351	-1.52	-	ferric (Fe+3) ABC superfamily ATP binding cassette transporter, binding protein	Transport
OG1RF_12352	-1.46	-	ABC superfamily ATP binding cassette transporter, ABC protein	Transport
OG1RF_12353	-1.43	-	ferric (Fe+3) ABC superfamily ATP binding cassette transporter, membrane protein	Transport
OG1RF_12354	-1.12	-	ABC superfamily ATP binding cassette transporter, membrane protein	Transport
OG1RF_12380	1.06	*rpmB2*	50S ribosomal protein L28	Transcription and translation
OG1RF_12421	-1.77	-	S-layer protein	Surface protein
OG1RF_12425	-2.70	*trePP*	glycosyl hydrolase	Metabolism
OG1RF_12426	-2.69	*yvdM*	beta-phosphoglucomutase	Metabolism
OG1RF_12441	-1.21	-	hypothetical protein	Hypothetical
OG1RF_12453	1.25	-	WxL domain surface protein	Surface protein
OG1RF_12455	1.26	-	hypothetical protein	Hypothetical
OG1RF_12456	1.23	-	WxL domain surface protein	Surface protein
OG1RF_12460	1.70	*lrgB*	murein hydrolase regulator LrgB	Signaling and regulation
OG1RF_12461	1.61	*lrgA*	murein hydrolase regulator LrgA	Signaling and regulation
OG1RF_12480	-1.06	-	DEAH-box family ATP-dependent helicase	Transcription and translation
OG1RF_12484	-1.14	-	hypothetical protein	Hypothetical
OG1RF_12485	-1.01	-	phosphatidylglycerol--membrane-oligosaccharide glycerophosphotransferase	Unclassified
OG1RF_12523	-1.10	-	hydantoinase/oxoprolinase	Metabolism
OG1RF_12535	1.18	*croR*	response regulator	Signaling and regulation
OG1RF_12536	1.09	*croS*	sensor histidine kinase	Signaling and regulation
#Manual annotation in red.				

Supplementary Table C4 | RNA-Seq results comparing *croR::TnΔsrtAΔhtrA* and *ΔsrtAΔhtrA.*

Genes with significant differences in abundance of mRNAs were determined using a P-Value and false discovery rate (FDR) cutoff of 0.05. The LogFC represents the log2 change between biological triplicates of *croR::TnΔsrtAΔhtrA* and *ΔsrtAΔhtrA* when grown to mid-log phase in TSB supplemented with 0.25% glucose.

Locus Tag	LogFC	Gene	Annotation	Manual classification
OG1RF_10019	-0.71	*manX2*	PTS system mannose transporter subunit IIAB	Transport
OG1RF_10020	-0.63	*manY*	PTS family mannose/fructose/sorbose porter component IIC	Transport
OG1RF_10029	1.03	-	Hypothetical protein	Hypothetical
OG1RF_10054	1.28	*purR*	Purine operon repressor	Signaling and regulation
OG1RF_10090	-1.59	-	Putative lipoprotein	Unclassified
OG1RF_10095	-2.86	*serS*	Serine--trna ligase	Transcription and translation
OG1RF_10099	-4.33	*arcA*	Arginine deiminase	Unclassified
OG1RF_10100	-2.32	*arcB*	Ornithine carbamoyltransferase	Unclassified
OG1RF_10133	-0.67	*deoB*	Phosphopentomutase	Metabolism
OG1RF_10134	-0.74	*deoD*	Purine-nucleoside phosphorylase	Metabolism
OG1RF_10148	1.39	*thiD*	Phosphomethylpyrimidine kinase	Unclassified
OG1RF_10172	0.54	*adk*	Adenylate kinase	Metabolism
OG1RF_10180	2.18	-	Hypothetical protein	Hypothetical
OG1RF_10181	1.81	-	M20D family peptidase	Unclassified
OG1RF_10187	1.26	*brnQ*	LIVCS family branched-chain amino acid: cation symporter	Transport
OG1RF_10192	1.37	-	Hypothetical protein	Hypothetical
OG1RF_10210	1.23	*hslO*	Chaperonin hslo	Protease/Chaperone
OG1RF_10211	1.53	*dus*	Trna-dihydrouridine synthase	Unclassified
OG1RF_10213	2.03	*licT*	Transcription anti-terminator lict	Transcription and translation
OG1RF_10228	0.97	*pyrDA*	Dihydroorotate oxidase	Metabolism
OG1RF_10232	0.68	*srpG*	Cysteine synthase	Metabolism
OG1RF_10269	-0.94	-	Hypothetical protein	Hypothetical
OG1RF_10270	-0.89	-	Hypothetical protein	Hypothetical
OG1RF_10282	1.10	-	Vitamin-B12 independent methionine synthase	Metabolism
OG1RF_10286	0.94	-	Membrane protein	Unclassified
OG1RF_10288	2.51	*nhaC*	Na+/H+ antiporter nhac	Metabolism
OG1RF_10293	0.92	-	Mannitol operon transcriptional anti-terminator	Unclassified
OG1RF_10349	1.15	*dapF*	Diaminopimelate epimerase	Unclassified
OG1RF_10353	-1.19	-	Lema family protein	Unclassified
OG1RF_10382	0.92	-	Hypothetical protein	Hypothetical
OG1RF_10391	1.95	-	MATE efflux family protein	Metabolism
OG1RF_10421	-0.96	-	Hypothetical protein	Hypothetical
OG1RF_10429	0.84	*trmB*	Trna (guanine-N (7)-)-methyltransferase	Unclassified
OG1RF_10481	-3.35	*pbp5*	Beta-lactamase	Cell division/cell envelope
OG1RF_10485	1.32	-	Cell wall surface anchor family protein	Surface protein
OG1RF_10495	1.17	*glnQ*	ABC superfamily ATP binding cassette transporter, ABC protein	Transport
OG1RF_10496	0.97	*glnP*	Amino acid ABC superfamily ATP binding cassette transporter, binding/permease protein	Transport
OG1RF_10497	-1.07	*uvrB*	Excision endonuclease subunit uvrb	DNA repair and recombination
OG1RF_10516	-1.08	-	Acyltransferase	Unclassified
OG1RF_10530	1.01	-	Type 2 phosphatidic acid phosphatase	Unclassified
OG1RF_10590	1.53	-	APC family amino acid-polyamine-organocation transporter	Transport

Supplementary table C4 (*continued*.)				
OG1RF_10601	1.50	-	potassium uptake protein	Metabolism
OG1RF_10613	1.25	-	hypothetical protein	Hypothetical
OG1RF_10614	1.44	-	hypothetical protein	Hypothetical
OG1RF_10616	0.96	-	cellulose synthase catalytic subunit	Metabolism
OG1RF_10626	1.44	-	hypothetical protein	Hypothetical
OG1RF_10627	-2.51	*aad*	aldehyde-alcohol dehydrogenase	Metabolism
OG1RF_10655	1.00	-	glucose uptake protein	Metabolism
OG1RF_10656	1.26	-	amino acid permease	transport
OG1RF_10660	-1.04	*rep*	ATP-dependent DNA helicase	DNA repair and recombination
OG1RF_10667	1.19	-	hypothetical protein	Hypothetical
OG1RF_10672	1.49	-	GNAT family acetyltransferase	Unclassified
OG1RF_10674	-0.60	*ppx2*	exopolyphosphatase	Unclassified
OG1RF_10707	-2.90	-	DNA repair exonuclease	DNA repair and recombination
OG1RF_10712	0.65	*folD*	bifunctional methylenetetrahydrofolate dehydrogenase/methylenetetrahydrofolate cyclohydrolase	Unclassified
OG1RF_10718	0.94	*recN*	DNA repair protein RecN	DNA repair and recombination
OG1RF_10722	-0.93	*mraW*	S-adenosyl-methyltransferase MraW	Unclassified
OG1RF_10723	-1.88	-	cell division protein	Cell division/cell envelope
OG1RF_10740	-1.07	*sfsA*	sugar fermentation stimulation protein	Metabolism
OG1RF_10752	-2.16	-	PTS family lactose/cellobiose (lac) porter component IIC	Transport
OG1RF_10754	-1.14	-	GNAT family acetyltransferase	Unclassified
OG1RF_10765	-0.90	*drrC*	daunorubicin resistance protein	Unclassified
OG1RF_10766	-1.98	-	6-aminohexanoate hydrolase	Unclassified
OG1RF_10772	-0.73	-	cof family protein	Unclassified
OG1RF_10774	1.68	-	xanthine/uracil permease family protein	Transport
OG1RF_10784	1.17	*csrS*	sensor histidine kinase CsrS	Signaling and regulation
OG1RF_10858	2.25	-	MFS family major facilitator transporter	Transport
OG1RF_10875	1.45	-	hypothetical protein	Hypothetical
OG1RF_10876	1.76	-	hypothetical protein	Hypothetical
OG1RF_10895	1.71	*glnP*	glutamine ABC superfamily ATP binding cassette transporter, membrane protein	Transport
OG1RF_10897	1.44	*glnH*	glutamine ABC superfamily ATP binding cassette transporter, binding protein	Transport
OG1RF_10898	1.78	*glnQ*	ABC superfamily ATP binding cassette transporter, ABC protein	Transport
OG1RF_10926	-0.82	*recU*	recombination protein U	DNA repair and recombination
OG1RF_10932	0.75	*nth*	endonuclease III	DNA repair and recombination
OG1RF_10953	1.28	-	oxygen-insensitive NADPH nitroreductase	Metabolism
OG1RF_10965	-0.85	-	response regulator	Signaling and regulation
OG1RF_10966	-0.58	-	sensor histidine kinase	Signaling and regulation
OG1RF_10967	-0.61	-	hypothetical protein	Hypothetical
OG1RF_10968	-0.64	-	hypothetical protein	Hypothetical
OG1RF_10972	1.53	-	hypothetical protein	Hypothetical
OG1RF_10973	1.21	-	hypothetical protein	Hypothetical
OG1RF_10987	1.09	-	hypothetical protein	Hypothetical
OG1RF_10994	2.33	*ade*	adenine deaminase	Unclassified
OG1RF_10995	2.72	*mtaD*	putative S-adenosylhomocysteine deaminase	Unclassified
OG1RF_11014	0.74	*yckE*	beta-glucosidase	Metabolism

Supplementary table C4 (*continued*.)				
OG1RF_11020	-0.72	-	hypothetical protein	Hypothetical
OG1RF_11033	-1.04	-	sulfatase	Unclassified
OG1RF_11036	-0.90	*ftsW*	E1-E2 family cation-transporting ATPase	Metabolism
OG1RF_11071	2.94	*rodA*	FtsW/RodA/SpovE family cell division protein	Cell division/cell envelope
OG1RF_11073	-2.62	-	LysR family transcriptional regulator	Signaling and regulation
OG1RF_11083	-0.79	*yhgF*	YhgF like protein	Unclassified
OG1RF_11140	-0.81	*mgtA2*	magnesium-importing ATPase	Unclassified
OG1RF_11153	1.05	-	membrane protein	Unclassified
OG1RF_11154	0.95	-	integral membrane protein	Unclassified
OG1RF_11158	1.29	-	MFS family drug resistance transporter	Transport
OG1RF_11164	0.93	-	VanZ/RDD domain protein	Unclassified
OG1RF_11172	0.79	-	hypothetical protein	Hypothetical
OG1RF_11190	-0.85	-	hypothetical protein	Hypothetical
OG1RF_11207	-1.39	*atpF1*	V-type ATPase, subunit F	Metabolism
OG1RF_11208	-0.65	*atpI*	proton (H+) or sodium (Na+) translocating V-type ATPase (V-ATPase), subunit I	Metabolism
OG1RF_11210	-1.34	*atpE*	proton (H+) or sodium (Na+) translocating V-type ATPase (V-ATPase), subunit E	Metabolism
OG1RF_11211	-0.76	*atpC*	proton (H+) or sodium (Na+) translocating V-type ATPase (V-ATPase), subunit C	Metabolism
OG1RF_11213	-0.98	*atpA*	ATP synthase F1 subcomplex subunit alpha	Metabolism
OG1RF_11214	-1.04	*atpB*	proton (H+) or sodium (Na+) translocating V-type ATPase (V-ATPase), subunit B	Metabolism
OG1RF_11215	-0.83	*atpD*	V-type ATP synthase subunit D	Metabolism
OG1RF_11216	-0.76	-	hypothetical protein	Hypothetical
OG1RF_11219	0.83	-	beta-lactamase	Cell division/cell envelope
OG1RF_11221	1.54	*lysA*	diaminopimelate decarboxylase	Metabolism
OG1RF_11230	1.14	*sacT*	SacPA operon anti-terminator	Signaling and regulation
OG1RF_11231	1.01	*ptsG*	PTS family glucose porter, IICBA component	Transport
OG1RF_11239	-2.50	-	transposon family protein	Unclassified
OG1RF_11253	-0.70	*tig2*	peptidyl-prolyl isomerase	Unclassified
OG1RF_11261	1.05	-	hypothetical protein	Hypothetical
OG1RF_11265	-0.82	-	LysM domain-containing protein	Transport
OG1RF_11266	1.00	*cmk*	cytidylate kinase	Unclassified
OG1RF_11267	0.79	*rpsA*	30S ribosomal protein S1	Transcription and translation
OG1RF_11268	0.63	*engA*	ribosome-associated GTPase EngA	Transcription and translation
OG1RF_11280	0.80	*aroE*	shikimate dehydrogenase	Metabolism
OG1RF_11281	1.10	*aroF*	phospho-2-dehydro-3-deoxyheptonate aldolase	Metabolism
OG1RF_11283	1.01	*aroC*	chorismate synthase	Metabolism
OG1RF_11284	0.70	*tyrA*	prephenate dehydrogenase	Metabolism
OG1RF_11287	0.88	*pheA*	prephenate dehydratase	Unclassified
OG1RF_11288	-0.57	*psr*	transcriptional regulator	Signaling and regulation
OG1RF_11293	0.65	-	CPA1 family monovalent cation:proton (H+) antiporter-1	Transport
OG1RF_11305	1.09	*ndh*	NADH dehydrogenase	Metabolism
OG1RF_11307	2.12	-	GNAT family acetyltransferase	Unclassified
OG1RF_11308	3.04	-	N-acetyltransferase	Unclassified
OG1RF_11310	1.49	-	multidrug ABC superfamily ATP binding cassette transporter, ABC protein	Transport
OG1RF_11314	1.14	*katA*	catalase	Unclassified

Supplementary table C4 (*continued*.)				
OG1RF_11326	1.19	-	hypothetical protein	Hypothetical
OG1RF_11355	0.82	*plsY*	acyl-phosphate glycerol 3-phosphate acyltransferase	Unclassified
OG1RF_11442	1.61	*mdlB*	multidrug ABC superfamily ATP binding cassette transporter, ABC protein	Transport
OG1RF_11443	1.31	*mdlA*	multidrug ABC superfamily ATP binding cassette transporter, ABC protein	Transport
OG1RF_11464	-1.16	-	hypothetical protein	Hypothetical
OG1RF_11485	1.21	*fabG2*	3-oxoacyl-ACP reductase	Metabolism
OG1RF_11486	0.94	-	hypothetical protein	Hypothetical
OG1RF_11489	1.69	*purD*	phosphoribosylamine--glycine ligase	Metabolism
OG1RF_11494	1.58	*purL*	phosphoribosylformylglycinamidine synthase	Metabolism
OG1RF_11504	0.78	*ilvE*	branched-chain-amino-acid transaminase	Unclassified
OG1RF_11507	1.11	-	hypothetical protein	Hypothetical
OG1RF_11523	1.40	-	LysR family transcriptional regulator	Signaling and regulation
OG1RF_11525	1.28	*sprE*	SprE protein	Signaling and regulation
OG1RF_11526	1.13	*gelE*	gelatinase	Signaling and regulation
OG1RF_11527	1.81	*fsrC*	sensor histidine kinase FsrC	Signaling and regulation
OG1RF_11528	1.51	*fsrB*	FsrB protein	Signaling and regulation
OG1RF_11573	0.68	*murC*	UDP-N-acetylmuramate--L-alanine ligase	Cell division/cell envelope
OG1RF_11605	1.41	-	hypothetical protein	Hypothetical
OG1RF_11606	1.08	-	bicyclomycin resistance protein	Unclassified
OG1RF_11624	0.78	*tpiA*	triose-phosphate isomerase	Unclassified
OG1RF_11625	0.67	*pgk*	phosphoglycerate kinase	Metabolism
OG1RF_11628	0.88	-	YitT family protein	Unclassified
OG1RF_11630	1.66	-	hypothetical protein	Hypothetical
OG1RF_11631	1.56	-	putative phosphomethylpyrimidine kinase	Unclassified
OG1RF_11641	-1.24	*rarA*	replication-associated recombination protein A	DNA repair and recombination
OG1RF_11653	1.34	-	amino acid permease	Transport
OG1RF_11656	-1.17	-	ABC superfamily ATP binding cassette transporter, permease protein	Transport
OG1RF_11657	-1.50	-	ABC superfamily ATP binding cassette transporter, ABC protein	Transport
OG1RF_11663	1.71	-	ABC superfamily ATP binding cassette transporter, ABC/membrane protein	Transport
OG1RF_11664	1.63	-	ABC superfamily ATP binding cassette transporter, ABC/membrane protein	Transport
OG1RF_11665	1.06	*cydB*	cytochrome D ubiquinol oxidase subunit II	Transport
OG1RF_11666	1.04	*cydA*	cytochrome D ubiquinol oxidase subunit I	Transport
OG1RF_11673	0.72	*trmU*	tRNA (5-methyl aminomethyl-2-thiouridylate)-methyltransferase	Unclassified
OG1RF_11693	1.43	-	cobalt (Co2+) ABC superfamily ATP binding cassette transporter, membrane protein	Transport
OG1RF_11694	1.07	-	ABC superfamily ATP binding cassette transporter, ABC protein	Transport
OG1RF_11695	1.39	-	hypothetical protein	Hypothetical
OG1RF_11697	-0.83	-	hypothetical protein	Hypothetical
OG1RF_11722	0.71	-	hypothetical protein	Hypothetical
OG1RF_11723	0.76	-	brp/Blh family beta-carotene 15,15'-monooxygenase	Unclassified

Supplementary table C4 (*continued*.)				
OG1RF_11732	-0.64	*rmlB*	dTDP glucose 4,6-dehydratase	Metabolism
OG1RF_11733	-0.79	*rfbC*	dTDP-4-dehydrorhamnose 3,5-epimerase	Unclassified
OG1RF_11748	-1.07	*phzF2*	phenazine biosynthesis protein PhzF family protein	Unclassified
OG1RF_11753	2.34	*treB*	PTS family trehalose porter, IIBC component	Transport
OG1RF_11766	-4.54	-	multidrug ABC superfamily ATP binding cassette transporter, ABC protein	Transport
OG1RF_11767	-3.37	-	ABC superfamily ATP binding cassette transporter, membrane protein	Transport
OG1RF_11793	-1.45	*clpB*	chaperone protein ClpB	Protease/ Chaperone
OG1RF_11797	3.82	*pbuX*	xanthine permease	Metabolism
OG1RF_11798	3.81	*xpt*	xanthine phosphoribosyltransferase	Metabolism
OG1RF_11860	1.16	*guaC*	GMP reductase	Unclassified
OG1RF_11892	-0.69	*typA*	GTP-binding protein TypA/BipA	Unclassified
OG1RF_11903	0.86	*gcp*	O-sialoglycoprotein endopeptidase	Unclassified
OG1RF_11904	0.72	*rimI*	ribosomal-protein-alanine acetyltransferase	Unclassified
OG1RF_11907	-0.83	*pbp4*	penicillin-binding protein 4	Cell division/cell envelope
OG1RF_11922	2.26	-	M protein trans-acting positive regulator	Signaling and regulation
OG1RF_11923	1.71	-	hypothetical protein	Hypothetical
OG1RF_11925	1.41	-	hypothetical protein	Hypothetical
OG1RF_11926	1.26	-	cro/CI family transcriptional regulator	Signaling and regulation
OG1RF_11931	0.97	*upp2*	uracil phosphoribosyltransferase	Unclassified
OG1RF_11977	2.29	*licT2*	transcription anti-terminator LicT	Unclassified
OG1RF_12013	-1.51	*opuAA2*	glycine betaine/L-proline ABC superfamily ATP binding cassette transporter, ABC protein	Transport
OG1RF_12014	-1.26	-	glycine betaine/carnitine/choline ABC superfamily ATP binding cassette transporter	Transport
OG1RF_12027	-0.72	*coaB*	phosphopantothenate--cysteine ligase	Unclassified
OG1RF_12031	1.70	-	integral membrane protein	Unclassified
OG1RF_12035	0.96	-	RNA methyltransferase	Transcription and translation
OG1RF_12064	-1.71	-	hypothetical protein	Hypothetical
OG1RF_12065	-0.74	*nudF*	ADP-ribose diphosphatase	Metabolism
OG1RF_12066	-1.15	-	hypothetical protein	Hypothetical
OG1RF_12067	-1.00	*telA*	tellurite resistance protein	Unclassified
OG1RF_12070	1.03	-	hypothetical protein	Hypothetical
OG1RF_12072	-0.75	*mutY*	A/G-specific adenine glycosylase	Unclassified
OG1RF_12075	1.18	-	integral membrane protein	Unclassified
OG1RF_12084	0.64	-	ABC superfamily ATP binding cassette transporter, ABC protein	Transport
OG1RF_12104	0.84	-	O-methyltransferase	Unclassified
OG1RF_12109	-0.90	*dltD*	D-alanyl-lipoteichoic acid biosynthesis protein DltD	Cell division/cell envelope
OG1RF_12110	-1.73	*dltC*	D-alanine--D-alanine ligase	Cell division/cell envelope
OG1RF_12112	-1.10	*dltA*	D-alanine--D-alanine ligase	Cell division/cell envelope
OG1RF_12115	-1.05	*nrdD*	anaerobic ribonucleoside-triphosphate reductase large subunit	Unclassified
OG1RF_12132	2.19	*yniG*	EmrB/QacA family drug resistance transporter	Transport
OG1RF_12152	1.60	-	hypothetical protein	Hypothetical
OG1RF_12158	-1.28	*penA*	penicillin-binding protein 2B	Cell division/cell envelope
OG1RF_12178	0.95	*accA*	acetyl-coA carboxylase carboxyl transferase subunit alpha	Metabolism

Supplementary table C4 (*continued*.)				
OG1RF_12179	1.00	*accD*	Acetyl-coa carboxylase carboxyl transferase subunit beta	Metabolism
OG1RF_12180	0.67	*accC*	Acetyl-coa carboxylase subunit A	Metabolism
OG1RF_12181	0.69	*fabZ2*	(3R)-hydroxymyristoyl-ACP dehydratase	Metabolism
OG1RF_12183	0.83	*fabF2*	Beta-ketoacyl-acyl-carrier-protein synthase II	Metabolism
OG1RF_12184	0.85	*fabG3*	3-oxoacyl-ACP reductase	Metabolism
OG1RF_12185	0.74	*fabD*	Malonyl-coa-[acyl-carrier-protein] transacylase	Metabolism
OG1RF_12186	0.74	*fabK*	Enoyl-ACP reductase	Metabolism
OG1RF_12200	1.34	*trxB3*	Thioredoxin-disulfide reductase	Metabolism
OG1RF_12238	1.70	-	NCS2 family xanthine/uracil permease family protein	Transport
OG1RF_12267	-2.18	-	Permease protein	Transport
OG1RF_12268	-2.40	-	ABC superfamily ATP binding cassette transporter, ABC protein	Transport
OG1RF_12269	-3.87	-	RND transporter	Transport
OG1RF_12271	-1.01	*cdr*	Coa-disulfide reductase	Unclassified
OG1RF_12272	-1.81	-	Rhodanese family protein	Unclassified
OG1RF_12284	1.02	-	Sulfate transporter/STAS domain protein	Transport
OG1RF_12302	1.83	-	DAACS family dicarboxylate/amino acid:cation symporter	Transport
OG1RF_12333	-0.86	*mreC*	Rod shape-determining protein mrec	Cell division/cell envelope
OG1RF_12339	0.96	-	Formate/nitrite transporter	Transport
OG1RF_12354	2.42	-	ABC superfamily ATP binding cassette transporter, membrane protein	Transport
OG1RF_12359	1.78	-	Yitt family protein	Unclassified
OG1RF_12394	-0.68	-	Yicc like protein	Unclassified
OG1RF_12420	1.55	*mscL*	Large conductance mechanosensitive channel protein	Transport
OG1RF_12425	1.54	*trePP*	Glycosyl hydrolase	Metabolism
OG1RF_12426	1.41	*yvdM*	Beta-phosphoglucomutase	Metabolism
OG1RF_12473	1.10	-	Dihydrouridine synthase	Unclassified
OG1RF_12474	1.12	-	ABC superfamily ATP binding cassette transporter, membrane protein	Transport
OG1RF_12475	0.94	-	ABC superfamily ATP binding cassette transporter, ABC protein	Transport
OG1RF_12485	0.86	-	Phosphatidylglycerol--membrane-oligosaccharide glycerophosphotransferase	Unclassified
OG1RF_12489	-1.05	-	Putative lipoprotein	Unclassified
OG1RF_12492	0.61	*rpoC*	DNA-directed RNA polymerase subunit beta prime	Transcription and translation
OG1RF_12493	0.60	*rpoB*	DNA-directed RNA polymerase subunit beta	Transcription and translation
OG1RF_12500	-4.92	-	Cell-envelope associated acid phosphatase	Signaling and regulation
OG1RF_12510	0.81	*ndh3*	NADH dehydrogenase	Metabolism
OG1RF_12529	0.96	-	Brp/Blh family beta-carotene 15,15'-monooxygenase	Unclassified
OG1RF_12535	-4.36	*croR*	Response regulator	Signaling and regulation
OG1RF_12536	-4.20	*croS*	Sensor histidine kinase	Signaling and regulation
[#]Manual annotation in red.				

Supplementary Table C5 | RNA-Seq results showing 164 consensus genes identified when compared across 3 sets of RNA data.

ΔsrtAΔhtrA vs WT; *ΔsrtAΔhtrA* vs *ΔsrtA*; *ΔsrtAΔhtrA* vs *ΔhtrA*. Genes with significant differences in abundance of mRNAs were determined using a P value and false discovery rate (FDR) cutoff of 0.05. The values represent the log2 fold change between biological triplicates of Δ*srtA*Δ*htrA* compared to respective strains when grown to mid-log phase in TSB supplemented with 0.25% glucose.

Locus Tag	*WT*	Δ*srtA*	Δ*htrA*	Genes[#]	Annotation	Manual Classification
OG1RF_10040	1.17	1.25	1.38	-	PIN domain-containing protein	Unclassified
OG1RF_10041	1.09	1.17	1.32	*ispF*	2-C-methyl-D-erythritol 2,4-cyclo diphosphate synthase	Metabolism
OG1RF_10113	-1.19	-1.20	-1.20	-	cob(I)yrinic acid a, c-diamide adenosyltransferase	Unclassified
OG1RF_10136	-1.97	-2.71	-1.59	-	iron (Fe3+) ABC superfamily ATP binding cassette transporter, binding protein	Transport
OG1RF_10180	-1.66	-1.80	-1.77	-	hypothetical protein	Hypothetical
OG1RF_10181	-1.72	-1.64	-1.53	-	M20D family peptidase	Unclassified
OG1RF_10182	-1.45	-1.45	-1.30	-	ABC superfamily ATP binding cassette transporter, ABC protein	Transport
OG1RF_10208	1.11	1.28	1.21	*hpt*	hypoxanthine phosphoribosyltransferase	Unclassified
OG1RF_10209	1.21	1.23	1.30	*ftsH*	cell division protein FtsH	Cell division/cell envelope
OG1RF_10223	-2.08	-1.30	-1.91	-	hypothetical protein	Hypothetical
OG1RF_10224	-1.58	-1.26	-1.61	-	hypothetical protein	Hypothetical
OG1RF_10228	-1.17	-1.49	-1.16	*pyrDA*	dihydroorotate oxidase	Metabolism
OG1RF_10353	3.39	3.89	2.90	-	LemA family protein	Unclassified
OG1RF_10354	3.54	3.94	2.90	-	hypothetical protein	Hypothetical
OG1RF_10356	-0.99	-0.87	-1.04	*nrdE*	ribonucleotide-diphosphate reductase subunit alpha	Metabolism
OG1RF_10357	-1.01	-1.10	-1.10	*nrdI*	ribonucleotide-diphosphate reductase subunit gamma	Metabolism
OG1RF_10379	-1.32	-1.40	-1.29	-	phage integrase family site-specific recombinase	DNA repair and recombination
OG1RF_10423	3.35	2.88	2.02	*prsA*	peptidyl-prolyl cis-trans isomerase	Protease/ Chaperone
OG1RF_10476	-1.49	-1.80	-1.47	-	hypothetical protein	Hypothetical
OG1RF_10528	-1.29	-1.65	-1.42	-	rRNA methylase	Transcription and translation
OG1RF_10529	-1.48	-1.71	-1.50	-	radical SAM protein	Unclassified
OG1RF_10589	-1.04	-1.26	-1.12	-	cation efflux family protein	Transport
OG1RF_10590	-1.12	-1.57	-1.30	-	APC family amino acid-polyamine-organocation transporter	Transport
OG1RF_10613	-1.13	-1.07	-1.12	-	hypothetical protein	Hypothetical
OG1RF_10614	-2.00	-2.25	-1.50	-	hypothetical protein	Hypothetical
OG1RF_10615	-1.90	-2.22	-1.26	-	group 2 glycosyl transferase	Metabolism
OG1RF_10616	-1.80	-2.24	-1.29	-	cellulose synthase catalytic subunit	Metabolism
OG1RF_10617	-2.00	-2.36	-1.32	-	hypothetical protein	Hypothetical
OG1RF_10618	-1.89	-2.29	-1.28	-	hypothetical protein	Hypothetical
OG1RF_10626	-1.98	-2.45	-2.13	-	hypothetical protein	Hypothetical
OG1RF_10672	-1.08	-1.17	-1.27	-	GNAT family acetyltransferase	Unclassified
OG1RF_10707	2.05	1.30	1.59	-	DNA repair exonuclease	DNA repair and recombination

Supplementary table C5 (*continued*.)

OG1RF_10817	-1.64	-2.01	-1.86	*malR*	phage integrase family site-specific recombinase	DNA repair and recombination
OG1RF_10818	-1.47	-1.98	-1.95	-	nitroreductase	Metabolism
OG1RF_10820	-1.21	-1.95	-1.74	-	LytR family response regulator	Signaling and regulation
OG1RF_10838	-2.58	-2.82	-2.00	-	NRAMP family Mn2+/Fe2+ transporter	Transport
OG1RF_10869	1.72	1.21	1.60	*ebpA*	von Willebrand factor type A domain-containing protein	Surface protein
OG1RF_10870	1.81	1.46	1.83	*ebpB*	cell wall surface anchor family protein	Surface protein
OG1RF_10871	1.86	1.41	1.87	*ebpC*	cell wall surface anchor family protein	Surface protein
OG1RF_10895	-1.69	-1.93	-1.79	*glnP*	glutamine ABC superfamily ATP binding cassette transporter, membrane protein	Transport
OG1RF_10896	-1.38	-1.71	-1.37	*glnM*	amino acid ABC superfamily ATP binding cassette transporter, membrane protein	Transport
OG1RF_10897	-1.47	-1.71	-1.45	*glnH*	glutamine ABC superfamily ATP binding cassette transporter, binding protein	Transport
OG1RF_10922	-1.29	-1.71	-1.66	-	hypothetical protein	Hypothetical
OG1RF_10952	1.64	1.39	1.42	-	hypothetical protein	Hypothetical
OG1RF_10975	0.98	1.02	1.01	-	crossover junction endodeoxyribonuclease	DNA repair and recombination
OG1RF_11045	-1.85	-1.55	-2.24	-	hypothetical protein	Hypothetical
OG1RF_11046	-1.50	-1.31	-1.66	-	hypothetical protein	Phage
OG1RF_11047	-1.58	-1.29	-1.60	-	cro/CI family transcriptional regulator	Phage
OG1RF_11048	-1.83	-2.02	-2.95	-	hypothetical protein	Phage
OG1RF_11049	-2.35	-2.36	-3.33	-	DNA replication protein	Phage
OG1RF_11050	-2.21	-2.27	-3.32	-	DNA replication protein	Phage
OG1RF_11051	-2.18	-2.29	-3.30	-	hypothetical protein	Phage
OG1RF_11052	-2.54	-2.58	-3.66	-	RinA family transcriptional regulator	Phage
OG1RF_11053	-3.23	-3.29	-3.58	-	transposase	Phage
OG1RF_11054	-3.66	-3.58	-4.16	-	hypothetical protein	Phage
OG1RF_11055	-3.49	-3.52	-3.89	-	TP901-1 family phage major tail protein	Phage
OG1RF_11056	-3.55	-3.46	-3.84	-	hypothetical protein	Phage
OG1RF_11057	-3.74	-3.67	-4.26	-	hypothetical protein	Phage
OG1RF_11058	-3.56	-3.73	-4.04	-	ABC superfamily ATP binding cassette transporter permease subunit	Phage
OG1RF_11059	-3.68	-3.85	-4.24	-	phage tail protein	Phage
OG1RF_11060	-3.83	-3.88	-4.22	-	phage structural protein	Phage
OG1RF_11061	-3.81	-3.87	-4.21	-	hypothetical protein	Phage
OG1RF_11062	-3.59	-3.75	-4.11	-	holin	Phage
OG1RF_11063	-4.15	-4.11	-4.57	*amiD2*	N-acetylmuramoyl-L-alanine amidase	Phage
OG1RF_11064	-1.17	-1.00	-1.34	*truB*	tRNA pseudouridine synthase B	Metabolism
OG1RF_11065	-1.23	-1.09	-1.41	*ribF*	riboflavin biosynthesis protein RibF	Metabolism
OG1RF_11066	-1.29	-0.99	-1.42	-	GNAT family acetyltransferase	Unclassified
OG1RF_11067	-2.29	-1.64	-2.94	-	PadR family transcriptional regulator	Signaling and regulation
OG1RF_11068	-2.93	-2.29	-3.39	-	hypothetical protein	Hypothetical

Supplementary table C5 (*continued*.)

OG1RF_11069	-2.12	-1.41	-2.58	-	putative transcriptional regulator	Signaling and regulation
OG1RF_11070	-4.41	-3.78	-4.72	*ftsW*	FtsW/RodA/SpovE family cell division protein	Cell division/cell envelope
OG1RF_11071	-3.85	-3.40	-4.15	*rodA*	FtsW/RodA/SpovE family cell division protein	Cell division/cell envelope
OG1RF_11075	-1.06	-0.99	-1.25	*hemN*	coproporphyrinogen dehydrogenase	Metabolism
OG1RF_11086	-1.23	-1.48	-1.20	-	hypothetical protein	Hypothetical
OG1RF_11157	-1.71	-1.56	-1.54	-	cro/CI family transcriptional regulator	Signaling and regulation
OG1RF_11207	1.94	1.71	1.97	*atpF1*	V-type ATPase, subunit F	Metabolism
OG1RF_11208	2.21	1.69	1.91	*atpI*	proton (H+) or sodium (Na+) translocating V-type ATPase (V-ATPase), subunit I	Metabolism
OG1RF_11209	2.00	1.55	1.76	*atpK*	proton (H+) or sodium (Na+) translocating V-type ATPase (V-ATPase), subunit K	Metabolism
OG1RF_11210	1.83	1.36	1.63	*atpE*	proton (H+) or sodium (Na+) translocating V-type ATPase (V-ATPase), subunit E	Metabolism
OG1RF_11211	1.94	1.39	1.62	*atpC*	proton (H+) or sodium (Na+) translocating V-type ATPase (V-ATPase), subunit C	Metabolism
OG1RF_11212	1.95	1.36	1.72	*atpF2*	V-type ATP synthase subunit F	Metabolism
OG1RF_11213	1.75	1.34	1.55	*atpA*	ATP synthase F1 subcomplex subunit alpha	Metabolism
OG1RF_11214	1.58	1.21	1.39	*atpB*	proton (H+) or sodium (Na+) translocating V-type ATPase (V-ATPase), subunit B	Metabolism
OG1RF_11215	1.64	1.23	1.54	*atpD*	V-type ATP synthase subunit D	Metabolism
OG1RF_11216	1.59	1.17	1.34	-	hypothetical protein	Hypothetical
OG1RF_11219	-0.97	-1.05	-1.01	-	beta-lactamase	Cell division/cell envelope
OG1RF_11230	-2.20	-1.98	-2.39	*sacT*	SacPA operon antiterminator	Signaling and regulation
OG1RF_11231	-1.93	-1.91	-2.23	*ptsG*	PTS family glucose porter, IICBA component	Transport
OG1RF_11239	1.15	1.80	2.03	-	transposon family protein	Unclassified
OG1RF_11260	-3.40	-3.11	-3.22	-	brp/Blh family beta-carotene 15,15'-monooxygenase	Metabolism
OG1RF_11261	-2.20	-2.09	-2.45	-	hypothetical protein	Hypothetical
OG1RF_11308	-2.44	-1.63	-3.25	-	N-acetyltransferase	Unclassified
OG1RF_11384	1.64	1.73	1.10	-	permease protein	Transport
OG1RF_11442	-1.83	-1.57	-2.18	*mdlB*	multidrug ABC superfamily ATP binding cassette transporter, ABC protein	Transport
OG1RF_11443	-1.40	-1.25	-1.82	*mdlA*	multidrug ABC superfamily ATP binding cassette transporter, ABC protein	Transport
OG1RF_11462	3.31	3.52	2.37	-	hypothetical protein	Hypothetical
OG1RF_11463	3.30	3.48	2.27	-	PspC domain-containing protein	Unclassified
OG1RF_11464	3.75	3.69	2.42	-	hypothetical protein	Hypothetical
OG1RF_11485	-1.29	-1.25	-1.25	*fabG2*	3-oxoacyl-ACP reductase	Metabolism
OG1RF_11490	-1.48	-1.12	-1.17	*purH*	bifunctional purine biosynthesis protein PurH	Metabolism
OG1RF_11523	-1.67	-1.45	-1.40	-	LysR family transcriptional regulator	Signaling and regulation

Supplementary table C5 (*continued*.)						
OG1RF_11569	1.93	2.11	1.87	-	integral membrane protein	Unclassified
OG1RF_11607	-0.88	-1.26	-1.06	-	membrane-oligosaccharide glycerophosphotransferase	Metabolism
OG1RF_11656	3.20	2.43	2.79	-	ABC superfamily ATP binding cassette transporter, permease protein	Signaling and regulation
OG1RF_11657	3.26	2.64	2.97	-	ABC superfamily ATP binding cassette transporter, ABC protein	Signaling and regulation
OG1RF_11663	-1.80	-1.71	-1.93	-	ABC superfamily ATP binding cassette transporter, ABC/membrane protein	Transport
OG1RF_11664	-2.06	-2.00	-2.30	-	ABC superfamily ATP binding cassette transporter, ABC/membrane protein	Transport
OG1RF_11671	-1.03	-1.02	-1.01	-	hypothetical protein	Hypothetical
OG1RF_11672	-1.11	-0.97	-1.09	-	major facilitator family transporter	Transport
OG1RF_11680	-1.25	-0.98	-1.36	-	ABC superfamily ATP binding cassette transporter, ABC protein	Transport
OG1RF_11681	-1.32	-1.21	-1.38	*hipO2*	aminoacylase	Unclassified
OG1RF_11683	-2.03	-1.58	-2.15	-	ABC superfamily ATP binding cassette transporter, membrane protein	Transport
OG1RF_11684	-1.77	-1.50	-1.91	-	ABC superfamily ATP binding cassette transporter, binding protein	Transport
OG1RF_11694	-1.75	-1.70	-1.85	-	ABC superfamily ATP binding cassette transporter, ABC protein	Transport
OG1RF_11695	-1.32	-1.46	-1.50	-	hypothetical protein	Hypothetical
OG1RF_11720	-1.85	-1.34	-1.90	-	group 2 glycosyl transferase	Metabolism
OG1RF_11751	2.78	2.27	2.61	-	hypothetical protein	Hypothetical
OG1RF_11766	2.90	2.97	2.95	-	multidrug ABC superfamily ATP binding cassette transporter, ABC protein	Transport
OG1RF_11767	2.99	3.24	3.18	-	ABC superfamily ATP binding cassette transporter, membrane protein	Transport
OG1RF_11793	1.58	1.89	1.49	*clpB*	chaperone protein ClpB	Protease/ chaperone
OG1RF_11797	-2.69	-2.13	-2.87	*pbuX*	xanthine permease	Metabolism
OG1RF_11798	-3.23	-2.66	-3.59	*xpt*	xanthine phosphoribosyltransferase	Metabolism
OG1RF_11861	-1.54	-1.31	-1.64	-	NCS2 family xanthine/uracil permease	Transport
OG1RF_11875	-1.85	-1.54	-1.69	-	acyl-CoA thioester hydrolase	Metabolism
OG1RF_11903	-0.92	-1.04	-1.00	*gcp*	O-sialoglycoprotein endopeptidase	Unclassified
OG1RF_11904	-0.97	-1.36	-1.24	*rimI*	ribosomal-protein-alanine acetyltransferase	Unclassified
OG1RF_11905	-1.05	-1.36	-1.11	*rimI2*	ribosomal-protein-alanine acetyltransferase	Unclassified
OG1RF_11922	-1.60	-1.48	-1.97	-	M protein trans-acting positive regulator	Signaling and regulation
OG1RF_11923	-1.61	-1.59	-1.99	-	hypothetical protein	Hypothetical
OG1RF_11925	-2.05	-2.39	-2.24	-	hypothetical protein	Hypothetical
OG1RF_11926	-1.88	-2.31	-2.15	-	cro/CI family transcriptional regulator	Signaling and regulation

Supplementary table C5 (*continued*.)						
OG1RF_11927	-2.85	-3.30	-2.96	*azlC*	LIV-E family branched chain amino acid exporter AzlC	Transport
OG1RF_11928	-3.02	-3.58	-3.19	*azlD*	LIV-E family branched-chain amino acid exporter AzlD	Transport
OG1RF_12031	-1.67	-2.06	-1.75	-	integral membrane protein	Unclassified
OG1RF_12063	1.35	1.36	1.52	*mtnN*	MTA/SAH nucleosidase	Metabolism
OG1RF_12064	1.21	1.17	1.54	-	hypothetical protein	Hypothetical
OG1RF_12065	1.33	1.30	1.40	*nudF*	ADP-ribose diphosphatase	Metabolism
OG1RF_12066	2.75	2.25	1.97	-	hypothetical protein	Hypothetical
OG1RF_12067	2.20	1.69	1.56	*telA*	tellurite resistance protein	Unclassified
OG1RF_12127	-1.76	-1.53	-1.64	*tenA*	thiaminase	Metabolism
OG1RF_12128	-1.33	-1.35	-1.42	-	cobalt transporter	Transport
OG1RF_12129	-1.62	-1.58	-1.71	-	ABC superfamily ATP binding cassette transporter, ABC protein	Transport
OG1RF_12130	-0.95	-1.07	-1.14	-	ABC superfamily ATP binding cassette transporter, membrane protein	Transport
OG1RF_12152	-1.63	-1.15	-1.62	-	hypothetical protein	Hypothetical
OG1RF_12158	1.67	1.46	2.11	*penA*	penicillin-binding protein 2B	Cell division/cell envelope
OG1RF_12267	5.23	4.07	4.95	-	permease protein	Transport
OG1RF_12268	5.21	4.50	5.15	-	ABC superfamily ATP binding cassette transporter, ABC protein	Transport
OG1RF_12269	5.18	4.56	5.32	-	RND transporter	Transport
OG1RF_12294	-1.09	-1.13	-1.22	*pmr1*	P-ATPase superfamily P-type ATPase cation transporter	Transport
OG1RF_12325	-1.18	-1.40	-1.04	-	putative lipoprotein	Unclassified
OG1RF_12380	1.27	1.06	1.11	*rpmB2*	50S ribosomal protein L28	Transcription and translation
OG1RF_12421	-1.88	-1.77	-2.39	-	S-layer protein	Surface protein
OG1RF_12425	-1.95	-2.70	-2.07	*trePP*	glycosyl hydrolase	Metabolism
OG1RF_12426	-1.88	-2.69	-1.86	*yvdM*	beta-phosphoglucomutase	Metabolism
OG1RF_12453	2.16	1.25	1.89	-	WxL domain surface protein	Surface protein
OG1RF_12455	2.09	1.26	1.73	-	hypothetical protein	Hypothetical
OG1RF_12456	1.97	1.23	1.78	-	WxL domain surface protein	Surface protein
OG1RF_12460	1.68	1.70	2.03	*lrgB*	murein hydrolase regulator LrgB	Signaling and regulation
OG1RF_12461	1.68	1.61	1.61	*lrgA*	murein hydrolase regulator LrgA	Signaling and regulation
OG1RF_12480	-1.14	-1.06	-1.15	-	DEAH-box family ATP-dependent helicase	Transcription and translation
OG1RF_12484	-1.28	-1.14	-1.40	-	hypothetical protein	Hypothetical
OG1RF_12523	-1.37	-1.10	-1.11	-	hydantoinase/oxoprolinase	Metabolism
OG1RF_12535	1.44	1.18	1.88	*croR*	response regulator	Signaling and regulation
OG1RF_12536	1.41	1.09	1.80	*croS*	sensor histidine kinase	Signaling and regulation
[#]Manual annotation in red.						

Supplementary Table C6 | 81 genes which show opposite in fold-change expression in *croR::TnΔsrtAΔhtrA* vs *ΔsrtAΔhtrA*; *ΔsrtA* vs *ΔsrtAΔhtrA* postulated as CroR-regulated genes.

Locus Tag	*croR::TnΔsrtAΔhtrA* vs *ΔsrtAΔhtrA*	*ΔsrtAΔhtrA* vs *ΔsrtA*	Gene	Annotation
OG1RF_10180	2.18	-1.80	-	Hypothetical protein
OG1RF_10181	1.81	-1.64	-	M20D family peptidase
OG1RF_10228	0.97	-1.49	*pyrDA*	Dihydroorotate oxidase
OG1RF_10590	1.53	-1.57	-	APC family amino acid-polyamine-organocation transporter
OG1RF_10613	1.25	-1.07	-	Hypothetical protein
OG1RF_10614	1.44	-2.25	-	Hypothetical protein
OG1RF_10616	0.96	-2.24	-	Cellulose synthase catalytic subunit
OG1RF_10626	1.44	-2.45	-	Hypothetical protein
OG1RF_10672	1.49	-1.17	-	GNAT family acetyltransferase
OG1RF_10707	-2.90	1.30	-	DNA repair exonuclease
OG1RF_10784	1.17	-0.87	*csrS*	Sensor histidine kinase csrs
OG1RF_10875	1.45	-2.48	-	Hypothetical protein
OG1RF_10876	1.76	-2.19	-	Hypothetical protein
OG1RF_10895	1.71	-1.93	*glnP*	Glutamine ABC superfamily ATP binding cassette transporter, membrane protein
OG1RF_10897	1.44	-1.71	*glnH*	Glutamine ABC superfamily ATP binding cassette transporter, binding protein
OG1RF_10898	1.78	-1.45	*glnQ*	ABC superfamily ATP binding cassette transporter, ABC protein
OG1RF_10953	1.28	-1.36	-	Oxygen-insensitive NADPH nitroreductase
OG1RF_11071	2.94	-3.40	-	Ftsw/roda/spove family cell division protein
OG1RF_11207	-1.39	1.71	-	V-type atpase, subunit F
OG1RF_11208	-0.65	1.69	*atpI*	Proton (H+) or sodium (Na+) translocating V-type atpase (V-atpase), subunit I
OG1RF_11210	-1.34	1.36	*atpE*	Proton (H+) or sodium (Na+) translocating V-type atpase (V-atpase), subunit E
OG1RF_11211	-0.76	1.39	*atpC*	Proton (H+) or sodium (Na+) translocating V-type atpase (V-atpase), subunit C
OG1RF_11213	-0.98	1.34	*atpA*	ATP synthase F1 subcomplex subunit alpha
OG1RF_11214	-1.04	1.21	*atpB*	Proton (H+) or sodium (Na+) translocating V-type atpase (V-atpase), subunit B
OG1RF_11215	-0.83	1.23	*atpD*	V-type ATP synthase subunit D
OG1RF_11216	-0.76	1.17	-	Hypothetical protein
OG1RF_11219	0.83	-1.05	-	Beta-lactamase
OG1RF_11221	1.54	-1.58	*lysA*	Diaminopimelate decarboxylase
OG1RF_11230	1.14	-1.98	*sacT*	Sacpa operon antiterminator
OG1RF_11231	1.01	-1.91	*ptsG*	PTS family glucose porter, IICBA component
OG1RF_11239	-2.50	1.80	-	Transposon family protein
OG1RF_11261	1.05	-2.09	-	Hypothetical protein
OG1RF_11308	3.04	-1.63	-	N-acetyltransferase
OG1RF_11442	1.61	-1.57	*mdlB*	Multidrug ABC superfamily ATP binding cassette transporter, ABC protein
OG1RF_11443	1.31	-1.25	*mdlA*	Multidrug ABC superfamily ATP binding cassette transporter, ABC protein
OG1RF_11464	-1.16	3.69	-	Hypothetical protein
OG1RF_11485	1.21	-1.25	*fabG2*	3-oxoacyl-ACP reductase
OG1RF_11523	1.40	-1.45	-	Lysr family transcriptional regulator
OG1RF_11525	1.28	-2.40	*sprE*	Spre protein
OG1RF_11526	1.13	-2.38	*gelE*	Gelatinase
OG1RF_11527	1.81	-1.72	*fsrC*	Sensor histidine kinase fsrc
OG1RF_11528	1.51	-1.57	*fsrB*	Fsrb protein

Supplementary table C6 (*continued.*)				
OG1RF_11573	0.68	-1.48	*murC*	UDP-N-acetylmuramate--L-alanine ligase
OG1RF_11606	1.08	-1.14	-	Bicyclomycin resistance protein
OG1RF_11656	-1.17	2.43	-	ABC superfamily ATP binding cassette transporter, permease protein
OG1RF_11657	-1.50	2.64	-	ABC superfamily ATP binding cassette transporter, ABC protein
OG1RF_11663	1.71	-1.71	-	ABC superfamily ATP binding cassette transporter, ABC/membrane protein
OG1RF_11664	1.63	-2.00	-	ABC superfamily ATP binding cassette transporter, ABC/membrane protein
OG1RF_11694	1.07	-1.70	-	ABC superfamily ATP binding cassette transporter, ABC protein
OG1RF_11695	1.39	-1.46	-	Hypothetical protein
OG1RF_11720	0.88	-1.34	-	Group 2 glycosyl transferase
OG1RF_11766	-4.54	2.97	-	Multidrug ABC superfamily ATP binding cassette transporter, ABC protein
OG1RF_11767	-3.37	3.24	-	ABC superfamily ATP binding cassette transporter, membrane protein
OG1RF_11793	-1.45	1.89	*clpB*	Chaperone protein clpb
OG1RF_11797	3.82	-2.13	*pbuX*	Xanthine permease
OG1RF_11798	3.81	-2.66	*xpt*	Xanthine phosphoribosyltransferase
OG1RF_11903	0.86	-1.04	*gcp*	O-sialoglycoprotein endopeptidase
OG1RF_11904	0.72	-1.36	*rimI*	Ribosomal-protein-alanine acetyltransferase
OG1RF_11922	2.26	-1.48	-	M protein trans-acting positive regulator
OG1RF_11923	1.71	-1.59	-	Hypothetical protein
OG1RF_11925	1.41	-2.39	-	Hypothetical protein
OG1RF_11926	1.26	-2.31	-	Cro/CI family transcriptional regulator
OG1RF_12064	-1.71	1.17	-	Hypothetical protein
OG1RF_12065	-0.74	1.30	*nudF*	ADP-ribose diphosphatase
OG1RF_12066	-1.15	2.25	-	Hypothetical protein
OG1RF_12067	-1.00	1.69	*telA*	Tellurite resistance protein
OG1RF_12130	1.46	-1.07	-	ABC superfamily ATP binding cassette transporter, membrane protein
OG1RF_12152	1.60	-1.15	-	Hypothetical protein
OG1RF_12158	-1.28	1.46	*penA*	Penicillin-binding protein 2B
OG1RF_12267	-2.18	4.07	-	Permease protein
OG1RF_12268	-2.40	4.50	-	ABC superfamily ATP binding cassette transporter, ABC protein
OG1RF_12269	-3.87	4.56	-	Integrating conjugative element protein
OG1RF_12333	-0.86	0.98	*mreC*	Rod shape-determining protein mrec
OG1RF_12354	2.42	-1.12	-	ABC superfamily ATP binding cassette transporter, membrane protein
OG1RF_12425	1.54	-2.70	*trePP*	Glycosyl hydrolase
OG1RF_12426	1.41	-2.69	*yvdM*	Beta-phosphoglucomutase
OG1RF_12453	-1.10	1.25	-	Wxl domain surface protein
OG1RF_12455	-1.74	1.26	-	Hypothetical protein
OG1RF_12485	0.86	-1.01	-	Phosphatidylglycerol--membrane-oligosaccharide glycerophosphotransferase
OG1RF_12535	-4.36	1.18	*croR*	Response regulator
OG1RF_12536	-4.20	1.09	*croS*	Sensor histidine kinase
[#]Manual annotation in red.				

Supplementary Table C7 | RNA-Seq results comparing *ΔsrtA* and WT.

Genes with significant differences in abundance of mRNAs were determined using a P-Value and false discovery rate (FDR) cutoff of 0.05. The LogFC represents the log_2 change between biological triplicates of *ΔsrtA* and WT when grown to mid-log phase in TSB supplemented with 0.25% glucose.

Locus tag	logFC	Gene	Annotation
OG1RF_10026	-1.89	*malX*	PTS family maltose and glucose porter, IIABC component
OG1RF_10101	2.61	*arcC*	Carbamate kinase
OG1RF_10235	-1.56	*celB*	PTS family lactose-N, N'-diacetylchitobiose-beta-glucoside (lac) porter component IIBC
OG1RF_10296	-1.40	*mtlA2*	PTS family mannitol porter, EIICB component
OG1RF_10317	-1.63	*dctM*	TRAP-T family tripartite ATP-independent periplasmic transporter, membrane protein
OG1RF_10341	-1.924	-	PTS system mannose/fructose/sorbose transporter subunit IID
OG1RF_11140	1.93	*mgtA2*	Magnesium-importing ATPase
OG1RF_11529	1.17	*fsrA*	FsrA response regulator
OG1RF_12280	-1.50	-	Cytosine/purine permease
OG1RF_12327	-10.46	*srtA*	Sortase SrtA

Supplementary Table C8 | RNA-Seq results comparing *croS::TnΔsrtAΔhtrA* and *ΔsrtAΔhtrA.*

Genes with significant differences in abundance of mRNAs were determined using a PValue and false discovery rate (FDR) cutoff of 0.05. The LogFC represents the log2 change between biological triplicates of *croS::TnΔsrtAΔhtrA* and *ΔsrtAΔhtrA* when grown to mid-log phase in TSB supplemented with 0.25% glucose.

Locus tag	LogFC	Gene	Annotation	Manual classification
OG1RF_10003	-1.32	*yaaA*	S4 domain-containing protein yaaa	Transcription and translation
OG1RF_10004	-1.31	*recF*	Recombination protein F	DNA repair and recombination
OG1RF_10005	-0.76	*gyrB*	DNA topoisomerase subunit B	Transcription and translation
OG1RF_10013	-0.81	*purA*	Adenylosuccinate synthase	Metabolism
OG1RF_10016	0.79	-	ABC superfamily ATP binding cassette transporter, ABC protein	Transport
OG1RF_10018	-0.78	*manX*	PTS family mannose/fructose/sorbose porter component IIB	Transport
OG1RF_10019	-1.22	*manX2*	PTS system mannose transporter subunit IIAB	Transport
OG1RF_10020	-1.24	*manY*	PTS family mannose/fructose/sorbose porter component IIC	Transport
OG1RF_10021	-1.20	-	PTS system mannose/fructose/sorbose transporter subunit IID	Transport
OG1RF_10022	-0.91	-	Hypothetical protein	Hypothetical
OG1RF_10029	1.40	-	Hypothetical protein	Hypothetical
OG1RF_10036	-0.58	*proA*	Glutamate-5-semialdehyde dehydrogenase	Metabolism
OG1RF_10040	-0.77	-	PIN domain-containing protein	Unclassified
OG1RF_10041	-0.84	*ispF*	2-C-methyl-D-erythritol 2,4-cyclo diphosphate synthase	Metabolism
OG1RF_10042	-0.48	*gltX*	Glutamate-trna ligase	Transcription and translation
OG1RF_10049	-0.89	*veg*	Veg protein	Unclassified
OG1RF_10056	1.70	-	5'-nucleotidase	Metabolism
OG1RF_10061	-0.84	*ruvB*	Crossover junction ATP-dependent DNA helicase ruvb	Transcription and translation
OG1RF_10068	1.19	*fabG*	3-oxoacyl-ACP reductase	Metabolism
OG1RF_10069	1.16	-	Hypothetical protein	Hypothetical
OG1RF_10070	1.09	*orf4*	Hypothetical protein	Hypothetical
OG1RF_10071	1.37	*gls24b*	Stress response regulator Gls24	Unclassified
OG1RF_10072	1.17	*gls24*	Stress response regulator Gls24	Unclassified
OG1RF_10073	1.41	*glsB*	Transglycosylase associated protein	Unclassified
OG1RF_10079	-1.60	-	Major facilitator family transporter	Transport
OG1RF_10080	-1.19	-	Hypothetical protein	Hypothetical
OG1RF_10090	-1.23	-	Putative lipoprotein	Unclassified
OG1RF_10092	-3.49	*pfoR*	Perfringolysin O regulator protein	Signaling and regulation
OG1RF_10093	-5.00	*sdaB*	L-serine dehydratase, iron-sulfur-dependent subunit beta	Metabolism
OG1RF_10094	-3.38	*sdaA*	L-serine dehydratase, iron-sulfur-dependent subunit alpha	Metabolism
OG1RF_10095	-3.47	*serS*	Serine--trna ligase	Transcription and translation

Supplementary table C8 (*continued*.)				
OG1RF_10098	-1.09	*argR*	Arginine repressor	Transcription and translation
OG1RF_10099	-2.35	*arcA*	Arginine deiminase	Unclassified
OG1RF_10100	-4.30	*arcB*	Ornithine carbamoyltransferase	Unclassified
OG1RF_10103	1.18	-	UIT3 family protein	Unclassified
OG1RF_10110	-0.71	-	Gntr family transcriptional regulator	Signaling and regulation
OG1RF_10122	1.05	*deoC*	Deoxyribose-phosphate aldolase	Metabolism
OG1RF_10133	-0.71	*deoB*	Phosphopentomutase	Metabolism
OG1RF_10134	-0.57	*deoD*	Purine-nucleoside phosphorylase	Metabolism
OG1RF_10142	-0.68	-	Resolvase family site-specific recombinase	DNA repair and recombination
OG1RF_10148	2.77	*thiD*	Phosphomethylpyrimidine kinase	Unclassified
OG1RF_10149	0.71	*cfa*	Cyclopropane-fatty-acyl-phospholipid synthase	Metabolism
OG1RF_10180	2.10	-	Hypothetical protein	Hypothetical
OG1RF_10181	1.24	-	M20D family peptidase	Unclassified
OG1RF_10200	0.98	*pth*	Aminoacyl-trna hydrolase	Transcription and translation
OG1RF_10210	1.70	*hslO*	Chaperonin hslo	Protease/Chaperone
OG1RF_10211	1.89	*dus*	Trna-dihydrouridine synthase	Unclassified
OG1RF_10226	1.67	*fabF*	3-oxoacyl-(acyl-carrier-protein) synthase II	Unclassified
OG1RF_10227	1.30	*fabZ*	(3R)-hydroxymyristoyl-ACP dehydratase	Unclassified
OG1RF_10228	2.45	*pyrDA*	Dihydroorotate oxidase	Metabolism
OG1RF_10236	0.85	-	Rpir family transcriptional regulator	Signaling and regulation
OG1RF_10259	-1.15	-	Response regulator	Signaling and regulation
OG1RF_10260	-1.07	-	Sensor histidine kinase	Signaling and regulation
OG1RF_10265	1.06	-	Ankyrin repeat family protein	Unclassified
OG1RF_10266	0.71	-	Amidohydrolase	Unclassified
OG1RF_10269	-1.00	-	Hypothetical protein	Hypothetical
OG1RF_10270	-1.15	-	Hypothetical protein	Hypothetical
OG1RF_10275	1.96	-	Sodium/dicarboxylate symporter family protein	Transport
OG1RF_10276	1.76	*allD*	Ureidoglycolate dehydrogenase	Metabolism
OG1RF_10277	1.66	-	UIT9 family protein	Unclassified
OG1RF_10278	1.39	*atzC*	N-isopropylammelide isopropylaminohydrolase	Unclassified
OG1RF_10282	1.55	-	Vitamin-B12 independent methionine synthase	Metabolism
OG1RF_10288	3.37	*nhaC*	Na+/H+ antiporter nhac	Metabolism
OG1RF_10306	0.84	-	Hypothetical protein	Hypothetical
OG1RF_10307	1.20	*lmrB*	MFS family lincomycin resistance protein lmrb	Unclassified
OG1RF_10308	1.00	-	Merr family transcriptional regulator	Signaling and regulation
OG1RF_10313	-2.15	*idnO*	Gluconate 5-dehydrogenase	Metabolism
OG1RF_10326	0.90	*dtpT*	POT family proton (H+)-dependent oligopeptide transporter	Transport
OG1RF_10337	-0.97	-	AMP-binding family protein	Unclassified
OG1RF_10350	-0.83	-	Transcriptional regulator	Signaling and regulation
OG1RF_10351	-0.89	*nagB*	Glucosamine-6-phosphate deaminase	Metabolism
OG1RF_10353	-1.57	-	Lema family protein	Unclassified

Supplementary table C8 (*continued*.)				
OG1RF_10354	-1.90	-	Hypothetical protein	Hypothetical
OG1RF_10355	1.51	*nrdF*	Ribonucleotide-diphosphate reductase subunit beta	Metabolism
OG1RF_10356	1.48	*nrdE*	Ribonucleotide-diphosphate reductase subunit alpha	Metabolism
OG1RF_10357	1.44	*nrdI*	Ribonucleotide-diphosphate reductase subunit gamma	Metabolism
OG1RF_10360	-1.85	*feoB*	Feob family ferrous iron (Fe2+) uptake protein	Metabolism
OG1RF_10365	3.01	-	Hypothetical protein	Hypothetical
OG1RF_10366	2.85	*tyrS*	Tyrosine-trna ligase	Transcription and translation
OG1RF_10367	1.34	-	Decarboxylase	Metabolism
OG1RF_10368	1.54	-	Amino acid permease	transport
OG1RF_10369	3.23	*nhaC2*	Na+/H+ antiporter nhac	Metabolism
OG1RF_10371	2.32	-	Yehr like protein	Unclassified
OG1RF_10383	-1.11	-	Hypothetical protein	Hypothetical
OG1RF_10386	-1.00	-	Nitroreductase	#N/A
OG1RF_10391	1.99	-	MATE efflux family protein	#N/A
OG1RF_10398	0.90	-	Hypothetical protein	Hypothetical
OG1RF_10399	0.68	*murE*	UDP-N-acetylmuramoyl-L-alanyl-D-glutamate--L-lysine ligase	Cell division/cell envelope
OG1RF_10404	-0.94	*csn*	Csn1 family CRISPR-associated protein	Unclassified
OG1RF_10410	0.83	-	Putative acetyltransferase	Unclassified
OG1RF_10421	-0.76	-	Hypothetical protein	Hypothetical
OG1RF_10423	-0.75	*prsA*	Peptidyl-prolyl cis-trans isomerase	Protease/ Chaperone
OG1RF_10428	1.84	*ytmP*	Phosphotransferase enzyme family protein	Unclassified
OG1RF_10429	1.94	*trmB*	Trna (guanine-N (7)-)-methyltransferase	Unclassified
OG1RF_10431	4.80	*fruK*	1-phosphofructokinase	Metabolism
OG1RF_10436	-1.88	-	GNAT family acetyltransferase	Unclassified
OG1RF_10441	1.53	-	Hypothetical protein	Hypothetical
OG1RF_10442	0.79	-	Putative lipoprotein	Unclassified
OG1RF_10446	-1.32	-	Hypothetical protein	Hypothetical
OG1RF_10476	1.48	-	Hypothetical protein	Hypothetical
OG1RF_10481	-3.14	*pbp5*	Beta-lactamase	Cell division/cell envelope
OG1RF_10487	-1.79	-	Wxl domain surface protein	Surface protein
OG1RF_10488	-1.41	-	Wxl domain surface protein	Surface protein
OG1RF_10489	-1.32	-	Wxl domain surface protein	Surface protein
OG1RF_10490	-1.55	-	Cell wall surface anchor family protein	Surface protein
OG1RF_10491	-1.45	-	Hypothetical protein	Hypothetical
OG1RF_10495	0.97	*glnQ*	ABC superfamily ATP binding cassette transporter, ABC protein	Transport
OG1RF_10496	0.86	*glnP*	Amino acid ABC superfamily ATP binding cassette transporter, binding/permease protein	Transport
OG1RF_10497	-1.01	*uvrB*	Excision endonuclease subunit uvrb	DNA repair and recombination
OG1RF_10499	-2.81	-	Hypothetical protein	Hypothetical
OG1RF_10517	1.25	*metK*	Methionine adenosyltransferase	Unclassified

Supplementary table C8 (*continued*.)				
OG1RF_10521	-0.70	-	ABC superfamily ATP binding cassette transporter, membrane protein	Transport
OG1RF_10522	-0.85	-	Multidrug resistance ABC superfamily ATP binding cassette transporter, membrane protein	Transport
OG1RF_10525	0.72	-	Tetr family transcriptional regulator	Signaling and regulation
OG1RF_10528	0.74	-	Rrna methylase	Transcription and translation
OG1RF_10529	0.62	-	Radical SAM protein	Unclassified
OG1RF_10530	0.94	-	Type 2 phosphatidic acid phosphatase	Unclassified
OG1RF_10531	-0.98	-	Hypothetical protein	Hypothetical
OG1RF_10534	0.48	*leuS*	Leucyl-trna synthetase	Transcription and translation
OG1RF_10541	0.87	-	Transglycosylase-associated protein	Unclassified
OG1RF_10542	2.35	-	Hypothetical protein	Hypothetical
OG1RF_10543	1.98	-	Hypothetical protein	Hypothetical
OG1RF_10546	0.96	-	Gntr family transcriptional regulator	Signaling and regulation
OG1RF_10585	-2.66	-	M protein trans-acting positive regulator	Signaling and regulation
OG1RF_10589	1.65	-	Cation efflux family protein	Transport
OG1RF_10590	1.39	-	APC family amino acid-polyamine-organocation transporter	Transport
OG1RF_10591	1.24	-	GNAT family acetyltransferase	Unclassified
OG1RF_10600	-0.64	-	Putative calcium-transporting atpase	Metabolism
OG1RF_10601	3.90	-	Potassium uptake protein	Metabolism
OG1RF_10605	-1.11	-	Aldo/keto reductase 2 family oxidoreductase	Metabolism
OG1RF_10607	0.72	*mutM*	DNA-formamidopyrimidine glycosylase	Metabolism
OG1RF_10612	0.66	-	Hypothetical protein	Hypothetical
OG1RF_10613	1.62	-	Hypothetical protein	Hypothetical
OG1RF_10614	2.46	-	Hypothetical protein	Hypothetical
OG1RF_10615	2.37	-	Group 2 glycosyl transferase	Metabolism
OG1RF_10616	2.02	-	Cellulose synthase catalytic subunit	Metabolism
OG1RF_10617	1.97	-	Hypothetical protein	Hypothetical
OG1RF_10618	1.88	-	Hypothetical protein	Hypothetical
OG1RF_10623	-1.04	-	Putative glycerol dehydrogenase	Metabolism
OG1RF_10626	1.37	-	Hypothetical protein	Hypothetical
OG1RF_10627	-2.08	*aad*	Aldehyde-alcohol dehydrogenase	Metabolism
OG1RF_10631	-0.75	*mvk*	Mevalonate kinase	Metabolism
OG1RF_10645	1.05	-	Integral membrane protein	Unclassified
OG1RF_10655	0.68	-	Glucose uptake protein	Metabolism
OG1RF_10656	1.02	-	Amino acid permease	transport
OG1RF_10657	-0.79	*metG*	Methionine--trna ligase	Transcription and translation
OG1RF_10660	-1.69	*rep*	ATP-dependent DNA helicase	DNA repair and recombination
OG1RF_10662	-0.71	-	Primase-like protein	Unclassified
OG1RF_10675	-0.69	*ung2*	Uracil-DNA glycosylase	Transcription and translation
OG1RF_10685	2.51	*rgfB*	Endonuclease/exonuclease/phosphatase family protein rgfb	Unclassified

Supplementary table C8 (*continued*.)				
OG1RF_10707	-2.52	-	DNA repair exonuclease	DNA repair and recombination
OG1RF_10712	1.12	*folD*	Bifunctional methylenetetrahydrofolate dehydrogenase/methylenetetrahydrofolate cyclohydrolase	Unclassified
OG1RF_10713	0.76	*xseA*	Exodeoxyribonuclease VII large subunit	DNA repair and recombination
OG1RF_10716	0.74	*hlyA*	Hemolysin A	Unclassified
OG1RF_10717	1.56	*argR3/ ahrC*	Arginine repressor	Signaling and regulation
OG1RF_10718	1.22	*recN*	DNA repair protein recn	DNA repair and recombination
OG1RF_10727	0.62	*murG*	UDP-N-acetylglucosamine-N-acetylmuramyl- (pentapeptide) pyrophosphoryl-undecaprenol N-acetylglucosamine transferase	Unclassified
OG1RF_10728	0.67	*ftsQ*	Cell division protein ftsq	Cell division/cell envelope
OG1RF_10739	-1.20	-	Hypothetical protein	Hypothetical
OG1RF_10740	-1.32	*sfsA*	Sugar fermentation stimulation protein	Metabolism
OG1RF_10753	-1.60	*bglA2*	6-phospho-beta-glucosidase	Metabolism
OG1RF_10754	-0.65	-	GNAT family acetyltransferase	Unclassified
OG1RF_10770	0.86	-	Aspartate aminotransferase	Unclassified
OG1RF_10772	-1.50	-	Cof family protein	Unclassified
OG1RF_10774	1.59	-	Xanthine/uracil permease family protein	Transport
OG1RF_10778	1.20	*pfkA*	6-phosphofructokinase	Metabolism
OG1RF_10780	1.93	-	Nucleic acid-binding protein	Transcription and translation
OG1RF_10784	1.10	*csrS*	Sensor histidine kinase csrs	Signaling and regulation
OG1RF_10811	0.81	*cna*	Collagen adhesion protein	Surface protein
OG1RF_10817	1.76	*malR*	Phage integrase family site-specific recombinase	DNA repair and recombination
OG1RF_10819	1.68	-	Membrane protein	Unclassified
OG1RF_10820	2.27	-	Lytr family response regulator	Signaling and regulation
OG1RF_10823	-0.89	-	ATP-binding nuclease	DNA repair and recombination
OG1RF_10824	-0.91	-	Uvrd/REP helicase	DNA repair and recombination
OG1RF_10825	-1.19	-	Hypothetical protein	Hypothetical
OG1RF_10832	-1.15	-	Phage integrase family site-specific recombinase	DNA repair and recombination
OG1RF_10840	1.78	-	Hypothetical protein	Hypothetical
OG1RF_10841	2.19	*traC*	Oligopeptide ABC superfamily ATP binding cassette transporter, binding protein	Transport
OG1RF_10852	0.67	*galR*	Galactose operon repressor galr	Signaling and regulation
OG1RF_10853	1.64	-	Hypothetical protein	Hypothetical
OG1RF_10858	1.94	-	MFS family major facilitator transporter	Transport
OG1RF_10875	1.14	-	Hypothetical protein	Hypothetical
OG1RF_10876	1.21	-	Hypothetical protein	Hypothetical
OG1RF_10890	-0.85	*rexB*	Exonuclease rexb	DNA repair and recombination
OG1RF_10891	-0.81	*addA*	ATP-dependent nuclease subunit A	DNA repair and recombination
OG1RF_10915	0.78	*dkgB*	2,5-diketo-D-gluconate reductase	Metabolism
OG1RF_10922	1.18	-	Hypothetical protein	Hypothetical

Supplementary table C8 (*continued*.)				
OG1RF_10927	0.54	-	Ypsa like protein	Unclassified
OG1RF_10929	1.39	-	Site-specific DNA-methyltransferase	DNA repair and recombination
OG1RF_10930	1.24	*taq*	Putative carboxypeptidase Taq	Unclassified
OG1RF_10931	1.25	*dnaD*	Putative DNA replication protein dnad	Transcription and translation
OG1RF_10932	1.35	*nth*	Endonuclease III	DNA repair and recombination
OG1RF_10947	-0.71	*rho*	Transcription termination factor Rho	Transcription and translation
OG1RF_10953	1.99	-	Oxygen-insensitive NADPH nitroreductase	Metabolism
OG1RF_10962	-2.23	-	Hypothetical protein	Hypothetical
OG1RF_10963	-2.18	-	Degv family protein	Unclassified
OG1RF_10966	-0.55	-	Sensor histidine kinase	Signaling and regulation
OG1RF_10968	-0.63	-	Hypothetical protein	Hypothetical
OG1RF_10974	-0.85	-	Hypothetical protein	Hypothetical
OG1RF_10975	-0.92	-	Crossover junction endodeoxyribonuclease	DNA repair and recombination
OG1RF_10976	-0.96	-	Hypothetical protein	Hypothetical
OG1RF_10984	-0.72	-	Transcriptional regulator	Signaling and regulation
OG1RF_10987	1.53	-	Hypothetical protein	Hypothetical
OG1RF_10993	1.73	-	Spermidine/putrescine ABC superfamily ATP binding cassette transporter	Transport
OG1RF_10994	2.15	*ade*	Adenine deaminase	Unclassified
OG1RF_10995	2.17	*mtaD*	Putative S-adenosylhomocysteine deaminase	Unclassified
OG1RF_11000	-2.65	-	M protein trans-acting positive regulator	Signaling and regulation
OG1RF_11001	-2.34	-	Hypothetical protein	Hypothetical
OG1RF_11014	1.38	*yckE*	Beta-glucosidase	Metabolism
OG1RF_11015	0.94	-	Gfo/Idh/moca family oxidoreductase	Metabolism
OG1RF_11022	1.24	-	ABC superfamily ATP binding cassette transporter, binding protein	Transport
OG1RF_11023	1.34	-	ABC superfamily ATP binding cassette transporter, membrane protein	Transport
OG1RF_11024	1.20	-	ABC superfamily ATP binding cassette transporter, ABC protein	Transport
OG1RF_11033	-0.59	-	Sulfatase	Unclassified
OG1RF_11034	-0.68	-	Methyltransferase	Unclassified
OG1RF_11036	-1.00	-	E1-E2 family cation-transporting atpase	Metabolism
OG1RF_11037	1.00	-	Cell wall surface anchor family protein	Surface protein
OG1RF_11046	-1.41	-	Hypothetical protein	Phage
OG1RF_11047	-1.37	-	Cro/CI family transcriptional regulator	Phage
OG1RF_11053	-1.81	-	Transposase	Phage
OG1RF_11054	-1.95	-	Hypothetical protein	Phage
OG1RF_11055	-1.97	-	TP901-1 family phage major tail protein	Phage
OG1RF_11056	-1.80	-	Hypothetical protein	Phage
OG1RF_11068	2.09	-	Hypothetical protein	Hypothetical
OG1RF_11073	-2.33	-	Lysr family transcriptional regulator	Signaling and regulation
OG1RF_11083	-0.77	*yhgF*	Yhgf like protein	Unclassified

Supplementary table C8 (continued.)				
OG1RF_11089	0.86	-	Hypothetical protein	Hypothetical
OG1RF_11090	1.10	-	Hypothetical protein	Hypothetical
OG1RF_11097	-1.72	-	Tetr family transcriptional regulator	Signaling and regulation
OG1RF_11101	-5.15	-	Yhge/Pip domain protein	Unclassified
OG1RF_11111	3.27	-	Hypothetical protein	Hypothetical
OG1RF_11131	1.67	-	ABC superfamily ATP binding cassette transporter, ABC protein	Transport
OG1RF_11132	0.88	-	Mar family transcriptional regulator	Signaling and regulation
OG1RF_11135	1.52	-	Sugar ABC superfamily ATP binding cassette transporter, sugar-binding protein	Transport
OG1RF_11140	-0.78	*mgtA2*	Magnesium-importing atpase	Unclassified
OG1RF_11146	0.93	*gldA*	Glycerol dehydrogenase	Metabolism
OG1RF_11148	0.76	*dhaK*	Dihydroxyacetone kinase	Metabolism
OG1RF_11150	1.13	-	Hypothetical protein	Hypothetical
OG1RF_11155	-0.98	*cspA*	Cold shock protein cspa	Unclassified
OG1RF_11156	1.12	-	Hypothetical protein	Hypothetical
OG1RF_11158	2.07	-	MFS family drug resistance transporter	Transport
OG1RF_11164	0.63	-	Vanz/RDD domain protein	Unclassified
OG1RF_11189	-1.45	*ziaA*	Zinc-exporting atpase	Transport
OG1RF_11190	-0.90	-	Hypothetical protein	Hypothetical
OG1RF_11191	-0.72	*cvpA*	Colicin V production protein cvpa family protein	Unclassified
OG1RF_11197	-0.74	-	ABC superfamily ATP binding cassette transporter, membrane protein	Transport
OG1RF_11200	-1.68	-	Hypothetical protein	Hypothetical
OG1RF_11207	-1.11	*atpF1*	V-type atpase, subunit F	Metabolism
OG1RF_11208	-1.01	*atpI*	Proton (H+) or sodium (Na+) translocating V-type atpase (V-atpase), subunit I	Metabolism
OG1RF_11209	-1.04	*atpK*	Proton (H+) or sodium (Na+) translocating V-type atpase (V-atpase), subunit K	Metabolism
OG1RF_11210	-1.14	*atpE*	Proton (H+) or sodium (Na+) translocating V-type atpase (V-atpase), subunit E	Metabolism
OG1RF_11211	-0.84	*atpC*	Proton (H+) or sodium (Na+) translocating V-type atpase (V-atpase), subunit C	Metabolism
OG1RF_11212	-1.10	*atpF2*	V-type ATP synthase subunit F	Metabolism
OG1RF_11213	-1.09	*atpA*	ATP synthase F1 subcomplex subunit alpha	Metabolism
OG1RF_11214	-1.12	*atpB*	Proton (H+) or sodium (Na+) translocating V-type atpase (V-atpase), subunit B	Metabolism
OG1RF_11215	-1.02	*atpD*	V-type ATP synthase subunit D	Metabolism
OG1RF_11216	-1.02	-	Hypothetical protein	Hypothetical

Supplementary table C8 (continued.)				
OG1RF_11219	1.05	-	Beta-lactamase	Cell division/cell envelope
OG1RF_11220	1.27	*fbp*	Fructose-1,6-bisphosphatase	Metabolism
OG1RF_11221	2.05	*lysA*	Diaminopimelate decarboxylase	Metabolism
OG1RF_11225	1.57	-	Hypothetical protein	Hypothetical
OG1RF_11231	0.78	*ptsG*	PTS family glucose porter, IICBA component	Transport
OG1RF_11239	-1.27	-	Transposon family protein	Unclassified
OG1RF_11241	0.82	*dnaG*	DNA primase	Transcription and translation
OG1RF_11242	0.70	*sigA*	RNA polymerase sigma factor siga	Transcription and translation
OG1RF_11252	-1.71	-	Hypothetical protein	Hypothetical
OG1RF_11253	-1.48	*tig2*	Peptidyl-prolyl isomerase	Unclassified
OG1RF_11255	0.78	-	Cell surface hydrolase	Cell division/cell envelope
OG1RF_11260	2.42	-	Brp/Blh family beta-carotene 15,15'-monooxygenase	Metabolism
OG1RF_11261	2.45	-	Hypothetical protein	Hypothetical
OG1RF_11263	1.32	-	Hypothetical protein	Hypothetical
OG1RF_11264	1.16	*recQ*	ATP-dependent helicase recq	DNA repair and recombination
OG1RF_11266	1.97	*cmk*	Cytidylate kinase	Unclassified
OG1RF_11267	0.93	*rpsA*	30S ribosomal protein S1	Transcription and translation
OG1RF_11269	-0.64	*hup*	DNA-binding protein HU	Transcription and translation
OG1RF_11270	1.08	-	Hypothetical protein	Hypothetical
OG1RF_11271	1.19	-	Hypothetical protein	Hypothetical
OG1RF_11272	1.19	-	IDEAL domain protein	Unclassified
OG1RF_11276	-0.64	*cca*	Trna adenylyltransferase	Unclassified
OG1RF_11280	2.17	*aroE*	Shikimate dehydrogenase	Metabolism
OG1RF_11281	2.60	*aroF*	Phospho-2-dehydro-3-deoxyheptonate aldolase	Metabolism
OG1RF_11282	1.84	*aroB*	3-dehydroquinate synthase	Metabolism
OG1RF_11283	1.62	*aroC*	Chorismate synthase	Metabolism
OG1RF_11284	1.09	*tyrA*	Prephenate dehydrogenase	Metabolism
OG1RF_11285	1.09	*aroA*	3-phosphoshikimate 1-carboxyvinyltransferase	Metabolism
OG1RF_11286	0.90	*aroK*	Shikimate kinase	Metabolism
OG1RF_11287	0.87	*pheA*	Prephenate dehydratase	Unclassified
OG1RF_11288	-0.61	*psr*	Transcriptional regulator	Signaling and regulation
OG1RF_11293	0.89	-	CPA1 family monovalent cation:proton (H+) antiporter-1	Transport
OG1RF_11297	-0.56	-	Iron-sulfur cluster-binding protein	Unclassified
OG1RF_11298	-1.21	*lexA*	Repressor lexa	Unclassified
OG1RF_11299	-0.83	-	Hypothetical protein	Hypothetical
OG1RF_11306	-1.21	-	Mutt/NUDIX family protein	Unclassified
OG1RF_11307	1.46	-	GNAT family acetyltransferase	Unclassified
OG1RF_11308	3.80	-	N-acetyltransferase	Unclassified
OG1RF_11310	2.17	-	Multidrug ABC superfamily ATP binding cassette transporter, ABC protein	Transport

Supplementary table C8 (continued.)				
OG1RF_11311	1.72	-	ABC superfamily ATP binding cassette transporter, ABC/membrane protein	Transport
OG1RF_11314	1.47	*katA*	Catalase	Unclassified
OG1RF_11315	0.88	*phrB*	Deoxyribodipyrimidine photolyase	Unclassified
OG1RF_11320	0.64	*scrR*	Sucrose operon repressor scrr	Signaling and regulation
OG1RF_11321	1.49	-	Hypothetical protein	Hypothetical
OG1RF_11322	1.11	*yckE2*	Beta-glucosidase	Unclassified
OG1RF_11323	1.49	*bglP2*	Phosphotransferase system (PTS) beta-glucoside-specific enzyme IIBCA component	Transport
OG1RF_11328	-1.26	*pflA*	Pyruvate formate-lyase activating enzyme	Unclassified
OG1RF_11329	-1.40	*pflB*	Formate acetyltransferase	Unclassified
OG1RF_11330	-0.77	*gyrA2*	DNA topoisomerase subunit A	Transcription and translation
OG1RF_11331	-0.75	*parE*	DNA topoisomerase (ATP-hydrolyzing) pare	Transcription and translation
OG1RF_11390	-1.39	-	Putative lipoprotein	Unclassified
OG1RF_11392	0.64	-	S41A family carboxy-terminal peptidase	Unclassified
OG1RF_11394	0.57	*msrA2*	Peptide-methionine-(S)-S-oxide reductase	Unclassified
OG1RF_11398	1.76	*hlyIII*	Hemolysin III	Unclassified
OG1RF_11401	-0.68	*recJ*	Single-stranded-DNA-specific exonuclease recj	DNA repair and recombination
OG1RF_11411	0.85	*ffh*	Signal recognition particle protein	Unclassified
OG1RF_11412	0.77	-	Transcriptional regulator	Signaling and regulation
OG1RF_11420	-0.89	-	Gntr family sugar-binding transcriptional regulator	Signaling and regulation
OG1RF_11430	1.42	*pyrB*	Aspartate carbamoyltransferase	Unclassified
OG1RF_11431	1.35	*pyrP*	NCS family uracil:cation symporter	Transport
OG1RF_11432	1.71	*upp*	Uracil phosphoribosyltransferase	Unclassified
OG1RF_11436	0.62	*fhs*	Formate--tetrahydrofolate ligase	Unclassified
OG1RF_11437	2.47	*cspA2*	Cold shock protein cspa	Unclassified
OG1RF_11438	1.29	*ebsa*	Ebsa protein	Unclassified
OG1RF_11439	-0.97	*rnhA*	Ribonuclease HI	DNA repair and recombination
OG1RF_11442	0.84	*mdlB*	Multidrug ABC superfamily ATP binding cassette transporter, ABC protein	Transport
OG1RF_11443	0.97	*mdlA*	Multidrug ABC superfamily ATP binding cassette transporter, ABC protein	Transport
OG1RF_11444	0.74	*yneF*	Hypothetical protein	Hypothetical
OG1RF_11456	1.00	-	Methyl-accepting chemotaxis family protein	Unclassified
OG1RF_11457	-0.86	*cap4C*	UTP--glucose-1-phosphate uridylyltransferase	Unclassified
OG1RF_11458	-0.85	*gpsA*	Glycerol-3-phosphate dehydrogenase (NAD(P) (+))	Metabolism
OG1RF_11486	1.95	-	Hypothetical protein	Hypothetical

Supplementary table C8 (continued.)

OG1RF_11502	-1.06	*oppA2*	Oligopeptide ABC superfamily ATP binding cassette transporter, binding protein	Transport
OG1RF_11505	1.02	-	Hypothetical protein	Hypothetical
OG1RF_11519	3.02	*gspA1*	General stress protein A	Unclassified
OG1RF_11520	2.85	*gspA2*	General stress protein A	Unclassified
OG1RF_11523	1.23	-	Lysr family transcriptional regulator	Signaling and regulation
OG1RF_11525	1.71	*sprE*	Spre protein	Signaling and regulation
OG1RF_11526	1.84	*gelE*	Gelatinase	Signaling and regulation
OG1RF_11527	2.20	*fsrC*	Sensor histidine kinase fsrc	Signaling and regulation
OG1RF_11528	2.15	*fsrB*	Fsrb protein	Signaling and regulation
OG1RF_11529	1.26	*fsrA*	Fsra response regulator	Signaling and regulation
OG1RF_11544	0.98	*ntcA2*	Global nitrogen regulator ntca	Signaling and regulation
OG1RF_11573	1.24	*murC*	UDP-N-acetylmuramate--L-alanine ligase	Cell division/cell envelope
OG1RF_11580	1.07	*ysxC*	Ribosome biogenesis GTP-binding protein ysxc	Transcription and translation
OG1RF_11581	1.06	*clpX*	ATP-dependent Clp protease ATP-binding subunit	Unclassified
OG1RF_11594	0.81	-	Pyridine nucleotide-disulfide family oxidoreductase	Unclassified
OG1RF_11598	1.70	*yedF*	PTS family porter component IIABC	Transport
OG1RF_11599	1.11	-	Gntr family transcriptional regulator	Signaling and regulation
OG1RF_11600	-1.24	-	Hypothetical protein	Hypothetical
OG1RF_11601	1.49	-	GNAT family acetyltransferase	Unclassified
OG1RF_11602	0.69	-	Putative calcium-transporting atpase	Metabolism
OG1RF_11605	1.38	-	Hypothetical protein	Hypothetical
OG1RF_11606	0.98	-	Bicyclomycin resistance protein	Unclassified
OG1RF_11607	0.85	-	Membrane-oligosaccharide glycerophosphotransferase	Metabolism
OG1RF_11627	1.91	*cggR*	Central glycolytic genes regulator	Signaling and regulation
OG1RF_11628	1.04	-	Yitt family protein	Unclassified
OG1RF_11629	1.87	*ywlG*	Hypothetical protein	Hypothetical
OG1RF_11630	2.18	-	Hypothetical protein	Hypothetical
OG1RF_11631	2.42	-	Putative phosphomethylpyrimidine kinase	Unclassified
OG1RF_11633	0.71	*hisS*	Histidine-trna ligase	Transcription and translation
OG1RF_11634	1.62	-	Hypothetical protein	Hypothetical
OG1RF_11635	0.61	*dtd*	D-tyrosyl-trna(Tyr) deacylase	Unclassified
OG1RF_11636	0.64	*relA*	GTP diphosphokinase	Metabolism
OG1RF_11637	-0.75	-	Rsme family RNA methyltransferase	Unclassified
OG1RF_11641	-1.18	*rarA*	Replication-associated recombination protein A	DNA repair and recombination
OG1RF_11642	2.79	-	Hypothetical protein	Hypothetical
OG1RF_11644	-0.65	*ackA*	Acetate kinase	Metabolism
OG1RF_11653	1.05	-	Amino acid permease	Transport
OG1RF_11655	-1.58	-	Cfr family radical SAM enzyme	Unclassified
OG1RF_11656	-1.00	-	ABC superfamily ATP binding cassette transporter, permease protein	Transport

Supplementary table C8 (continued.)				
OG1RF_11657	-1.00	-	ABC superfamily ATP binding cassette transporter, ABC protein	Transport
OG1RF_11661	0.62	*ubiA*	1,4-dihydroxy-2-naphthoate octaprenyltransferase	Unclassified
OG1RF_11663	1.35	-	ABC superfamily ATP binding cassette transporter, ABC/membrane protein	Transport
OG1RF_11664	1.38	-	ABC superfamily ATP binding cassette transporter, ABC/membrane protein	Transport
OG1RF_11669	1.37	-	Superoxide dismutase	DNA repair and recombination
OG1RF_11672	1.16	-	Major facilitator family transporter	Transport
OG1RF_11673	1.22	*trmU*	Trna (5-methyl aminomethyl-2-thiouridylate)-methyltransferase	Unclassified
OG1RF_11689	0.68	-	Hypothetical protein	Hypothetical
OG1RF_11690	1.06	-	Hypothetical protein	Hypothetical
OG1RF_11691	0.91	-	Femab family peptidoglycan biosynthesis protein	Cell division/cell envelope
OG1RF_11693	0.97	-	Cobalt (Co2+) ABC superfamily ATP binding cassette transporter, membrane protein	Transport
OG1RF_11694	0.90	-	ABC superfamily ATP binding cassette transporter, ABC protein	Transport
OG1RF_11695	1.21	-	Hypothetical protein	Hypothetical
OG1RF_11699	-1.10	*nifJ*	Pyruvate:ferredoxin oxidoreductase	Metabolism
OG1RF_11705	0.65	*glpQ*	Glycerophosphodiester phosphodiesterase	Metabolism
OG1RF_11722	0.67	-	Hypothetical protein	Hypothetical
OG1RF_11723	0.55	-	Brp/Blh family beta-carotene 15,15'-monooxygenase	Unclassified
OG1RF_11732	-0.51	*rmlB*	Dtdp glucose 4,6-dehydratase	Metabolism
OG1RF_11742	1.85	-	Transcriptional regulator tspo	Signaling and regulation
OG1RF_11747	-0.98	-	Fis family DNA-binding protein	Signaling and regulation
OG1RF_11748	-1.10	*phzF2*	Phenazine biosynthesis protein phzf family protein	Unclassified
OG1RF_11751	-0.89	-	Hypothetical protein	Hypothetical
OG1RF_11753	1.84	*treB*	PTS family trehalose porter, IIBC component	Transport
OG1RF_11758	0.76	-	Arac family DNA-binding response regulator	Signaling and regulation
OG1RF_11766	-3.84	-	Multidrug ABC superfamily ATP binding cassette transporter, ABC protein	Transport
OG1RF_11767	-3.36	-	ABC superfamily ATP binding cassette transporter, membrane protein	Transport
OG1RF_11768	-1.38	*trpS*	Tryptophan--trna ligase	Transcription and translation
OG1RF_11793	-1.22	*clpB*	Chaperone protein clpb	Protease/ Chaperone
OG1RF_11794	4.93	-	Hypothetical protein	Hypothetical
OG1RF_11795	0.76	*purB*	Adenylosuccinate lyase	Metabolism
OG1RF_11796	0.70	*purK2*	Phosphoribosylaminoimidazole carboxylase atpase subunit purk	Metabolism
OG1RF_11797	4.01	*pbuX*	Xanthine permease	Metabolism
OG1RF_11798	4.17	*xpt*	Xanthine phosphoribosyltransferase	Metabolism

Supplementary table C8 (continued.)				
OG1RF_11822	-1.01	-	ATP-binding protein	Unclassified
OG1RF_11823	-1.52	-	Methyltransferase	Metabolism
OG1RF_11825	-0.88	*sufB*	ABC superfamily ATP binding cassette transporter, membrane protein	Transport
OG1RF_11826	-0.79	-	Nifu family SUF system fes assembly protein	Unclassified
OG1RF_11827	-0.79	*csd*	Selenocysteine lyase/cysteine desulfurase	Unclassified
OG1RF_11828	-0.55	*sufD*	Iron-sulfur ABC superfamily ATP binding cassette transporter, membrane protein	Transport
OG1RF_11830	0.93	*frr*	Ribosome recycling factor	Transcription and translation
OG1RF_11831	0.92	*pyrH*	UMP kinase	Unclassified
OG1RF_11832	0.66	*tsf*	Elongation factor EF1B	Transcription and translation
OG1RF_11833	0.86	*rpsB*	30S ribosomal protein S2	Transcription and translation
OG1RF_11849	0.91	*zurR*	Fur family transcriptional regulator zurr	Signaling and regulation
OG1RF_11850	-2.04	-	Hypothetical protein	Hypothetical
OG1RF_11856	-0.68	*pgcA*	Bifunctional phosphoglucomutase/phosphomannomutase	Unclassified
OG1RF_11860	0.86	*guaC*	GMP reductase	Unclassified
OG1RF_11863	-0.83	-	Metallo-beta-lactamase superfamily protein	Cell division/cell envelope
OG1RF_11869	1.55	-	PTS system transporter subunit IIA	Transport
OG1RF_11871	-1.54	-	Hypothetical protein	Hypothetical
OG1RF_11892	-0.75	*typA*	GTP-binding protein typa/bipa	Unclassified
OG1RF_11895	1.65	-	Voltage-gated chloride channel family protein	Metabolism
OG1RF_11903	1.81	*gcp*	O-sialoglycoprotein endopeptidase	Unclassified
OG1RF_11904	1.62	*rimI*	Ribosomal-protein-alanine acetyltransferase	Unclassified
OG1RF_11905	1.77	*rimI2*	Ribosomal-protein-alanine acetyltransferase	Unclassified
OG1RF_11907	-0.56	*pbp4*	Penicillin-binding protein 4	Cell division/cell envelope
OG1RF_11908	-0.59	-	Hypothetical protein	Hypothetical
OG1RF_11916	0.86	*metQ*	ABC superfamily ATP binding cassette transporter, binding protein	Transport
OG1RF_11917	0.97	*metI*	Metal ion ABC superfamily ATP binding cassette transporter, membrane protein	Transport
OG1RF_11918	0.94	*metN*	ABC superfamily ATP binding cassette transporter, ABC protein	Transport
OG1RF_11921	-0.52	*ftsW2*	Ftsw/roda/spove family cell division protein	Cell division/cell envelope
OG1RF_11922	1.98	-	M protein trans-acting positive regulator	Signaling and regulation
OG1RF_11923	1.90	-	Hypothetical protein	Hypothetical
OG1RF_11925	2.54	-	Hypothetical protein	Hypothetical
OG1RF_11926	2.51	-	Cro/CI family transcriptional regulator	Signaling and regulation
OG1RF_11930	0.88	-	Hypothetical protein	Hypothetical
OG1RF_11951	-1.43	-	Selenium-dependent molybdenum hydroxylase 1	Unclassified

Supplementary table C8 (continued.)				
OG1RF_11958	-2.93	*ygeY*	M20/dape family protein ygey	Unclassified
OG1RF_11963	0.78	-	Putative transcriptional regulator	Signaling and regulation
OG1RF_11969	0.88	*ampC*	Beta-lactamase	Cell division/cell envelope
OG1RF_11971	1.07	-	Multidrug resistance ABC superfamily ATP binding cassette transporter, membrane protein	Transport
OG1RF_11972	1.54	-	Multidrug resistance ABC superfamily ATP binding cassette transporter, ABC/membrane protein	Transport
OG1RF_11973	1.37	-	Tetr family transcriptional regulator	Signaling and regulation
OG1RF_11976	1.19	*bglF*	PTS system transporter subunit I	Transport
OG1RF_11977	2.18	*licT2*	Transcription antiterminator lict	Unclassified
OG1RF_12000	-0.76	*nadE2*	NAD (+) synthase	Metabolism
OG1RF_12001	-0.74	-	Nicotinate phosphoribosyltransferase	Unclassified
OG1RF_12013	-1.87	*opuAA 2*	Glycine betaine/L-proline ABC superfamily ATP binding cassette transporter, ABC protein	Transport
OG1RF_12014	-1.64	-	Glycine betaine/carnitine/choline ABC superfamily ATP binding cassette transporter	Transport
OG1RF_12022	1.29	*potC*	Spermidine/putrescine ABC superfamily ATP binding cassette transporter, membrane protein	Transport
OG1RF_12023	0.96	*potB*	Spermidine/putrescine ABC superfamily ATP binding cassette transporter, membrane protein	Transport
OG1RF_12024	0.92	*potA*	Spermidine/putrescine ABC superfamily ATP binding cassette transporter, ABC protein	Transport
OG1RF_12025	0.80	-	Cro/CI family transcriptional regulator	Signaling and regulation
OG1RF_12031	1.57	-	Integral membrane protein	Unclassified
OG1RF_12035	0.84	-	RNA methyltransferase	Transcription and translation
OG1RF_12042	0.81	*cyaA*	Adenylate cyclase	Unclassified
OG1RF_12047	1.39	*spxA*	Regulatory protein Spx	Signaling and regulation
OG1RF_12049	1.17	*lmrA*	Multidrug resistance ABC transporter ATP-binding and permease	Transport
OG1RF_12050	-1.92	-	HAD-superfamily hydrolase	Cell division/cell envelope
OG1RF_12056	-0.69	-	Hypothetical protein	Hypothetical
OG1RF_12057	-0.54	-	Snf2 family protein	Unclassified
OG1RF_12058	-0.75	*sbcC*	Exonuclease sbcc	DNA repair and recombination
OG1RF_12059	-0.76	*sbcD*	Exonuclease sbcd	DNA repair and recombination
OG1RF_12063	-0.72	*mtnN*	MTA/SAH nucleosidase	Metabolism
OG1RF_12064	-1.25	-	Hypothetical protein	Hypothetical
OG1RF_12065	-1.05	*nudF*	ADP-ribose diphosphatase	Metabolism
OG1RF_12066	-1.06	-	Hypothetical protein	Hypothetical
OG1RF_12067	-0.60	*telA*	Tellurite resistance protein	Unclassified
OG1RF_12068	-1.01	-	Mutt/NUDIX family protein	Unclassified

Supplementary table C8 (continued.)				
OG1RF_12070	1.73	-	Hypothetical protein	Hypothetical
OG1RF_12079	-1.51	-	Brp/Blh family beta-carotene 15,15'-monooxygenase	Unclassified
OG1RF_12081	-0.51	*rplJ*	50S ribosomal protein L10	Transcription and translation
OG1RF_12091				
OG1RF_12096	0.87	-	Membrane protein	Unclassified
OG1RF_12102	-1.83	*trxB2*	Thioredoxin-disulfide reductase	Unclassified
OG1RF_12103	-1.59	*ahpC*	Peroxiredoxin	Unclassified
OG1RF_12105	-0.72	*lplA2*	Lipoate-protein ligase	Unclassified
OG1RF_12106	-0.59	-	Metallo-beta-lactamase	Cell division/cell envelope
OG1RF_12112	-0.66	*dltA*	D-alanine--D-alanine ligase	Cell division/cell envelope
OG1RF_12115	-1.79	*nrdD*	Anaerobic ribonucleoside-triphosphate reductase large subunit	Unclassified
OG1RF_12116	-1.50	*nrdG*	Pyruvate formate-lyase activating enzyme	Unclassified
OG1RF_12117	-1.74	*dinB*	DNA-directed DNA polymerase IV	Transcription and translation
OG1RF_12121	0.80	*yabA*	Initiation-control protein yaba	Unclassified
OG1RF_12122	0.76	*yaaT*	Stage 0 sporulation protein yaat	Unclassified
OG1RF_12123	0.54	*holB*	DNA-directed DNA polymerase III subunit delta	Transcription and translation
OG1RF_12127	2.30	*tenA*	Thiaminase	Metabolism
OG1RF_12128	2.33	-	Cobalt transporter	Transport
OG1RF_12129	1.99	-	ABC superfamily ATP binding cassette transporter, ABC protein	Transport
OG1RF_12130	3.07	-	ABC superfamily ATP binding cassette transporter, membrane protein	Transport
OG1RF_12132	1.80	*yniG*	Emrb/qaca family drug resistance transporter	Transport
OG1RF_12135	2.70	*thiD2*	Phosphomethylpyrimidine kinase	Unclassified
OG1RF_12136	2.53	*thiE*	Thiamine-phosphate diphosphorylase	Unclassified
OG1RF_12138	1.93	*thiW*	Thiw protein	Transport
OG1RF_12141	-0.73	-	Galactose-1-phosphate uridylyltransferase	Unclassified
OG1RF_12155	1.76	-	Brp/Blh family beta-carotene 15,15'-monooxygenase	Unclassified
OG1RF_12158	-1.51	*penA*	Penicillin-binding protein 2B	Cell division/cell envelope
OG1RF_12178	0.84	*accA*	Acetyl-coa carboxylase carboxyl transferase subunit alpha	Metabolism
OG1RF_12179	0.83	*accD*	Acetyl-coa carboxylase carboxyl transferase subunit beta	Metabolism
OG1RF_12180	0.70	*accC*	Acetyl-coa carboxylase subunit A	Metabolism
OG1RF_12181	1.01	*fabZ2*	(3R)-hydroxymyristoyl-ACP dehydratase	Metabolism
OG1RF_12183	1.04	*fabF2*	Beta-ketoacyl-acyl-carrier-protein synthase II	Metabolism
OG1RF_12184	1.19	*fabG3*	3-oxoacyl-ACP reductase	Metabolism

Supplementary table C8 (continued.)

OG1RF_12185	1.19	*fabD*	Malonyl-coa-[acyl-carrier-protein] transacylase	Metabolism
OG1RF_12186	1.41	*fabK*	Enoyl-ACP reductase	Metabolism
OG1RF_12188	1.34	*fabH*	Beta-ketoacyl-acyl-carrier-protein synthase III	Metabolism
OG1RF_12189	0.82	-	Marr family transcriptional regulator	Signaling and regulation
OG1RF_12195	1.27	-	Hypothetical protein	Hypothetical
OG1RF_12196	-0.84	*yugI*	General stress protein 13	Unclassified
OG1RF_12200	2.61	*trxB3*	Thioredoxin-disulfide reductase	Metabolism
OG1RF_12225	0.67	*cspA3*	Cold shock protein cspa	Unclassified
OG1RF_12229	1.04	-	Hypothetical protein	Hypothetical
OG1RF_12254	-0.79	-	Amidinotransferase	Unclassified
OG1RF_12267	-1.87	-	Permease protein	Transport
OG1RF_12268	-1.96	-	ABC superfamily ATP binding cassette transporter, ABC protein	Transport
OG1RF_12269	-2.47	-	RND transporter	Transport
OG1RF_12271	-1.41	*cdr*	Coa-disulfide reductase	Unclassified
OG1RF_12297	-0.66	*truA2*	Trna-pseudouridine synthase I	Unclassified
OG1RF_12304	-1.69	-	Alpha/beta knot family protein	Unclassified
OG1RF_12306	-0.56	-	Trna binding domain-containing protein	Unclassified
OG1RF_12307	-0.62	-	Universal stress protein	Unclassified
OG1RF_12309	-0.75	*pepA2*	Glutamyl aminopeptidase	Unclassified
OG1RF_12311	-0.65	*traC2*	Peptide ABC superfamily ATP binding cassette transporter, binding protein	Transport
OG1RF_12322	-1.21	-	Hypothetical protein	Hypothetical
OG1RF_12323	1.55	-	Hypothetical protein	Hypothetical
OG1RF_12324	1.18	-	PTT family thiamin transporter	Transport
OG1RF_12331	1.30	-	Lipase	Unclassified
OG1RF_12337	-0.82	-	Hydrolase	Cell division/cell envelope
OG1RF_12349	2.40	*pepT2*	Tripeptide aminopeptidase	Unclassified
OG1RF_12350	2.04	-	Oligopeptide ABC superfamily ATP binding cassette transporter, binding protein	Transport
OG1RF_12362	-0.85	*ftsY*	Cell division protein ftsy	Cell division/cell envelope
OG1RF_12368	-1.14	-	Oligopeptide ABC superfamily ATP binding cassette transporter, membrane protein	Transport
OG1RF_12370	-1.10	-	ABC superfamily ATP binding cassette transporter, ABC protein	Transport
OG1RF_12391	0.93	*gmk2*	Guanylate kinase	Unclassified
OG1RF_12392	-1.08	-	Serine-type D-Ala-D-Ala carboxypeptidase	Unclassified
OG1RF_12394	-1.08	-	Yicc like protein	Unclassified
OG1RF_12395	-1.05	-	Hypothetical protein	Hypothetical
OG1RF_12405	4.81	*gnd2*	6-phosphogluconate dehydrogenase	Unclassified
OG1RF_12417	0.54	-	Hypothetical protein	Hypothetical
OG1RF_12425	1.64	*trePP*	Glycosyl hydrolase	Metabolism
OG1RF_12426	1.51	*yvdM*	Beta-phosphoglucomutase	Metabolism

Supplementary table C8 (continued.)				
OG1RF_12432	1.06	*msrB*	Peptide-methionine (R)-S-oxide reductase	Unclassified
OG1RF_12438	1.24	*ymdA*	2',3'-cyclic-nucleotide 2'-phosphodiesterase	Unclassified
OG1RF_12442	1.48	-	FMN reductase	Unclassified
OG1RF_12450	1.02	-	Hypothetical protein	Hypothetical
OG1RF_12452	-1.06	*ubiD*	Ubid family decarboxylase	Surface protein
OG1RF_12454	-1.06	*ubiD2*	Ubid family decarboxylase	Surface protein
OG1RF_12466	1.48	-	ABC superfamily ATP binding cassette transporter, ABC protein	Transport
OG1RF_12473	1.80	-	Dihydrouridine synthase	Unclassified
OG1RF_12475	1.55	-	ABC superfamily ATP binding cassette transporter, ABC protein	Transport
OG1RF_12476	2.00	-	PTS family fructose/mannitol (fru) porter component IIA	Transport
OG1RF_12477	1.72	-	PTS family ascorbate porter, IIB component	Transport
OG1RF_12484	1.21	-	Hypothetical protein	Hypothetical
OG1RF_12485	0.49	-	Phosphatidylglycerol--membrane-oligosaccharide glycerophosphotransferase	Unclassified
OG1RF_12487	-0.76	*rplM*	50S ribosomal protein L13	Transcription and translation
OG1RF_12489	-1.07	-	Putative lipoprotein	Unclassified
OG1RF_12490	-1.16	*gntK*	Gluconokinase	Metabolism
OG1RF_12499	0.79	-	Chitin binding protein	Unclassified
OG1RF_12500	-3.23	-	Cell-envelope associated acid phosphatase	Signaling and regulation
OG1RF_12505	-1.02	-	Hypothetical protein	Hypothetical
OG1RF_12508	-0.83	-	Thiamine biosynthesis lipoprotein	Unclassified
OG1RF_12520	1.21	-	Hypothetical protein	Hypothetical
OG1RF_12521	1.20	-	Cro/CI family zinc-binding transcriptional regulator	Signaling and regulation
OG1RF_12522	1.26	-	Hypothetical protein	Hypothetical
OG1RF_12529	1.04	-	Brp/Blh family beta-carotene 15,15'-monooxygenase	Unclassified
OG1RF_12534	-1.49	-	Rpir family transcriptional regulator	Signaling and regulation
OG1RF_12535	-1.22	*croR*	Response regulator	Signaling and regulation
OG1RF_12536	-2.19	*croS*	Sensor histidine kinase	Signaling and regulation
OG1RF_12538	0.81	*guaB*	IMP dehydrogenase	Metabolism
OG1RF_12539	0.63	-	Hypothetical protein	Hypothetical
OG1RF_12547	0.86	*mycA*	Myosin-cross-reactive antigen	Unclassified
OG1RF_12551	-1.40	*srlE*	PTS family glucitol/sorbitol porter, IIB component	Transport
OG1RF_12573	1.10	-	Gntr family transcriptional regulator	Signaling and regulation
Manual annotation in red.				

REFERENCES

Agudelo Higuita, N. I. and M. M. Huycke (2014). Enterococcal Disease, Epidemiology, and Implications for Treatment. Enterococci: From Commensals to Leading Causes of Drug Resistant Infection. M. S. Gilmore, D. B. Clewell, Y. Ike and N. Shankar. Boston.

Ahn, S. J., J. A. C. Lemos and R. A. Burne (2005). "Role of HtrA in growth and competence of Streptococcus mutans UA159." Journal of Bacteriology **187**(9): 3028-3038.

Alonzo, F., 3rd, B. Xayarath, J. C. Whisstock and N. E. Freitag (2011). "Functional analysis of the Listeria monocytogenes secretion chaperone PrsA2 and its multiple contributions to bacterial virulence." Mol Microbiol **80**(6): 1530-1548.

Anders, S., P. T. Pyl and W. Huber (2015). "HTSeq--a Python framework to work with high-throughput sequencing data." Bioinformatics **31**(2): 166-169.

Asai, K., Kawamura, F., Sadaie, Y., & Takahashi, H. (1997). Isolation and characterization of a sporulation initiation mutation in the Bacillus subtilis secA gene. Journal of Bacteriology, **179**(2), 544-547. doi:DOI 10.1128/jb.179.2.544-547.1997

Backert, S., Bernegger, S., Skorko-Glonek, J., & Wessler, S. (2018). Extracellular HtrA serine proteases: An emerging new strategy in bacterial pathogenesis. Cell Microbiol, **20**(6), e12845. doi:10.1111/cmi.12845

Baek, K. T., C. S. Vegge and L. Brondsted (2011). "HtrA chaperone activity contributes to host cell binding in Campylobacter jejuni." Gut Pathog **3**: 13.

Bakker, D., A. M. Buckley, A. de Jong, V. J. van Winden, J. P. Verhoeks, O. P. Kuipers, G. R. Douce, E. J. Kuijper, W. K. Smits and J. Corver (2014). "The HtrA-like protease CD3284 modulates virulence of Clostridium difficile." Infect Immun **82**(10): 4222-4232.

Banerjee, A. and I. Biswas (2008). "Markerless multiple-gene-deletion system for Streptococcus mutans." Appl Environ Microbiol **74**(7): 2037-2042.

Barakat, M., P. Ortet, C. Jourlin-Castelli, M. Ansaldi, V. Mejean and D. E. Whitworth (2009). "P2CS: a two-component system resource for prokaryotic signal transduction research." Bmc Genomics **10**.

Barbieri, C. M. and A. M. Stock (2008). "Universally applicable methods for monitoring response regulator aspartate phosphorylation both in vitro and in vivo using Phos-tag-based reagents." Anal Biochem **376**(1): 73-82.

Baumler, A. J., J. G. Kusters, I. Stojiljkovic and F. Heffron (1994). "Salmonella typhimurium loci involved in survival within macrophages." Infect Immun **62**(5): 1623-1630.

Bendezu, F. O. and P. A. de Boer (2008). "Conditional lethality, division defects, membrane involution, and endocytosis in mre and mrd shape mutants of Escherichia coli." J Bacteriol **190**(5): 1792-1811.

Biswas, S. and I. Biswas (2005). "Role of HtrA in surface protein expression and biofilm formation by Streptococcus mutans." Infect Immun **73**(10): 6923-6934.

Boehm, M., J. Lind, S. Backert and N. Tegtmeyer (2015). "Campylobacter jejuni serine protease HtrA plays an important role in heat tolerance, oxygen resistance, host cell adhesion, invasion, and transmigration." Eur J Microbiol Immunol (Bp) **5**(1): 68-80.

Boucher, J. C., J. Martinez-Salazar, M. J. Schurr, M. H. Mudd, H. Yu and V. Deretic (1996). "Two distinct loci affecting conversion to mucoidy in Pseudomonas aeruginosa in cystic fibrosis encode homologs of the serine protease HtrA." J Bacteriol **178**(2): 511-523.

Boucher, P. E., Murakami, K., Ishihama, A., & Stibitz, S. (1997). Nature of DNA binding and RNA polymerase interaction of the Bordetella pertussis BvgA transcriptional activator at the fha promoter. J Bacteriol, **179**(5), 1755-1763.

Bourgogne, A., D. A. Garsin, X. Qin, K. V. Singh, J. Sillanpaa, S. Yerrapragada, Y. Ding, S. Dugan-Rocha, C. Buhay, H. Shen, G. Chen, G. Williams, D. Muzny, A. Maadani, K. A. Fox, J. Gioia, L. Chen, Y. Shang, C. A. Arias, S. R. Nallapareddy, M. Zhao, V. P. Prakash, S. Chowdhury, H. Jiang, R. A. Gibbs, B. E. Murray, S. K. Highlander and G. M. Weinstock (2008). "Large scale variation in Enterococcus faecalis illustrated by the genome analysis of strain OG1RF." Genome Biol **9**(7): R110.

Bourgogne, A., S. G. Hilsenbeck, G. M. Dunny and B. E. Murray (2006). "Comparison of OG1RF and an isogenic fsrB deletion mutant by transcriptional analysis: the Fsr system of Enterococcus faecalis is more than the activator of gelatinase and serine protease." J Bacteriol **188**(8): 2875-2884.

Bourgogne, A., K. V. Singh, K. A. Fox, K. J. Pflughoeft, B. E. Murray and D. A. Garsin (2007). "EbpR is important for biofilm formation by activating expression of the endocarditis and biofilm-associated pilus operon (ebpABC) of Enterococcus faecalis OG1RF." J Bacteriol **189**(17): 6490-6493.

Bourgogne, A., L. C. Thomson and B. E. Murray (2010). "Bicarbonate enhances expression of the endocarditis and biofilm associated pilus locus, ebpR-ebpABC, in Enterococcus faecalis." BMC Microbiol **10**: 17.

Brunskill, E. W. and K. W. Bayles (1996). "Identification of LytSR-regulated genes from Staphylococcus aureus." J Bacteriol **178**(19): 5810-5812.

Burton, M. J. and D. C. Mabey (2009). "The global burden of trachoma: a review." PLoS Negl Trop Dis **3**(10): e460.

Caparon, M. G., R. T. Geist, J. Perez-Casal and J. R. Scott (1992). "Environmental regulation of virulence in group A streptococci: transcription of the gene encoding M protein is stimulated by carbon dioxide." J Bacteriol **174**(17): 5693-5701.

Capra, E. J. and M. T. Laub (2012). "Evolution of two-component signal transduction systems." Annu Rev Microbiol **66**: 325-347.

Champion, O. L., A. V. Karlyshev, N. J. Senior, M. Woodward, R. La Ragione, S. L. Howard, B. W. Wren and R. W. Titball (2010). "Insect infection model for Campylobacter jejuni reveals that O-methyl phosphoramidate has insecticidal activity." J Infect Dis **201**(5): 776-782.

Chakraborty, S., & Kenney, L. J. (2018). A New Role of OmpR in Acid and Osmotic Stress in Salmonella and E. coli. Front Microbiol, **9**, 2656. doi:10.3389/fmicb.2018.02656

Chakraborty, S., Winardhi, R. S., Morgan, L. K., Yan, J., & Kenney, L. J. (2017). Non-canonical activation of OmpR drives acid and osmotic stress responses in single bacterial cells. Nat Commun, 8(1), 1587.

Chatfield, S. N., K. Strahan, D. Pickard, I. G. Charles, C. E. Hormaeche and G. Dougan (1992). "Evaluation of Salmonella typhimurium strains harbouring defined mutations in htrA and aroA in the murine salmonellosis model." Microb Pathog **12**(2): 145-151.

Clausen, T., Kaiser, M., Huber, R., & Ehrmann, M. (2011). HTRA proteases: regulated proteolysis in protein quality control. Nat Rev Mol Cell Biol, 12(3), 152-162. doi:10.1038/nrm3065

Chitlaru, T., G. Zaide, S. Ehrlich, I. Inbar, O. Cohen and A. Shafferman (2011). "HtrA is a major virulence determinant of Bacillus anthracis." Mol Microbiol **81**(6): 1542-1559.

Cho, H., T. Uehara and T. G. Bernhardt (2014). "Beta-lactam antibiotics induce a lethal malfunctioning of the bacterial cell wall synthesis machinery." Cell **159**(6): 1300-1311.

Chong, K. K. L., W. H. Tay, B. Janela, A. M. H. Yong, T. H. Liew, L. Madden, D. Keogh, T. M. S. Barkham, F. Ginhoux, D. L. Becker and K. A. Kline (2017). "Enterococcus faecalis Modulates Immune Activation and Slows Healing During Wound Infection." J Infect Dis **216**(12): 1644-1654.

Citron, D. M., E. J. Goldstein, C. V. Merriam, B. A. Lipsky and M. A. Abramson (2007). "Bacteriology of moderate-to-severe diabetic foot infections and in vitro activity of antimicrobial agents." J Clin Microbiol **45**(9): 2819-2828.

Clausen, T., M. Kaiser, R. Huber and M. Ehrmann (2011). "HTRA proteases: regulated proteolysis in protein quality control." Nat Rev Mol Cell Biol **12**(3): 152-162.

Cole, J. N., J. A. Aquilina, P. G. Hains, A. Henningham, K. S. Sriprakash, M. G. Caparon, V. Nizet, M. Kotb, S. J. Cordwell, S. P. Djordjevic and M. J. Walker (2007). "Role of group A Streptococcus HtrA in the maturation of SpeB protease." Proteomics **7**(24): 4488-4498.

Coleman, J. L., J. T. Crowley, A. M. Toledo and J. L. Benach (2013). "The HtrA protease of Borrelia burgdorferi degrades outer membrane protein BmpD and chemotaxis phosphatase CheX." Mol Microbiol **88**(3): 619-633.

Comenge, Y., R. Quintiliani, Jr., L. Li, L. Dubost, J. P. Brouard, J. E. Hugonnet and M. Arthur (2003). "The CroRS two-component regulatory system is required for intrinsic beta-lactam resistance in Enterococcus faecalis." J Bacteriol **185**(24): 7184-7192.

Contreras-Martel, C., A. Martins, C. Ecobichon, D. M. Trindade, P. J. Mattei, S. Hicham, P. Hardouin, M. E. Ghachi, I. G. Boneca and A. Dessen (2017). "Molecular architecture of the PBP2-MreC core bacterial cell wall synthesis complex." Nat Commun **8**(1): 776.

Cortes, G., B. de Astorza, V. J. Benedi and S. Alberti (2002). "Role of the htrA gene in Klebsiella pneumoniae virulence." Infect Immun **70**(9): 4772-4776.

Cowburn, D. (1997). "Peptide recognition by PTB and PDZ domains." Current opinion in structural biology **7**(6): 835-838.

Dai, Z. and T. M. Koehler (1997). "Regulation of anthrax toxin activator gene (atxA) expression in Bacillus anthracis: temperature, not CO2/bicarbonate, affects AtxA synthesis." Infect Immun **65**(7): 2576-2582.

Dale, J. L., J. L. Nilson, A. M. T. Barnes and G. M. Dunny (2017). "Restructuring of Enterococcus faecalis biofilm architecture in response to antibiotic-induced stress." NPJ Biofilms Microbiomes **3**: 15.

Danese, P. N. and T. J. Silhavy (1997). "The sigma(E) and the Cpx signal transduction systems control the synthesis of periplasmic protein-folding enzymes in Escherichia coli." Genes Dev **11**(9): 1183-1193.

Danese, P. N., W. B. Snyder, C. L. Cosma, L. J. Davis and T. J. Silhavy (1995). "The Cpx two-component signal transduction pathway of Escherichia coli regulates transcription of the gene specifying the stress-inducible periplasmic protease, DegP." Genes Dev **9**(4): 387-398.

Daniel, R. A. and J. Errington (2003). "Control of cell morphogenesis in bacteria: two distinct ways to make a rod-shaped cell." Cell **113**(6): 767-776.

Darmon, E., D. Noone, A. Masson, S. Bron, O. P. Kuipers, K. M. Devine and J. M. van Dijl (2002). "A novel class of heat and secretion stress-responsive genes is controlled by the autoregulated CssRS two-component system of Bacillus subtilis." J Bacteriol **184**(20): 5661-5671.

Day, C. L. and M. G. Hinds (2002). "HtrA--a renaissance protein." Structure **10**(6): 737-739.

Del Papa, M. F. and M. Perego (2011). "Enterococcus faecalis virulence regulator FsrA binding to target promoters." J Bacteriol **193**(7): 1527-1532.

den Blaauwen, T., M. A. de Pedro, M. Nguyen-Disteche and J. A. Ayala (2008). "Morphogenesis of rod-shaped sacculi." FEMS Microbiol Rev **32**(2): 321-344.

Depardieu, F., I. Podglajen, R. Leclercq, E. Collatz and P. Courvalin (2007). "Modes and modulations of antibiotic resistance gene expression." Clin Microbiol Rev **20**(1): 79-114.

Desai, S. K., Winardhi, R. S., Periasamy, S., Dykas, M. M., Jie, Y., & Kenney, L. J. (2016). The horizontally-acquired response regulator SsrB drives a Salmonella lifestyle switch by relieving biofilm silencing. Elife, **5**. doi:10.7554/eLife.10747

Djoric, D. and C. J. Kristich (2015). "Oxidative stress enhances cephalosporin resistance of Enterococcus faecalis through activation of a two-component signaling system." Antimicrob Agents Chemother **59**(1): 159-169.

Djoric, D., & Kristich, C. J. (2017). Extracellular SalB contributes to intrinsic cephalosporin resistance and cell envelope integrity in Enterococcus faecalis. J Bacteriol. doi:10.1128/JB.00392-17

Dorneles, E. M., N. Sriranganathan and A. P. Lage (2015). "Recent advances in Brucella abortus vaccines." Vet Res **46**: 76.

Ducret, A., E. M. Quardokus and Y. V. Brun (2016). "MicrobeJ, a tool for high throughput bacterial cell detection and quantitative analysis." Nat Microbiol **1**(7): 16077.

Dundar, H., D. A. Brede, S. L. La Rosa, A. O. El-Gendy, D. B. Diep and I. F. Nes (2015). "The fsr Quorum-Sensing System and Cognate Gelatinase Orchestrate the Expression and Processing of Proprotein EF_1097 into the Mature Antimicrobial Peptide Enterocin O16." J Bacteriol **197**(13): 2112-2121.

Ehrmann, M. and T. Clausen (2004). "Proteolysis as a regulatory mechanism." Annu Rev Genet **38**: 709-724.

Elzer, P. H., S. D. Hagius, G. T. Robertson, R. W. Phillips, J. V. Walker, M. B. Fatemi, F. M. Enright and R. M. Roop, 2nd (1996). "Behaviour of a high-temperature-requirement A (HtrA) deletion mutant of Brucella abortus in goats." Res Vet Sci **60**(1): 48-50.

Elzer, P. H., R. W. Phillips, G. T. Robertson and R. M. Roop, 2nd (1996). "The HtrA stress response protease contributes to resistance of Brucella abortus to killing by murine phagocytes." Infect Immun **64**(11): 4838-4841.

Fabret, C., Feher, V. A., & Hoch, J. A. (1999). Two-component signal transduction in Bacillus subtilis: how one organism sees its world. J Bacteriol, **181**(7), 1975-1983.

Fang, K., X. Jin and S. H. Hong (2018). "Probiotic Escherichia coli inhibits biofilm formation of pathogenic E. coli via extracellular activity of DegP." Sci Rep **8**(1): 4939.

Fanning, A. S. and J. M. Anderson (1996). "Protein-protein interactions: PDZ domain networks." Curr Biol **6**(11): 1385-1388.

Flannagan, R. S., D. Aubert, C. Kooi, P. A. Sokol and M. A. Valvano (2007). "Burkholderia cenocepacia requires a periplasmic HtrA protease for growth under thermal and osmotic stress and for survival in vivo." Infect Immun **75**(4): 1679-1689.

Flemming, H. C., J. Wingender, U. Szewzyk, P. Steinberg, S. A. Rice and S. Kjelleberg (2016). "Biofilms: an emergent form of bacterial life." Nat Rev Microbiol **14**(9): 563-575.

Flores-Mireles, A. L., J. S. Pinkner, M. G. Caparon and S. J. Hultgren (2014). "EbpA vaccine antibodies block binding of Enterococcus faecalis to fibrinogen to prevent catheter-associated bladder infection in mice." Sci Transl Med **6**(254): 254ra127.

Fogg, P. C. M., D. J. Rigden, J. R. Saunders, A. J. McCarthy and H. E. Allison (2011). "Characterization of the relationship between integrase, excisionase and antirepressor activities associated with a superinfecting Shiga toxin encoding bacteriophage." Nucleic Acids Research **39**(6): 2116-2129.

Frank, K. L., P. S. Guiton, A. M. Barnes, D. A. Manias, O. N. Chuang-Smith, P. L. Kohler, A. R. Spaulding, S. J. Hultgren, P. M. Schlievert and G. M. Dunny (2013). "AhrC and Eep are biofilm infection-associated virulence factors in Enterococcus faecalis." Infect Immun **81**(5): 1696-1708.

Gao, P., K. L. Pinkston, S. R. Nallapareddy, A. van Hoof, B. E. Murray and B. R. Harvey (2010). "Enterococcus faecalis rnjB is required for pilin gene expression and biofilm formation." J Bacteriol **192**(20): 5489-5498.

Gao, R. and A. M. Stock (2009). "Biological insights from structures of two-component proteins." Annu Rev Microbiol **63**: 133-154.

Garcia-Granja, P. E., J. Lopez, I. Vilacosta, C. Ortiz-Bautista, T. Sevilla, C. Olmos, C. Sarria, C. Ferrera, I. Gomez and J. A. San Roman (2015). "Polymicrobial Infective Endocarditis: Clinical Features and Prognosis." Medicine (Baltimore) **94**(49): e2000.

Gardino, A. K. and D. Kern (2007). "Functional dynamics of response regulators using NMR relaxation techniques." Methods Enzymol **423**: 149-165.

Ge, X., R. Wang, J. Ma, Y. Liu, A. N. Ezemaduka, P. R. Chen, X. Fu and Z. Chang (2014). "DegP primarily functions as a protease for the biogenesis of beta-barrel outer membrane proteins in the Gram-negative bacterium Escherichia coli." FEBS J **281**(4): 1226-1240.

Ghosh, M., Wang, L. C., Ramesh, R., Morgan, L. K., Kenney, L. J., & Anand, G. S. (2017). Lipid-Mediated Regulation of Embedded Receptor Kinases via Parallel Allosteric Relays. Biophys J, **112**(4), 643-654. doi:10.1016/j.bpj.2016.12.027

Gjodsbol, K., J. J. Christensen, T. Karlsmark, B. Jorgensen, B. M. Klein and K. A. Krogfelt (2006). "Multiple bacterial species reside in chronic wounds: a longitudinal study." Int Wound J **3**(3): 225-231.

Gloeckl, S., V. A. Ong, P. Patel, J. D. Tyndall, P. Timms, K. W. Beagley, J. A. Allan, C. W. Armitage, L. Turnbull, C. B. Whitchurch, M. Merdanovic, M. Ehrmann, J. C. Powers, J. Oleksyszyn, M. Verdoes, M. Bogyo and W. M. Huston (2013). "Identification of a serine protease inhibitor which causes inclusion vacuole reduction and is lethal to Chlamydia trachomatis." Mol Microbiol **89**(4): 676-689.

Goh, H. M. S., M. H. A. Yong, K. K. L. Chong and K. A. Kline (2017). "Model systems for the study of Enterococcal colonization and infection." Virulence **8**(8): 1525-1562.

Gold, H. S. (2001). "Vancomycin-resistant enterococci: mechanisms and clinical observations." Clin Infect Dis **33**(2): 210-219.

Gottesman, S., S. Wickner and M. R. Maurizi (1997). "Protein quality control: triage by chaperones and proteases." Genes Dev **11**(7): 815-823.
Granok, A. B., D. Parsonage, R. P. Ross and M. G. Caparon (2000). "The RofA binding site in Streptococcus pyogenes is utilized in multiple transcriptional pathways." J Bacteriol **182**(6): 1529-1540.

Graslund, S., J. Sagemark, H. Berglund, L. G. Dahlgren, A. Flores, M. Hammarstroem, I. Johansson, T. Kotenyova, M. Nilsson, P. Nordlund and J. Weigelt (2008). "The use of systematic N- and C-terminal deletions to promote production and structural studies of recombinant proteins." Protein Expression and Purification **58**(2): 210-221.

Groicher, K. H., B. A. Firek, D. F. Fujimoto and K. W. Bayles (2000). "The Staphylococcus aureus lrgAB operon modulates murein hydrolase activity and penicillin tolerance." J Bacteriol **182**(7): 1794-1801.

Guberman, J. M., A. Fay, J. Dworkin, N. S. Wingreen and Z. Gitai (2008). "PSICIC: noise and asymmetry in bacterial division revealed by computational image analysis at sub-pixel resolution." PLoS Comput Biol **4**(11): e1000233.

Guiton, P. S., C. S. Hung, L. E. Hancock, M. G. Caparon and S. J. Hultgren (2010). "Enterococcal biofilm formation and virulence in an optimized murine model of foreign body-associated urinary tract infections." Infect Immun **78**(10): 4166-4175.

Guiton, P. S., C. S. Hung, K. A. Kline, R. Roth, A. L. Kau, E. Hayes, J. Heuser, K. W. Dodson, M. G. Caparon and S. J. Hultgren (2009). "Contribution of autolysin and Sortase

a during Enterococcus faecalis DNA-dependent biofilm development." Infect Immun **77**(9): 3626-3638.

Gushchin, I., Melnikov, I., Polovinkin, V., Ishchenko, A., Yuzhakova, A., Buslaev, P., . . . Gordeliy, V. (2017). Mechanism of transmembrane signaling by sensor histidine kinases. Science, **356**(6342). doi:10.1126/science.aah6345

Hancock, L. and M. Perego (2002). "Two-component signal transduction in Enterococcus faecalis." J Bacteriol **184**(21): 5819-5825.

Hancock, L. E. and M. Perego (2004). "The Enterococcus faecalis fsr two-component system controls biofilm development through production of gelatinase." J Bacteriol **186**(17): 5629-5639.

Hasselblatt, H., R. Kurzbauer, C. Wilken, T. Krojer, J. Sawa, J. Kurt, R. Kirk, S. Hasenbein, M. Ehrmann and T. Clausen (2007). "Regulation of the sigmaE stress response by DegS: how the PDZ domain keeps the protease inactive in the resting state and allows integration of different OMP-derived stress signals upon folding stress." Genes Dev **21**(20): 2659-2670.

Heimesaat, M. M., M. Alutis, U. Grundmann, A. Fischer, N. Tegtmeyer, M. Bohm, A. A. Kuhl, U. B. Gobel, S. Backert and S. Bereswill (2014). "The role of serine protease HtrA in acute ulcerative enterocolitis and extra-intestinal immune responses during Campylobacter jejuni infection of gnotobiotic IL-10 deficient mice." Front Cell Infect Microbiol **4**: 77.

Hidron, A. I., J. R. Edwards, J. Patel, T. C. Horan, D. M. Sievert, D. A. Pollock, S. K. Fridkin, T. National Healthcare Safety Network and F. Participating National Healthcare Safety Network (2008). "NHSN annual update: antimicrobial-resistant pathogens associated with healthcare-associated infections: annual summary of data reported to the National Healthcare Safety Network at the Centers for Disease Control and Prevention, 2006-2007." Infect Control Hosp Epidemiol **29**(11): 996-1011.

Hollenbeck, B. L. and L. B. Rice (2012). "Intrinsic and acquired resistance mechanisms in enterococcus." Virulence **3**(5): 421-433.

Holtje, J. V. (1998). "Growth of the stress-bearing and shape-maintaining murein sacculus of Escherichia coli." Microbiol Mol Biol Rev **62**(1): 181-203.

Hoy, B., T. Geppert, M. Boehm, F. Reisen, P. Plattner, G. Gadermaier, N. Sewald, F. Ferreira, P. Briza, G. Schneider, S. Backert and S. Wessler (2012). "Distinct roles of secreted HtrA proteases from gram-negative pathogens in cleaving the junctional protein and tumor suppressor E-cadherin." J Biol Chem **287**(13): 10115-10120.

Hoy, B., M. Lower, C. Weydig, G. Carra, N. Tegtmeyer, T. Geppert, P. Schroder, N. Sewald, S. Backert, G. Schneider and S. Wessler (2010). "Helicobacter pylori HtrA is a

new secreted virulence factor that cleaves E-cadherin to disrupt intercellular adhesion." EMBO Rep **11**(10): 798-804.

Humnabadkar, V., K. R. Prabhakar, A. Narayan, S. Sharma, S. Guptha, P. Manjrekar, M. Chinnapattu, V. Ramachandran, S. P. Hameed, S. Ravishankar and M. Chatterji (2014). "UDP-N-acetylmuramic acid l-alanine ligase (MurC) inhibition in a tolC mutant Escherichia coli strain leads to cell death." Antimicrob Agents Chemother **58**(10): 6165-6171.

Humphreys, S., A. Stevenson, A. Bacon, A. B. Weinhardt and M. Roberts (1999). "The alternative sigma factor, sigmaE, is critically important for the virulence of Salmonella typhimurium." Infect Immun **67**(4): 1560-1568.

Hung, D. L., T. L. Raivio, C. H. Jones, T. J. Silhavy and S. J. Hultgren (2001). "Cpx signaling pathway monitors biogenesis and affects assembly and expression of P pili." EMBO J **20**(7): 1508-1518.

Huston, W. M., C. Theodoropoulos, S. A. Mathews and P. Timms (2008). "Chlamydia trachomatis responds to heat shock, penicillin induced persistence, and IFN-gamma persistence by altering levels of the extracytoplasmic stress response protease HtrA." BMC Microbiol **8**: 190.

Hyyrylainen, H. L., A. Bolhuis, E. Darmon, L. Muukkonen, P. Koski, M. Vitikainen, M. Sarvas, Z. Pragai, S. Bron, J. M. van Dijl and V. P. Kontinen (2001). "A novel two-component regulatory system in Bacillus subtilis for the survival of severe secretion stress." Mol Microbiol **41**(5): 1159-1172.

Hyyrylainen, H. L., B. C. Marciniak, K. Dahncke, M. Pietiainen, P. Courtin, M. Vitikainen, R. Seppala, A. Otto, D. Becher, M. P. Chapot-Chartier, O. P. Kuipers and V. P. Kontinen (2010). "Penicillin-binding protein folding is dependent on the PrsA peptidyl-prolyl cis-trans isomerase in Bacillus subtilis." Molecular Microbiology **77**(1): 108-127.

Ingmer, H. and L. Brondsted (2009). "Proteases in bacterial pathogenesis." Res Microbiol **160**(9): 704-710.

Isaac, D. D., J. S. Pinkner, S. J. Hultgren and T. J. Silhavy (2005). "The extracytoplasmic adaptor protein CpxP is degraded with substrate by DegP." Proc Natl Acad Sci U S A **102**(49): 17775-17779.

Jin, T. and M. Inouye (1993). "Ligand binding to the receptor domain regulates the ratio of kinase to phosphatase activities of the signaling domain of the hybrid Escherichia coli transmembrane receptor, Taz1." J Mol Biol **232**(2): 484-492.

Johnson, K., I. Charles, G. Dougan, D. Pickard, P. O'Gaora, G. Costa, T. Ali, I. Miller and C. Hormaeche (1991). "The role of a stress-response protein in Salmonella typhimurium virulence." Mol Microbiol **5**(2): 401-407.

Jones, C. H., T. C. Bolken, K. F. Jones, G. O. Zeller and D. E. Hruby (2001). "Conserved DegP protease in gram-positive bacteria is essential for thermal and oxidative tolerance and full virulence in Streptococcus pyogenes." Infect Immun **69**(9): 5538-5545.

Jones, C. H., P. N. Danese, J. S. Pinkner, T. J. Silhavy and S. J. Hultgren (1997). "The chaperone-assisted membrane release and folding pathway is sensed by two signal transduction systems." EMBO J **16**(21): 6394-6406.

Jorgensen, J. H., M. J. Ferraro, W. A. Craig, G. V. Doern, S. M. Finegold, J. Fung-Tomc, S. L. Hansen, J. Hindler, L. B. Reller, J. M. Swenson, F. C. Tenover, R. T. Testa, M. A. Wikler and National Committee for Clinical Laboratory Standards. (1997). Methods for dilution antimicrobial susceptibility tests for bacteria that grow aerobically--fourth edition; approved standard. Wayne, PA, NCCLS.

Jousselin, A., C. Manzano, A. Biette, P. Reed, M. G. Pinho, A. E. Rosato, W. L. Kelley and A. Renzoni (2016). "The Staphylococcus aureus Chaperone PrsA Is a New Auxiliary Factor of Oxacillin Resistance Affecting Penicillin-Binding Protein 2A." Antimicrobial Agents and Chemotherapy **60**(3): 1656-1666.

Kandaswamy, K., T. H. Liew, C. Y. Wang, E. Huston-Warren, U. Meyer-Hoffert, K. Hultenby, J. M. Schroder, M. G. Caparon, S. Normark, B. Henriques-Normark, S. J. Hultgren and K. A. Kline (2013). "Focal targeting by human beta-defensin 2 disrupts localized virulence factor assembly sites in Enterococcus faecalis." Proc Natl Acad Sci U S A **110**(50): 20230-20235, “Copyright (2013) National Academy of Sciences.”

Kang, K. H., J. S. Lee, M. Yoo and I. Jin (2010). "The influence of HtrA expression on the growth of Streptococcus mutans during acid stress." Mol Cells **29**(3): 297-304.

Kellogg, S. L. and C. J. Kristich (2016). "Functional Dissection of the CroRS Two-Component System Required for Resistance to Cell Wall Stressors in Enterococcus faecalis." J Bacteriol **198**(8): 1326-1336.

Kellogg, S. L., J. L. Little, J. S. Hoff and C. J. Kristich (2017). "Requirement of the CroRS Two-Component System for Resistance to Cell Wall-Targeting Antimicrobials in Enterococcus faecium." Antimicrob Agents Chemother **61**(5).

Kenney, L. J. (2002). Structure/function relationships in OmpR and other winged-helix transcription factors. Curr Opin Microbiol**, 5**(2), 135-141.

Kenney, L. J. (2018). The role of acid stress in Salmonella pathogenesis. Curr Opin Microbiol, **47**, 45-51. doi:10.1016/j.mib.2018.11.006.

Kemp, K. D., K. V. Singh, S. R. Nallapareddy and B. E. Murray (2007). "Relative contributions of Enterococcus faecalis OG1RF sortase-encoding genes, srtA and bps

(srtC), to biofilm formation and a murine model of urinary tract infection." Infect Immun **75**(11): 5399-5404.

Kim, D. Y. and K. K. Kim (2005). "Structure and function of HtrA family proteins, the key players in protein quality control." J Biochem Mol Biol **38**(3): 266-274.

Kline, K. A., A. L. Kau, S. L. Chen, A. Lim, J. S. Pinkner, J. Rosch, S. R. Nallapareddy, B. E. Murray, B. Henriques-Normark, W. Beatty, M. G. Caparon and S. J. Hultgren (2009). "Mechanism for sortase localization and the role of sortase localization in efficient pilus assembly in Enterococcus faecalis." J Bacteriol **191**(10): 3237-3247.

Kochan, T. J. and S. Dawid (2013). "The HtrA protease of Streptococcus pneumoniae controls density-dependent stimulation of the bacteriocin blp locus via disruption of pheromone secretion." J Bacteriol **195**(7): 1561-1572.

Kolmar, H., P. R. Waller and R. T. Sauer (1996). "The DegP and DegQ periplasmic endoproteases of Escherichia coli: specificity for cleavage sites and substrate conformation." J Bacteriol **178**(20): 5925-5929.

Koretke, K. K., A. N. Lupas, P. V. Warren, M. Rosenberg and J. R. Brown (2000). "Evolution of two-component signal transduction." Molecular Biology and Evolution **17**(12): 1956-1970.

Kristich, C. J., V. T. Nguyen, T. Le, A. M. Barnes, S. Grindle and G. M. Dunny (2008). "Development and use of an efficient system for random mariner transposon mutagenesis to identify novel genetic determinants of biofilm formation in the core Enterococcus faecalis genome." Appl Environ Microbiol **74**(11): 3377-3386.

Krojer, T., J. Sawa, E. Schafer, H. R. Saibil, M. Ehrmann and T. Clausen (2008). "Structural basis for the regulated protease and chaperone function of DegP." Nature **453**(7197): 885-890.

Laddomada, F., M. M. Miyachiro and A. Dessen (2016). "Structural Insights into Protein-Protein Interactions Involved in Bacterial Cell Wall Biogenesis." Antibiotics (Basel) **5**(2).

Lawrence, A., T. Fraser, A. Gillett, J. D. Tyndall, P. Timms, A. Polkinghorne and W. M. Huston (2016). "Chlamydia Serine Protease Inhibitor, targeting HtrA, as a New Treatment for Koala Chlamydia infection." Sci Rep **6**: 31466.

Le Breton, Y., G. Boel, A. Benachour, H. Prevost, Y. Auffray and A. Rince (2003). "Molecular characterization of Enterococcus faecalis two-component signal transduction pathways related to environmental stresses." Environ Microbiol **5**(5): 329-337.

Le Breton, Y., C. Muller, Y. Auffray and A. Rince (2007). "New insights into the Enterococcus faecalis CroRS two-component system obtained using a differential-display random arbitrarily primed PCR approach." Appl Environ Microbiol **73**(11): 3738-3741.

Lebreton, F., R. J. L. Willems and M. S. Gilmore (2014). Enterococcus Diversity, Origins in Nature, and Gut Colonization. Enterococci: From Commensals to Leading Causes of Drug Resistant Infection. M. S. Gilmore, D. B. Clewell, Y. Ike and N. Shankar. Boston.

Letunic, I., T. Doerks and P. Bork (2015). "SMART: recent updates, new developments and status in 2015." Nucleic Acids Res **43**(Database issue): D257-260.

Lewis, C., H. Skovierova, G. Rowley, B. Rezuchova, D. Homerova, A. Stevenson, J. Spencer, J. Farn, J. Kormanec and M. Roberts (2009). "Salmonella enterica Serovar Typhimurium HtrA: regulation of expression and role of the chaperone and protease activities during infection." Microbiology **155**(Pt 3): 873-881.

Li, H. and R. Durbin (2009). "Fast and accurate short read alignment with Burrows-Wheeler transform." Bioinformatics **25**(14): 1754-1760.

Li, S. R., N. Dorrell, P. H. Everest, G. Dougan and B. W. Wren (1996). "Construction and characterization of a Yersinia enterocolitica O:8 high-temperature requirement (htrA) isogenic mutant." Infect Immun **64**(6): 2088-2094.

Lipinska, B., S. Sharma and C. Georgopoulos (1988). "Sequence analysis and regulation of the htrA gene of Escherichia coli: a sigma 32-independent mechanism of heat-inducible transcription." Nucleic Acids Res **16**(21): 10053-10067.

Liu, W., & Hulett, F. M. (1997). Bacillus subtilis PhoP binds to the phoB tandem promoter exclusively within the phosphate starvation-inducible promoter. J Bacteriol, **179**(20), 6302-6310.

Livak, K. J., & Schmittgen, T. D. (2001). Analysis of relative gene expression data using real-time quantitative PCR and the 2(-Delta Delta C(T)) Method. Methods, **25**(4), 402-408. doi:10.1006/meth.2001.1262

Lowe, A. M., P. A. Lambert and A. W. Smith (1995). "Cloning of an Enterococcus faecalis endocarditis antigen: homology with adhesins from some oral streptococci." Infect Immun **63**(2): 703-706.

Lu, H., Y. Yamaoka and D. Y. Graham (2005). "Helicobacter pylori virulence factors: facts and fantasies." Curr Opin Gastroenterol **21**(6): 653-659.

Lyon, W. R. and M. G. Caparon (2003). "Trigger factor-mediated prolyl isomerization influences maturation of the Streptococcus pyogenes cysteine protease." J Bacteriol **185**(12): 3661-3667.

Lyon, W. R. and M. G. Caparon (2004). "Role for serine protease HtrA (DegP) of Streptococcus pyogenes in the biogenesis of virulence factors SpeB and the hemolysin streptolysin S." Infect Immun **72**(3): 1618-1625.

Maki, D. G. and W. A. Agger (1988). "Enterococcal bacteremia: clinical features, the risk of endocarditis, and management." Medicine (Baltimore) **67**(4): 248-269.

Malet, H., F. Canellas, J. Sawa, J. Yan, K. Thalassinos, M. Ehrmann, T. Clausen and H. R. Saibil (2012). "Newly folded substrates inside the molecular cage of the HtrA chaperone DegQ." Nat Struct Mol Biol **19**(2): 152-157.

Manias, D. A. and G. M. Dunny (2018). "Expression of Adhesive Pili and the Collagen-binding Adhesin ACE is Activated by ArgR Family Transcription Factors in Enterococcus faecalis." J Bacteriol.

Marsh, J. W., V. A. Ong, W. B. Lott, P. Timms, J. D. Tyndall and W. M. Huston (2017). "CtHtrA: the lynchpin of the chlamydial surface and a promising therapeutic target." Future Microbiol **12**: 817-829.

Marsh, J. W., B. A. Wee, J. D. Tyndall, W. B. Lott, R. J. Bastidas, H. D. Caldwell, R. H. Valdivia, L. Kari and W. M. Huston (2015). "A Chlamydia trachomatis strain with a chemically generated amino acid substitution (P370L) in the cthtrA gene shows reduced elementary body production." BMC Microbiol **15**: 194.

Martinez-Hackert, E. and A. M. Stock (1997). "Structural relationships in the OmpR family of winged-helix transcription factors." J Mol Biol **269**(3): 301-312.

Mascher, T., M. Heintz, D. Zahner, M. Merai and R. Hakenbeck (2006). "The CiaRH system of Streptococcus pneumoniae prevents lysis during stress induced by treatment with cell wall inhibitors and by mutations in pbp2x involved in beta-lactam resistance." J Bacteriol **188**(5): 1959-1968.

Matos, R. C., N. Lapaque, L. Rigottier-Gois, L. Debarbieux, T. Meylheuc, B. Gonzalez-Zorn, F. Repoila, F. Lopes Mde and P. Serror (2013). "Enterococcus faecalis prophage dynamics and contributions to pathogenic traits." PLoS Genet **9**(6): e1003539.

McBride, S. M., V. A. Fischetti, D. J. Leblanc, R. C. Moellering, Jr. and M. S. Gilmore (2007). "Genetic diversity among Enterococcus faecalis." PLoS One **2**(7): e582.

McNeill, K. and I. R. Hamilton (2003). "Acid tolerance response of biofilm cells of Streptococcus mutans." FEMS Microbiol Lett **221**(1): 25-30.

Mecsas, J., P. E. Rouviere, J. W. Erickson, T. J. Donohue and C. A. Gross (1993). "The activity of sigma E, an Escherichia coli heat-inducible sigma-factor, is modulated by expression of outer membrane proteins." Genes Dev **7**(12B): 2618-2628.

Mende, D. R., I. Letunic, J. Huerta-Cepas, S. S. Li, K. Forslund, S. Sunagawa and P. Bork (2017). "proGenomes: a resource for consistent functional and taxonomic annotations of prokaryotic genomes." Nucleic Acids Res **45**(D1): D529-D534.

Mielich-Suss, B., J. Schneider and D. Lopez (2013). "Overproduction of flotillin influences cell differentiation and shape in Bacillus subtilis." MBio **4**(6): e00719-00713.

Missiakas, D. and S. Raina (1997). "Protein misfolding in the cell envelope of Escherichia coli: new signaling pathways." Trends Biochem Sci **22**(2): 59-63.

Missiakas, D. and S. Raina (1997). "Signal transduction pathways in response to protein misfolding in the extracytoplasmic compartments of E. coli: role of two new phosphoprotein phosphatases PrpA and PrpB." EMBO J **16**(7): 1670-1685.

Mizuno, T. (1997). Compilation of all genes encoding two-component phosphotransfer signal transducers in the genome of Escherichia coli. DNA Res, **4**(2), 161-168.

Mohamed, J. A., F. Teng, S. R. Nallapareddy and B. E. Murray (2006). "Pleiotrophic effects of 2 Enterococcus faecalis sagA-like genes, salA and salB, which encode proteins that are antigenic during human infection, on biofilm formation and binding to collagen type i and fibronectin." J Infect Dis **193**(2): 231-240.

Mohamedmohaideen, N. N., S. K. Palaninathan, P. M. Morin, B. J. Williams, M. Braunstein, S. E. Tichy, J. Locker, D. H. Russell, W. R. Jacobs, Jr. and J. C. Sacchettini (2008). "Structure and function of the virulence-associated high-temperature requirement A of Mycobacterium tuberculosis." Biochemistry **47**(23): 6092-6102.

Muller, C., Y. Le Breton, T. Morin, A. Benachour, Y. Auffray and A. Rince (2006). "The response regulator CroR modulates expression of the secreted stress-induced SalB protein in Enterococcus faecalis." J Bacteriol **188**(7): 2636-2645.

Muller, C., S. Massier, Y. Le Breton and A. Rince (2018). "The role of the CroR response regulator in resistance of Enterococcus faecalis to D-cycloserine is defined using an inducible receiver domain." Mol Microbiol **107**(3): 416-427.

Mylonakis, E., M. Engelbert, X. Qin, C. D. Sifri, B. E. Murray, F. M. Ausubel, M. S. Gilmore and S. B. Calderwood (2002). "The Enterococcus faecalis fsrB gene, a key component of the fsr quorum-sensing system, is associated with virulence in the rabbit endophthalmitis model." Infect Immun **70**(8): 4678-4681.

Nagalakshmi, U., K. Waern and M. Snyder (2010). "RNA-Seq: a method for comprehensive transcriptome analysis." Curr Protoc Mol Biol **Chapter 4**: Unit 4 11 11-13.

Nakayama, J., Y. Cao, T. Horii, S. Sakuda, A. D. Akkermans, W. M. de Vos and H. Nagasawa (2001). "Gelatinase biosynthesis-activating pheromone: a peptide lactone that mediates a quorum sensing in Enterococcus faecalis." Mol Microbiol **41**(1): 145-154.

Nakayama, J., S. Chen, N. Oyama, K. Nishiguchi, E. A. Azab, E. Tanaka, R. Kariyama and K. Sonomoto (2006). "Revised model for Enterococcus faecalis fsr quorum-sensing

system: the small open reading frame fsrD encodes the gelatinase biosynthesis-activating pheromone propeptide corresponding to staphylococcal agrd." J Bacteriol **188**(23): 8321-8326.

Nallapareddy, S. R., J. Sillanpaa, J. Mitchell, K. V. Singh, S. A. Chowdhury, G. M. Weinstock, P. M. Sullam and B. E. Murray (2011). "Conservation of Ebp-type pilus genes among Enterococci and demonstration of their role in adherence of Enterococcus faecalis to human platelets." Infect Immun **79**(7): 2911-2920.

Nallapareddy, S. R., K. V. Singh, J. Sillanpaa, D. A. Garsin, M. Hook, S. L. Erlandsen and B. E. Murray (2006). "Endocarditis and biofilm-associated pili of Enterococcus faecalis." J Clin Invest **116**(10): 2799-2807.

Nallapareddy, S. R., K. V. Singh, J. Sillanpaa, M. Zhao and B. E. Murray (2011). "Relative contributions of Ebp Pili and the collagen adhesin ace to host extracellular matrix protein adherence and experimental urinary tract infection by Enterococcus faecalis OG1RF." Infect Immun **79**(7): 2901-2910.

Narberhaus, F., M. Obrist, F. Fuhrer and S. Langklotz (2009). "Degradation of cytoplasmic substrates by FtsH, a membrane-anchored protease with many talents." Res Microbiol **160**(9): 652-659.

Narberhaus, F., W. Weiglhofer, H. M. Fischer and H. Hennecke (1998). "Identification of the Bradyrhizobium japonicum degP gene as part of an operon containing small heat-shock protein genes." Arch Microbiol **169**(2): 89-97.

Nielsen, H. V., A. L. Flores-Mireles, A. L. Kau, K. A. Kline, J. S. Pinkner, F. Neiers, S. Normark, B. Henriques-Normark, M. G. Caparon and S. J. Hultgren (2013). "Pilin and sortase residues critical for endocarditis- and biofilm-associated pilus biogenesis in Enterococcus faecalis." J Bacteriol **195**(19): 4484-4495.

Nielsen, H. V., A. L. Flores-Mireles, A. L. Kau, K. A. Kline, J. S. Pinkner, F. Neiers, S. Normark, B. Henriques-Normark, M. G. Caparon and S. J. Hultgren (2013). "Pilin and sortase residues critical for endocarditis- and biofilm-associated pilus biogenesis in Enterococcus faecalis." Journal of bacteriology **195**(19): 4484-4495.

Nielsen, H. V., P. S. Guiton, K. A. Kline, G. C. Port, J. S. Pinkner, F. Neiers, S. Normark, B. Henriques-Normark, M. G. Caparon and S. J. Hultgren (2012). "The metal ion-dependent adhesion site motif of the Enterococcus faecalis EbpA pilin mediates pilus function in catheter-associated urinary tract infection." MBio **3**(4): e00177-00112.

Noone, D., A. Howell and K. M. Devine (2000). "Expression of ykdA, encoding a Bacillus subtilis homologue of HtrA, is heat shock inducible and negatively autoregulated." J Bacteriol **182**(6): 1592-1599.

Okada, A., Y. Gotoh, T. Watanabe, E. Furuta, K. Yamamoto and R. Utsumi (2007). "Targeting two-component signal transduction: A novel drug discovery system." Two-Component Signaling Systems, Pt A **422**: 386-395.

Okura, M., M. Osaki, N. Fittipaldi, M. Gottschalk, T. Sekizaki and D. Takamatsu (2011). "The minor pilin subunit Sgp2 is necessary for assembly of the pilus encoded by the srtG cluster of Streptococcus suis." J Bacteriol **193**(4): 822-831.

Page, M. J. and E. Di Cera (2008). "Evolution of peptidase diversity." J Biol Chem **283**(44): 30010-30014.

Pallen, M. J. and B. W. Wren (1997). "The HtrA family of serine proteases." Mol Microbiol **26**(2): 209-221.

Patterson, J. E., A. H. Sweeney, M. Simms, N. Carley, R. Mangi, J. Sabetta and R. W. Lyons (1995). "An analysis of 110 serious enterococcal infections. Epidemiology, antibiotic susceptibility, and outcome." Medicine (Baltimore) **74**(4): 191-200.

Patton, D. L., M. Askienazy-Elbhar, J. Henry-Suchet, L. A. Campbell, A. Cappuccio, W. Tannous, S. P. Wang and C. C. Kuo (1994). "Detection of Chlamydia trachomatis in fallopian tube tissue in women with postinfectious tubal infertility." Am J Obstet Gynecol **171**(1): 95-101.

Paulsen, I. T., L. Banerjei, G. S. Myers, K. E. Nelson, R. Seshadri, T. D. Read, D. E. Fouts, J. A. Eisen, S. R. Gill, J. F. Heidelberg, H. Tettelin, R. J. Dodson, L. Umayam, L. Brinkac, M. Beanan, S. Daugherty, R. T. DeBoy, S. Durkin, J. Kolonay, R. Madupu, W. Nelson, J. Vamathevan, B. Tran, J. Upton, T. Hansen, J. Shetty, H. Khouri, T. Utterback, D. Radune, K. A. Ketchum, B. A. Dougherty and C. M. Fraser (2003). "Role of mobile DNA in the evolution of vancomycin-resistant Enterococcus faecalis." Science **299**(5615): 2071-2074.

Pedersen, L. L., M. Radulic, M. Doric and Y. Abu Kwaik (2001). "HtrA homologue of Legionella pneumophila: an indispensable element for intracellular infection of mammalian but not protozoan cells." Infect Immun **69**(4): 2569-2579.

Phillips, R. W., P. H. Elzer, G. T. Robertson, S. D. Hagius, J. V. Walker, M. B. Fatemi, F. M. Enright and R. M. Roop, 2nd (1997). "A Brucella melitensis high-temperature-requirement A (htrA) deletion mutant is attenuated in goats and protects against abortion." Res Vet Sci **63**(2): 165-167.
Phillips, R. W. and R. M. Roop, 2nd (2001). "Brucella abortus HtrA functions as an authentic stress response protease but is not required for wild-type virulence in BALB/c mice." Infect Immun **69**(9): 5911-5913.

Pinholt, M., C. Ostergaard, M. Arpi, N. E. Bruun, H. C. Schonheyder, K. O. Gradel, M. Sogaard, J. D. Knudsen and N. Danish Collaborative Bacteraemia (2014). "Incidence,

clinical characteristics and 30-day mortality of enterococcal bacteraemia in Denmark 2006-2009: a population-based cohort study." Clin Microbiol Infect **20**(2): 145-151.

Pinkston, K. L., P. Gao, D. Diaz-Garcia, J. Sillanpaa, S. R. Nallapareddy, B. E. Murray and B. R. Harvey (2011). "The Fsr quorum-sensing system of Enterococcus faecalis modulates surface display of the collagen-binding MSCRAMM Ace through regulation of gelE." J Bacteriol **193**(17): 4317-4325.

Ponting, C. P. (1997). "Evidence for PDZ domains in bacteria, yeast, and plants." Protein Sci **6**(2): 464-468.

Popham, D. L. and K. D. Young (2003). "Role of penicillin-binding proteins in bacterial cell morphogenesis." Curr Opin Microbiol **6**(6): 594-599.

Poquet, I., V. Saint, E. Seznec, N. Simoes, A. Bolotin and A. Gruss (2000). "HtrA is the unique surface housekeeping protease in Lactococcus lactis and is required for natural protein processing." Mol Microbiol **35**(5): 1042-1051.

Price, N. L. and T. L. Raivio (2009). "Characterization of the Cpx regulon in Escherichia coli strain MC4100." J Bacteriol **191**(6): 1798-1815.

Purdy, G. E., M. Hong and S. M. Payne (2002). "Shigella flexneri DegP facilitates IcsA surface expression and is required for efficient intercellular spread." Infect Immun **70**(11): 6355-6364.

Qin, X., K. V. Singh, G. M. Weinstock and B. E. Murray (2000). "Effects of Enterococcus faecalis fsr genes on production of gelatinase and a serine protease and virulence." Infect Immun **68**(5): 2579-2586.

Qin, X., K. V. Singh, G. M. Weinstock and B. E. Murray (2001). "Characterization of fsr, a regulator controlling expression of gelatinase and serine protease in Enterococcus faecalis OG1RF." J Bacteriol **183**(11): 3372-3382.

Raivio, T. L., Popkin, D. L., & Silhavy, T. J. (1999). The Cpx envelope stress response is controlled by amplification and feedback inhibition. J Bacteriol, **181**(17), 5263-5272.

Redford, P., P. L. Roesch and R. A. Welch (2003). "DegS is necessary for virulence and is among extraintestinal Escherichia coli genes induced in murine peritonitis." Infect Immun **71**(6): 3088-3096.

Redford, P. and R. A. Welch (2006). "Role of sigma E-regulated genes in Escherichia coli uropathogenesis." Infect Immun **74**(7): 4030-4038.

Rekart, M. L., M. Gilbert, R. Meza, P. H. Kim, M. Chang, D. M. Money and R. C. Brunham (2013). "Chlamydia public health programs and the epidemiology of pelvic inflammatory disease and ectopic pregnancy." J Infect Dis **207**(1): 30-38.

Resto-Ruiz, S. I., D. Sweger, R. H. Widen, N. Valkov and B. E. Anderson (2000). "Transcriptional activation of the htrA (High-temperature requirement A) gene from Bartonella henselae." Infect Immun **68**(10): 5970-5978.

Reynolds, P. E. (1989). "Structure, biochemistry and mechanism of action of glycopeptide antibiotics." Eur J Clin Microbiol Infect Dis **8**(11): 943-950.

Rigoulay, C., J. M. Entenza, D. Halpern, E. Widmer, P. Moreillon, I. Poquet and A. Gruss (2005). "Comparative analysis of the roles of HtrA-like surface proteases in two virulent Staphylococcus aureus strains." Infect Immun **73**(1): 563-572.

Rosch, J. and M. Caparon (2004). "A Microdomain for Protein Secretion in Gram-Positive Bacteria." Science **304**(5676): 1513-1515.

Rosch, J. W. and M. G. Caparon (2005). "The ExPortal: an organelle dedicated to the biogenesis of secreted proteins in Streptococcus pyogenes." Mol Microbiol **58**(4): 959-968.

Roy, A., A. Kucukural and Y. Zhang (2010). "I-TASSER: a unified platform for automated protein structure and function prediction." Nat Protoc **5**(4): 725-738.

Ruiz, N. and T. J. Silhavy (2005). "Sensing external stress: watchdogs of the Escherichia coli cell envelope." Curr Opin Microbiol **8**(2): 122-126.

Ruiz, N., B. Wang, A. Pentland and M. Caparon (1998). "Streptolysin O and adherence synergistically modulate proinflammatory responses of keratinocytes to group A streptococci." Molecular Microbiology **27**(2): 337-346.

Salama, N. R., B. Shepherd and S. Falkow (2004). "Global transposon mutagenesis and essential gene analysis of Helicobacter pylori." J Bacteriol **186**(23): 7926-7935.

Sarvas, M., C. R. Harwood, S. Bron and J. M. van Dijl (2004). "Post-translocational folding of secretory proteins in Gram-positive bacteria." Biochim Biophys Acta **1694**(1-3): 311-327.

Sawa, J., H. Malet, T. Krojer, F. Canellas, M. Ehrmann and T. Clausen (2011). "Molecular adaptation of the DegQ protease to exert protein quality control in the bacterial cell envelope." J Biol Chem **286**(35): 30680-30690.

Schaller, G. E., S. H. Shiu and J. P. Armitage (2011). "Two-Component Systems and Their Co-Option for Eukaryotic Signal Transduction." Current Biology **21**(9): R320-R330.

Schindelin, J., I. Arganda-Carreras, E. Frise, V. Kaynig, M. Longair, T. Pietzsch, S. Preibisch, C. Rueden, S. Saalfeld, B. Schmid, J. Y. Tinevez, D. J. White, V. Hartenstein,

K. Eliceiri, P. Tomancak and A. Cardona (2012). "Fiji: an open-source platform for biological-image analysis." Nat Methods **9**(7): 676-682.

Schlievert, P. M., P. J. Gahr, A. P. Assimacopoulos, M. M. Dinges, J. A. Stoehr, J. W. Harmala, H. Hirt and G. M. Dunny (1998). "Aggregation and binding substances enhance pathogenicity in rabbit models of Enterococcus faecalis endocarditis." Infect Immun **66**(1): 218-223.

Schneewind, O. and D. Missiakas (2014). "Sec-secretion and sortase-mediated anchoring of proteins in Gram-positive bacteria." Biochim Biophys Acta **1843**(8): 1687-1697.

Schurr, M. J., H. Yu, J. M. Martinez-Salazar, J. C. Boucher and V. Deretic (1996). "Control of AlgU, a member of the sigma E-like family of stress sigma factors, by the negative regulators MucA and MucB and Pseudomonas aeruginosa conversion to mucoidy in cystic fibrosis." J Bacteriol **178**(16): 4997-5004.

Sebert, M. E., L. M. Palmer, M. Rosenberg and J. N. Weiser (2002). "Microarray-based identification of htrA, a Streptococcus pneumoniae gene that is regulated by the CiaRH two-component system and contributes to nasopharyngeal colonization." Infect Immun **70**(8): 4059-4067.

Shankar, N., C. V. Lockatell, A. S. Baghdayan, C. Drachenberg, M. S. Gilmore and D. E. Johnson (2001). "Role of Enterococcus faecalis surface protein Esp in the pathogenesis of ascending urinary tract infection." Infect Immun **69**(7): 4366-4372.

Sievers, F., A. Wilm, D. Dineen, T. J. Gibson, K. Karplus, W. Li, R. Lopez, H. McWilliam, M. Remmert, J. Soding, J. D. Thompson and D. G. Higgins (2011). "Fast, scalable generation of high-quality protein multiple sequence alignments using Clustal Omega." Mol Syst Biol **7**: 539.

Sillanpaa, J., C. Chang, K. V. Singh, M. C. Montealegre, S. R. Nallapareddy, B. R. Harvey, H. Ton-That and B. E. Murray (2013). "Contribution of individual Ebp Pilus subunits of Enterococcus faecalis OG1RF to pilus biogenesis, biofilm formation and urinary tract infection." PLoS One **8**(7): e68813.

Smeds, A., P. Varmanen and A. Palva (1998). "Molecular characterization of a stress-inducible gene from Lactobacillus helveticus." J Bacteriol **180**(23): 6148-6153.

Snyder, H., S. L. Kellogg, L. M. Skarda, J. L. Little and C. J. Kristich (2014). "Nutritional control of antibiotic resistance via an interface between the phosphotransferase system and a two-component signaling system." Antimicrob Agents Chemother **58**(2): 957-965.

Snyder, W. B. and T. J. Silhavy (1992). "Enhanced export of beta-galactosidase fusion proteins in prlF mutants is Lon dependent." J Bacteriol **174**(17): 5661-5668.

Sonnhammer, E. L., G. von Heijne and A. Krogh (1998). "A hidden Markov model for predicting transmembrane helices in protein sequences." Proc Int Conf Intell Syst Mol Biol **6**: 175-182.

Spiess, C., A. Beil and M. Ehrmann (1999). "A temperature-dependent switch from chaperone to protease in a widely conserved heat shock protein." Cell **97**(3): 339-347.

Stephenson, K. and J. A. Hoch (2002). "Two-component and phosphorelay signal-transduction systems as therapeutic targets." Current Opinion in Pharmacology **2**(5): 507-512.

Swamy, K. H., C. H. Chung and A. L. Goldberg (1983). "Isolation and characterization of protease do from Escherichia coli, a large serine protease containing multiple subunits." Arch Biochem Biophys **224**(2): 543-554.

Taylor, B. L. and I. B. Zhulin (1999). "PAS domains: internal sensors of oxygen, redox potential, and light." Microbiol Mol Biol Rev **63**(2): 479-506.

Tegtmeyer, N., Y. Moodley, Y. Yamaoka, S. R. Pernitzsch, V. Schmidt, F. R. Traverso, T. P. Schmidt, R. Rad, K. G. Yeoh, H. Bow, J. Torres, M. Gerhard, G. Schneider, S. Wessler and S. Backert (2016). "Characterisation of worldwide Helicobacter pylori strains reveals genetic conservation and essentiality of serine protease HtrA." Mol Microbiol **99**(5): 925-944.

Teixeira, N., S. Varahan, M. J. Gorman, K. L. Palmer, A. Zaidman-Remy, R. Yokohata, J. Nakayama, L. E. Hancock, A. Jacinto, M. S. Gilmore and M. de Fatima Silva Lopes (2013). "Drosophila host model reveals new enterococcus faecalis quorum-sensing associated virulence factors." PLoS One **8**(5): e64740.

Thomas, V. C., L. R. Thurlow, D. Boyle and L. E. Hancock (2008). "Regulation of autolysis-dependent extracellular DNA release by Enterococcus faecalis extracellular proteases influences biofilm development." J Bacteriol **190**(16): 5690-5698.

Tjalsma, H., Antelmann, H., Jongbloed, J. D., Braun, P. G., Darmon, E., Dorenbos, R., . . . van Dijl, J. M. (2004). Proteomics of protein secretion by Bacillus subtilis: separating the "secrets" of the secretome. Microbiol Mol Biol Rev, **68**(2), 207-233. doi:10.1128/MMBR.68.2.207-233.2004.

Ton-That, H. and O. Schneewind (2003). "Assembly of pili on the surface of Corynebacterium diphtheriae." Mol Microbiol **50**(4): 1429-1438.
Tsirigos, K. D., C. Peters, N. Shu, L. Kall and A. Elofsson (2015). "The TOPCONS web server for consensus prediction of membrane protein topology and signal peptides." Nucleic Acids Res **43**(W1): W401-407.

Tschauner, K., Hornschemeyer, P., Muller, V. S., & Hunke, S. (2014). Dynamic interaction between the CpxA sensor kinase and the periplasmic accessory protein CpxP mediates

signal recognition in E. coli. PLoS One**,** **9**(9), e107383. doi:10.1371/journal.pone.0107383.

Tsui, H. C., S. K. Keen, L. T. Sham, K. J. Wayne and M. E. Winkler (2011). "Dynamic distribution of the SecA and SecY translocase subunits and septal localization of the HtrA surface chaperone/protease during Streptococcus pneumoniae D39 cell division." MBio **2**(5).

Tu, Z. M., G. Y. He, K. X. X. Li, M. J. J. Chen, J. L. Chang, L. Chen, Q. Yao, D. P. P. Liu, H. Ye, J. T. Shi and X. Q. Wu (2005). "An improved system for competent cell preparation and high efficiency plasmid transformation using different Escherichia coli strains." Electronic Journal of Biotechnology **8**(1): 113-120.

Typas, A., M. Banzhaf, C. A. Gross and W. Vollmer (2011). "From the regulation of peptidoglycan synthesis to bacterial growth and morphology." Nat Rev Microbiol **10**(2): 123-136.

Waller, P. R. and R. T. Sauer (1996). "Characterization of degQ and degS, Escherichia coli genes encoding homologs of the DegP protease." J Bacteriol **178**(4): 1146-1153.

Walsh, N. P., B. M. Alba, B. Bose, C. A. Gross and R. T. Sauer (2003). "OMP peptide signals initiate the envelope-stress response by activating DegS protease via relief of inhibition mediated by its PDZ domain." Cell **113**(1): 61-71.

Wang, L. C., Morgan, L. K., Godakumbura, P., Kenney, L. J., & Anand, G. S. (2012). The inner membrane histidine kinase EnvZ senses osmolality via helix-coil transitions in the cytoplasm. EMBO J, **31**(11), 2648-2659. doi:10.1038/emboj.2012.99

Weiner, L. M., A. K. Webb, B. Limbago, M. A. Dudeck, J. Patel, A. J. Kallen, J. R. Edwards and D. M. Sievert (2016). "Antimicrobial-Resistant Pathogens Associated With Healthcare-Associated Infections: Summary of Data Reported to the National Healthcare Safety Network at the Centers for Disease Control and Prevention, 2011-2014." Infect Control Hosp Epidemiol **37**(11): 1288-1301.

Wessler, S., G. Schneider and S. Backert (2017). "Bacterial serine protease HtrA as a promising new target for antimicrobial therapy?" Cell Commun Signal **15**(1): 4.

Wilken, C., K. Kitzing, R. Kurzbauer, M. Ehrmann and T. Clausen (2004). "Crystal structure of the DegS stress sensor: How a PDZ domain recognizes misfolded protein and activates a protease." Cell **117**(4): 483-494.

Williams, K., P. C. Oyston, N. Dorrell, S. Li, R. W. Titball and B. W. Wren (2000). "Investigation into the role of the serine protease HtrA in Yersinia pestis pathogenesis." FEMS Microbiol Lett **186**(2): 281-286.

Wilson, R. L., L. L. Brown, D. Kirkwood-Watts, T. K. Warren, S. A. Lund, D. S. King, K. F. Jones and D. E. Hruby (2006). "Listeria monocytogenes 10403S HtrA is necessary for resistance to cellular stress and virulence." Infect Immun **74**(1): 765-768.

Wu, C., A. Mishra, J. Yang, J. O. Cisar, A. Das and H. Ton-That (2011). "Dual function of a tip fimbrillin of Actinomyces in fimbrial assembly and receptor binding." J Bacteriol **193**(13): 3197-3206.

Wu, X., L. Lei, S. Gong, D. Chen, R. Flores and G. Zhong (2011). "The chlamydial periplasmic stress response serine protease cHtrA is secreted into host cell cytosol." BMC Microbiol **11**: 87.

Wyrick, P. B. (2010). "Chlamydia trachomatis persistence in vitro: an overview." J Infect Dis **201 Suppl 2**: S88-95.

Xu, W., Flores-Mireles, A. L., Cusumano, Z. T., Takagi, E., Hultgren, S. J., & Caparon, M. G. (2017). Host and bacterial proteases influence biofilm formation and virulence in a murine model of enterococcal catheter-associated urinary tract infection. NPJ Biofilms Microbiomes, **3**, 28. doi:10.1038/s41522-017-0036-z

Yang, J. and Y. Zhang (2015). "I-TASSER server: new development for protein structure and function predictions." Nucleic Acids Res **43**(W1): W174-181.

Zhang, L. H., Y. Li, Y. P. Wen, G. W. Lau, X. B. Huang, R. Wu, Q. G. Yan, Y. Huang, Q. Zhao, X. P. Ma, X. T. Wen and S. J. Cao (2016). "HtrA Is Important for Stress Resistance and Virulence in Haemophilus parasuis." Infection and Immunity **84**(8): 2209-2219.

Zurawa-Janicka, D., Wenta, T., Jarzab, M., Skorko-Glonek, J., Glaza, P., Gieldon, A., Lipinska, B. (2017). Structural insights into the activation mechanisms of human HtrA serine proteases. *Arch Biochem Biophys*, **621**, 6-23. doi:10.1016/j.abb.2017.04.004